Modelling and Optimization of Remote Laser Welding Galvanized Steels Using Statistical Methodologies

by

Yanglin Shi [redacted]

Supervisor: Professor Stuart Barnes

Master of Science by Research in Engineering

Warwick Manufacturing Group, University of Warwick

April 2016

Abstract

This thesis is written under the circumstance of "Remote Laser Welding (RLW) System for Eco & Resilient Automotive Factories" project, of which goals are to configure, integrate, test and validate application of RLW system in automotive assembly line. The goal of this study is to identify the RLW process window and optimal parameters setting for four different material stack-ups in the configuration of lap joint.

One-Factor-at-A-Time method is used to determine the process window in which sound welds, free from visible defects such as spatter, cut-through, burn-through and insufficient weld, are produced. One step further, sound welds are transversely cross-sectioned and geometric profiles (top concavity, interface width, penetration and bottom concavity) are measured and compared to industrial standards. Eventually, it is determined that within power [3, 4] kW, speed [2.5,5.5] m/min, gap [0.15, 0.30] mm, welds fulfilling visual and non-visual requirements could be produced for stack-up of DX56D+Z 1.00 mm plus DX54D+Z 1.00 mm.

Paired mean hypothesis test between stack-up of 0.75 mm DX56D+Z plus 1.00 mm DX54D+Z and stack-up of 0.75 mm DX56D+Z plus 1.80 mm DX56D+Z is performed with the objective of testing whether lower thickness is a significant factor affecting the process. The results reveal insignificance. The process modelling is therefore simplified to focus on the stack-up with greatest lower thickness. Thanks to this result, it significantly reduces the total experimental work.

Response surfaces between process parameters (power, speed and gap) and cross-section geometric profile (top concavity and penetration) are built, based on the data collected from the Box-Behnken Design experiments carried out on the stack-up of 0.75 mm DX54D+Z and 1.8 mm DX56D+Z. Optimization with the purpose of increasing speed (reduced weld time), lowering the power (saved energy) and delivering "right" quality is performed on the four stack-ups. It is concluded that: for stack-up of 0.75 mm DX56D+Z plus 1.8 mm DX 54D+Z, the optimal results are speed at 3.30 m/min, power at 3.80 kW, and gap at 0.15 mm; for stack-up of 0.75 mm DX56D+Z sheet plus 1.00 mm DX52D+Z or 1.00 mm DX 54D+Z, optimal results are: speed at 3.86 m/min, power at 3.19 kW, and gap at 0.18 mm; for stack-up 0.75 mm DX56D+Z plus 0.70 mm DX53D+Z, optimal results are: speed at 4.65 m/min, power at 3.20 kW, and gap at 0.15 mm.

Key words: RLW, Galvanized steel, Hypothesis testing, BBD, RSM, Modelling and

Optimization

Acknowledgement

My involvement in the RLW European commission project is an extraordinary experience. It gives me a chance to learn, think and choose.

I would like to firstly express my gratitude to Professor Darek Ceglarek, who is such a diligent and dedicated person whose enthusiasm and devotion to research will never rank in the second place in the world. It is very thought-provoking to work with him.

My gratitude also goes to Professor Kevin Neailey, Professor Stuart Barnes and Jennifer Kirkwood. Many thanks to Professor Stuart and Kevin for giving good advice. Great thanks to Jennifer Kirkwood for assisting me in every process of getting experimental work done and thesis written.

My sincere thanks also go to Mr David Moseley, Mr David Williams and Mr David Cooper. All of them, the kindest and most professional individuals I have ever met, helped me through the process of writing this thesis. Gratitude also goes to colleagues Abhishek Das, Dr Pasquale Franciosa and Selim Yilmazer. Should there not be their support, this thesis could never have been finally finished. In addition, great thanks to Gabriele Gattere who was an exchange student from University of Polimi Milano in Italy with good knowledge on laser welding and Andrés Ortiz Arroyave who worked on this project for his Master's degree before me. Without any of them, I could not have finished this thesis.

Finally, thanks to my parents and younger sister. Thanks for their continuous support and love.

Contents

Abbreviation

Abbreviation	Full name
BIW	Body-in-White
OEM	Original Equipment Manufacturer
PLW	Proximity Laser Welding
RLW	Remote Laser Welding
RSW	Resistance Spot Welding
SU	Stack-up
TSB	Technology Strategy Board
HAZ	Heat Affected Zone
WMG	Warwick Manufacturing Group
IPG	IPG Photonics Corporate
COMAU	COnsorzio MAcchine Utensili, Italian company, part of Fiat Group
ABSL	Application BoxSmart Laser
VHN	Vickers Hardness Number

List of Figures

List of Tables

1. Introduction

This study is derived from a prestigious British OEM's research project of applying Remote Laser Welding (RLW) to doors in a body-in-white (BIW) assembly in the configuration of lap joint. Lap joint configuration is illustrated in Figure1. 1. The door of interest consists of four stack-ups as listed in Table1. 1. The materials are all galvanized steels. The goal of this study is to firstly find out process window within which right quality weld joints without defects according to industrial standards could be produced. Secondly, within the identified process window, the optimal condition under which with least power and fastest speed, meanwhile the right quality of weld joints is achieved is to be investigated and concluded.

Figure1. 1 Lap joint configuration (from Ford Welding Standards, Appendix F)

Table1. 1 Four different stack-ups for door of interest

Stack-up	Upper material designation	Upper thickness	Lower material designation	Lower thickness
SU1	DX56D+Z	0.75 mm	DX52D+Z	1.00 mm
SU2	DX56D+Z	0.75 mm	DX54D+Z	1.80 mm

SU3	DX56D+Z	0.75 mm	DX54D+Z	1.00 mm
SU4	DX56D+Z	0.75 mm	DX53D+Z	0.70 mm

The reasons why galvanized steel and RLW have been gaining continuous attention in automotive industry are investigated. In automotive industry, durability improvement and fuel consumption reduction have been the main pursuits these years. The corrosion resistance of material contributes to the improvement of durability, and weight reduction helps to decrease fuel consumption (Zhao et al., 2012,Mei et al., 2009, Chen et al., 2012). Galvanized steel, in possess of the merit of better corrosion resistance than mere alloy steel without coating, has been increasingly used as BIW panels. Meanwhile, RLW technique, due to its characteristics of non-contact and smaller weld area, enables those panels to be designed with smaller flanges, consequently it even reduces the overall weight of the BIW.

In BIW assembly line, different joining processes have been used to join metallic components, iron-carbon alloys with various shapes and geometries. The joints shall have sufficient tensile strength, stiffness and be free from defects such as cracks and spatters for the sake of surface aesthetics. Meanwhile, considering manufacturing engineering and plant management, the joining processes are required to deliver high level of flexibility and productivity.

Resistance Spot Welding (RSW) is the most widely used joining process in today's OEMs' plants. RSW is a fusion welding mode and the base materials are heated by the flow of an electric current. The electrodes and base materials form into an electric

circular, and by means of Joule effect, the base materials are molten and joined together. This process works for non-galvanized steels efficiently. However, when welding galvanized sheet steel, the life of RSW electrode is excessively short (Zhao et al., 2012).

Proximity Laser Welding (PLW) is an alternative of RSW with outstanding merit of shorter cycle time. It also has many other advantages e.g. deep penetration, high speed, small heat affected zone (HAZ), fine welding bead quality, low heat input, fibre beam delivery and no direct contact (Zhao et al., 2012, Mei et al., 2009, Chen et al., 2012). However, PLW is much more expensive than RSW and has the risks of collision and contamination of the scanner.

With the development of disk and fibre laser, RLW has emerged as another alternative. By the application of long focal lenses, RLW welding scanner can be set at a distance of more than 1 m away from the workpiece instead of standing off at a distance in the order of magnitude of centimetres. This merit helps to eliminate the risk of collision and contamination. In addition, by tilting two galvanometric mirrors in the laser welding scanner, the laser beam could cover a wide working area at high speed (Grupp et al., 2003, Kang et al., 2011). Benefit from it, the repositioning time of RLW is significantly shortened, limiting to several milliseconds compared to several seconds of RSW and PLW. Despite all the advantages, some difficulties still prevent RLW process from being used flexibly and efficiently in welding galvanized steels. The main concern is caused by the fact that the boiling temperature of zinc (906 °C) is much lower than the melting temperature of steel (1530 °C), resulting in unstable process where the vaporization of zinc would block the plasma and causes severe expulsion of melted material. Fortunately, this problematic concern has been

studied widely in academia, and different solutions have been proposed. One direction focuses on pre-treatment of the welding surfaces by either adding additional elements (Baardsen, 1975) or removing zinc-coating (Pennington, 1987) to eliminate the vaporization phenomenon, which seems to lack the feasibility of industrial application. Another direction focuses on adjusted laser beam such as dual focus beam (Banas and Doyle, 1987) , oscillated laser beam (Stol and Martukanitz, 2004) , fast frequency modulation of laser power (Schmidt et al., 2008) and etc. The other direction concentrates on creating a gap between the two metal sheets for the zinc to degas. (Rito et al., 1988) suggested to create the gap by loose contact or inserting spacers. (Petrick, 1990) used pre-stamped projection technique to create V-shape tabs in the lower part which acts as the required gap. (Colombo et al., 2012) believed that dimplings that are protrusions from the lower sheet, created by laser, had an advantage over others as it shows the industrial feasibility of mass production.

In this study, the chosen solution is to create a gap using shims as illustrated in Figure 1. 2. In order to increase the consistency and reduce the variation of the gap, a specifically designed fixture is used and will be introduced in detail in Chapter 5- Experimental Set-up. One-Factor-at-a-Time method is applied to figure out the process window, and then Response Surface Methodology (RSM) is used to establish the correlation models between process parameters and weld-joint geometric structure and the optimal process parameters are obtained.

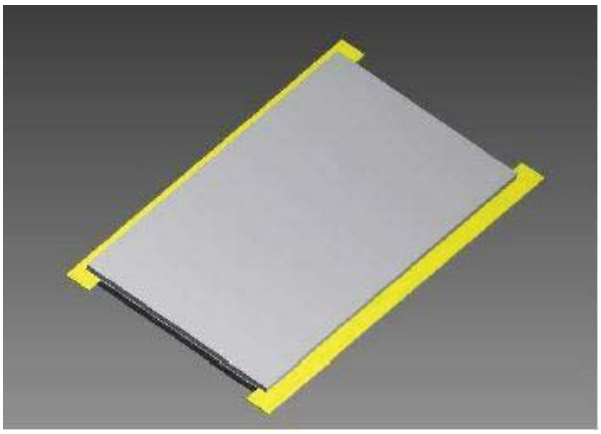

Figure 1. 2 Shims in yellow to create the gap between two coupons

When it comes to establishing correlation models between process parameters and process outputs and the optimal process parameters, a great number of studies have been carried out in literature. Different methodologies such as RSM (Benyounis et al., 2005a, Benyounis et al., 2005b, Manonmani et al., 2007, Rizzi et al., 2011, Khan et al., 2011, Zhao et al., 2012, Padmanaban and Balasubramanian, 2010), Artificial Neural Network Method (Vitek et al., 1998, Jeng et al., 2000), Taguchi methodology (Sathiya et al., 2011, Lee et al., 2006, Pan et al., 2005, Anawa and Olabi, 2008, Olabi and Anawa, 2006) and etc. were applied. In this study, thanks to RSM's advantages over other methods in this context, it is chosen as the methodology for correlation modelling and optimization.

However, the aforementioned optimization studies are all committed to optimize certain mechanical property or weld bead profile from a structural point of view, in the ambition of delivering weld joints with "best" quality. Differently, this study changes the focus to improve the efficiency of the process from the view point of industrial engineering, aiming to shorten process cycle time, reduce energy

consumption and deliver weld joints with “right” quality. Thanks to the proposed problem-solving roadmap in Chapter 4-Methodology, this study accomplishes the goals by conducting experiments on one material stack-up and the correlation models could be shared among four stack-ups. It helps reduce tedious repeats of experimentation.

In the end, it is concluded that within power [3, 4] kW, speed [2.5,5.5] m/min, gap [0.15, 0.30] mm, weld joints fulfilling visual and non-visual requirements could be soundly produced for stack-up of DX56D+Z 1.00 mm plus DX54D+Z 1.00 mm. For stack-up of 0.75 mm DX56D+Z plus 1.8 mm DX 54D+Z , the optimal results are speed at 3.30 m/min, power at 3.80 kW, and gap at 0.15 mm; For stack-up of 0.75 mm DX56D+Z sheet plus 1.00 mm DX52D+Z or 1.00 mm DX 54D+Z, optimal results are: speed at 3.86 m/min, power at 3.19 kW, and gap at 0.18 mm; For stack-up 0.75 mm DX56D+Z plus 0.70 mm DX53D+Z, optimal results are: speed at 4.65 m/min, power at 3.20 kW, and gap at 0.15 mm.

2. Research background

This thesis is written under the circumstance of "Remote Laser Welding System for Eco & Resilient Automotive Factories" project, the goals of which are to configure, integrate, test and validate application of RLW system in automotive assembly. Before this project, another project named Technology Strategy Board (TSB) has been carried out in Warwick Manufacturing Group (WMG) with the objective of defining RLW process engineering guidelines. These two projects utilize the same RLW system located in Warwick manufacturing centre, University of Warwick. The system integrates an IPG 4 kW laser source and a COMAU Smartlaser. Thanks to the results shared from TSB, tremendous useful information is ready to use.

In this chapter, the architecture of RLW and major conclusions of TSB project relevant to this study are introduced. Afterwards, automotive weld quality definition of lap-joint welds is presented.

2.1 RLW system

The RLW system, integrating an IPG 4 kW laser source and a COMAU Smartlaser in a cell is illustrated in Figure 2. 1. The laser source is a 4 kW high brightness fibre laser and COMAU Smartlaser is an industrial robot with a 4-axis robotic arm integrated with an optical focussing and addressing arm. RLW process could produce similar weld joints as PLW (deep penetration, narrow HAZ and etc.). However, unlike PLW, RLW process does not utilize inertia shield gas to protect the weld keyhole. Therefore, it does not have the effect of plasma suppression. There are two nozzles mounted on the scanner to direct compressed air onto the weld area and expel the generated fumes, but this does not have the effect of suppression of plasma

in the weld pool. An additional air-knife is used to blow away the melted material particles and prevent the optics from contamination.

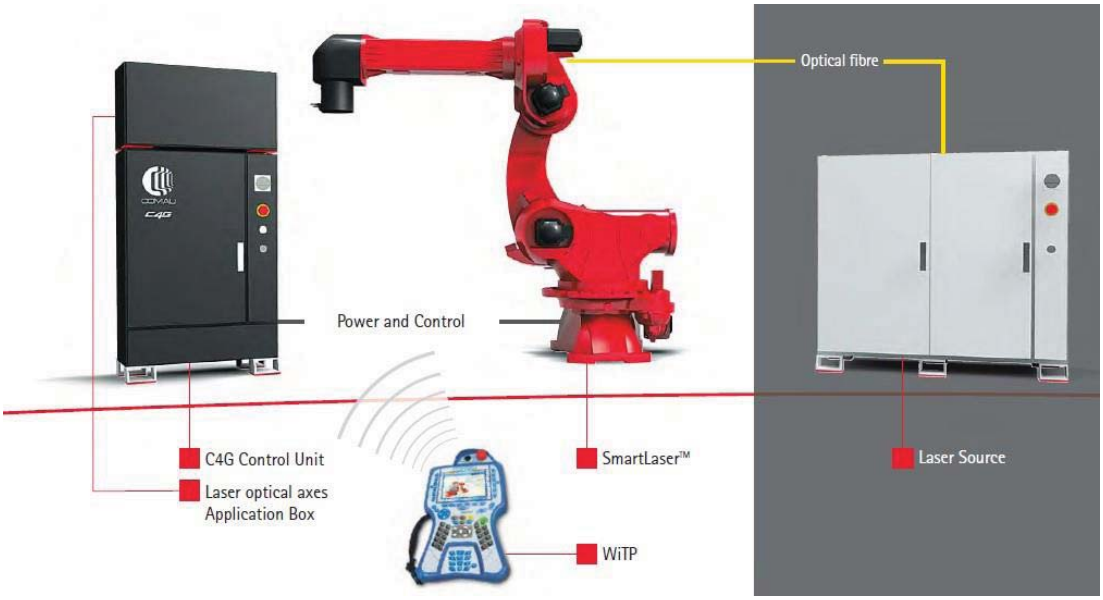

Figure 2. 1 WMG RLW system (Source: COMAU)

2.1.1 Laser source

The Ytterbium Fibre Laser (YLR-4000) from IPG Photonics could emit 4 kW power at maximum. The power is supplied by 8 modules. Within each module, an array of pump diodes launch electromagnetic radiation at 960 nm into the delivery fibre, which transmits the 960 nm radiation into another section of the same fibre in which silica is dooped with Ytterbium. This material could generate radiation at 1070 nm through physical mechanism of population inversion and stimulated emission. In this way, the pump diodes light is transformed into laser beam. Through the application of an optical combiner, the laser from different modules is coupled together. The

coupled laser is directed to the workpiece by the usage of a delivering fibre with a diameter of 200 μm and a collimation and focusing system. The IPG 4 kW laser source technical specification is shown in Table 2. 1; Figure 2. 2 shows the interior of the IPG laser box and Figure 2. 3 shows one single module inside the laser box.

Table 2. 1 Technical specification of IPG YLR-4000

	IPG YLR-4000 (Yetterbium Fibre Laser)
Laser wavelength	1070 nm
Available laser power	4 kW
Operating mode	Continuous wave
Number of power module	8
Feed fibre diameter	200 μm
M^2	Source (at output of delivery fibre) =21.4 Smartlaser (at workpiece) =31.4
Maximum modulation frequency	5000 Hz
Output power variation	± 0.5 %

Cooling mode	Water

Note: M^2, known as beam quality factor, represents the degree of variation of a beam from an ideal Gaussian beam. It reflects how well a collimated laser beam can be focused to a small spot, or how well a divergent laser source can be collimated.

Figure 2. 2 IPG YLR-4000 laser source with 8 modules inside

Figure 2. 3 A module of IPG YLR-4000 laser (Source : IPG)

2.1.2 COMAU Smart Laser

2.1.2.1 Robotic system and scanning head

COMAU Smartlaser integrates a classical NH1 (COMAU's internal code) 4-axis robot (called anthropomorphic arm, Arm 2, in Figure 2. 4) with an optical arm (called focusing and addressing arm, Arm 1, in Figure 2. 4) that is used to direct the laser beam to the workpiece in high dynamics. The focusing of the laser beam could be achieved at a range of distance between 750 mm and 1100 mm through adjusting lens positions in arm 2. This adjusting mechanism is realized through utilizing an electronic cam controlled by 3 motorized axes. Thanks to this solution, the focusing axis has low inertia and can move at the speed of 4 m/s at maximum and the acceleration could be as high as 8 times of gravitational acceleration (8g). After the beam is focalized, the 2-axis rotating mirror could generate movement in x and y dimensions at a speed in the range of 150 – 250 rad/s. Compared to other robotic system integrated with 2D scanner having maximum acceleration of 1g, SmartLaser has substantially improved in acceleration. RLW system's specific features are listed in Table 2. 2.

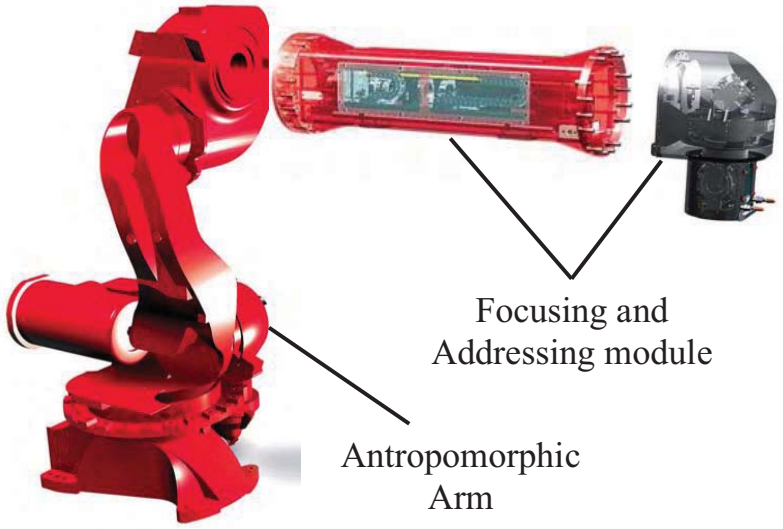

Figure 2. 4 Robotic arm and scanning head (Source: COMAU)

Table 2. 2 Operating range of every axis of the robot (Source : COMAU, Appendix C)

Specific Features			
Number of axes		7	
Repeatability (mm)		+/-0.07	
Installation position		floor	
Protection class		IP65	
ARM1	axis 3	stroke (mm)	+0.1 to +315.0
		speed (m/s)	3
	axis 4	stroke (°)	+/- 140
		speed (°/s)	1289
	axis 5	stroke (°)	+10 / -7.5
		speed (°/s)	945

ARM2			
	axis 1	stroke (°)	+/-180
		speed (°/s)	108
	axis 2	stroke (°)	+75/-55
		speed (°/s)	104
	axis 3	stroke (°)	+110/-170
		speed (°/s)	110
	axis 4	stroke (°)	+/-282
		speed (°/s)	190
Operating areas	A	(mm)	3396.13
	B	(mm)	2863.41
	C	(mm)	900
	D	(mm)	1686.75
	E	(mm)	387.66

The magnification ratio of the optical chain is 3. Therefore, with the feed fibre diameter of 200 μm, the laser beam waist diameter is 600 μm.

2.1.2.2 Controlling system

The controlling system has two separate modules. C4G is a typical COMAU control module for robots. The Application Box Smart Laser (ABSL) module is an additional module for the laser system. ABSL is powered by C4G control and does

not require separate connection to power suppliers. They are usually delivered together as a whole as shown in Figure 2. 5.

Figure 2. 5 Control box of the RLW system (Source : COMAU)

2.2 WMG TSB project

In TSB project, useful guidelines for applying RLW technique to volume manufacturing have been concluded through thousands of experiments and tests. In this section, the guidelines regarding welding zinc-coated steels, which are closely relevant to this study, are highlighted. The TSB report is attached as Appendix D in this thesis.

***Guideline 1**: A laser weld stitch, if being used as a direct substitute for a resistance spot, should be at least 25 mm in length.*

***Guideline 2**: For coated steels, material stack combination that includes zinc coated steels requires an interface gap between 0.1 mm and 0.25 mm.*

***Guideline 3**: Any combination of the following grades of steel can be readily and acceptably welded: DC04, DC05, DX54, DX55, HSLA, BH (up to 260), XF (up to 350), DP (up to 600), boron steels (up to 1200), 304, EN8 EN16, EN30.*

***Guideline 4**: For DX54, the thickness combinations in green, shown in Table 2. 3, are able to produce good weld joints in term of lap shear strength.*

Table 2. 3 Permissible material thickness combinations for DX54 (Source: TSB report)

Material Capability: DX54: Expected Lap shear strength								
		Top						
		0.7	1	1.5	1.7	2	2 (boron)	3
Bottom	0.7	4.6	5.1		5.8	5.8	6	
	1	5.1	7.4	7.7		6.2		
	1.5		7.8	11.4				
	1.7	5.5			12.7			
	2	5.8	8.2			17.8		
	2 (boron)	6	9.4					
	3							17.2

***Guideline 5**: Material stack combinations where one or both materials are coated with zinc are readily weldable if a suitable interface gap is maintained, and the optimum value of the gap is 0.18 mm.*

***Guideline 6**: The allowed incident angle of the laser beam to workpieces surface is 30 degrees from perpendicular.*

2.3 Industrial weld quality definition

According to (Juran et al., 1999), fitness for intended use to customer's satisfaction is a modern and widely accepted definition of quality. Following this logic, a weld joint is considered as of good quality if it presents sufficient strength, reliability, durability and neat appearance within its life cycle. Strength means the resistance to fail under a

constant load and it is a crucial characteristic for the weld bead as the joined components are all structural of the body frame. When a vehicle is riding, dynamic loads under different working conditions are forced on the structural components, therefore reliability is another aspect for the customers to judge whether a product conveys the image of good quality. Durability relates to performance degradation over time. Usually customers expect the product to serve without major failures within its entire life cycle. The appearance of the weld is an important contributor for perceived quality and homogeneous welds not only reduce the risk of corrosion but also give an impression of premium quality and high technology to the customers. Strength, reliability and durability need to be tested. The tests could either be destructive or non-destructive. Appearance could be subjectively evaluated.

In Ford internal standards (Appendix F), the above mentioned characteristics could be inferred from macro evaluation or metallographic assessment of weld bead, which means there are correlations (in Figure 2. 6) between those characteristics and the KPIs defined in the Ford standards. The defined KPIs are:

- Weld length
- Interface width
- Penetration
- Root convexity
- Top surface concavity
- Bottom surface concavity
- Undercut

- Porosity
- Spatter
- Top surface cracks
- Cut-through
- Burn-through
- Weld discontinuity
- Hardness

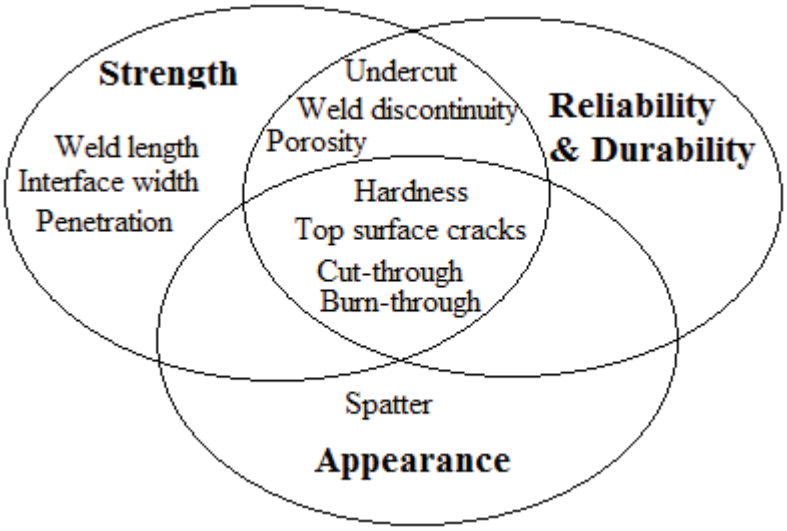

Figure 2. 6 Correlation between four characteristics and Ford KPIs

As illustrated in Figure 2. 6, Weld length, interface width and penetration are considered to be only relevant to strength. Spatter affects the appearance. Top concavity and bottom concavity are thought to influence both strength and appearance of the weld. Undercut, weld discontinuity and porosity influence strength, reliability and durability. Cut-through, burn-through, top surface cracks and hardness affect strength, reliability, durability and appearance. The definitions of the indicators are presented as below:

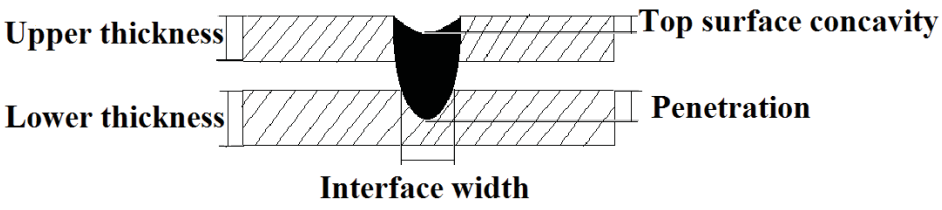

Figure 2. 7 Partial penetration mode of laser welding

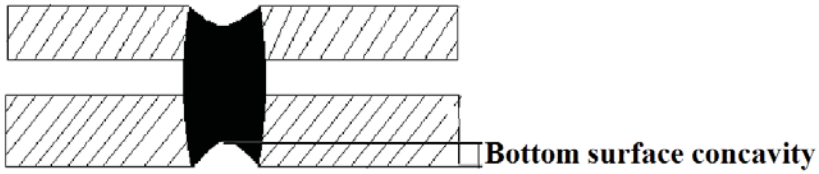

Figure 2. 8 Full penetration mode of laser welding

Length

The weld length is a main factor determining the strength. In Ford Standard (see in Appendix E), d1 is defined as the design length and d2 is defined as the weld length as illustrated in Figure 2. 9. The weld length is considered as the effective length. In TSB project, it has been concluded that only if the weld length (d1) shall be longer than 25 mm, the property of welded joints could replace a resistance spot welded joint. Therefore, the limit of length is:

$$\text{Weld length} \geq 25 \text{ mm}$$

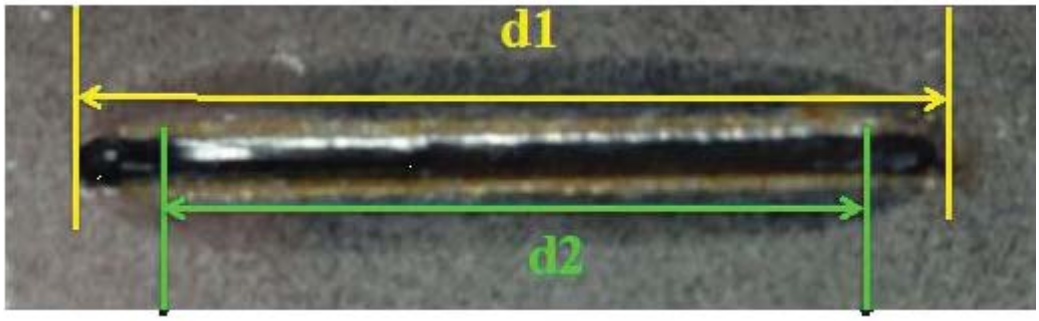

Figure 2. 9 Length (Source: Ford Standards)

Interface width

The horizontal distance in weld interface as illustrated in Figure 2. 7 is the most relevant characteristic for strength. In Ford standard, the minimum value of it is considered as a linear function of the thinner sheet and in this study the function is:

$$\text{Interface width} \geq 0.9 \times \text{thinner thickness}$$

Penetration

Penetration is another key parameter characterizing strength. In several works, penetration has been investigated as the main factor, for example (Benyounis et al., 2005a). As illustrated in Figure 2. 7 and Figure 2. 8, penetration could be partial and complete of the lower thickness thanks to the amount of energy input. In some studies, the penetration is measured from the upper sheet surface. Instead, in Ford standard and ANSI/AWS standards, it is measured as the depth of welded area in the lower sheet. This thesis follows the latter definition. Regard to Ford standard, the minimum penetration into the lower sheet is required to reach 30 % of the lower thickness. That is to say:

$$\text{Penetration} \geq 0.3 \times \text{lower thickness}$$

Root convexity

Root convexity (R), also named as sagging or pitting, is defined as the protrusion that extends over the external surface of the lower sheet material as illustrated in Figure 2. 10. Excessive protrusion not only deteriorates the weld appearance but also reduces the weld corrosion resistance. Therefore the maximum of it is limited to:

$$\text{Root concavity} \leq 0.2\ \text{mm} + (0.3 \times \text{lower thickness})$$

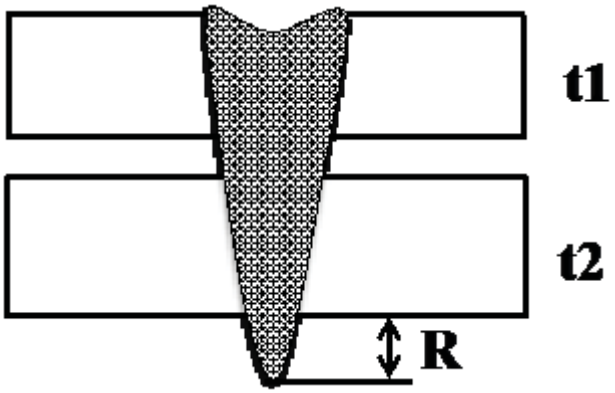

Figure 2. 10 Root convexity (from Arroyave, A.O., 2012)

Top surface concavity

Top surface concavity is a pit that extends from the surface of the upper sheet as illustrated in Figure 2. 7. The cause could be the effect of gravity linked with a reduction of surface tension when the material is melted or a large gap between the weld sheets. It causes a reduction in strength consequently. The maximum acceptable limit is :

$$\text{Top surface concavity} \leq 0.5 \times \text{upper thickness}$$

Bottom surface concavity

Bottom surface concavity is the depth of the pit from the lower surface of the lower sheet as shown in Figure 2. 8. Basically it is caused by excessive melting of the weld pool material so that the tension force of the surface cannot hold the vapour and some of it drops. In addition, vaporization of the weld pool might cause such depression. In literature no limit of such defect has been defined, however it is found, in TSB project, presentation of such defect damages strength and appearance of the weld. The length is limited to:

$$\text{Bottom surface concavity} \leq 0.5 \times \text{upper thickness}$$

Undercut

The definition of undercut (U) is a slot of mission material between the HAZ and the melted material in Figure 2. 11. This defect has a great effect on reliability and fatigue behaviour of the weld due to the fact that small radius of such defect concentrates stresses and leads to failures under repetitive cycles of load. To avoid such failures, the total length of undercut should be:

$$\text{Undercut length} \leq 0.2 \times \text{Design length}$$

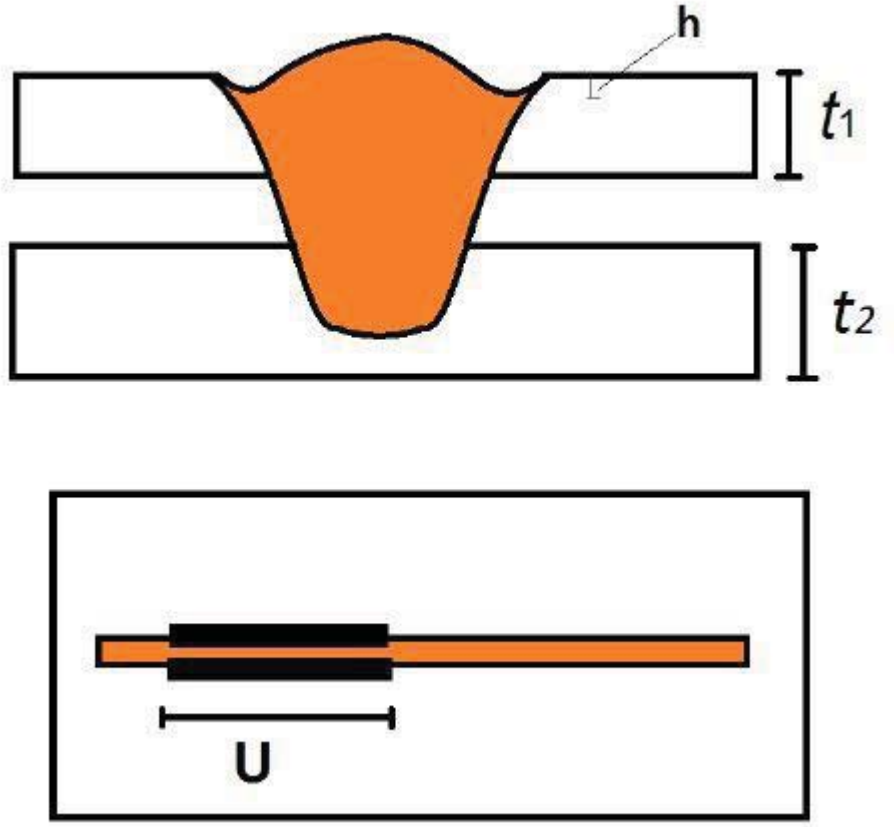

Figure 2. 11 Undercut

Porosity

Porosity is generated by the entrapment of gas in the welded material during the solidification phase illustrated in Figure 2. 12. The entrapped pores not only deteriorate the strength but also affect the fatigue life of the components. Such pores are impossible to be visually observed and cross-section could theoretically help to calculate the sum of all pores length. In Ford standard, the limitation is set as:

$$\text{Porosity length} \leq 0.3 \times \text{upper thickness}$$

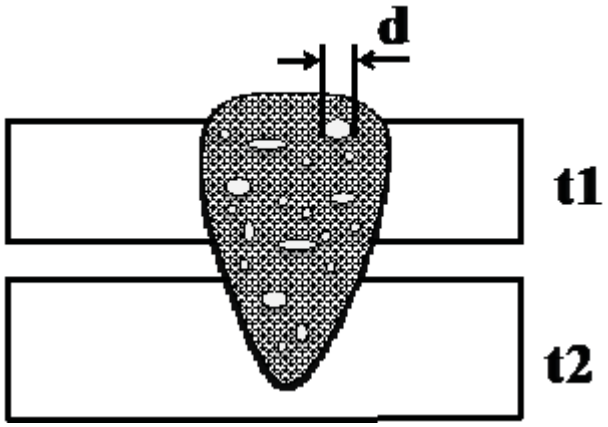

Figure 2. 12 Porosity (from Arroyave, A.0., 2012)

Spatter

Spatters are small metal particles projected from the weld pool in Figure 2. 13. This phenomenon is generally caused by the pore generation. The occurring of it badly deteriorates the appearance of the weld. The limit of such defects is depended on the required surface finish level.

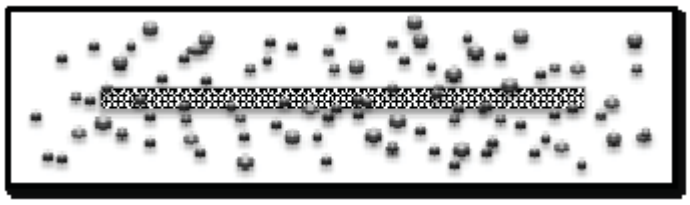

Figure 2. 13 Spatter (from Arroyave, A.O., 2012)

Top surface cracks

There are two types of cracks, hot cracks and cold cracks. They are crucial to welding process since they not only severely affect strength of the joint but also

reliability and durability. For those reasons in Ford standards top surface cracks are not allowed.

Not allowed

Cut-through

Cut-through is the absence of upper material in the weld joint as shown in Figure 2. 14. This defect affects the mechanical resistance and fatigue life of the weld joint. The limit of it is:

$$\text{Cut} - \text{through} \ \leq 0.2 \ \times \text{length}$$

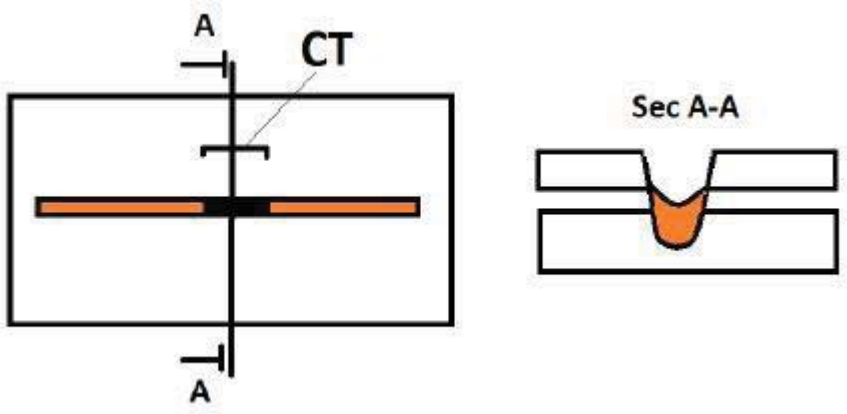

Figure 2. 14 Cut-through

Burn-through

Burn-through is the absence of material of both upper and lower sheets as illustrated in Figure 2. 15. The presence of it highly deteriorates strength, reliability and durability, and appearance of the weld joint. Therefore, in Ford standards, such defect is not allowed.

Not allowed

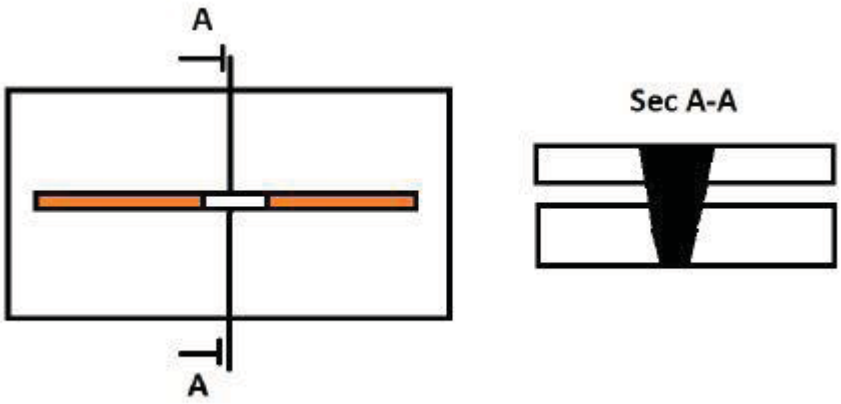

Figure 2. 15 Burn-through

Weld discontinuity

Weld discontinuity means a part of the weld is not welded. It might happen due to sudden stop of energy supply during the welding process. It affects the strength of the weld joint due to insufficiency of weld length. The limit of it is:

$$\text{Weld discontinuity} \leq 0.2 \times \text{Design length}$$

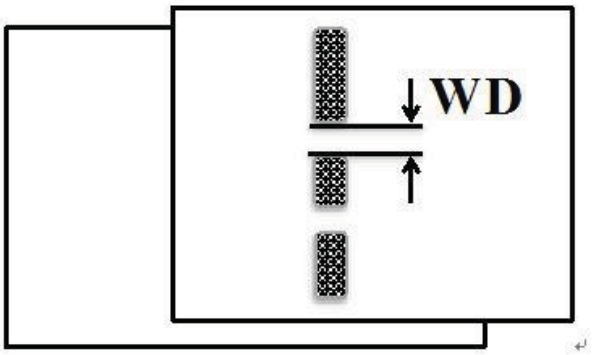

Figure 2. 16 Weld discontinuity (from Arroyave, A.O., 2012)

Hardness

To make sure the weld could obtain good mechanical property, the hardness of HAZ and weld area must be inside the requested threshold. It has been stated in TSB project that the hardness of a laser weld joint is comparable to a resistance spot welded one. The limit of hardness should be:

$$\text{Hardness} \leq 400 \text{ VHN}$$

VHN-unit, Vickers Hardness Number

3. Literature review

In order to establish sufficient knowledge and achieve the goals of this study, a substantial literature review has been made. The history of "Laser" and development of laser application in automotive industry was briefly reviewed and summarized. Concerning the process of welding galvanized steel with RLW, how a RLW system is integrated is reviewed to understand the working principles of such a system. The major issues related with welding galvanized steel by laser and solutions are carefully reviewed, and feasible solutions are found and integrated into the methodology roadmap in Chapter 4 to solve the problem.

3.1 Principle of Laser

"Laser", firstly proposed by Schawlow and Townes in 1958, is an acronym for Light Amplification by Stimulated Emission of Radiation. The basic components of laser construction include active media (serves as a means to amplify light), pumping source to excite the active media and optical resonator to provide optical feedback. The configuration of them is illustratively shown in Figure 3. 1. There are several different lasers with different laser construction. They are carbon dioxide (CO_2), carbon monoxide (CO), neodymium-doped yttrium aluminium garnet (YAG; Nd: YAG), neodymium glass (Nd: glass), ytterbium-doped YAG (Yb: YAG), erbium-doped YAG (Er: YAG), excimer (KrF, ArF, XeCl), diode and fibre lasers. Every laser has its own characteristics and advantages and disadvantages (Steen and Mazumder, 2010).

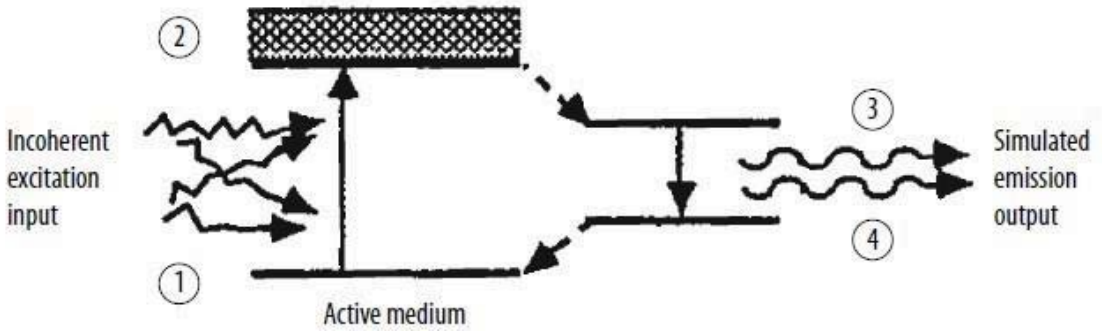

Figure 3. 1 Basic components of a laser construction, from (Steen and Mazumder, 2010)

3.2 Evolution of laser application in automotive industry

After laser came into being, it has been widely used in automotive industry. Figure 3. 2 gives a chronological record of laser application in automotive industry. It could be seen that laser was initially used in welding tailored blank butt and roof panel in proximity. PLW, operated closely to the workpiece due to its short focal length and beam quality (Higuchi, 2010), added the risk of scanner collision and contamination. RLW with stand-off more than 1 meter, came into being around 2006. It not only reduced the risk of collision and contamination but also significantly improved flexibility and productivity. This is why RLW is considered as a promising emerging technology, though more studies should be carried out to maturate the application of it in industry.

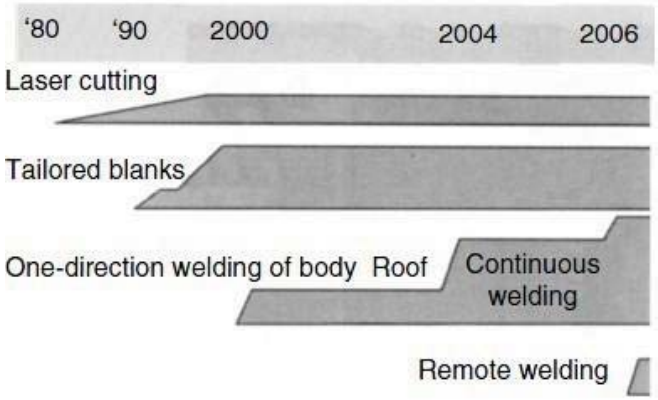

Figure 3. 2 Laser application development for automotive industry, from (Mori et al., 2010)

3.3 Working principles of RLW

RLW system normally integrates a commercial robotic arm, a 3D scanner, control system and laser source. Figure 3. 3 illustrates a robot and a scanner that are controlled by a PC-based controller. RLW can significantly reduce positioning time by application of 3D scanner, which helps to increase the productivity of the system. In addition, thanks to the long focal length and application of 3D scanner, RLW system extends the stand-off distance from the workpiece and enables welding evolved from merely two dimensions operation to three dimensions operation and becomes able to weld more complicated parts in space than merely simple parts such as roof panels. By this way, the flexibility is also significantly increased.

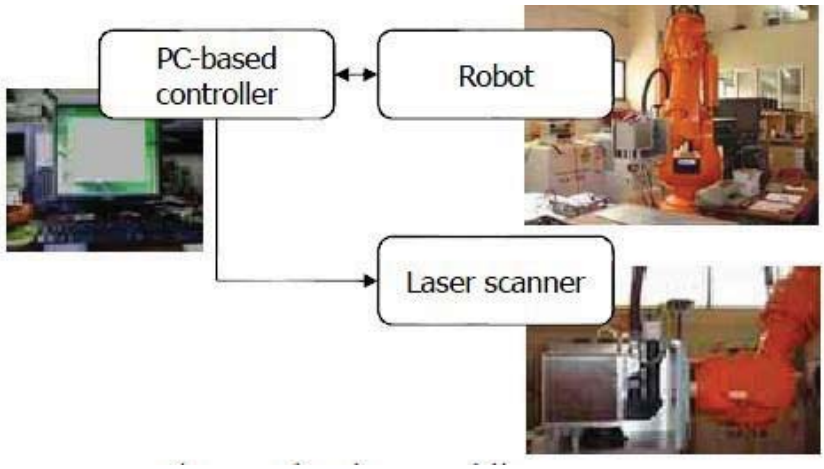

Figure 3. 3 An example of RLW system (adapted from (Kang et al., 2011))

Compared to conventional PLW, RLW is restricted to deliver process media like gases or metal fillers to the welding interaction zone (Grupp et al., 2003). Shielding gas could only be supplied independent of laser beam. One possibility is to integrate the gas supply nozzles into the clamping devices. With numerous welding stitches, the expenditure of this solution increases significantly. As shielding gases are usually very expensive, compressed air is often alternatively chosen to eliminate the effects of plasma (Grupp et al., 2003). (Grupp et al., 2003) also concluded when the system power is under 3kW, conrresponding to power density of $1.5 * 10^6$ W/cm^2, the weld depth (penetration) is not affected by the shielding gas. Figure 3. 4 summarizes the above mentioned phenomenon. When power density is over $1.5 * 10^6$ W/cm^2, helium plays a better role than argon in suppressing the effect of plasma.

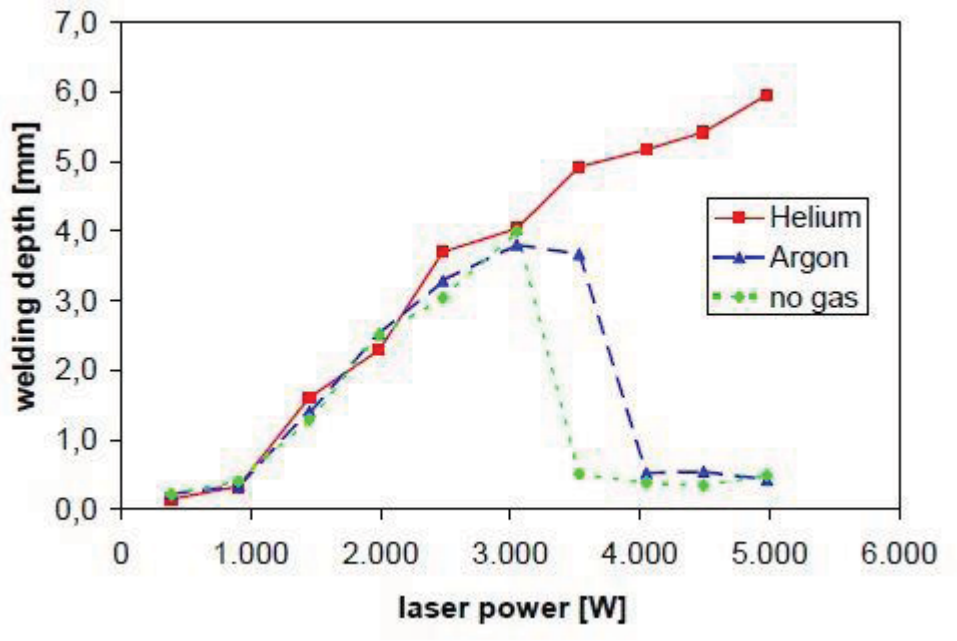

Figure 3. 4 Plasma shielding at high laser power [0.5, 6] kW; speed= 2m/min, mild steel, from Grupp et al., 2003

3.4 Conduction-limited vs Keyhole wleding

There are mainly two types of welding mechanism: conduction-limited welding (Figure 3. 5) and keyhole welding (Figure 3. 6). The former occurs when the power density is insufficient to boil the material in the weld pool. The latter provides sufficient energy per unit length to create vaporization in the weld pool and in consequence a stable hole occurs. The keyhole behaves like an optical black body in which the radiation enters and it is subjected to multiple reflections, as a result high percentage of energy is absorbed (Steen and Mazumder, 2010).

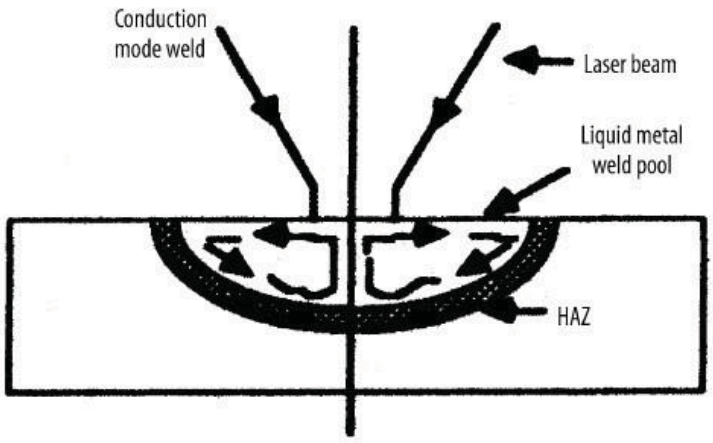

Figure 3. 5 Conduction welding mode, from (Steen and Mazumder, 2010)

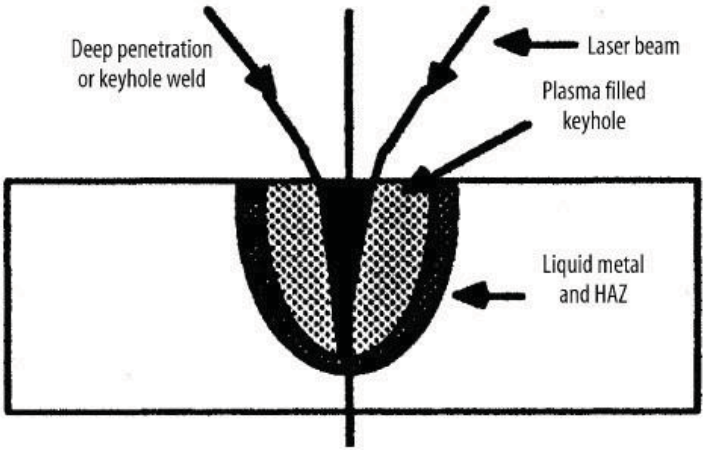

Figure 3. 6 Keyhole welding mode, from (Steen and Mazumder, 2010)

3.5 Zinc degassing solutions

In the occasion of laser welding galvanized steel, as described previously, due to the characteristic that the boiling temperature of zinc (906 °C) is much lower than the melting temperature of steel (1530 °C), zinc has already turned into vapour while steel is being heated up. There is high risk of expulsion of the weld metal (spatter) and considerable surface porosity and entrapped porosity in the weld joint if the gap is insufficient for the zinc vapour to exhaust (Zhao et al., 2012, Sinha et al., 2013, Bley et al., 2007, Chen et al., 2009, Fabbro et al., 2006, Schmidt et al., 2008, Yih-fong, 2006). Another problem induced by this zinc coating described by (Chen et al., 2009) is that Zinc gives rise to strongly ionized plasma and it affects the absorption and scattering of incident radiation and prevents the beam propagation through it, which results in penetration reduction, as well as seam discontinuity and seam narrowing.

A great many studies have discussed this problem and proposed solutions. U.S. Patent 3969604 proposed a way of adding additional elements to the surface which form a compound with the vaporized zinc (Baardsen, 1975). U.S. Patent 4642446 recommended to remove the zinc coating in the welding area and to replace it with a metal with higher boiling point like nickel (Pennington, 1987). U.S. Patent 4691093 used a dual focus beam to elongate the keyhole (Banas and Doyle, 1987). U.S. Patent 6740845 used oscillated laser beam along or transverse the weld seam (Stol and Martukanitz, 2004). (Schmidt et al., 2008) used fast frequency modulation of the laser power to join galvanized steel. (Chen et al., 2009) used vent holes which allowed zinc vapours to escape to solve this problem. U.S. Patent 5183992 suggested the sheets were positioned vertically, so that the gravitation force helps to

solve the problem (Bilge et al., 1993). According to U.S. Patent 4745257, this gap can be produced by loose contact or spacers (Rito et al., 1988). U.S. Patent 4916248 used pre-stamped projection technique to create V-shape tabs in the lower part which acts as the required clearance (Petrick, 1990). (Colombo et al., 2012) proposed dimplings technique which could be created by the pulsed laser believed had an advantage over others because of its industrial practicability.

In summary, the solutions could be mainly classified into three directions. One direction focused on creating clearance, another one focused on adjusting laser beam, and the other one concentrated on changing the property of zinc.

Auto industry's favourite solution is the creation of a gap between the to-be-welded sheets. Nowadays, in automotive industry, usually shims (difficult to control the consistency) or dimples (more realistic and under further investigation) are used to obtain an appropriate gap. (Steen and Mazumder, 2010) claimed the calculation of the gap size by physical and mathematical deduction. Equation 3. 1 is the theoretical conclusion. Figure 3. 7 is the schematic picture of laser welding zinc-coated steel with a small gap between the sheets for exhausting of the high-pressure zinc vapour. The conclusion of this study is that when the gap is less than 40% of upper thickness, it is possible to produce sound weld free from defects such as spatters and pitting.

Figure 3. 8 visually displays how this conclusion is referred.

Equation 3.1

$$2B\beta\Delta T \gg \frac{g}{t} \gg \frac{kVt_{zn}}{t^{\frac{3}{2}}}$$

Where

g: part –to-part gap

t: upper sheet thickness

k: a constant related to material properties

V: welding speed

B: a constant related to material properties, for galvanized mild steel B=1

β: coefficient of thermal expansion

ΔT: temperature change

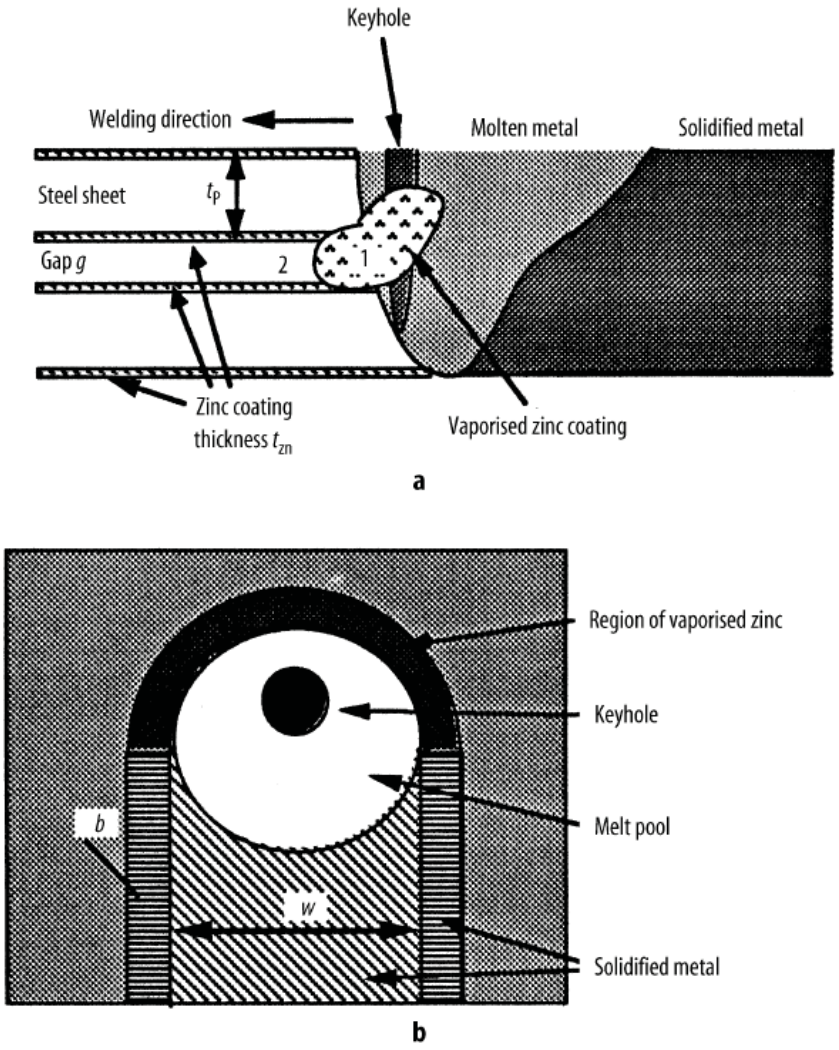

Figure 3. 7 Schematic picture of laser welding zinc-coated steel with a small gap between the sheets for exhausting of the high-pressure zinc vapour: a. side view, and b. top view (excerpted from Steen and Mazumder (2010))

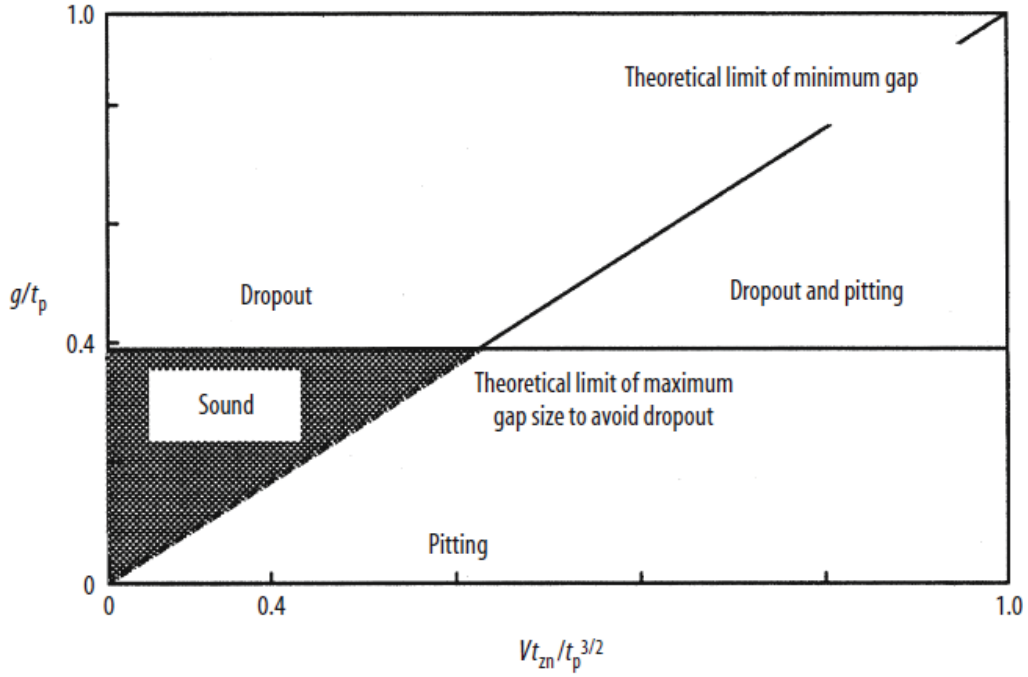

Figure 3. 8 Operational diagram for the welding of zinc-coated mild steel with a gap for zinc vapour exhaust (excerpted from Steen and Mazumder (2010))

In this study, the direction of creating an appropriate gap is chosen to avoid zinc vaporization. A fixture is specially designed to control the accuracy and consistency the gap to ensure the research quality.

3.6 Process modelling and optimization

(Benyounis and Olabi, 2008) wrote a comprehensive reference guide about modelling and optimization using statistical and numerical approaches of different welding processes by 2008. According to this review, welding input parameters play a significant role in determining the quality of a weld joints.

Design of experiments (DoE), evolutionary algorithms and computational network are widely used to develop mathematical relationship between the welding process input parameters and the output variables of the weld joint in order to determine the welding input parameters that lead to the desired weld quality (Benyounis and Olabi, 2008).

A comprehensive literature review of application of these methods in laser welding will be classified according to methodologies used to develop aforementioned correlations, i.e. Response Surface Methodology (RSM), Artificial Neural Network (ANN), Taguchi methods and other techniques.

RSM

(Benyounis et al., 2005b) has constructed empirical models using response surface methodology to predict heat input, penetration, welded zone width and heat affected zone width under differing laser power, welding speed and focal point position. A continuous 1.5 kW CO_2 laser was used to butt weld medium carbon steel. Box-Behnken design with full replicates was favoured as the experimental designing strategy. This investigation came to the conclusions that Box-Ben design worked well and the models developed could predict well which was demonstrated by confirmation experiments. Furthermore, welding speed has a negative effect on all the responses, whereas the laser power has positive effect. With the focused point going in the metal, the penetration significantly reduces and the HAZ width slightly reduces too, but weld width oppositely increases. They also found that heat input plays an important role in the weld-bead parameters dimension. Later on, based on the built model, (Benyounis et al., 2005a) optimized the process with the purposes of maximizing the penetration, minimizing the heat input, width of welded zone and

width of heat affected zone with the aid of both numerical and graphical optimization in design-expert software. They found in this research corresponding optimum process parameters are achievable, and full-depth penetration has a strong effect on the other bead parameters of interest.

(Manonmani et al., 2007) used a 2 kW solid state Nd:YAG laser to butt weld 2.5 mm thick AISI 304 stainless steel plate. Central Composite Design (CCD) was chosen to identify the trials. Beam power, welding speed and beam angle were related to depth of penetration, bead width and area of penetration. This investigation shows CCD is an easy tool to be used to analyse the process parameters on response. Beam power has a positive effect on all the response variables however beam angle and welding speed vice versa. Furthermore, it is also found there is small variation in weld width, which enlightens that weld width is not much affected by the input variables.

(Padmanaban and Balasubramanian, 2010) studied the influence of laser power, welding speed and focal position on the tensile strength of AZ31B magnesium alloy after being welded by a CO_2 laser in butt welding configuration. Thirty-three central composite face centred design with full replicates was selected. The results indicate the welding speed has the greatest influence on the tensile strength, followed by laser power and focal position. In addition, maximum tensile strength is obtained under the optimal process variable.

(Rizzi et al., 2011) investigated spectroscopic signals originated by the laser-induced plasma optical emission, energetic and metallographic characteristics of 2.5 kW CO_2 laser welded stainless steel lap joints simultaneously using RSM. Clear correlations between laser beam power, laser welding speed and response parameters: plasma plume temperature, joint penetration depth and melted area have been established.

The regression models could be a valuable starting point to develop a closed loop control of the responses within process window. Laser power was found to be the most influential variable. When the power is increased or welding speed is lowered, the penetration and melted area increase, on the contrary, the plasma temperature goes the opposite direction.

(Khan et al., 2011) related welding parameters (i.e. laser power, welding speed and focal position) to each of the weld characteristics (i.e. weld width, weld penetration depth, resistance length and shearing force) of a lap joint configuration of martensitic AISI 440FSe and AISI 416 stainless steels. The laser used is a CW 1.5 kW Nd:YAG. Full factorial design was applied in this study. Numerical and graphical methods are both applied to optimize the process based on the models obtained by RSM. Laser power and welding speed are concluded to be the most important factors affecting the weld bead geometry as well as shearing force. Fibre diameter has little effect on weld bead profile and shearing force. However, its interactions with others affect a great deal. Graphical optimization results were claimed to be quicker search of optimum. Strong and efficient weld joints could be obtained using the parameters from numerical optimization algorithm.

(Zhao et al., 2012) worked on rather thin-gauge galvanized steel with thickness of 0.4 mm in a lap joint configuration. They studies the effects laser power, speed, gap and defocus could bring to the weld width, weld penetration and concavity of the weld bead profile. The laser is an IPG YLR-1500 ytterbium 1.5 kW continuous mode laser. Uniform design was selected when designing experiments. The optimized process with the aim of max aspect radio, penetration divided by weld width.

Verification tests show positive feedback that weld joints with right quality were achieved under the setting of the optimal parameters.

Artificial neural network

(Vitek et al., 1998) have developed a model to predict the correlations between the controllable variables and the weld pool shape (penetration depth, width, half-width and total area) in the configuration of pulsed Nd:YAG laser welding of Al-alloy 5754. Neural network was chosen as the modelling methodology. The controllable parameters were travel speed, average power, pulse energy and pulse duration. They developed a routine to convert the shape parameters into a predicted weld profile which was based on the actual experimental weld profile data. This approach to predicting weld pool shapes allows for an instantaneous prediction of weld pool shape and therefore offers advantages in application where real-time predictions are needed and computationally intensive predictions are too slow.

(Jeng et al., 2000) have used both back propagation (BP) and learning vector quantization (LVQ) networks to relate work piece thickness, welding gap, power, speed and focal position to weld width, undercut and weld distortion in a butt joint configuration. Both these two techniques were proved to be successful in making predictions. The models are quite useful in selecting suitable welding parameters and avoiding inappropriate welding design. Limitations in the industrial application of laser welding for butt joints were removed by the work of this study.

Taguchi method

(Pan et al., 2005) studies the effect of Nd:YAG laser welding parameters (shielding gas type, laser energy, conveying speed, laser focus, pulse frequency and pulse shape) on the ultimate tensile strength of butt-welded thin plates of magnesium alloy using Taguchi method. The analytical results indicate that the pulse shape and the energy of the laser contributed the most. Accordingly, the optimal combination of welding parameters for this process is Argon as the shielding gas, a 360 W laser, a work piece speed of 25 mm/s, a laser focus distance of 0.0 mm, a pulse frequency of 160 Hz, and a type 3 pulse shape. The ultimate tension stress was at maximum an overlap of the welding zone of approximately 75%.

The purpose of the study by (Lee et al., 2006) is to optimize Nd:YAG laser welding parameters to seal an iodine-125 radioisotope seed into a titanium capsule. The accurate control of the melted length of the tube end was affected by the laser welding parameters (nozzle type, rotating speed, tilt angle, focal position, pumping voltage, pulse frequency, and pulse width). After being analysed and optimized by Taguchi and regression analysis method, it was found that the laser pulse width and focal position among the welding parameters had the greatest effects on the melted length. Optimal welding conditions were obtained through this study, and confirmation experiments validated this result very well.

(Olabi and Anawa, 2006) have investigated the effect of laser welding conditions on the toughness of dissimilar components. A CO_2 laser was used to weld 316 stainless steel and low carbon steel in the configuration of lap joint. Laser power, welding speed and focus position were considered as the process parameters of main effects to optimize the welding process in terms of mechanical properties. Taguchi method

was used to optimize the process. L-25 designed experiments were used. Impact strength was measured at room temperature by using universal pendulum impact tester. It was confirmed that Taguchi approach has decreased the number of experiments without negative effects on the results.

(Anawa and Olabi, 2008) have investigated ferrites (low-carbon steel)/austenitic (316 stainless steel) dissimilar lap welding joints under CO_2 laser welding using analysis of variation (ANOVA) and signal-to-noise ratio method. Laser power, welding speed, and focused position were considered as the main factors of the process. 3 factors, 5 levels L-25 orthogonal array was used as the strategy of designed experiments. Joint strength was determined using the notched-tensile strength method. Conclusions were made as following: laser power is the main factor affecting the process; the speed also has a strong negative effect on the response; however, focus position had no obvious effect on the tensile strength. The welding joints have better mechanical properties compared to the base metals. Furthermore, the models can predict adequately within the factors domain and optimal working conditions were obtained and confirmed through confirmation tests.

(Sathiya et al., 2011) have studied the correlation between input variables (i.e. shielding gases (argon, helium and nitrogen), beam power, travelling speed and focus position) and tensile strength and bead profiles (bead width and depth of penetration) with a 3.5 kW CO_2 cooled slab laser butt welding of 904 super austenitic stainless steel using Taguchi method. Taguchi approach is used as a statistical design of experiment technique for optimizing the selected welding parameters. Grey relational analysis and the desirability approach are applied by considering multiple output

variables simultaneously. Both analyses are proved to be accurate techniques to optimize the laser welding process.

Comparisons among the optimization techniques

According to (Benyounis and Olabi, 2008), RSM performs better than other techniques, especially ANN and GA, when a large number of experiments are not affordable. The trend in the modelling using RSM has a low order non-linear behaviour with a regular experimental domain and relatively small factors region, due to its limitation in building a model to fit the data over an irregular experimental region. Moreover, the main advantage of RSM is its ability to exhibit the factor contributions from the coefficients in the regression model. This ability is powerful in identifying the insignificant quadratic terms in the model and thereby can reduce the complexity of the problem. This technique required good definition of ranges for each factor to ensure that the response under consideration is changing in a regular manner within this range. The most popular designs within RSM designs are the central composite design (CCD) and Box-Behnken design (BBD). In regard to ANNs, it noted that ANNs perform better than other techniques, especially RSM when highly non-linear behaviour is the case. Also, this technique can build an efficient model using a small number of experiments; however the technique accuracy would be better when a larger number of experiments of experiments are used to develop a model. The ANN model itself provides little information about the design factors and their contribution to the response if further analysis has not been done. The most popular ANNs are learning vector quantization neural networks, back-propagation and counter-propagation networks. The Taguchi method is also one of the powerful optimization techniques which characterize with improving the product quality and

reliability at low cost. The optimization algorithm works by calculating singal-to-noise (SN) ratios for each combination and then the combination having a maximum S/N ratio is defined as the optimal setting. However, Taguchi's analysis approach of S/N ratio may lead to non-optimal solutions, less flexibility and the conduction of the needless experiments. In this study, the number of trials could be run is limited and the optimal solutions will be located within a relatively small region. Therefore, RSM is chosen as the ideal modelling algorithm and BBD experimental design is sufficient for this purpose. and methods used.

Table 3. 1 represents comparisons among those common modelling/optimizing techniques for laser welding. Table 3. 2 classifies all the aforementioned works into several groups based on different methods used and various characteristics of interest. Table 3. 3 provides detailed information about laser sources, material types, process parameters of interest, performance characteristics of interest, and methods used.

Table 3. 1 Comparison among the common modelling/optimizing techniques for laser welding (adapted fromBenyounis and Olabi (2008))

	RSM	ANNs	Taguchi
Computational time	Short	Long	Medium
Experimental domain	Regular only	Regular or irregular	Regular and irregular
Model developing	Yes	Yes	No

Optimization	Through model	Through model	Straight
Understanding	Easy	Moderate	Normal
Availability in software	Available	Available	Available
Optimization accuracy level	Very high	High	Normal
Application	Frequency	Frequently	Rarely

Table 3. 2 Summary of all the mentioned studies of modelling and optimizing for laser welding

	RSM	**Artificial neural network**	**Taguchi methods**
Weld-bead geometry	(Benyounis et al. (2005b), Benyounis et al. (2005a)) Manonmani et al. (2007) Rizzi et al. (2011) Khan et al. (2011) Zhao et al. (2012)	Vitek et al. (1998) Jeng et al. (2000)	Sathiya et al. (2011)
Mechanical properties	Padmanaban and Balasubramanian (2010) Khan et al. (2011)		Lee et al. (2006) Pan et al. (2005) Sathiya et al. (2011) Anawa and Olabi (2008) Olabi and Anawa (2006)

Table 3. 3 Summary of detailed information of the studies for modelling and optimizing of laser welding

	Laser type	Materials	Weld configuration	Input variables	Output variables	Methods
Manonmani et al. (2007)	CW 2 kW solid state Nd:YAG laser	2.5 mm austenitic stainless steel 304 sheet	Butt joint	Laser beam power [580, 750, 1000, 1250, 1420] Welding speed [580,750, 1000, 1250, 1420] Incident angle [82, 85,90,95, 98] (Shielding gas constant)	Penetration depth Bead width Penetration area	RSM (CCD)
(Benyounis et al. (2005b), Benyounis et al. (2005a))	CW 1.5 kW CO_2 laser	Medium carbon steel	Butt joint	Laser power [1200,1312, 1430] Weld speed [300, 500, 700] Focal point position [-2.5, -1.25, 0]	Penetration Weld zone width Heat affected zone width	RSM (BBD)

Rizzi et al. (2011)	CW 2.5 kW CO_2 laser	Stainless steel	Lap joint	Laser power [900, 1200, 1500] Welding speed [2400, 3000, 3600]	Plasma plume electron temperature Joint penetration Melt area	RSM (full factorial design)
Padmanaban and Balasubramanian (2010)	CW CO_2 laser	AZ31B magnesium alloy	Butt joint	Laser power [2500,3000, 3500] Welding speed [4500, 5000, 5500] Focal position [0,-1.5, -3]	Tensile strength	RSM (CCF-central composite face centered)
Khan et al. (2011)	CW1.5kW Nd:YAG laser	Martensitic AISI 440FSe and AISI 416 stainless steels	Lap joint	Laser power [800, 950, 1100] Welding speed [4500,6000,7500] Fiber diameter [300,-,400]	Weld width Penetration Resistance width Shearing force	RSM (FFD-full factorial design)
Zhao et al. (2012)	CW 1.5 kW ytterbium-doped fibre	0.4 mm galvanized	Lap joint	Laser power [550, 600, 650]	Weld depth	RSM (uniform design matrix)

	laser	SAE1004 steel		Welding speed [180, 210, 240] Prescribed gap [0.1, 0.15, 0.2] Defocus amount [0, -0.1, -0.2]	Weld width Concave	
Vitek et al. (1998)	Autogenous pulsed Nd:YAG laser	3 mm Aluminium alloy 5754 2mm alloy 6111	Plate test	Average power Weld speed Pulse energy Pulse duration	Penetration depth Top surface width Half-width Experimental weld profile	ANN
Jeng et al. (2000)			Butt joint	Work piece thickness Power Speed Focal position	Weld distortion Weld width undercut	ANN

				Gap		
Lee et al. (2006)	Pulse-pumped Nd:YAG laser	Titanium		Nozzle type Rotating speed Tilt angle Focal position Pumping voltage Pulse frequency Pulse width	Melted length	Taguchi method (orthogonal array)
Pan et al. (2005)	Pulsed 500W Nd:YAG laser	Magnesium alloy AZ31B	Butt joint	Shielding gas Laser energy Conveying speed Laser focus position Pulse frequency Pulse shap	Ultimate tension strength	Taguchi method (orthogonal array)

Sathiya et al. (2011)	3.5 kW cooled slab laser	Austenitic stainless steel AISI 904 SASS	Butt joint	Beam power Travelling speed Focal position Shielding gas(Argon, Nitrogen, Helium)	Bead width Depth of penetration Tensile strength	Taguchi method (3^3 full factorial design)
Anawa and Olabi (2008)	1.5 kW CO_2 laser	Ferritic(middle carbon mild steel) to austenitic(AISI 316 stainless steel)	Lap joint	Laser power Weld speed Focal position	Notched-tensile strength	Taguchi method (L-25 orthogonal array)
Olabi and Anawa (2006)	1.5 kW CO_2 laser	Ferritic(middle carbon mild steel) to austenitic(AISI 316 stainless steel)	Lap joint	Laser power Weld speed Focal position	Toughness Impact strength	Taguchi method (L-25 orthogonal array)

4. Methodologies

The goal of this study is to firstly figure out the process window within which weld joints free from visible defects and fulfilling requirements of weld joint geometry could be produced. Secondly, within the known process window, optimal welding condition could be identified where weld joints could be produced with "right" quality, least welding time and power consumption. Table 4. 1 lists out all the stack-ups of interest. The roadmap of achieving the goals is proposed in the following paragraph.

4.1 Problem-solving roadmap

Materials are welded in the configuration of lap joint. It could be seen that the four stack-ups share the same upper material but lower materials are different. According to EN10327 2004.6, the materials with different designations have same chemical composition but slightly different mechanical property. The significant difference among them is the lower thickness.

Table 4. 1 Stack-ups of case study

Stack-up	Upper material designation	Upper thickness	Lower material designation	Lower thickness
SU1	DX56D+Z	0.75 mm	DX52D+Z	1.00 mm
SU2	DX56D+Z	0.75 mm	DX54D+Z	1.8 mm
SU3	DX56D+Z	0.75 mm	DX54D+Z	1.00 mm

SU4	DX56D+Z	0.75 mm	DX53D+Z	0.70 mm

Figure 4. 1 illustrates the roadmap of achieving the goals. Firstly factors affecting the RLW process in the circumstance of welding galvanized steel are identified. In this step, fishbone diagram is used to analyse all potential factors systematically. After the factors of interest are selected, process window within which weld joints fulfilling all requirements could be produced is preliminarily specified using One-Factor-at-a-Time method. In the third step, statistical comparison analysis between SU2 and SU3 is carried out to check whether the lower thickness is significantly affecting the process. The assumption is if the influence is insignificant and negligible, modelling for four stack-ups could be simplified to only the stack-up with thickest lower material assuming the other three stack-ups share the model. In this case, the overall number of experiments could be significantly reduced. Otherwise, experimentation campaign needs to be repeated four times. Finally, optimization is performed on obtained models as the termination of the roadmap.

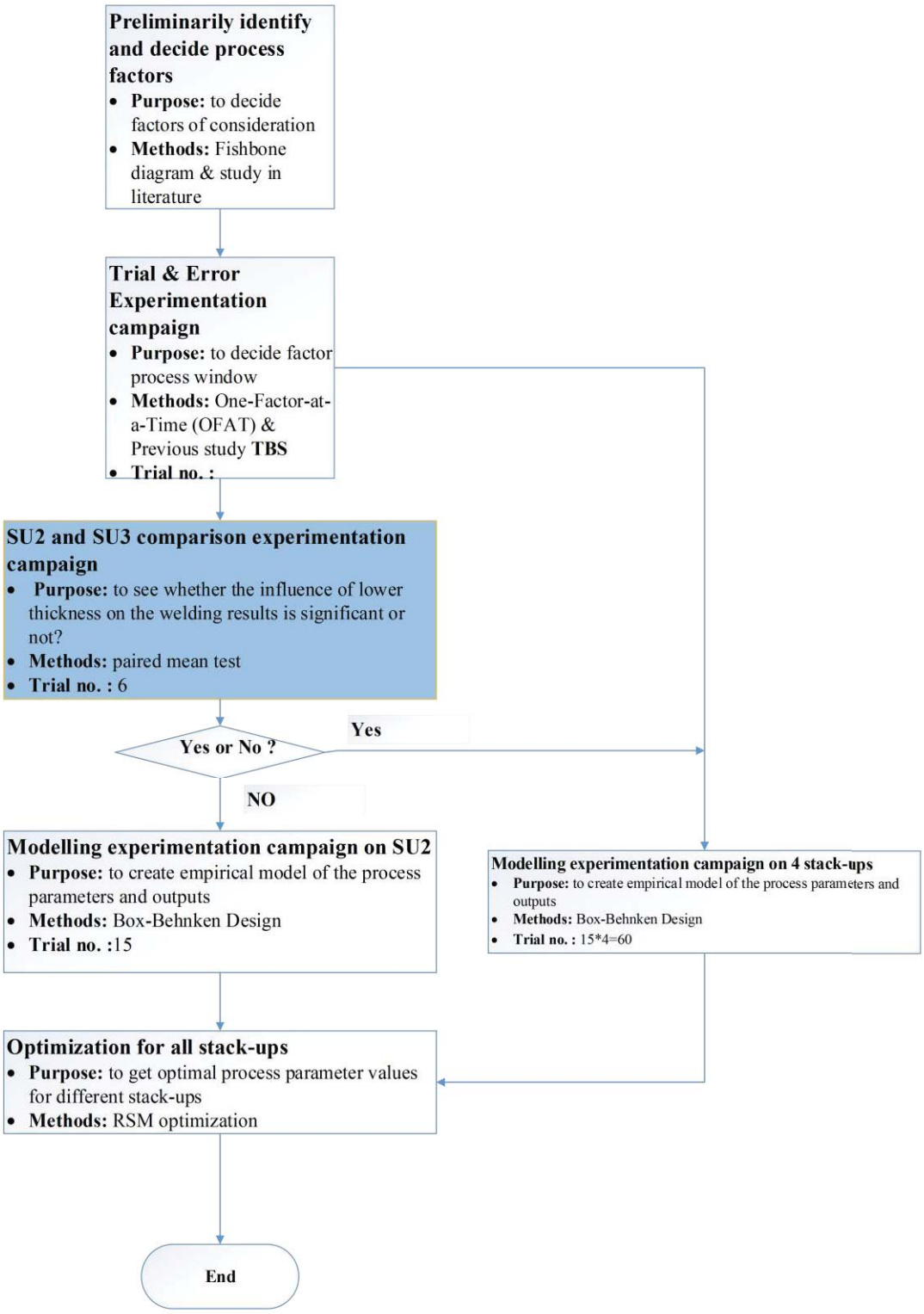

Figure 4. 1 Roadmap for achieving research objectives of this study

4.2 Identification of process factors

The process of laser welding galvanized steel is quite complicated with numerous factors affecting the outcomes. The controllable factors of interest should be identified and analysed how they are influencing the output, while the uncontrollable ones shall be kept as constants. (Steen and Mazumder, 2010) proposed all the factors that should be considered for a laser welding process are listed in Figure 4. 2.

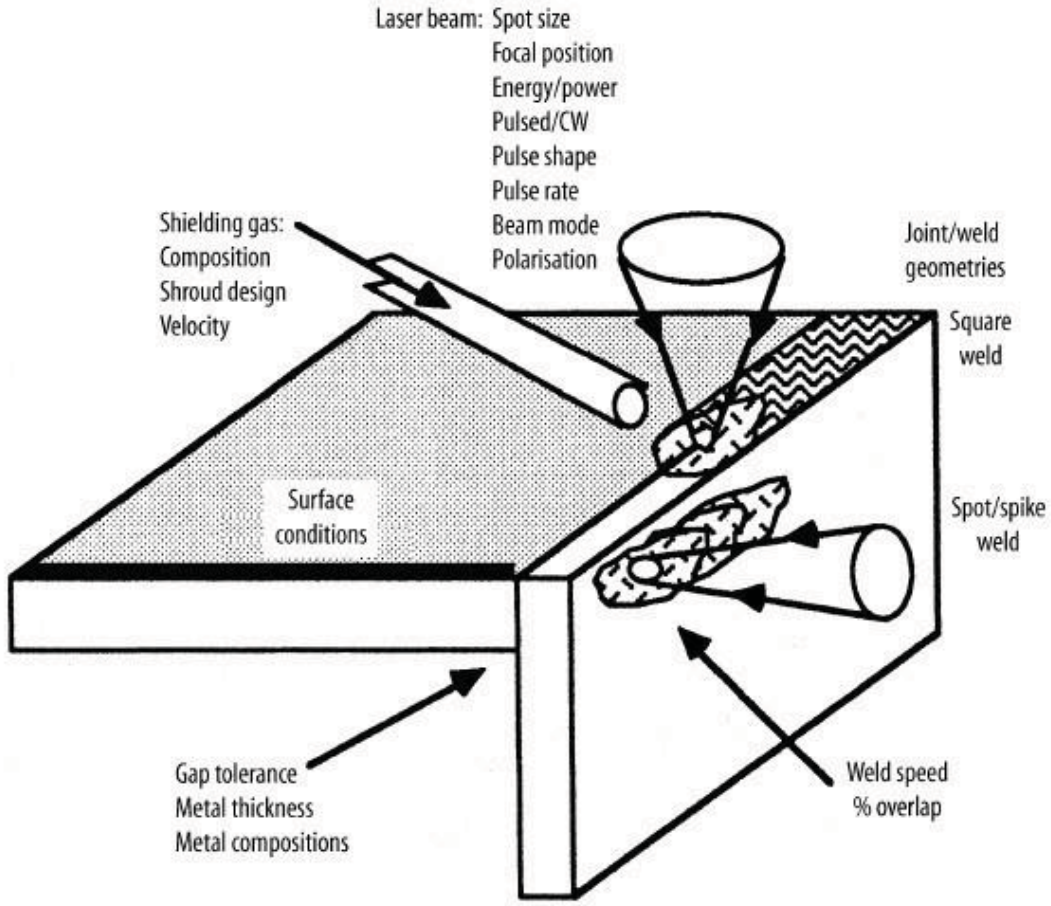

Figure 4. 2 All the needed to be considered process parameters for a laser welding systems, adapted from (Steen and Mazumder, 2010)

Laser beam

- Spot size: the nominal waist diameter of laser beam is 600 μm
- Focal position, the distance from focal point to material surface: the defocus is programmed to be 0
- Power: this is a controllable factor of interest
- Laser mode: Continuous Wave

Other process parameters

- Gap: this is a controllable factor of interest
- Incident angle: programmed to be perpendicular to the surface, but how the programming is done is not clear.
- Speed: this is a controllable factor of interest
- Material thickness: as listed in Table 4. 1
- Material compositions: further investigated in Chapter 5
- Shielding gas: no shielding gas, instead compressed air is used
- Weld geometry: lap joint configuration
- Surface condition: no surface treatment applied to simulate the real situation

- Environment: Warwick manufacturing centre, autumn, room temperature, no specific control of humidity

4.3 Methodology for process window identification

The factors to be further investigated are weld speed, power, and gap. The process window is screened based on the criteria that all weld joints are soundly welded free from visible defects such as spatter, cracks, cut-through and burn-through. The ranges of factors are preliminarily set as in Table 4. 2. According to TSB project, in the following ranges, all different welding behaviours could be covered, including sound weld, pitting, spatter, insufficient weld and etc.

Table 4. 2 Ranges of process factors

Factor	Type	Range	Unit
Speed	Variable	[1:12]	m/min
Power	Variable	[2:4]	kW
Gap	Variable	[0.05:0.5]	mm
Lower thickness	Variable	0.7, 1.0 and 1.8	mm

One-Factor-At-a-Time (OFAT), setting other process parameters as constant and changing merely the only chosen factor, is a simple methodology to roughly detect

the boundary of weld behaviour. The first step is to weld in the aforementioned range of process window, and then by visual inspection, the weld joints free from visible defects such as spatter, cracks, cut-through, burn-through and insufficient weld are selected out to be cross-sectioned and assessed. In the end, those weld joints fulfilling all quality standards (those standards in Chapter 2) are identified. And the process windows are decided. The whole process is described in Figure 4. 3.

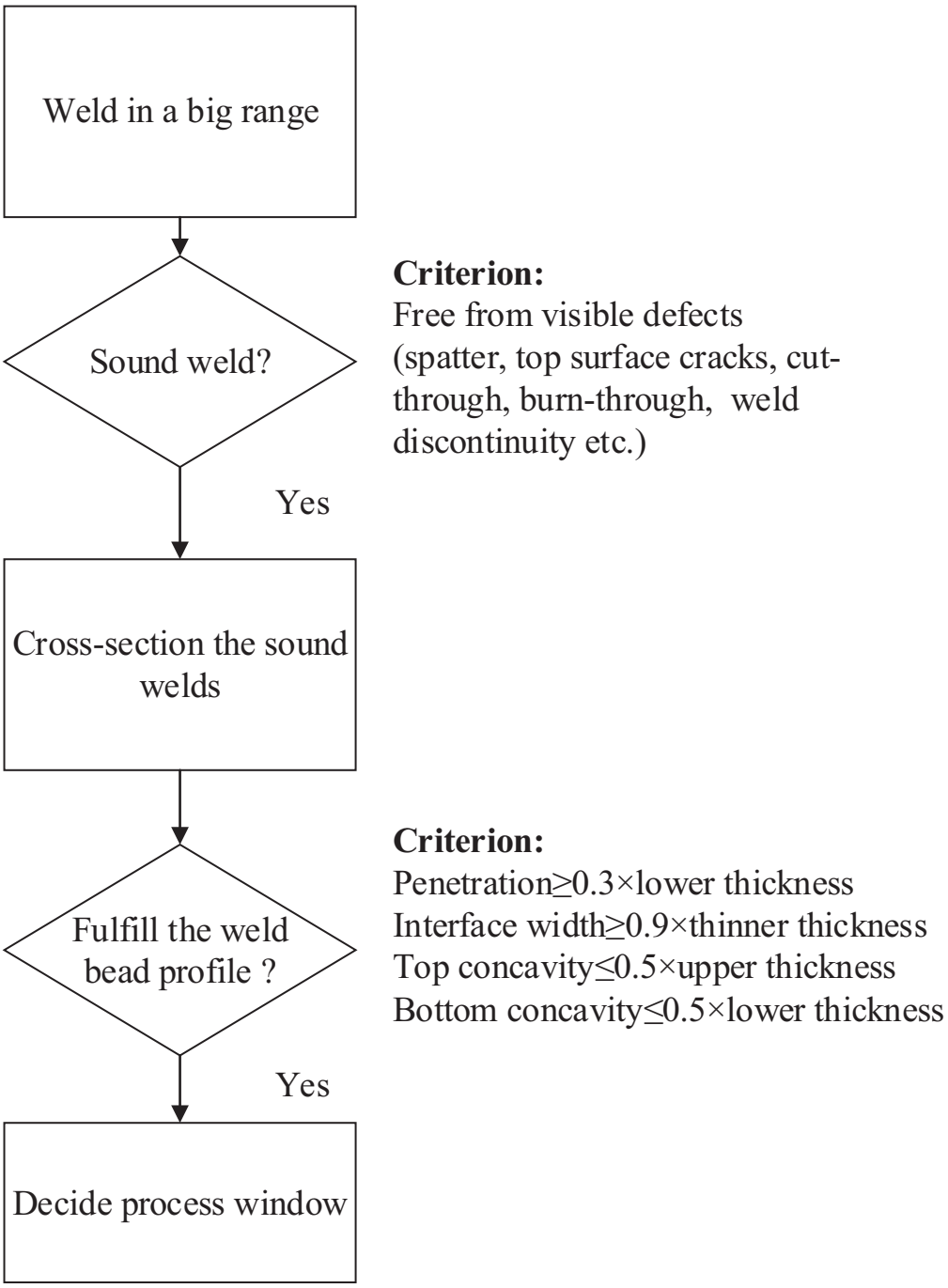

Figure 4. 3 Process to identify the process window

4.4 Paired mean test

To determine whether the lower thickness is a significant parameter to the laser welding process, paired mean test, a type of hypothesis test, is applied.

Paired mean t-test is a very useful testing technique when a comparison is needed. If the means of two groups are supposed to be same, the null hypothesis is: $H_0 : \mu_1 = \mu_2$. If it is assumed that $u_d = \mu_1 - \mu_2$, then the equivalent testing hypothesis is

$$H_0 : u_d = 0$$

$$H_0 : u_d \neq 0$$

The test statistic for the above hypothesis should be:

$$t = \frac{\bar{d}}{S_d/\sqrt{n}}$$

where $\bar{d} = \frac{1}{n}\sum_{j=1}^{n} d_j$ is the sample mean of the differences between pairs and n is the sample number.

$S_d = \left[\frac{\sum_{j=1}^{n}(d_j - \bar{d})^2}{n-1}\right]^2$ is the sample deviation of the paired differences.

In this test, if $t > t_{\alpha/2, n-1}$, the null hypothesis could be rejected at the probability of α to make a type 1 error.

4.5 Response surface methodology

Experimental Design

Box-Behnken Design (BBD) is chosen as the experimental design of this study. It is an efficient three-level design for fitting second order models based on balanced incomplete block designs, first developed by Box and Behnken in 1950. To illustrate the basic idea of BBD, let us assume the total number of process parameters is k. In BBD, factors are paired together, that is, in total k*(k-1)/2 pairs. Each pair is lined with a 2^2 factorial design, while the (k-2) factors remain in the centre. If the number of runs with all the process parameters in centre is denoted as n_c, then the total run of a BBD design with k parameters is $2k*(k-1)+n_c$. For instance, if k=3, then at least $12+n_c$ runs are needed. In Figure 4. 4, it graphically show the scattering structure of three factors three levels BBD. Usually in a BBD, in order to be efficient and reduce the number of trials, only the centre points are replicated for several times. Replicated centre points are very crucial for pure error and lack-of-fit analysis. When BBD is applied, it is assumed phase zero of factor screening and phase one of steepest ascent/descent with factorial design have been conducted and the region of experimentation contains the optimum.

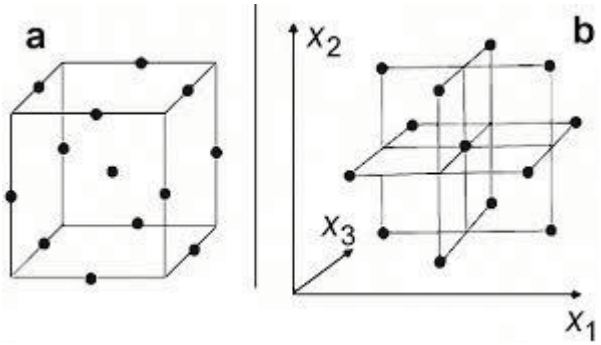

Figure 4. 4 Three factor three level Box-Behnken Design

Building empirical models

After obtaining the data from experimentation, the next stage is to build empirical models using the data. Generally speaking, the response variable y could be related to the k process parameters as the following, if there is linear correlation between them:

$$y = \beta_0 + \beta_1 x_1 + \beta_2 x_2 + \cdots + \beta_k x_k + \varepsilon$$

This model is called multiple linear regression model with k parameters, the $\beta_j, j = 0,1, \ldots, k$, are called regression coefficients.

However, sometimes the correlation could be much more complex. Thus second-order polynomial is chosen as a very good model to depict non-linear relationships. The second-order response surface with k=2process parameters, could be denoted as the following equation:

$$y = \beta_0 + \beta_1 x_1 + \beta_2 x_2 + \beta_{11} x_1^2 + \beta_{22} x_2^2 + \beta_{12} x_1 x_2 + \varepsilon$$

Seemingly the second-order model is different from the first order on and could be much hard to deal with and calculate the coefficient. However, if we let $x_3 = x_1^2, x_4 = x_2^2, x_5 = x_1 x_2, \beta_3 = \beta_{11}, \beta_4 = \beta_{22}$ and $\beta_5 = \beta_{12}$, then the model could be transformed into multiple linear regression model as well. That is,

$$y = \beta_0 + \beta_1 x_1 + \beta_2 x_2 + \beta_3 x_3 + \beta_4 x_4 + \beta_5 x_5 + \varepsilon$$

By doing so, first-order and second-order analysis are transformed into one mathematical problem. In order to estimate the coefficients of a model like above, the least square method is typically used. The purpose of it is to minimize the squares

of the errors between the observations and the predictions by the model. The observations could be denoted as

$$y_i = \beta_0 + \sum_{j=1}^{k} \beta_j x_{ij} + \varepsilon_i, i = 1,2, \dots n$$

Then the least squares function is

$$L = \sum_{i=1}^{n} \varepsilon_i^2$$

$$= \sum_{i=1}^{n} (y_i - \beta_0 - \sum_{j=1}^{k} \beta_j x_{ij})^2$$

The objective is to find a set of β's that minimizes the L function. Mathematically to do so, the first derivative of the equation should be equal to zero at the same time with the set of β's. That is,

$$\frac{\partial L}{\partial \beta_0} |_{b_0, b_1, \dots, b_k} = -2 \sum_{i=1}^{n} (y_i - b_0 - \sum_{j=1}^{k} b_j x_{ij}) = 0$$

and

$$\frac{\partial L}{\partial \beta_0} |_{b_0, b_1, \dots, b_k} = -2 \sum_{i=1}^{n} (y_i - b_0 - \sum_{j=1}^{k} b_j x_{ij}) x_{ij} = 0$$

Where j=1,2,…k.

If the above deduction is depicted in matrix form, it is like:

$$\mathbf{Y} = \mathbf{X\beta} + \boldsymbol{\varepsilon}$$

where

$\mathbf{Y} = [y_1, y_2, .., y_n]'$; $\mathbf{X} = \begin{bmatrix} 1 & x_{11} \cdots & x_{1k} \\ \vdots & \ddots & \vdots \\ 1 & x_{n1} \cdots & x_{nk} \end{bmatrix}$, $\boldsymbol{\beta} = [\beta_1, \beta_2, .., \beta_k]'$, and $\boldsymbol{\varepsilon} = [\varepsilon_1, \varepsilon_2, .., \varepsilon_n]'$

To make sure the squared error is minimized, then

$$\frac{\partial L}{\partial \boldsymbol{\beta}}|_{\mathbf{b}} = -\mathbf{2X'y} + \mathbf{2X'Xb} = 0$$

Then it could be simplified as

$$\mathbf{X'Xb = X'y, \text{ or } b} = (\mathbf{X'X})^{-1}\mathbf{X'y}$$

This series of equations are called normal equations of the least square.

Hypothesis testing in multiple regression

After achieving the set of β's, hypothesis testing could be applied to test whether the coefficients are statistically significant. The null hypothesis in this case is that

$$H_0: b_i = 0, i = 0,1, \ldots, k$$

$$H_1: b_j \neq 0, \text{at least one } j = 0,1, \ldots, k$$

The total sum of square (SST) could be divided into two components. One component comes from the regression model (usually denoted as SSR), whereas the left component is from the residual or error. The relationship could be described as below:

$$SST=SSR+SSE$$

After the previous stage of analysis, SST, SSR and SSE could be calculated with no difficulties. But manual calculation could be very complex, that is why some sophisticated softwares are widely adopted and appreciated by both researcher and practitioners, like Design Expert, Minitab, SPSS, R or even Microsoft Excel. The reason why this division is important is that a coefficient called R squared is a very persuasive indicator to distinguish whether the model is representative of the process at all. Following equation is how to calculate it.

$$R^2 = \frac{SSR}{SST} = \frac{SST - SSE}{SST} = 1 - \frac{SSE}{SST}$$

However, certain extreme case might occur in a regression model, that is when the model goes through every trial point and no lack-of-fit is available, or in other word, the total number of the trials done is equal to the total number of coefficients in the model, so that every trial result is so fully used which neglects the factor that random error always exists in any real physical experiment. In order to cope with this problem, another statistic called adjusted R^2 is proposed and it could be a more effective coefficient in evaluating the fitness of the deduced model.

$$R^2_{adj} = 1 - \frac{SSE/(n-p)}{SST/(n-1)} = 1 - \frac{n-1}{n-p}(1-R^2)$$

Where p means the degrees of error, or p=n-k-1.

Optimization

Graphical optimization

As mentioned in the brief introduction of RSM in Chapter 2, graphical optimization is a relatively straightforward approach in the case where there are only two process parameters and several response variables. By superimposing the contour plots of response variables onto the plane of process parameters, a region fulfilling all the constraints can be usually figured out and an optimum can be found within it.

Nevertheless, it is not unusual to encounter problems with more than just two process parameters and multiple responses in which case overlay the contour plots seems inefficient in that (k-2) parameters have to be held as constant. It might sometimes work for more than two parameters problems which are usually formulated and solved as constrained optimization problem. However, in such cases, formal optimization methods are more favourable.

Numerical optimization

Usually the optimization problem is formulated as a constrained optimization one. There are several frequently used methods to solve it. These methods are referred to as nonlinear programming methods. Direct search procedure and numerical algorithms like generalized reduced gradient (GRG) method, are used to find the optimum of such multiple response optimization problems. Another useful approach to optimization responses is to use the simultaneous optimization technique called desirability functions. In Design Expert, desirability function method is included.

The general idea is to convert each response variable y_i into an individual desirability function d_i that varies within the range [0,1], namely $0 \ll d_i \leq 1$. If the response fulfils the goal, $d_i = 1$; Otherwise, $d_i = 0$. Then if there are in total m response variables, the objective is to maximize the overall desirability $D = (d_1 d_2 \dots d_m)^{1/m}$.

The response variable could have maximum goal, minimum goal or a range goal. Different goals decide the way of constructing the individual desirability functions. When the weight value r=1, the desirability function is linear; r>1 makes it more important, while 0<r<1, it is less important.

If the goal is to maximize the certain response variable, then

$$d = \begin{cases} 0, y < T \\ (\frac{y - L}{T - L})^r, L \ll y \ll T \\ 1, y > T \end{cases}$$

If the goal is to minimize the certain response variable, then

$$d = \begin{cases} 1, y < T \\ (\frac{U - y}{U - T})^r, T \ll y \ll U \\ 0, y > T \end{cases}$$

Otherwise, the target is located between the lower limit (L) and the upper limit (U), then

$$d = \begin{cases} 0, y < L \\ (\frac{y - L}{T - L})^{r_1}, L \leq y \leq T \\ (\frac{U - y}{U - T})^{r_2}, T \ll y \ll U \\ 1, y > U \end{cases}$$

In the Design-Expert software, desirability functions are applied to solve constrained optimization problem. After the ultimate function is finally formulated, direct search methods are applied to reach the optimum.

5. Experimental set-up

This chapter gives an introduction of the experimental set-up. The fixture system is introduced regarding how it is developed and why it is able to ensure consistency of the gap. Experimental materials of interest are studied in terms of mechanical property and chemical composition. Metallographic analysis specification of the welding cross-section is also outlined in the end of this chapter.

5.1 RLW system

The experiments for this study are carried out in the RLW cell of Warwick Manufacturing Centre (Figure 5. 1). The system is programed to weld 25 mm stitches with perpendicular incident angle. The defocus is programmed to be 0.

- **Spot size:** the waist diameter of laser beam is nominally 600 μm. However, during the laser calibration, it is found that the diameter of the spot size ranges from 640 μm and 660 μm no matter the focal length is in the near field or far field, as illustrated in Figure 5. 2.

Figure 5. 1 RLW system in Warwick Manufacturing Centre

Focal Length	Parameter	Power			
		1 kW	2 kW	3 kW	4 Kw
Near Field (894 mm)	Beam Profile	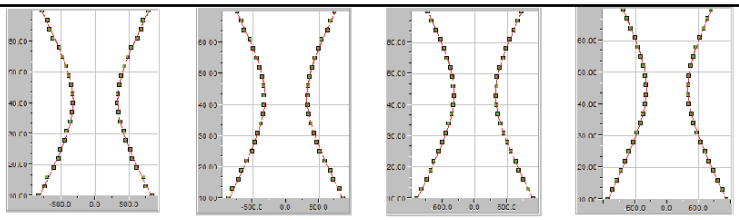			
	Power Density Distribution	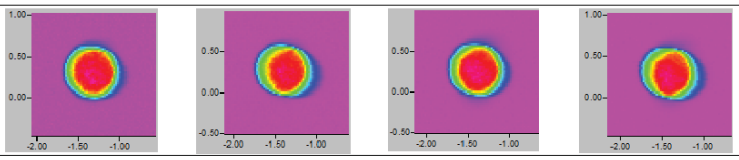			
	Beam Radius (mm)	0.328	0.321	0.323	0.325
Far Field (1216 mm)	Beam Profile	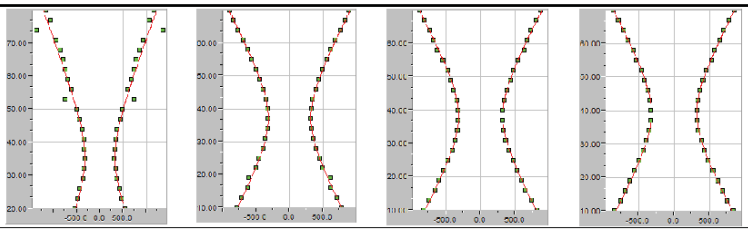			
	Power Density Distribution	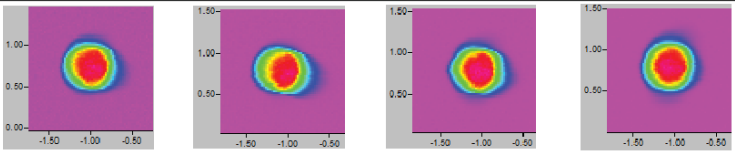			
	Beam Radius (mm)	0.327	0.319	0.321	0.322

Figure 5. 2 Laser beam quality measurement

5.2 Fixture

Fixture design contributes significantly to the repeatability of the experimentation. Therefore the fixture system of this study (in Figure 5. 3) has been designed to limit disturbing factors as much as possible. Two rectangle metals are used as clamps. The distance between these two clamps (L1) is adjustable and it can be reduced to a very small value to limit the un-flatness of the workpieces; the distance between the screws (L2) has been chosen to reduce possible curvature. In addition, the clamps are always tightened by a torque wrench precisely with the same load. Precise standardized stainless steel shims with gauges of 0.05 mm, 0.10 mm, 0.15 mm, 0.20 mm, 0.25 mm, 0.30 mm, 0.35 mm, 0.40 mm, 0.45 mm, 0.50 mm are used in this study.

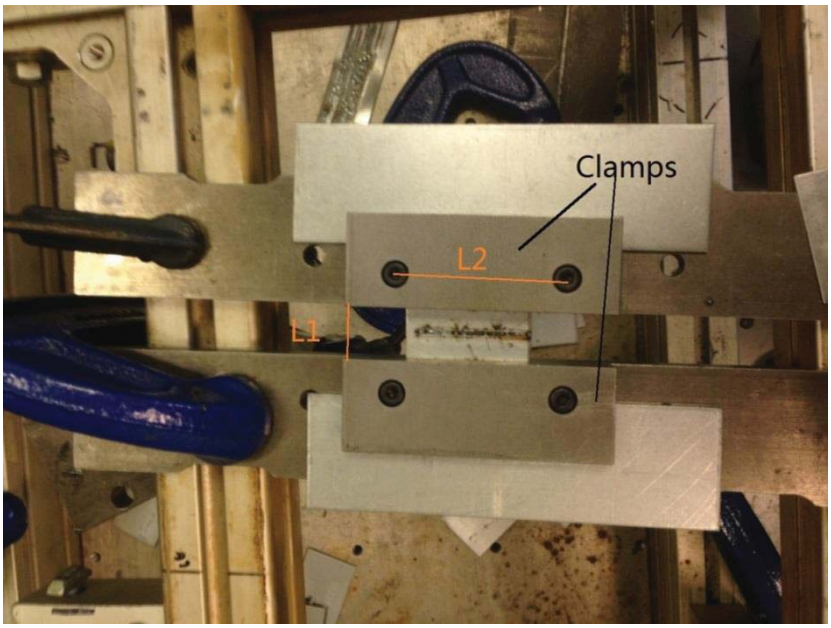

Figure 5. 3 Internal designed fixture for the study

5.3 Materials

This research problem rose from an industrial need as mentioned in Chapter 1. It is analysed and summarized that there are in total four stack-ups in terms of different material designation and thickness. There are listed for the second time in Table 5. 1.

It is found that the chemical composition of these materials is nominally same according to standards (EN 10327 2004.6). The chemical composition is as illustrated in Table 5. 2. However, the mechanical properties are slightly different （EN 10327 2004.6）. For each material, the mechanical properties are revealed respectively in Table 5. 4, Table 5. 5, Table 5. 6 and Table 5. 7.

Table 5. 1 Four stack-ups in a lap joint configuration in door L538

Stack-up	Upper material designation	Upper thickness (mm)	Lower material designation	Lower thickness (mm)
SU1	DX56D+Z	0.75	DX52D+Z	1.00
SU2	DX56D+Z	0.75	DX54D+Z	1.80
SU3	DX56D+Z	0.75	DX54D+Z	1.00
SU4	DX56D+Z	0.75	DX53D+Z	0.70

Table 5. 2 Chemical composition of DX56D+Z, DX54D+Z, DX52D+Z and DX53D+Z.

Chemical composition	**Max (%)**
C	0.12

Mn	0.6
P	0.1
S	0.045
Si	0.5
Ti	0.3

Table 5. 3 Permissible deviation of DX56D+Z, DX54D+Z, DX52D+Z and DX53D+Z

Chemical composition	Deviation (%)
C	0.02
Si	0.03
Mn	0.1
P	0.01
S	0.003
Al tot	0.1
Cr + Mo	0.05
Nb + Ti	0.02
V	0.02
B	0.001

Table 5. 4 Mechanical properties of DX56D+Z

Mechanical Properties (before galvanized)		
Strips, sheets; Uncoated; >0.7, <=3 mm	**Min**	**Max**
Yield stress (MPa)	120	180
Tensile stress (MPa)	270	350
Elongation, A (%)	39 L0=80 mm	
Strips, sheets; Uncoated; <=0.7 mm		
Yield stress (MPa)	120	180
Tensile stress (MPa)	270	350
Elongation, A (%)	37 L0=80 mm	

Table 5. 5 Mechanical properties of DX54D+Z

Mechanical Properties (before galvanized)		
Strips, sheets; Uncoated; >0.7, <=3 mm	**Min**	**Max**
Yield stress (MPa)	140	220
Tensile stress (MPa)	270	350

Elongation, A (%)	30 L0=80 mm	
Strips, sheets; Uncoated; <=0.7 mm	**Min**	**Max**
Yield stress (MPa)	140	220
Tensile stress (MPa)	270	350
Elongation, A (%)	30 L0=80 mm	

Table 5. 6 Mechanical properties of DX52D+Z

Mechanical Properties (before galvanized)		
Strips, sheets; Uncoated; >0.7, <=3 mm	**Min**	**Max**
Yield stress (MPa)	140	300
Tensile stress (MPa)	270	420
Elongation, A (%)	26 L0=80 mm	
Strips, sheets; Uncoated; <=0.7 mm	**Min**	**Max**
Yield stress (MPa)	140	300
Tensile stress (MPa)	270	420

Elongation, A (%)	24 L0=80 mm	

Table 5. 7 Mechanical properties of DX53D+Z

Mechanical Properties (before galvanized)		
Strips, sheets; Uncoated; >0.7, <=3 mm	**Min**	**Max**
Yield stress (MPa)	140	260
Tensile stress (MPa)	270	380
Elongation, A (%)	30 L0=80 mm	
Strips, sheets; Uncoated; <=0.7 mm	**Min**	**Max**
Yield stress(MPa)	140	260
Tensile stress (MPa)	270	380
Elongation, A (%)	28 L0=80 mm	

The coating of all the materials is Z100 which has the following characteristics (EN 10327 2004.6):

- Minimum total coating mass with a triple spot test is equal to 100 g/m^2 on both surface

- Minimum total coating mass with a single spot test is equal to 85 g/m^2 on both surface
- Theoretical guidance values for coating thickness per surface in the single spot test is equal to 7 µm
- Theoretical guidance values for coating range thickness per surface in the single spot test is between 5 to 12 µm
- Density is equal to 7.1 g/cm^3

To fit the material into the designed fixture, the samples have been prepared in small rectangle (25 mm × 40 mm) in Figure 5. 4. The tool used to cut the sample is the guillotine present in Warwick Manufacturing Centre. Every cut of guillotine imposes distortion to the samples and affects the final results. As mentioned in Chapter 1, in this study the appropriate gap is created by inserting two stainless steel shims between two samples as illustrated in Figure 5. 5.

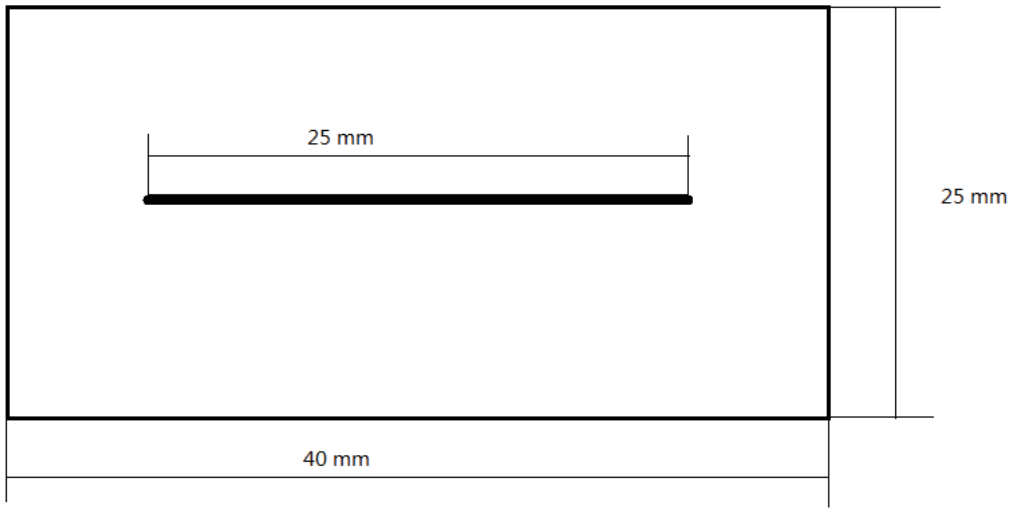

Figure 5. 4 Dimensions of a sample

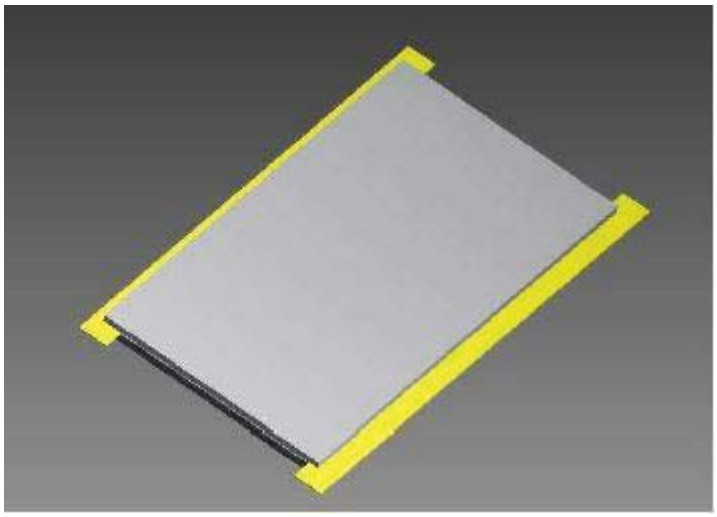

Figure 5. 5 Shims in yellow used in this study to create the gap

5.4 Metallographic analysis

After the samples are welded, top and bottom views of them are taken pictures of using a Panasonic G3 camera. Then the samples are cut into five pieces (in Figure 5. 6) using the Linear Precision Saw Buehler IsoMet 5000 as shown in Figure 5. 7. These five pieces are mounted into one Phenolic resin through the Automatic Mounting Press Buehler SimpliMet 1000 shown in Figure 5. 8. Before the acid etching, the surfaces to be analysed go through three phases of grinding and one phase of polishing using different discs on Sample Preparation System Buehler Pheonix 4000 shown in Figure 5. 9. After finishing the surface preparation, the acid etching uses a solution of 2% Nitrate for 25 seconds. Afterwards, the specimens are observed under optical microscope Leica DM 4000 M showing in Figure 5. 10 and images are captured with the help of Beuhler OmniMet Image Capturing software.

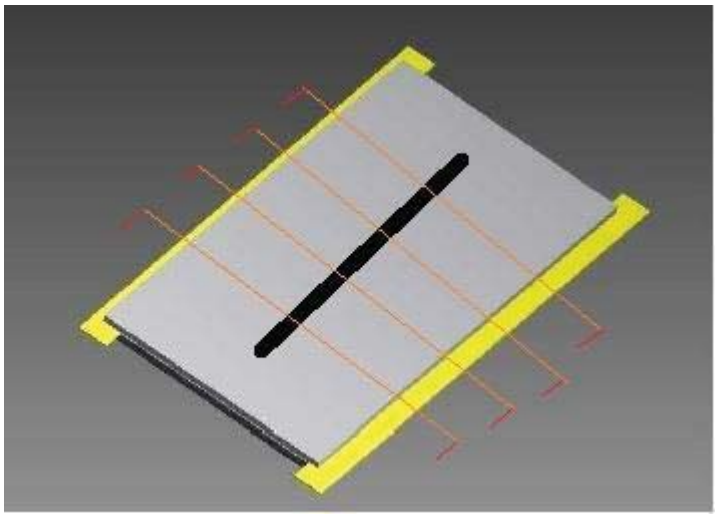

Figure 5. 6 The samples are cut into 5 pieces with equal length of 5 mm

Figure 5. 7 Linear Precision Saw Buehler IsoMet 500

Figure 5. 8 Automatic Mounting Press Buehler SimpliMet 1000

Figure 5. 9 Sample Preparation System Buehler Pheonix 4000

Figure 5. 10 Optical microscope Leica DM 4000 M

One example of sample cross-section is given in Figure 5. 11.

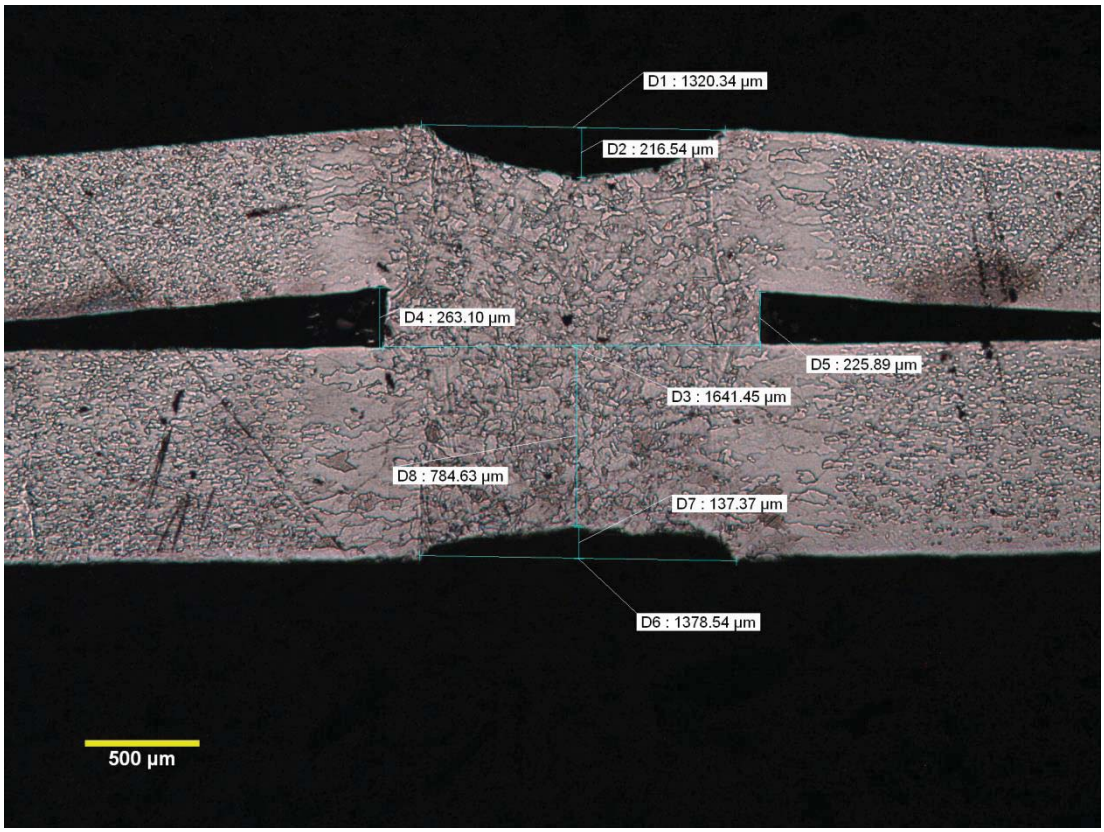

Figure 5. 11 Example of sample cross section.

The measured variables (referring to Figure 5. 12 and Figure 5. 13) are:

- Top concavity
- Interface width
- Penetration
- Bottom concavity (if applicable)

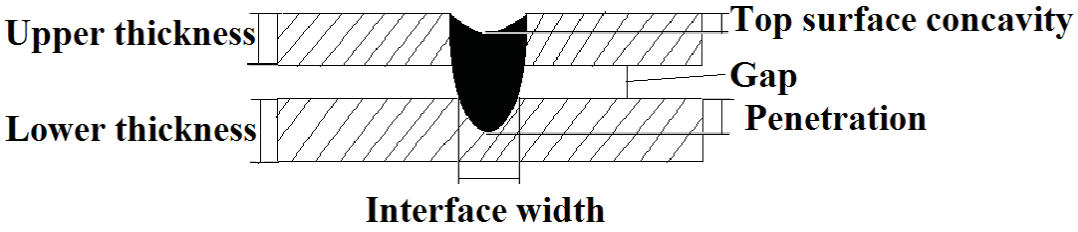

Figure 5. 12 Measured variables: top concavity, penetration, interface width and gap

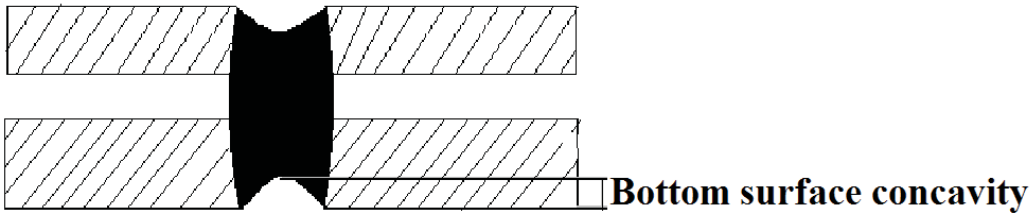

Figure 5. 13 Measured variable: bottom concavity (applicable case)

Except for penetration, it is visually clear to measure interface width, top and bottom concavity. The way how the boundary of penetration is detected is dependent on the microstructure present in the weld beam. As shown in Figure 5. 14, the welded material that has reached melting temperature displays the structure of martensite which is formed in carbon steel by quenching of austenite at such a high rate that carbon atoms do not have time to diffuse out of the crystal structure. The surrounding area that has not reached the melting temperature (namely Heat Affected Zone, HAZ) undergoes a microstructure change of crystalline grain dimension increase. The base material that is not much affected by the heat shows its own distinct microstructure. The Penetration is measured at the boundary of weld bead and HAZ as pointed out in Figure 5. 14. This detection is a subjective process by the measurer. Estimate errors

could be introduced. In order to limit the error introduced, the sample is cut into 5 pieces and all the measured variables are measured 5 times by the same measurer. The average value of these 5 measurements is used for modelling and optimization. Take the trial with speed at 3.00 m/min, power at 4 kW and gap of 0.20 mm as an instance, the cross-section displays as in Figure 5. 15 . The measured results of 5 repeats are collected (the raw data is missing). The average value of them is calculated and visualized using MATLAB and is shown in Table 5. 8, Figure 5. 16, Figure 5. 17, Figure 5. 18 and Figure 5. 19. The experimental results of Box-Behnken campaign follow the same logic of data pre-cleaning and the analytical results are attached in Appendix A and Appendix B.

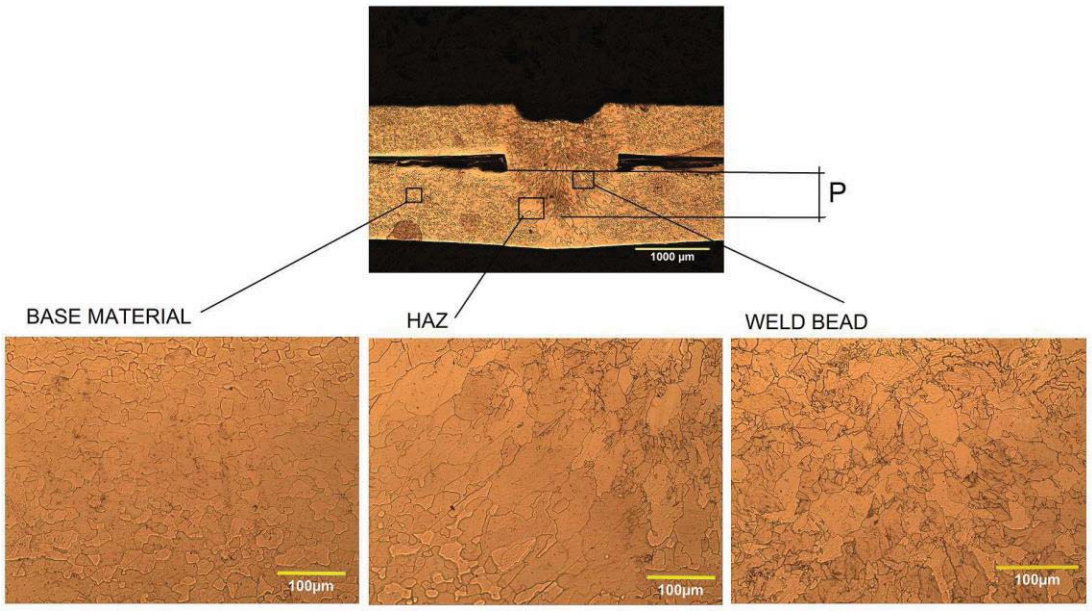

Figure 5. 14 Measurement of penetration

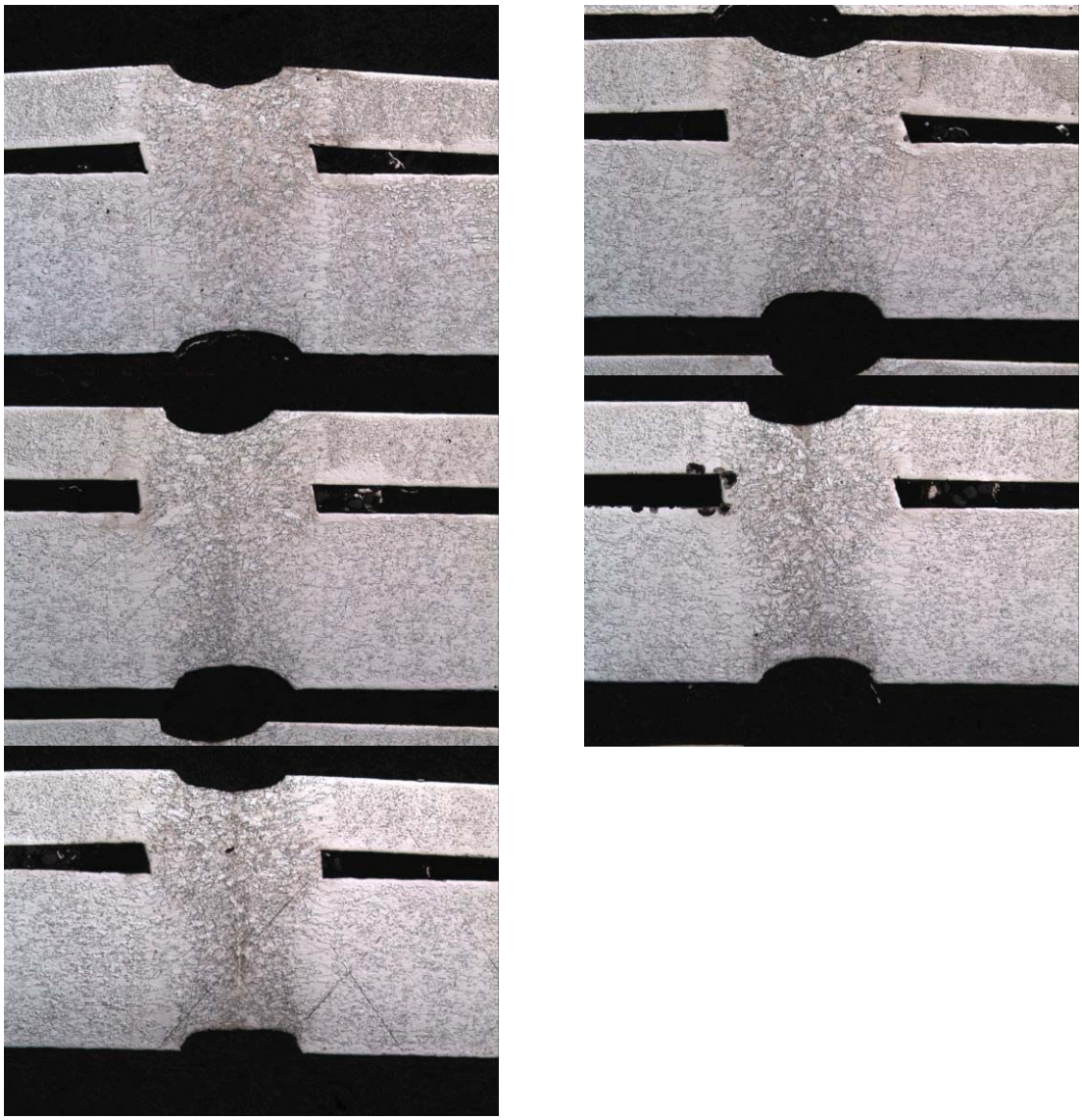

Figure 5. 15 Cross-section of five pieces under optical microscope: speed=3.00 m/min; power= 4.00 kW; gap=0.20 mm

Table 5. 8 Mean and variation value of measured variables: speed=3.00 m/min; power= 4.00 kW; gap=0.20 mm

Item	Mean (μm)	Variation (μm)
Top concavity	211.0	25.6
Interface width	1701.3	22.0
Penetration	1470.6	28.9
Bottom concavity	240.8	20.2

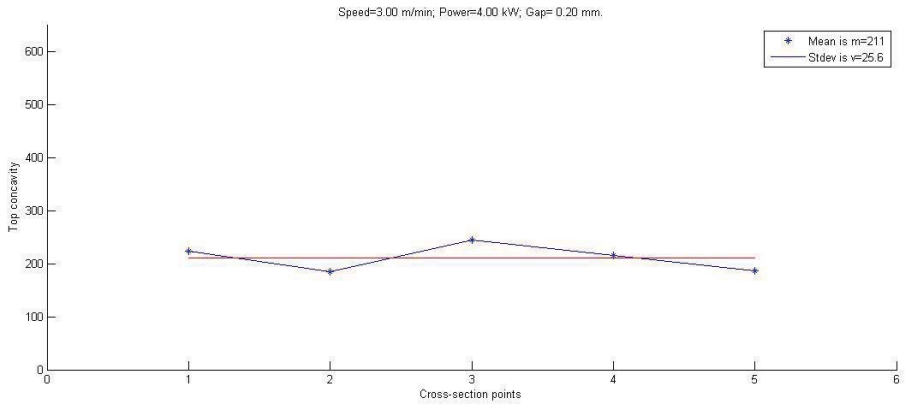

Figure 5. 16 Mean and variation value of top concavity: speed=3.00 m/min; power= 4.00 kW; gap=0.20 mm

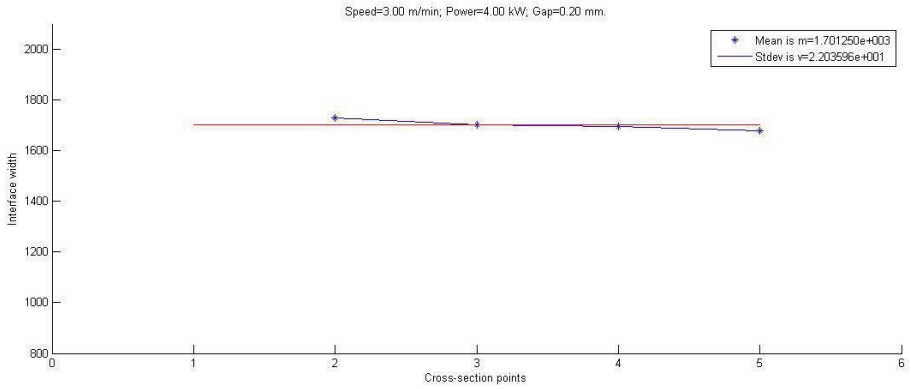

Figure 5. 17 Mean and variation value of interface width: speed=3.00 m/min; power= 4.00 kW; gap=0.20 mm

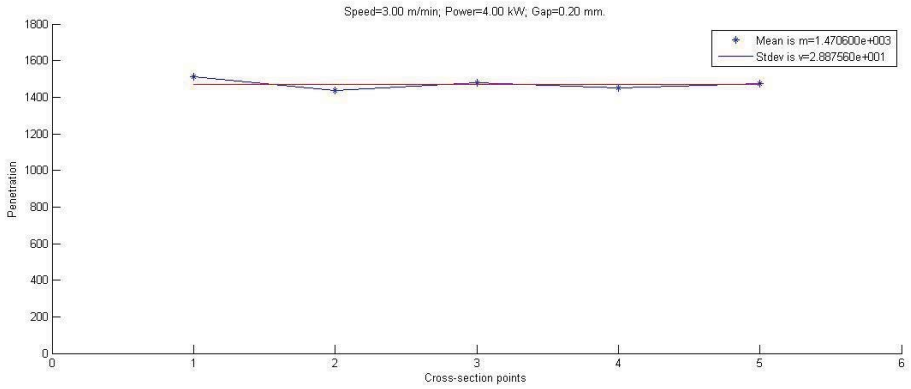

Figure 5. 18 Mean and variation value of penetration: speed=3.00 m/min; power= 4.00 kW; gap=0.20 mm

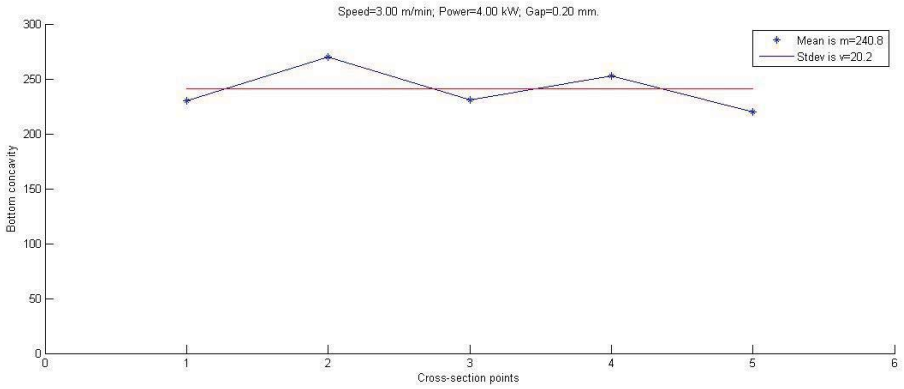

Figure 5. 19 Mean and variation value of penetration: speed=3.00 m/min; power= 4.00 kW; gap=0.20 mm

The aforementioned process of metallographic analysis is summarized in the following table.

Table 5. 9 Specification of the metallographic treatment for weld joints

Procedures	**Activity**	**Equipment**
Cross section	Four section cuts per weld	Linear Precision Saw Buehler IsoMet 5000
Mounting	- Pressure: 290 bar - Heating time: 1 min - Cooling time: 9 mins	Automatic Mounting Press Buehler SimpliMet 1000
Grinding	Abrasive disc P240	Sample Preparation System Buehler Phoenix

	- 5 mins - 150 rpm - 24N/lbs - complementary rotation - lubricant: water	4000
	Grinding disc 9 μm diamond - 5 min - 150 rpm - 24 N/lbs - complementary rotation - lubricant: plycristaline diamond suspension 9 μm	Sample Preparation System Buehler Phoenix 4000
	Trident disc 3 μm	Sample Preparation System Buehler Phoenix

	- 3 min - 150 rpm - 24N/lbs - complementary rotation - lubricant: plycristaline diamond suspension 3 μm	4000
Polishing	Polish micro cloth disc 0.05 μm - 2 min - 275 rpm - 22N/lbs - contrary rotation - lubricant : master prep polishing suspension and water	Sample Preparation System Buehler Phoenix 4000

Etcing	Solution: 2 % Nitrate solution (ethyl alcohol 98% and nitric acid 2 %) Time: 25 seconds	
Inspection	Measured variables: - Penetration - Interface width - Top concavity - Bottom concavity (if applicable) - Gap Repeats: 5 times as there are 5 pieces	- Optical microscope Leica DM 4000 M - Beuhler OmniMet Image Capturing Software

6. Experimental results and analysis

In this chapter, the design, execution and analysis of each experimental campaign are stated. In the first place, One-Factor-at-One-Time is applied to study the process window of RLW. Hundreds of trials are run in this stage; Secondly, in order to verify the proposition that the lower thickness is not significantly affecting the geometric profile under some condition, a comparison analysis campaign is run; Finally, experimental trials are designed and conducted to establish correlation models and optimal results are achieved.

6.1 Process window identification campaign

In this campaign, hundreds of experimental trials are run to identify the process window, which is a prerequisite for correlation modelling and optimization.

6.1.1 Design and execution of experiments

Power, speed and gap are three variables of interest. The trials are run on SU2 with upper thickness of 1.0 mm and lower thickness of 1.0 mm. The quality inspection process follows two steps. Weld joints are inspected visually to screen out defects like root convexity, undercut, spatter, top surface cracks, cut-through, burn-through and weld discontinuity. Those joints without the above mentioned defects are sent to be cross-sectioned and receive metallographic treatment. The geometric structure is measured and compared with the criteria to make sure quality requirements are fulfilled.

6.1.2 Observed defects

During the experimental process, the observed defects include burn-through, cut-through, spatter, insufficient weld. The other defects such as top surface cracks, root convexity are not observed.

- Burn-through

Shown in Figure 6. 1, occurs when the energy per length is too high. As described in the equation, actually when the power is too high or the speed is too slow, the energy tends to be high, which could leads to such defects.

$$\text{Energy} = \text{Power} \times \text{Time} = \frac{\text{Power} \times \text{Length}}{\text{Speed}}$$

Figure 6. 1 Burn-through: top surface and bottom surface

- Cut-through

This defect as shown in Figure 6. 2, occurs when the gap is big or speed is high. The reason is mainly because the equilibrium between the liquid thrust of melted material and vaporized plasma inside the keyhole is not easily reached. Unbalance of it resultes in the expulsion the upper material is certain spot of the weld length.

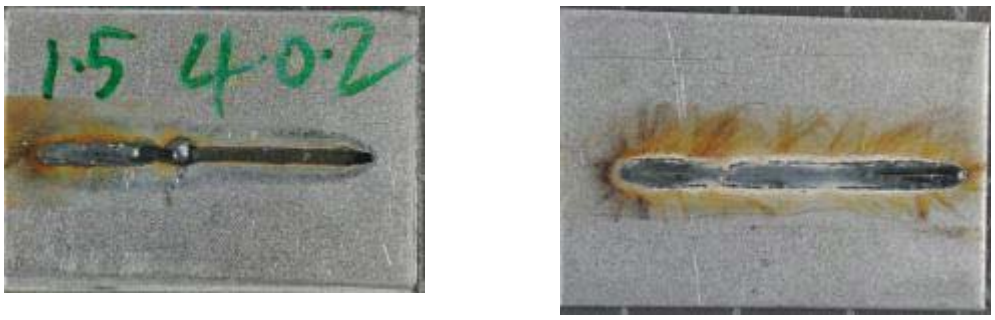

Figure 6. 2 Cut-through: top surface and bottom surface

- Spatter

Shown in Figure 6. 3, this defect is caused by the evacuation of the zinc vapour when the gap is too small.

Figure 6. 3 Spatter

- Insufficient weld

Insufficient weld tends to happen when power is low and speed is fast, as so the energy per length that is projected to the specimen is small. Together with cut-through it contributes to the formation of process window boundary.

$$\text{Energy} = \text{Power} \times \text{Time} = \frac{\text{Power} \times \text{Length}}{\text{Speed}}$$

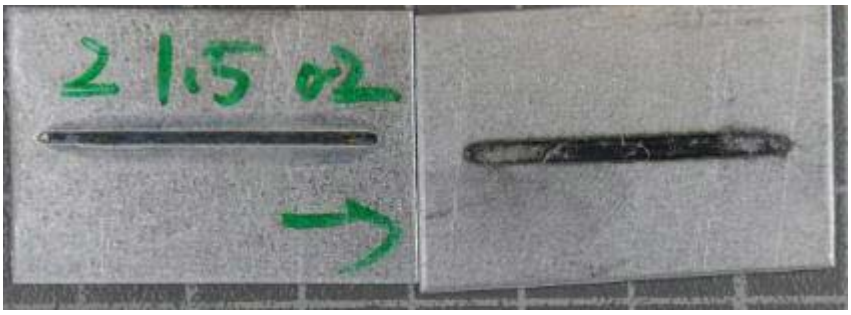

Figure 6. 4 Insufficient weld

The other visible defects such as root convexity, undercut, top surface cracks and weld discontinuity are not observed.

6.1.3 Experimental results of power of 4 kW, 3 kW and 2 kW

In the first step of OFAT method, power is set as a constant of 4 kW. Gap and speed are two variables. The range of gap is from 0 to 0.45mm and range of speed is from 1 m/min to 12 m/min. The design of experiments is listed in Table 6. 1

Table 6. 1 Experimental design for process window identification: power at 4 kW

Exp series	Power (kW)	Gap (mm)	Speed (m/min)	Trial no.	Results
1	4	0.20	[1: 0.5: 12]	21	Over welded, cut-through, burn through, insufficient weld.
2	4	0.30	[1:0.5:6]	10	Over weld, cut-through, burn-through, insufficient weld

3	4	0.35	[1:0.5:5]	8	Over welded, cut-through, burn through, insufficient weld.
4	4	0.40	4	1	not welded
5	4	0.45	4	1	not welded
6	4	0.15	4	1	welded
7	4	0.1	4	1	Spatter
8	4	0.05	4	1	Spatter
9	4	0	4	1	Spatter

In total, around 45 experiments have been conducted and the results are scattered onto a plane of gap and speed. The results are shown in Figure 6. 5. It could conclude that the gap range ensures weld joints without visual defects is from 0.15 mm to 0.35 mm. When gap is smaller than 0.15 mm, spatter occurs; when gap is over 0.35 mm, joints are not sufficiently welded.

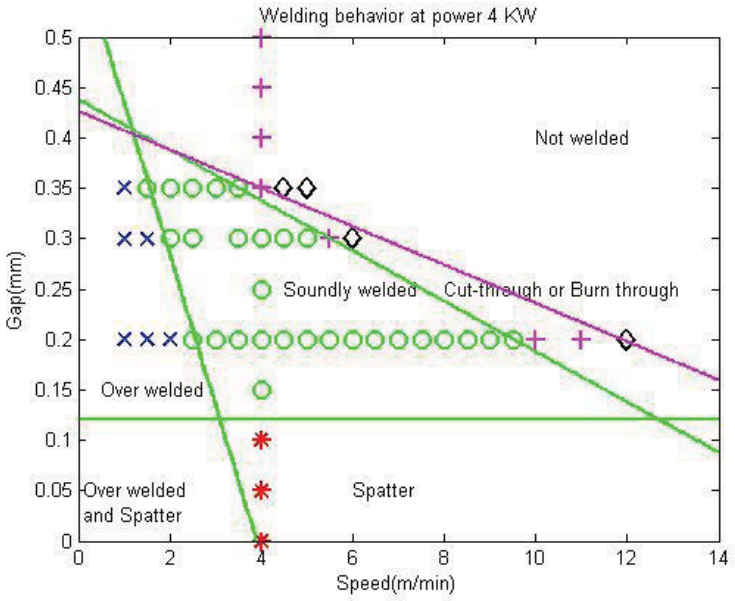

Figure 6. 5 Schematic figure of welding behaviour when power=4.00 kW

Following the same logic, when the power is set at 3 kW, trials as designed in Table 6. 2 are run. What could be observed in Figure 6. 6 is when the gap range is between 0.15 mm and 0.35 mm and speed between 2.0 m/min to 6.0 m/min, joints without visual defects could be produced.

Table 6. 2 Experimental design for process window identification: power at 3 kW

Exp series	Power (kW)	Gap (mm)	Speed (m/min)	Trial no.	Result
1	3	0.15	[1: 0.5: 7]	12	Over-welded and spatter, cut-through, burn-

					through, insufficient weld
2	3	0.30	[1: 0.5: 6]	11	Cut-through and burn-through
3	3	0.35	[1: 0.5: 4]	7	Variation of weld behaviours

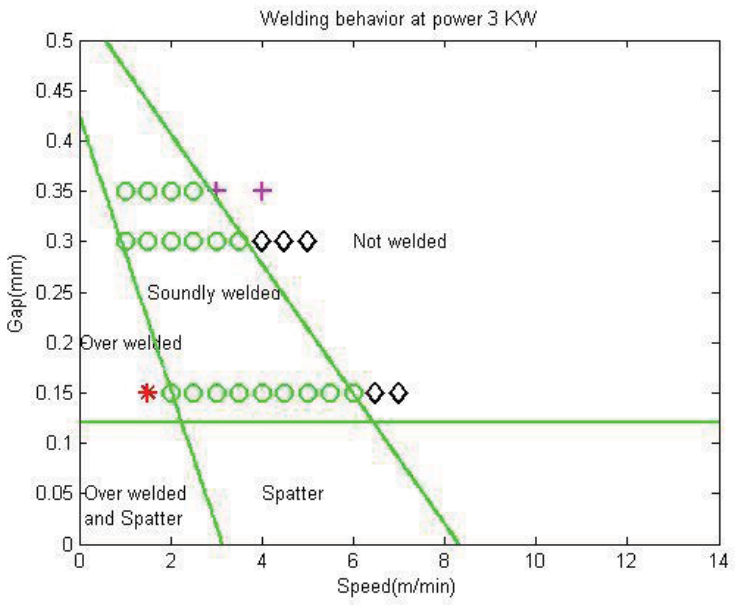

Figure 6. 6 Schematic figure of welding behaviour when power=3.00 kW

Similarly, when power is at 2 kW, it could be seen from Table 6. 3 and Figure 6. 7 that the feasible gap range is 0.2 mm to 0.4 mm and speed range is 1.5 m/min to 4.5 m/min.

Table 6. 3 Experimental design for process window identification: power at 2 kW

Exp series	Power (kW)	Gap (mm)	Speed (m/min)	Trial no.	Result
1	2	0.15	[1: 0.5: 3.5]	5	Over-welded and spatter
2	2	0.20	[1: 0.5: 3.5]	6	Over-weld, sufficient weld
3	2	0.30	[0.5: 0.5: 3]	6	Over-weld, sufficient weld
4	2	0.35	[0.5:0.5:2.5]	4	Over-weld, sufficient weld
5	2	0.40	[0.5: 0.5: 2]	4	Over-weld, sufficient weld

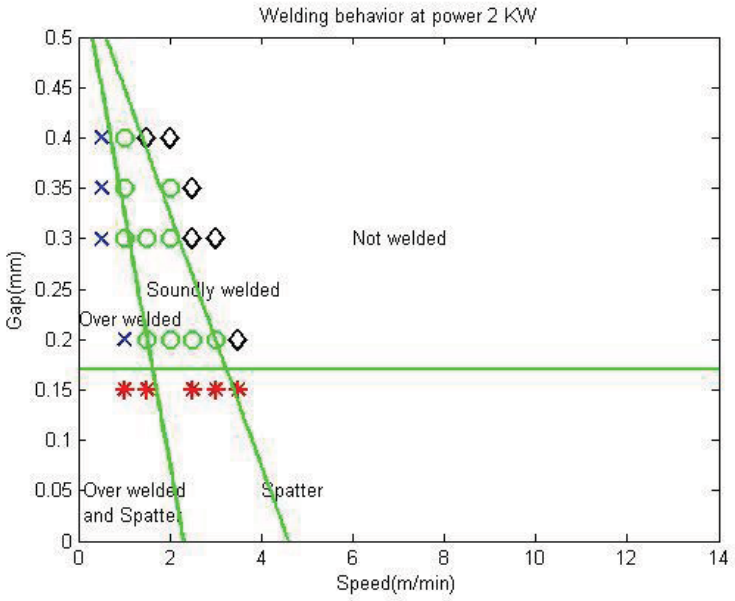

Figure 6. 7 Schematic figure of welding behaviour when power=2.00 kW

If the three figures are projected complementarily and shown in Figure 6. 8, it could been seen that the green lines encompass the Sound welded region at power of 4.00 kW; the blue lines encompass the same at power of 3.00 kW; and the red lines function similarly at the power of 2.00 kW. Combination of speed and gap in the yellow area could produce good weld joints at power 2.0 kW, 3.0 kW and 4.0 kW.

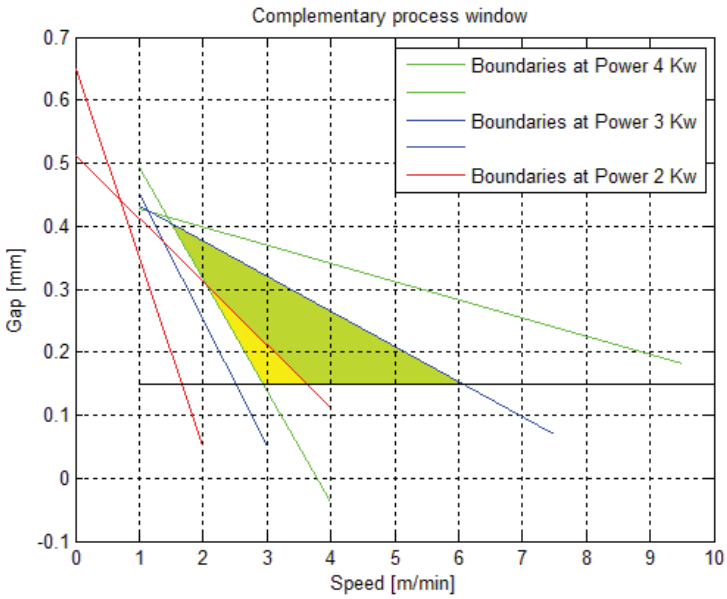

Figure 6. 8 Overlapped region in yellow at power 2.00 kW, 3.00 kW, and 4.00 kW. With right choice of combination of gap and speed, sound weld joints could be produced

Within the complementary process window, sound welds without visible defects could be produced. However, those welds might not fulfil the geometric profile requirements. Those geometric requirements are listed in Table 6. 4.

Table 6. 4 The criteria of constraints for stack-up: DX56D+Z 0.75 mm plus DX54D+Z 1.00 mm

Item	Equation	Value (μm)
Penetration	$\geq 0.3 \times t_{lower}$	≥ 300
Interface width	$\geq 0.9 \times t_{thinner}$	≥ 675
TS-concavity	$\leq 0.5 \times t_{upper}$	≤375
BS-concavity	$\leq 0.5 \times t_{lower}$	≤ 500

Determination of power window

In order to further inspect the fulfilment of geometric requirements, more experimental trials are run and the joints are cross-sectioned and receive metallographic treatment. The micrographs are shown in Figure 6. 9, Figure 6. 10 , Figure 6. 11, Figure 6. 12 and Figure 6. 13. The cross-section geometric data is summarized in Table 6. 5. Those experiments are run under the condition that the gap is at 0.20 mm, speed is at 4.00 m/min and power starts from 2.0 kW to 4.0 kW with a step of 0.5 kW.

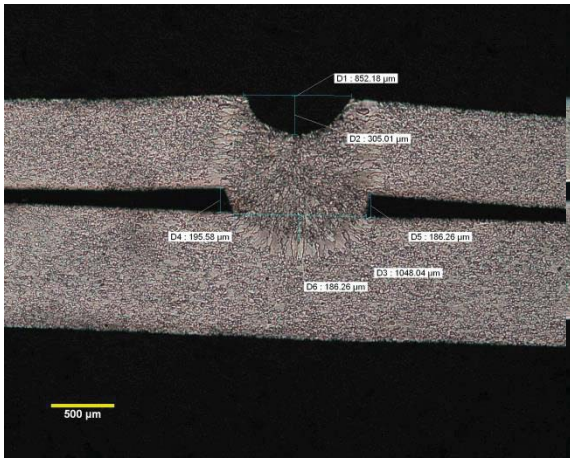

Figure 6. 9 (a) Process parameters : Power =2.00 kW, Speed=4.00 m/mim, Gap=0.20 mm ; Geometric dimensions: Top concavity =305.01 µm, Interface width= 1048.04 µm , Penetration= 186.26 µm,Bottom concavity=0; Status=NOK (insufficient penetration)

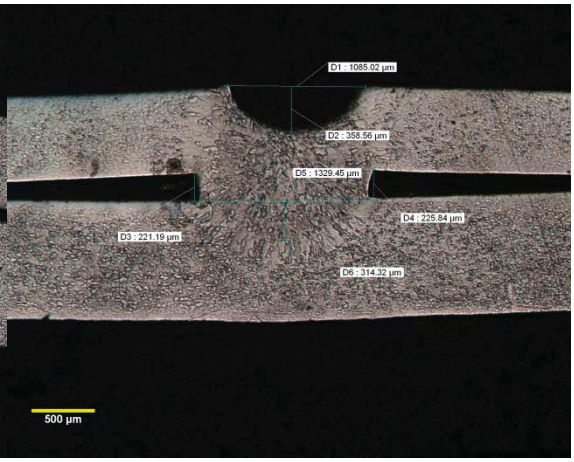

Figure 6. 10(b) Process parameters: Power=2.50 kW, Speed=4.00 m/min, Gap=0.20 mm ; Geometric dimensions: Top concavity=358.56 µm, Interface width = 1329.45 µm , Penetration=314.32 µm ,Bottom concavity=0; Status= Pending (considering standardized deviation of penetration, could not be decided.)

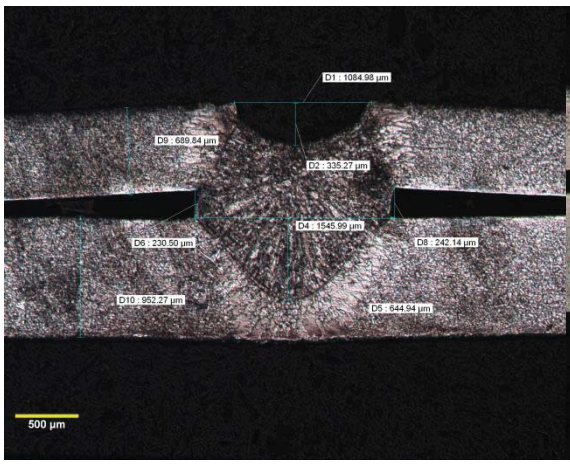

Figure 6. 11 (c) Process parameters: Power=3.00 kW, Speed=4.00 m/min, Gap=0.20 mm (c); Geometric dimensions: Top concavity = 335.27 µm; Interface width= 1549.99 µm; Penetration= 644.94 µm . Status=Pending (considering standard deviation of top concavity, could not be decided)

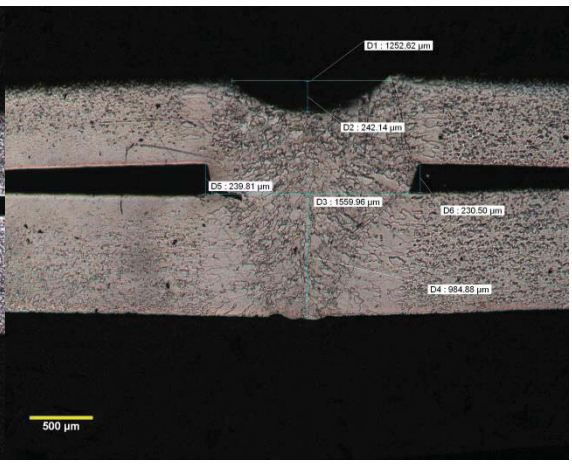

Figure 6. 12 (d) Process parameters : Power=3.50 kW, Speed=4.00 m/min, Gap=0.20 mm; Geometric dimensions: Top concavity =242.14 µm, Interface width=1559.96 µm, Penetration=984.88 µm ; Status=OK

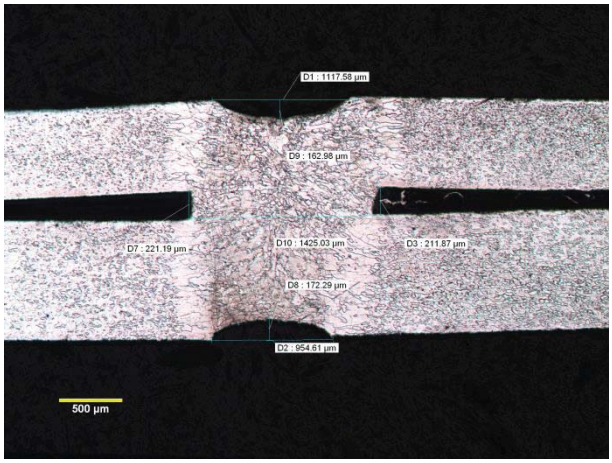

Figure 6. 13 (e) Process parameters: Power=4.00 kW, Speed=4.00 m/min, Gap=0.2 mm (e); Geometric dimensions: Top concavity=162.98 µm , Interface width=1424.03 µm , Penetration=954.61 µm full penetration, Bottom concavity= 172.29 µm; Status= OK

Table 6. 5 Cross-section geometric dimension measurements: Gap=0.20 mm, Speed= 4.0 m/min, Power =[2.0, 4.0] kW

	Power (kW)	Top concavity (μm)	Interface width (μm)	Penetration (μm)	Bottom width (μm)	Mode
1	2.00	305.01	1048.04	186.26	0.00	Full
2	2.50	358.56	1329.45	314.32	0.00	Full
3	3.00	335.27	1549.99	644.94	0.00	Full
4	3.50	242.14	1559.96	984.88	0.00	Full
5	4.00	162.98	1424.03	954.61	172.29	Partial
Gap=0.20 mm; Speed= 4.0 m/min; Power= [2.0, 4.0] kW						

Compared to the standards in Table 6. 4, weld joint (a) could not fulfil with a penetration of 186.26 μm where penetration is supposed to be over 300 μm; weld joint (b), (c), (d) and (e) fulfil the requirements, if the experimental errors are not considered. The weld profiles (a) (b) (c) show partial penetration; (d) and (e) show full penetration. (d) displays the threshold of bottom concavity occurrence. However, due to lack of replicates, there is no sufficient confidence of confirming this statement. Lack of replicates is an innate drawback of this study.

If the data in Table 6. 5 is scattered onto plane of power and length and shown in Figure 6. 14, and the results shows under 3.5 kW, top concavity, interface width and penetration shows linear relationship with power. Therefore, regression analysis is applied to them and shown in Figure 6. 15, it is statistically confident to claim penetration and interface width do have strong linear relationship with power, and the equations are:

$$\text{Penetration} = 545.3 * \text{Power} - 966.96, \ R^2 = 0.966;$$

$$\text{Interface width} = 352.26 * \text{Power} + 405.89, R^2 = 0.8876;$$

The fitness is checked by the determination coefficient (R^2). The value of R^2 is between 0 to1. Its value indicates the aptness of the regression model. This indicator explains the percentage that the experimental data could predict the weld results. If R^2 has a value of over 0.8, the model is considered to show enough confidence. Therefore, top concavity can't be concluded with linear correlation with power with R-squared 0.2944.

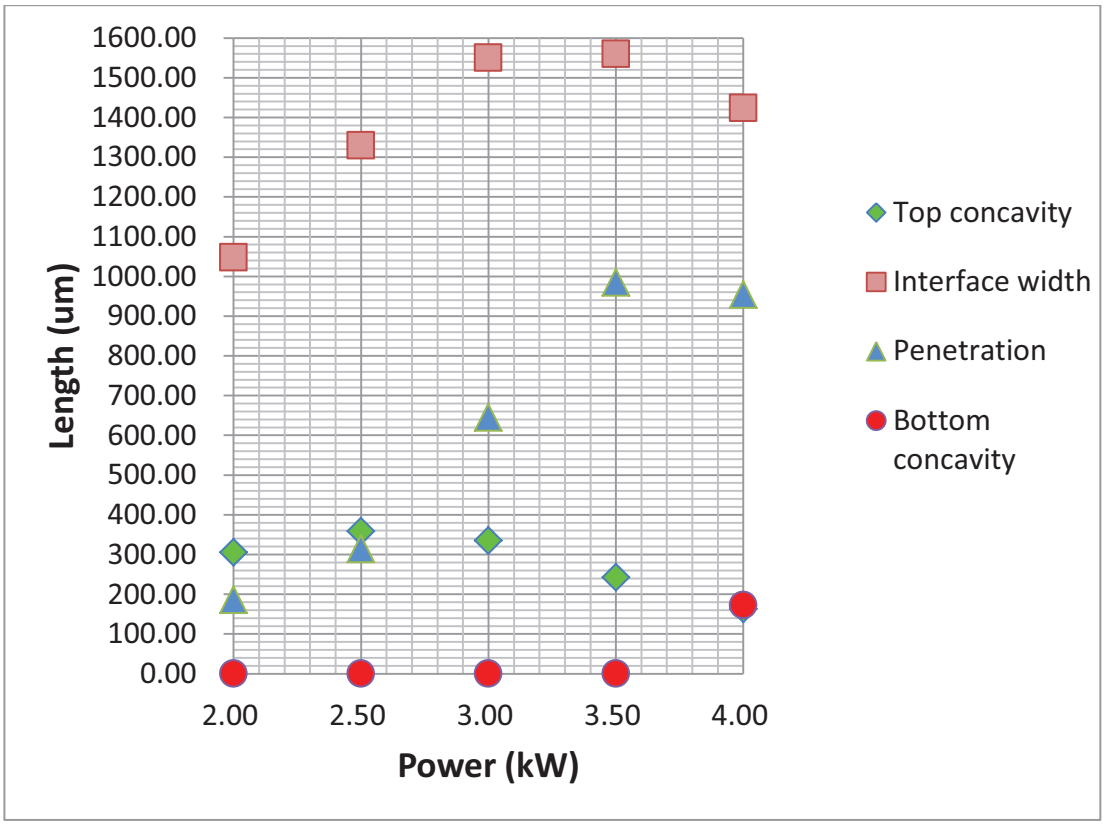

Figure 6. 14 Scattering plot of bead profile geometric dimensions: Gap=0.20 mm, Speed=4.0 m/min, Power= [2.0, 4.0] kW.

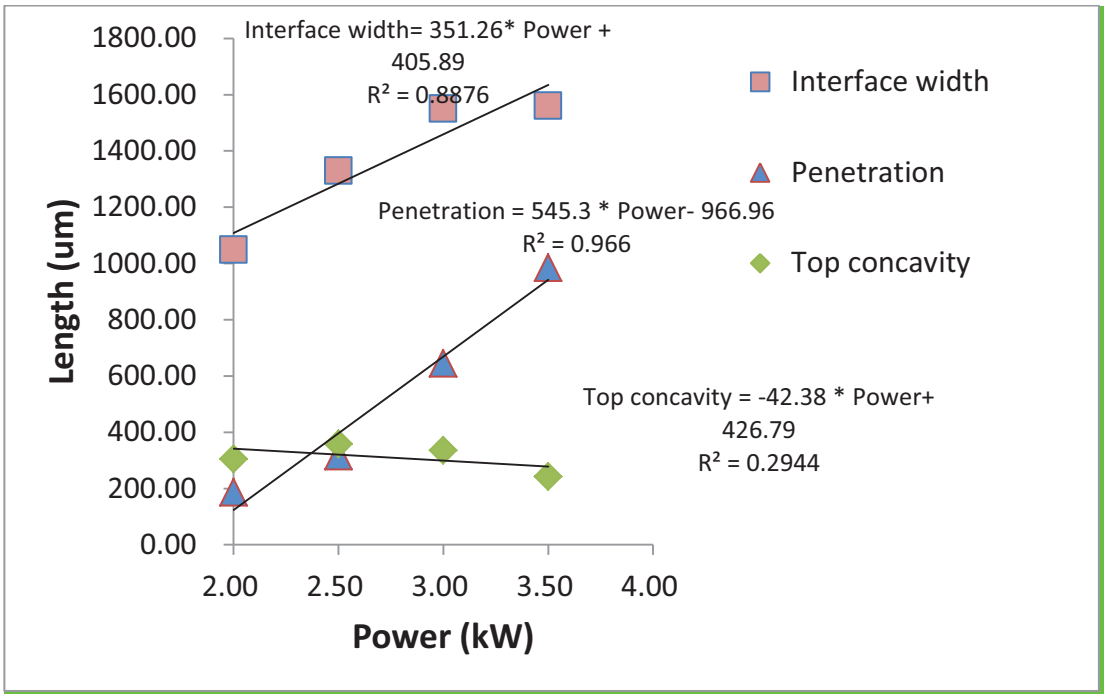

Figure 6. 15 Regression analysis of bead profile geometric dimensions: Gap=0.20 mm, Speed=4.0 m/min, Power= [2.0, 4.0] kW

In order to fulfil the requirement of penetration,

$$\text{Penetration} = 545.3 * \text{Power} - 966.96 \gg 0.3 * \text{lower thickness}$$

$$= 300 + 39 \text{ (error, referring to table 6.5)}$$

$$\text{Power} \geq \frac{300 + 50 + 966.96}{545.3} \approx 2.40\ kW$$

$$\text{Interface width} = 352.26 * \text{Power} + 405.89 \geq 1110.4\ \mu\text{m}$$

$$\geq 675\ \mu\text{m, power } [2.0,4.0]\ kW$$

Considering the errors that could occur during every stage of whole process and from worst case scenario, it is acceptable to claim when power is big than 2.40 kW, with a gap of 0.20 mm and speed of 4.0 m/min, the penetration could fulfil the requirements.

No matter what the power is, the interface width is always bigger than 1110.4 μm , which is absolutely bigger than the standard of 675 μm. Therefore, interface width is not a deciding factor for weld bead quality evaluation.

As to top concavity, though the value of weld (c) fulfils the requirements, however considering the possible error, it is hard to decide whether this requirement is truly fulfilled or not. Therefore, the power process window is determined as [3.0, 4.0] kW.

Determination of speed window

Similarly, with the objective of acquiring the process window for speed, 12 experiments are performed to investigate how speed influences the weld bead profile when gap is controlled at 0.20 mm and power is set as 4 kW. The speed starts from 2.50 m/min to 8.00 m/min, with a step of 0.5 m/min. Figure 6. 16 and Figure 6. 27 are the captured micrographs. And the results are summarized in Table 6. 6. Based on analysis, the process window for speed is concluded to be between 2.5 m/min and 5 m/min.

Table 6. 6 Cross-section geometric dimension measurements: Gap=0.20 mm, Power=4 kW, Speed= [2.5, 8] m/min

Speed	Top concavity	Interface width	Penetration	Bottom concavity	Mode

	(m/min)	(μm)	(μm)	(μm)	(μm)	
1	2.5	277.07	1478.53	670.56	279.43	Full
2	3.0	142.03	1424.96	766.02	172.29	Full
3	3.5	132.71	1441.22	763.74	172.36	Full
4	4.0	162.98	1425.03	782.32	172.29	Full
5	4.5		1258.25	849.92	112.92	Full
6	5.0	246.80	1443.65	533.20	0	Partial
7	5.5	286.38	1541.36	449.38	0	Partial
8	6.0	363.21	1355.07	435.00	0	Partial
9	6.5	305.01	1275.91	318.98	0	Partial
10	7.0	251.46	1115. 26	211.87	0	Partial
11	7.5	423.75	1196.74	179.34	0	Partial
12	8.0	260.77	905.70	60.54	0	Partial

Gap=0.20 mm, Power=4 kW, Speed= [2.5, 8] m/min

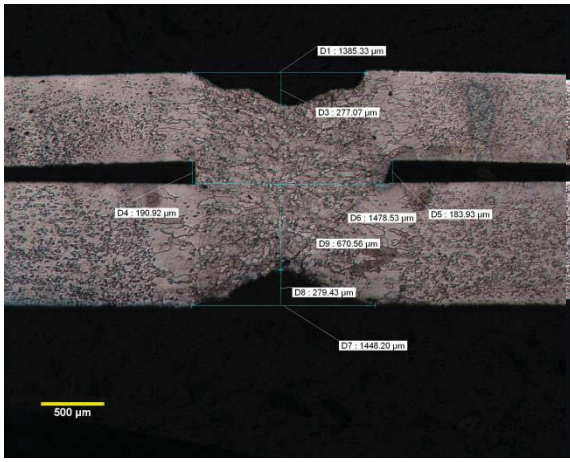

Figure 6. 16 (1) Power=4.00 kW, Speed=2.50 m/min, Gap=0.20 mm; Top concavity=277.07 µm, Interface width= 1478.53 µm, Penetration =670.56 µm, Bottom concavity=279.43 µm. Status=OK

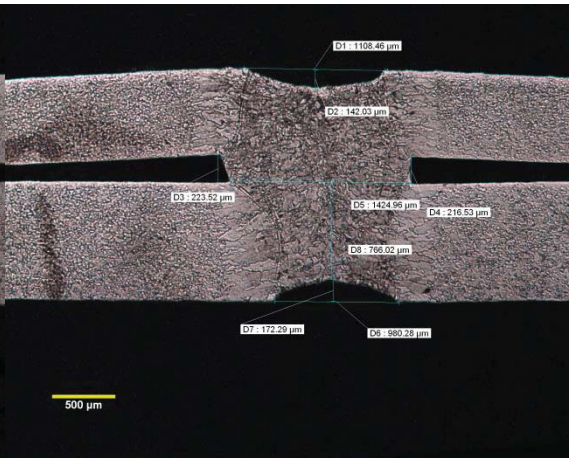

Figure 6. 17 (2) Power=4.00 Kw, Speed=3.00 m/min, Gap=0.20 mm; Top concavity=142.03 µm, Interface width =1424.96 µm , Penetration=766.02 µm , Bottom concavity =172.29 µm, Status=OK

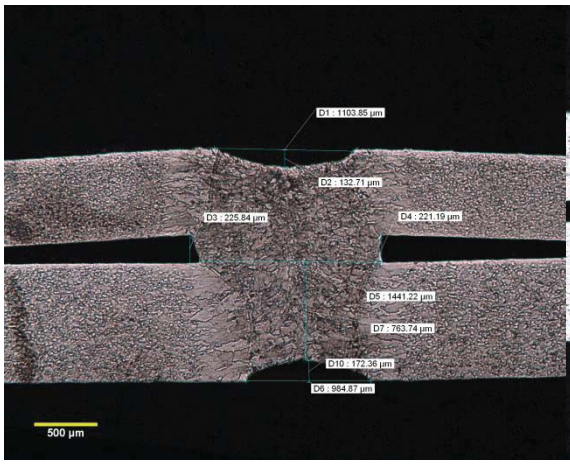

Figure 6. 18 (3) Process parameters: Power=4.00 kW, Speed=3.50 m/min, Gap=0.20 mm; Top concavity= 132.71 µm , Interface width= 1441.22 µm , Penetration= 763.74 µm , Bottom concavity=172.36 µm. Status=0K

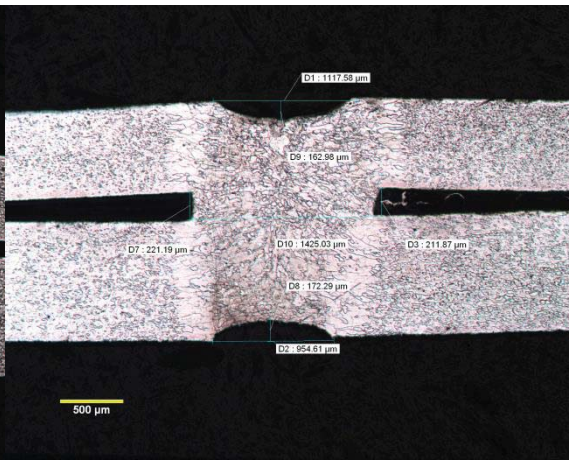

Figure 6. 19 (4) Process parameters: Power=4.00 Kw, Speed=4.00 m/min, Gap=0.20 mm; Top concavity=162.98 µm , Interface width= 1425.03 µm , Penetration=782.32 µm , Bottom concavity=172.29 µm. Status=OK

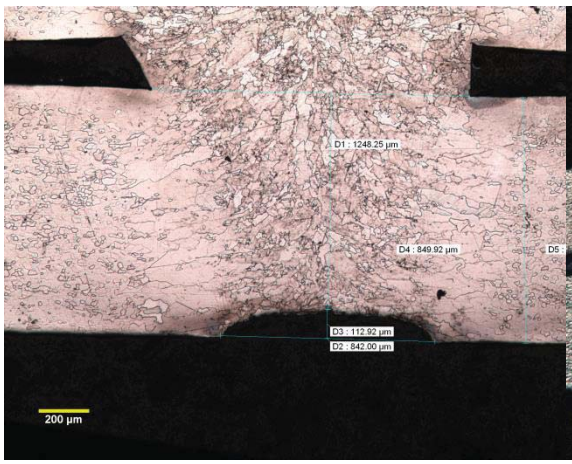

Figure 6. 20 (5) Process parameters: Power=4.00 kW, Speed=4.50 m/min, Gap=0.2 mm; Top concavity=missing, Interface width=1258.25 µm , Penetration=849.92 µm, Bottom concavity=112.92 µm . Status= OK (Top concavity information missing)

(note: the 500 μm micrograph is missing)

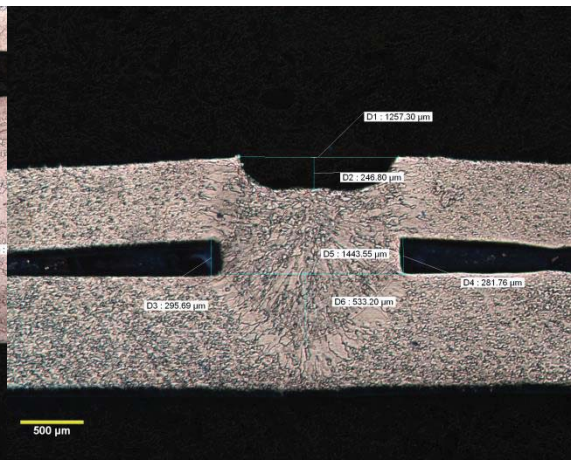

Figure 6. 21 (6) Process parameters: Power=4.00 kW, Speed=5.00 m/min, Gap=0.20 mm; Top concavity= 246.80 µm, Interface width= 1443.65 µm, Penetration= 533.20 µm, Bottom concavity=0. Status=OK

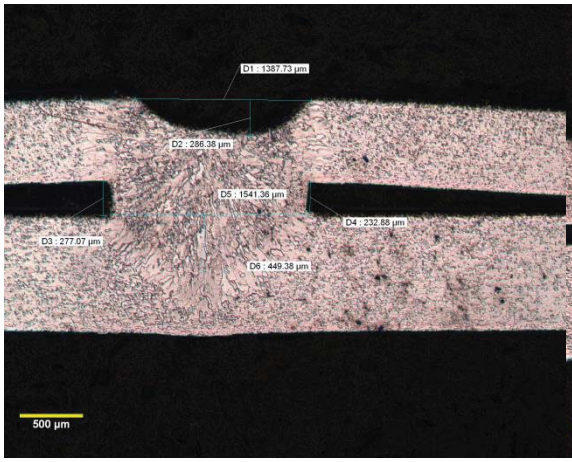

Figure 6. 22 (7) Process parameters: Power=4.00 kW, Speed=5.50 m/min, Gap=0.20 mm; Top concavity=286.38 µm, Interface width=1541.36 µm, Penetration=449.30 µm , Bottom concavity=0; Staust=OK

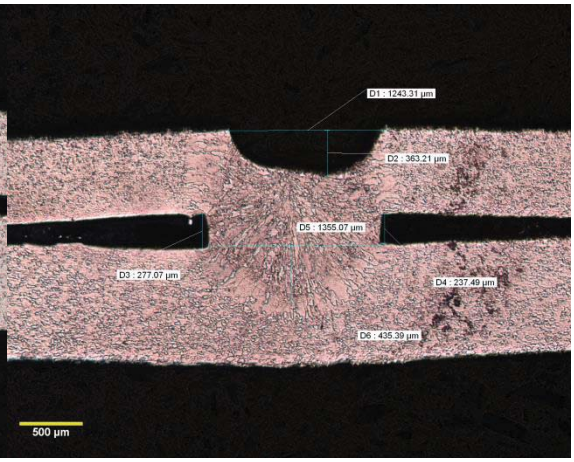

Figure 6. 23 (8) Process parameters: Power=4.00 kW, Speed=6.00 m/min, Gap=0.20 mm; Top concavity= 363.21 µm, Interface width 1355.07 µm, Penetration= 435.00 µm , Bottom concavity=0; Status=NOK (dangerous top concavity)

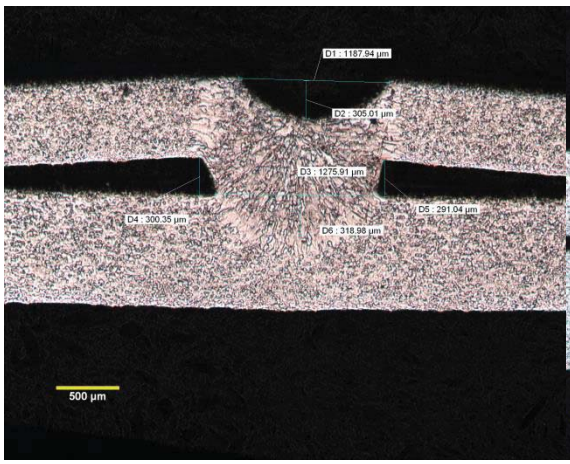

Figure 6. 24 (9) Process parameters: Power=4.00 kW, Speed=6.50 m/min, Gap=0.20 mm; Top concavity=305.01 µm , Interface width= 1275.91 µm, Penetration=318.98 µm, Bottom concavity= 0; Status=NOK (dangerous top concavity and penetration considering standard deviation)

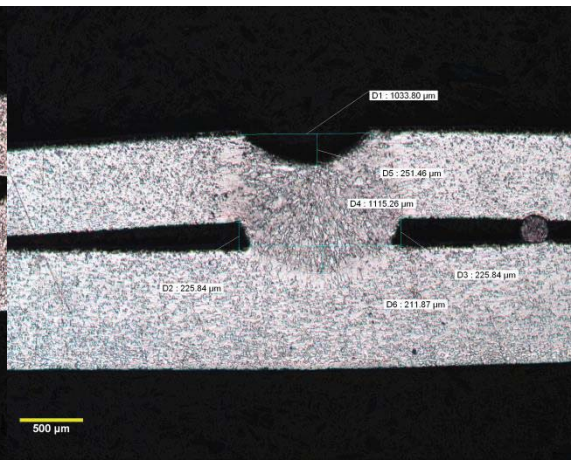

Figure 6. 25 (10) Process parameters: Power=4.00 kW, Speed=7.00 m/min, Gap=0.20 mm; Top concavity= 251.46 µm, Interface width= 1115. 26 µm, Penetration= 211.87 µm, Bottom concavity= 0; Status=NOK (insufficient penetration)

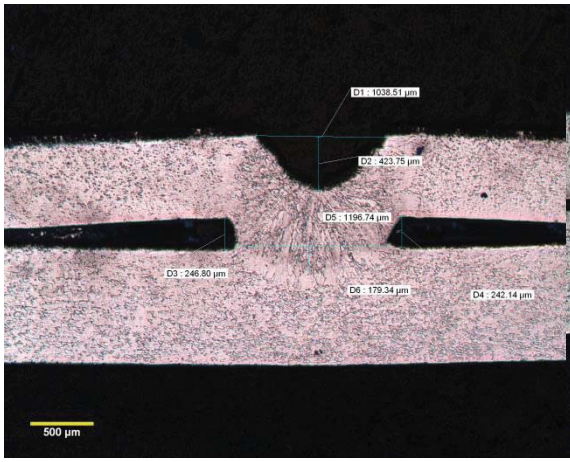

Figure 6. 26 (11) Process parameters: Power=4.00 kW, Speed=7.50 m/min, Gap=0.20 mm; Top concavity= 423.75 µm , Interface width=1196.74 µm, Penetration= 179.34 µm, Bottom concavity=0; Status=NOK (Excessive top concavity, insufficient penetration)

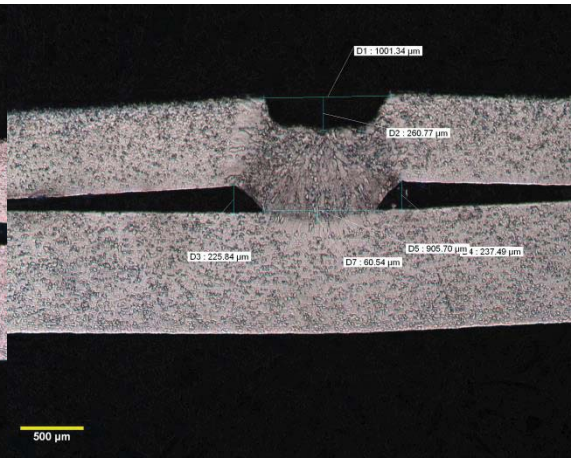

Figure 6. 27 (12) Process parameter: Power=4.00 kW, Speed=8.00 m/min, Gap=0.20 mm; Top concavity= 260.77 µm , Interface width= 905. 70 µm, Penetration= 60.54 µm, Bottom concavity= 0; Status= NOK (insufficient penetration)

Figure (1) to (5) show results are keyhole full penetration welding and the geometric dimensions all fulfil the prescribed standards. For figure (6), though the penetration

is partial penetration, the values have far surpasses the standard of 300 μm and other requirements are fulfilled as well.

From figure (7) is an exceptional case due the author's misconduct of data collection, and due to resource limitation, it is not possible to re-collect the data. The top concavity information is missing, and it is likely that it could fulfil the standard.

For figure (8) to (12), at least one geometric dimension-- either top concavity or penetration, could not meet the prescribed standard. Therefore those welds are considered as failed. It is interesting to conclude that interface width and bottom concavity standards are not setting strict requirements to the parameters as nearly all weld joints could meet the targets.

If the data is scattered onto a plane of speed and length, shown in Figure 6. 28, it could see that the welding behaviours are quite different in full penetration and partial penetration modes. In the full penetration mode (left of Figure 6. 28), the interface width seems to be a constant except (5), the penetration seems to have a linear relationship with speed. As the lower thickness is a constant, and penetration and bottom concavity has the following relationship, therefore top concavity shows the linear relationship with speed as well.

$$\text{Penetration} + \text{Bottom concavity} = \text{Lower thickness (full penetration mode)}$$

In partial penetration mode, the interface width seems to be a constant, and bottom concavity remains 0 as there is actually no bottom concavity at all. The interface width and penetration shows linear relationship with speed. The functions are:

$$\text{Penetration (l)} = 75.0 * \text{Speed} + 504, R^2 = 0.8564\ (Speed = [2.5, 4.5]\ m/min$$

$$\text{Penetration(r)} = -155.8 * \text{Speed} + 1325.3, R^2 = 0.9774\ (\text{Speed} = [5,8]\text{m/min})$$

Standard: Penetration(l) $\geq$ 500, considering bottom concavity

Standard: Penetration (r) $\geq$ 300

$$\text{Therefore, } 2.5 \leq \text{Speed} \leq \frac{1325.3 - 300 - error\ (39)}{155.8} = 6.33\ \text{m/min}$$

$$\text{Interface wid} = -181.6 * \text{Speed} + 2442.6, R^2 = 0.8471\ (Speed = [5,8]\ m/min)$$

Standard : Interface width $\geq$ 675

$$\text{Interface width} \geq -181.6 * 8 + 2442.6 = 989.8 \geq 675, \text{Speed} = [2.5, 8]\ \text{m/min}$$

The speed process window is decided as [2.5, 5.5] m/min by combining the analysis with the micrograph judgement.

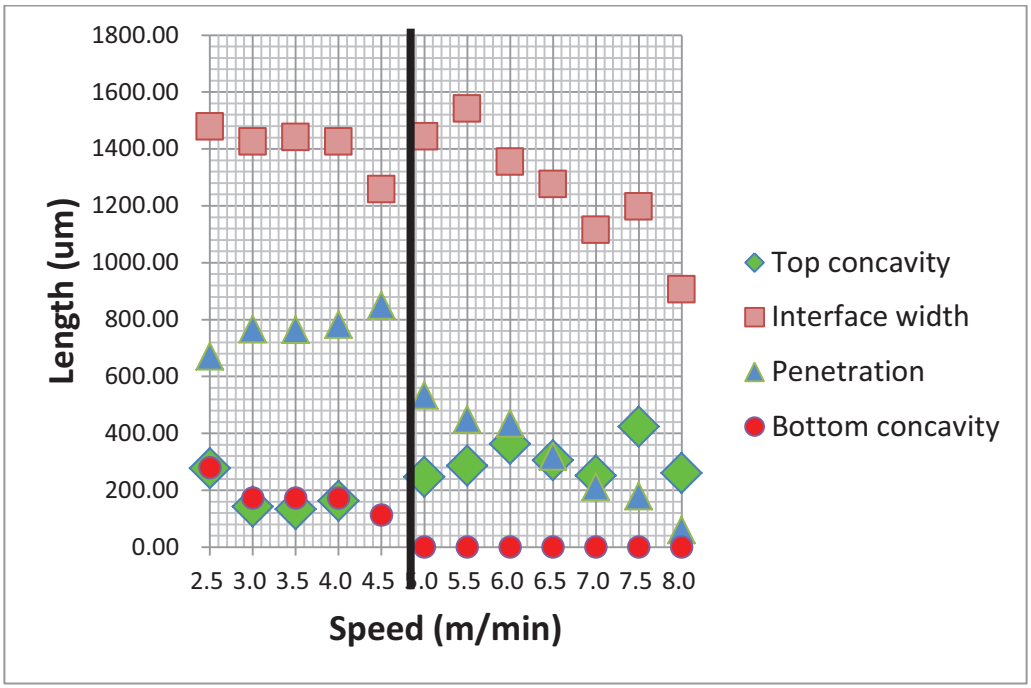

Figure 6. 28 Scattering plot of bead profile geometric dimensions: Gap=0.20 mm, Power=4 kW, Speed= [2.5, 8] m/min

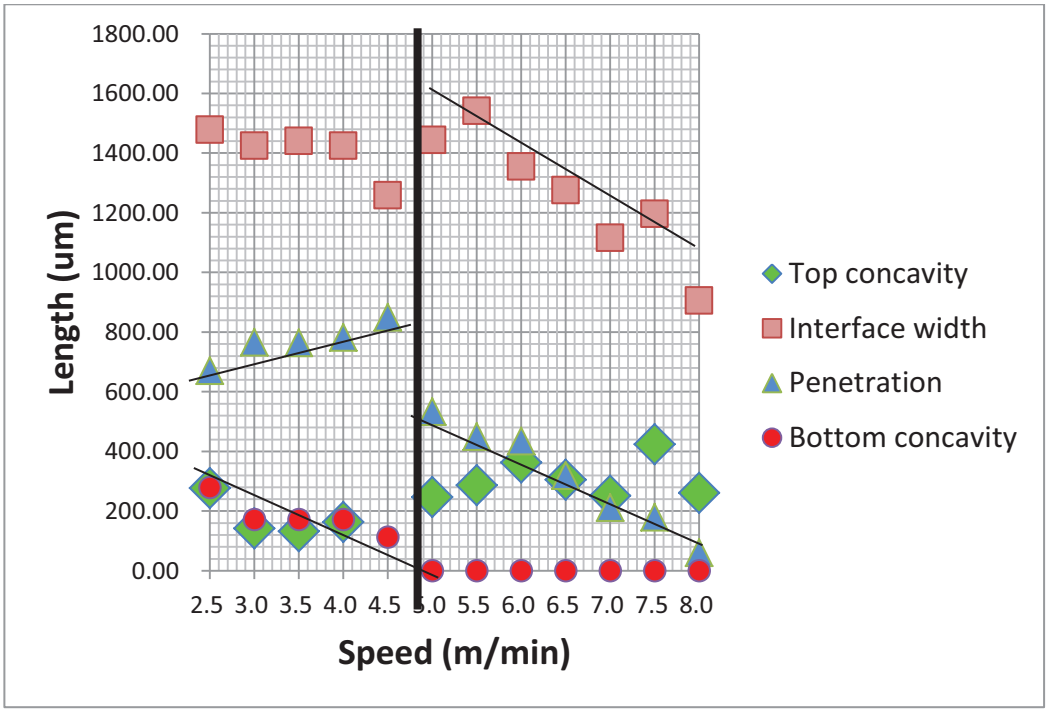

Figure 6. 29 Regression analysis of bead profile geometric dimensions: Gap=0.20 mm, Power=4 kw, Speed= [2.5, 8] m/min

Determination of gap window

10 experiments have been carried out to decide the range of gap from 0 to 0.45 mm. Power is set at 4 kW, and the speed is set at 4 m/min. Figure 6. 30 to Figure 6. 39 below indicate how the weld joints are affected by gap. These figures provide the weld surfaces instead of cross-sections as spatter is the main defect when gap is small and cut-through is the main defect when gap is big. Both defects are visible.

When the gap is 0 mm, 0.05 mm and 0.10 mm, spatter occurs on the surface of the specimen as shown in Figure 6. 30, Figure 6. 31 and Figure 6. 32. At gap 0.15 mm, 0.20 mm, 0.25 mm and 0.30 mm, the weld joints display nice appearances. When the gap is at 0.35 mm, 0.40 mm or 0.45 mm, defects such as cut-through or burn-through appear and they are considered as unacceptable weld joints. Therefore, it is concluded that the gap appropriate for producing sound weld joints is from 0.15 mm to 0.30 mm in this study.

Figure 6. 30 Power=4.00 kW; Speed= 4.00 m/min; Gap=0 mm, Status=NOK (Spatter, surface pores)

Figure 6. 31 Power=4.00 kW; Speed= 4.00 m/min; Gap=0.05 mm, Status=NOK (Spatter, surface pores)

Figure 6. 32 Power=4.00 kW; Speed= 4.00 m/min; Gap=0.10 mm, Status=NOK (Spatter, cut-though)

Figure 6. 33 Power=4.00 kW; Speed= 4.00 m/min; Gap=0.15 mm, Status=OK

Figure 6. 34 Power=4.00 kW; Speed= 4.00 m/min; Gap=0.20 mm, Status=OK

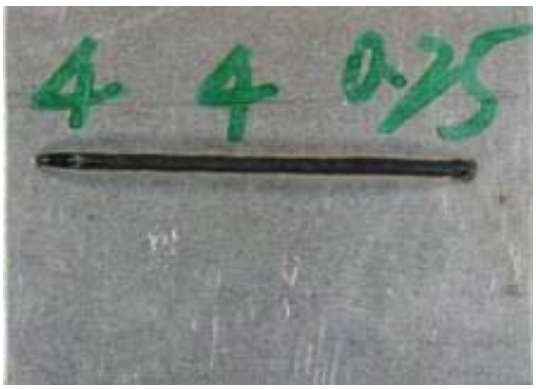

Figure 6. 35 Power=4.00 kW; Speed= 4.00 m/min; Gap=0.25 mm, Status=OK

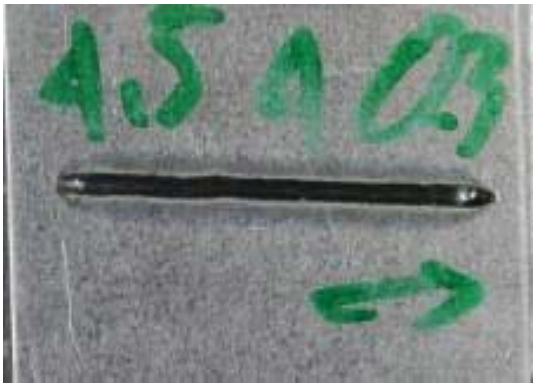

Figure 6. 36 Power=4.00 kW; Speed= 4.00 m/min; Gap=0.30 mm, Status=OK

Figure 6. 37 Power=4.00 kW; Speed= 4.00 m/min; Gap=0.35 mm, Status =NOK (Cut-through)

Figure 6. 38 Power=4.00 kW; Speed= 4.00 m/min; Gap=0.40 mm, Status=NOK (Cut-through, insufficient weld)

Figure 6. 39 Power=4.00 kW; Speed= 4.00 m/min; Gap=0.45 mm, Status=NOK (cut-through, insufficient weld

The major conclusion of this investigation is that the process windows are:

Power = [3.0, 4.0] kW, Speed= [2.5, 5.5] m/min, Gap= [0.15, 0.30] mm. One of two major objectives of this study is realized till now.

6.2 Stack-up comparison analysis campaign

6.2.1 Objective and experimental plan

The purpose of this campaign is to analyse whether the lower-thickness in the lap joint configuration influences the weld results. The reason why this campaign is of great value and importance is if the conclusion is insignificant, then modelling of four stack-ups could be simplified and just the stack-up with thickest lower thickness needs to be studied.

Two stack-ups: DX56D+Z 1.00 mm to DX54D+Z 1.00 mm and DX56D+Z 1.00 mm to DX56D+Z 1.8 mm are chosen to be investigated by paired mean hypothesis. Six pairs of experiments are planned and performed on these two material stack-ups as in Table 6. 7.

Table 6. 7 Results of the designed paired experiments

No.	**Speed**	**Power**	**Gap**	**Interface-width (μm)**		**Penetration (μm)**		**Top concavity (μm)**		**Top width (μm)**	
				0.75-1.00	0.75-1.80	0.75-1.00	0.75-1.80	0.75-1.00	0.75-1.80	0.75-1.00	0.75-1.80
1	4.50	4.00	0.20	1574	1579	576	529	275	271	1347	1404

2	5.00	4.00	0.20	1547	1455	589	465	279	290	1384	1319
3	5.50	4.00	0.20	1305	1456	356	379	176	288	1188	1234
4	6.00	4.00	0.20	1372	1313	362	342	364	295	1293	1032
5	6.50	4.00	0.20	1187	1241	261	291	291	286	1012	1057
6	7.00	4.00	0.20	1061	1225	225	296	249	308	995	1054

6.2.2 Analysis and discussion of the results

Twelve experiments are performed and geometric data is collected shown in Table 6. 7. As described in the chapter of methodology, the approach used to analyse this issue is paired mean hypothesis, which is a tool to test whether the effect brought by one factor at different values is significant or not.

u_d denotes the geometric structure difference between the two stack-ups. The null hypothesis is that the lower thickness does not affect the weld joint geometric structure, namely $u_d = 0$. The alternative hypothesis is that the lower thickness's effect is significant in defining the weld joint structure, that is to say, $u_d \neq 0$.

$$H_0 : u_d = 0$$

$$H_0 : u_d \neq 0$$

Table 6. 8 Paired means difference for weld joint geometry structure

	$d_{interface}$ (μm)	$d_{penetration}$ (μm)	$d_{topConcavity}$ (μm)	$d_{topWidth}$ (μm)
1	-5	47	4	-57

2	92	124	-11	65
3	-151	-23	-112	-46
4	59	20	69	261
5	-54	-30	5	-45
6	-164	-71	-59	-59
$\bar{\mathbf{d}}$	-37	11	-17.30	19.80
$\mathbf{s_d}$	106	68	61.90	127.2
t-value	-0.86	0.40	-0.69	0.38
p-value	0.43	0.71	0.52	0.718

The t-test results are listed in Table 6. 8, p-values for interface-width, penetration, top concavity and top width are all bigger that 5%. In this case, it could be concluded that the difference between the paired means is null. In other words, under these two welding setups, there is not much difference in the weld joint geometric structure. It is a positive conclusion as anticipated. If the lower thickness does not affect the welding process, models based on the thickest lower thickness could be used to predict all the other material stack-ups. Therefore, in this study, process modelling experimental campaign is only carried out on stack-up of DX56D+Z 0.75 mm and DX56D+Z 1.8 mm.

6.3 Process modelling campaign-RSM

6.3.1 Objectives and experimental design

To acquire the process empirical model which correlates the process parameters (speed, power and gap) and weld geometric structure (top concavity, penetration, interface with and bottom concavity) is the main objective of this campaign.

As concluded in the paired mean hypothesis testing section, the stack-up was selected to be DX56D+Z 0.75 mm to DX54D+Z 1.8 mm. The experiments are designed based on a three factors, three levels, Box-Behnken Design matrix with three centre point replicates with the help of Design Expert, referring to Table 6. 10. Factors considered are the aforementioned three parameters: speed, power, and gap. The chosen range of every process parameters are:

- Speed= [3.0, 5,0] m/min
- Power= [3.0,4,0] kW
- Gap =[0.15,0.25] mm

They are sub-regions of the process window defined previously. It ensures that weld joints fulfilling all standards could be obtained. The factors' notation, unit, and experimental design levels are listed in

Table 6. 9

Table 6. 9 Factors and experimental design levels

Notation	Factor	-1	0	1

$\mathbf{x_1}$ **(A)**	Speed (m/min)	3.00	4.00	5.00
$\mathbf{x_2}$ **(B)**	Power (kW)	3.00	3.50	4.00
$\mathbf{x_3}$ **(C)**	Gap (mm)	0.15	0.20	0.25

Table 6. 9, x1, x2 and x3 are coded variables. The transformation equations from the coded variables to natural variables are as follows:

$$\begin{cases} \text{Speed} = x_1 + 4.00 \\ \text{Power} = {}^{x_2}/_{2} + 3.50 \\ \text{Gap} = 0.05 * x_3 + 0.20 \end{cases}$$

Table 6. 10 Three factor Box-Behenken Design with 3 centre points and the experimental results

Natural No	Run No	Block	A	B	C	Speed (m/min)	Power (kW)	Gap (mm)	Top concavity (µm)	Interface-width (µm)	Penetration (µm)	Bottom concavity (µm)	Status
3	1	1	-1	1	0	3.00	4.00	0.20	245	1703	1477	231	OK
1	2	1	1	-1	1	5.00	3.00	0.25	472	1325	445	0	NOK
8	3	1	-1	0	-1	3.00	3.50	0.15	26	1278	1589	0	OK
10	4	1	0	-1	1	4.00	3.00	0.25	499	1199	458	0	NOK
5	5	1	0	0	0	4.00	3.50	0.20	514	1803	906	0	NOK
2	6	1	1	1	0	5.00	4.00	0.20	443	1702	793	0	NOK
7	7	1	-1	-1	0	3.00	3.00	0.20	233	1647	1598	136	OK
15	8	1	-1	0	1	3.00	3.50	0.25	509	1906	1527	202	NOK
9	9	1	0	0	0	4.00	3.50	0.20	334	1545	1234	0	OK

6	10	1	0	0	0	4.00	3.50	0.20	504	1735	839	0	NOK
14	11	1	0	-1	-1	4.00	3.00	0.15	142	1367	755	0	OK
11	12	1	1	0	-1	5.00	3.50	0.15	98	1337	559	0	OK
12	13	1	1	-1	0	5.00	3.00	0.20	456	1317	330	0	NOK
4	14	1	0	1	-1	4.00	4.00	0.15	41	1334	1745	0	OK
13	15	1	0	1	1	4.00	4.00	0.25	364	1625	1157	0	OK

Top concavity ≤ 375 μm;
Interface width ≥ 675 μm;
$Penetration \geq 540\ \mu m$;
bottom concavity ≤ 900 μm ;

All those with status of NOK, they fail due to top concavity or/and penetration.

6.3.2 Development of mathematical models

The designed fifteen experiments are carried out and geometric dimensional data is collected. The results are shown in Table 6. 10. The models obtained are:

Top concavity=324.30+55.06 *A-15.49*B +190.19* C

Penetration=1021.73-419.02*A+312.93*B -199.19* C

Analysis for Top concavity

Design Expert indicates top concavity model is linear with power, speed and gap. Table 6. 11 shows the result of "Fit summary" analysis. "Fit summary" is a method to identify the most appropriate correlation model for datasets, linear, quadratic or cubic. P-value shows the linear model is significant to explain the experimental data. ANOVA analysis (Table 6. 12) shows the linear model is statistically significant.

Table 6. 11 Fit analysis for top concavity modelling

Source	Sequential p-value	Lack of Fit p-value	Adjusted R-Squared	Predicted R-Squared	
Linear	0.0017	0.8456	0.6633	0.5514	Suggested
2FI	0.8725	0.7834	0.5739	0.2121	
Quadratic	0.3052	0.8265	0.65	-0.0364	

Cubic	0.8265	0.2893	Aliased

Table 6. 12 ANOVA table for Top concavity

Source	Sum of Squares	df	Mean Square	F Value	p-value Prob > F	
Model	2.94E+05	3	97944.3	10.19	0.0017	significant
A-A	21123.9	1	21123.9	2.2	0.1662	
B-B	242.56	1	242.56	0.025	0.8766	
C-C	2.66E+05	1	2.66E+05	27.73	0.0003	
Residual	1.06E+05	11	9608.25			
Lack of Fit	85409.74	10	8540.97	0.42	0.8456	Insignificant
Error	20280.98	1	20280.98			
Cor Total	4.00E+05	14				

If gap is set at 0.20 mm, the linear surface could be shown in Figure 6. 40 and it illustrates when power is big and speed is slow, the top concavity is small; while, when power is small and speed is big, the top concavity is big. Figure 6. 41 is the contour graph and it supports the conclusion.

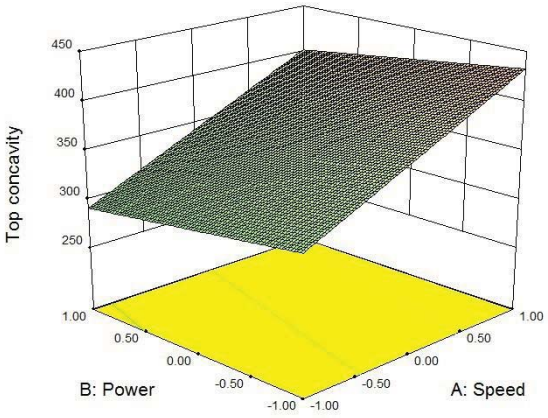

Figure 6. 40 3D graph to show the model of top concavity, gap at 0.20 mm

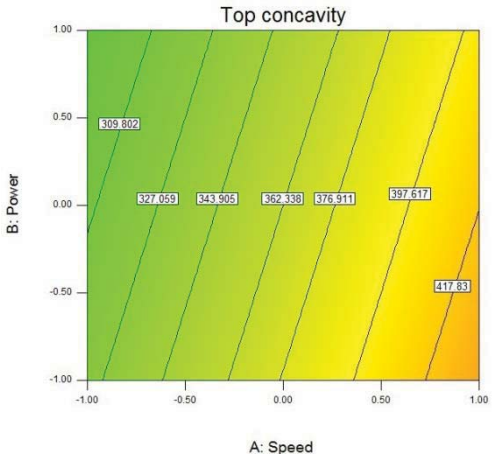

Figure 6. 41 Contour graph to show the model of top concavity, gap at 0.20 mm

Analysis of interface width

Though Design Expert suggest the model to be a linear one, the p-value is 9.06% and has surpassed the determination limit of 5%, which means the linear model is not significant to explain the experimental data, as shown in Table 6. 13 and Table 6. 14. The experimental data could not fit either quadratic or cubic model. Therefore, it is concluded no regression model is suitable for interface width.

Table 6. 13 Fit analysis for interface width modelling

Source	Sequential p-value	Lack of Fit p-value	Adjusted R-Squared	Predicted R-Squared	
Linear	0.0906	0.4031	0.2769	-0.0582	Suggested
2FI	0.5208	0.3839	0.2384	-0.7674	
Quadratic	0.1818	0.4427	0.503	-1.2046	
Cubic	0.4427		0.7695		Aliased

Table 6. 14 ANOVA analysis for interface width

Source	Sum of Squares	df	Mean Square	F Value	p-value Prob > F	
Model	3.05E+05	3	1.02E+05	2.79	0.0906	not significant
A-A	80318.9	1	80318.9	2.2	0.1662	
B-B	1.21E+05	1	1.21E+05	3.31	0.0961	
C-C	1.02E+05	1	1.02E+05	2.78	0.1238	
Residual	4.02E+05	11	36535			
Lack of Fit	3.90E+05	10	39024.16	3.35	0.4031	not significant
Pure Error	11643.38	1	11643.38			
Cor Total	7.07E+05	14				

Analysis of penetration

Same logic with top concavity, Design Expert suggests linear model for penetration, as p-value of it is far lower than 5%. The lack of fit p-valve is much higher than 5% and indicates insignificant. Quadratic and cubic are aliased to explain the available experimental data, shown in Table 6. 15 and Table 6. 16.

Table 6. 15 Fit analysis for penetration

Source	Sequential p-value	Lack of Fit p-value	Adjusted R-Squared	Predicted R-Squared	
Linear	0.0002	0.4676	0.7652	0.648	Suggested
2FI	0.6532	0.4315	0.7336	0.3998	
Quadratic	0.9087	0.3416	0.6144	-0.5998	
Cubic	0.3416		0.8963		Aliased

Table 6. 16 ANOVA analysis for penetration

Source	Sum of Squares	df	Mean Square	F Value	p-value Prob > F

Model	2665054.2	3	888351.3901	16.2110397	0.000238	significant
A-A	1936561.1	1	1936561.108	35.3392468	9.67E-05	
B-B	360545.67	1	360545.6738	6.57940123	0.026282	
C-C	99092.922	1	99092.92184	1.80829265	0.205785	
Residual	602790.78	11	54799.162			
Lack of Fit	578590.78	10	57859.0782	2.390871	0.46763	not significant
Pure Error	24200	1	24200			
Cor Total	3267845	14				

The linear model is as follows:

Penetration=1021.73-419.02*A+312.93*B -199.19* C;

If gap is set at 0.20 mm, the linear surface shows as in Figure 6. 42and it illustrates when power is big and speed is slow, penetration is big; while, when power is small and speed is big, penetration is small. Figure 6. 43 is the contour graph and it supports the conclusion.

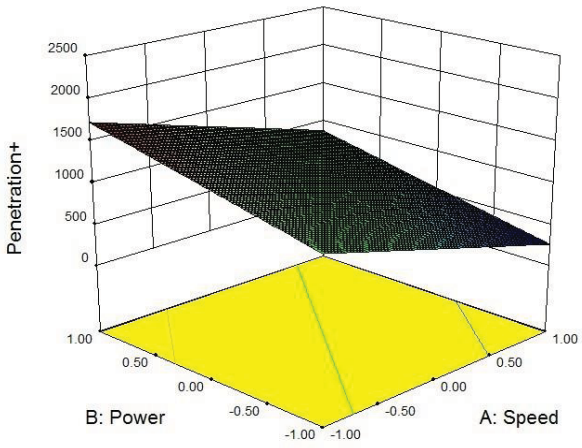

Figure 6. 42 3D graph to show the model of penetration, Gap at 0.20 mm

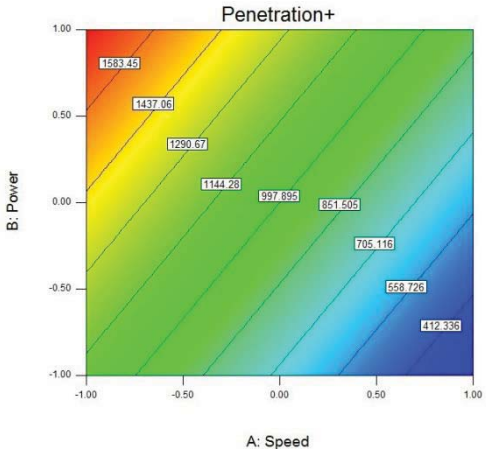

Figure 6. 43 Contour graph to show the model of penetration, Gap at 0.20 mm

Analysis of bottom Concavity

As shown in Table 6. 17 and Table 6. 18, the p-value for quadratic model is 6.77%, which has surpassed the threshold of 5%. Therefore, quadratic model is insignificant to explain the experimental results.

Table 6. 17 Fit analysis for bottom concavity

Source	Sequential p-value	Lack of Fit p-value	Adjusted R-Squared	Predicted R-Squared	
Linear	0.0881		0.2807	-0.0811	
2FI	0.595		0.2091	-1.2453	
Quadratic	0.0661		0.6651	-0.4003	Suggested
Cubic			1		Aliased

Table 6. 18 ANOVA analysis for penetration

Source	Sum of Squares	df	Mean Square	F Value	p-value Prob > F	
Model	59911.52	9	6656.84	4.09	0.0677	not significant
A-A	34111.72	1	34111.72	20.95	0.006	
B-B	495.04	1	495.04	0.3	0.6051	
C-C	13.87	1	13.87	8.52E-03	0.9301	
AB	5222.34	1	5222.34	3.21	0.1333	
AC	5669.78	1	5669.78	3.48	0.121	
BC	117.26	1	117.26	0.072	0.7991	
A^2	11655.17	1	11655.17	7.16	0.044	
B^2	5674.63	1	5674.63	3.49	0.1209	
C^2	3725.59	1	3725.59	2.29	0.1907	
Residual	8139.76	5	1627.95			
Lack of Fit	8139.76	4	2034.94			
Pure Error	0	1	0			
Cor Total	68051.28	14				

6.4 Optimization results for four stack-ups

One of the major objectives of this thesis is to find the optimal parameter setup to produce weld joints with least time, least power and "right" quality. In the case of RLW, faster speed is equivalent to reduce processing time and lower power helps to save cost. After we obtained the models of top concavity and penetration, the optimization problem could be formulated.

6.4.1 Optimization formulation for stack-up 0.75 mm-1.80 mm

Objectives:

$$\begin{cases} \text{Maximize speed} \\ \text{Minimize power} \end{cases}$$

Constraints:

$$\begin{cases} \text{Penetration} = 1030.46 - 495.15 * \text{A} + 192.30 * \text{Power} - 112.01 * \text{C} \\ \text{penetration} \geq 540\ \mu\text{m}; \\ Top\ concavity = 333.52 + 51.71 * A - 4.99 * B + 183.66 * C \\ \text{Top concavity} \leq 375\ \mu\text{m}; \\ \text{Interface width} \geq 675\ \mu\text{m}; \\ \text{bottom concavity} \leq 900\ \mu\text{m}; \end{cases}$$

After running the algorithm in Design-Experts, the results of stack-ups of 0.75 mm-1.8 mm are listed in Table 6. 19. The optimized desirability result is:

$$\begin{cases} \text{A} = -0.70 \\ \text{B} = 0.60 \\ \text{C} = -1.00 \end{cases}$$

According to the transformation equations:

$$\begin{cases} \text{Speed} = \text{A} + 4.00 = 3.30\ \text{m/min} \\ \text{Power} = {}^{\text{B}}/_{2} + 3.50 = 3.80\ \text{kW} \\ \text{Gap} = 0.05 * \text{C} + 0.20 = 0.15\ \text{mm} \end{cases}$$

Figure 6. 44 is the contour graph of desirability function at the aforementioned point. Figure 6. 45 is the contour graph with penetration as response on the plane of power and speed. Figure 6. 46 is the overlay plot of this situation on the plane of power and speed. In all these three graphs, the gap is at -1.00, namely 0.15 mm.

The predicted geometric structure dimensions are:

$$\begin{cases} \text{Top concavity} = 86.43\ \mu\text{m} \leq 375\ \mu\text{m} \\ \text{Interface width} = 1310.46\ \mu\text{m} \geq 675\ \mu\text{m} \\ Penetration = 1620\ \mu m \geq 540\ \mu m \\ \text{Bottom concavity} = 40.88\ \mu\text{m} \leq 900\mu\text{m} \end{cases}$$

Table 6. 19 Optimization results of stack-up 0.75 mm-1.80 mm

Number	A	B	C	Interface width (μm)	Top concavity (μm)	Bottom concavity (μm)	Penetration (μm)	Desirability
1	-0.70	0.60	-1.00	1310.46	86.4359	40.8799	1620	0.17458
2	-0.71	0.59	-1.00	1310.15	86.1887	41.5414	1620	0.174533
3	-0.69	0.61	-1.00	1310.8	86.7163	40.1288	1620	0.174513
4	-0.71	0.57	-1.00	1309.75	85.8615	42.4257	1620	0.174316
5	-0.73	0.56	-1.00	1309.28	85.4763	43.4711	1620	0.173838
6	-0.74	0.54	-1.00	1308.8	85.0825	44.5507	1620	0.173095
7	-0.69	0.62	-0.97	1329.56	92.2159	42.2794	1620	0.17197
8	-0.71	0.59	-0.97	1330.73	92.1491	44.2776	1620	0.171833

9	-0.76	0.52	-1.00	1308	84.4309	46.3527	1620	0.171296
10	-0.71	0.60	-0.95	1339.38	94.6991	45.3805	1620	0.170694
11	-0.77	0.50	-1.00	1307.36	83.9097	47.8097	1620	0.169331
12	-0.70	0.64	-0.90	1371.51	104.68	47.9454	1620	0.166215
13	-0.75	0.58	-0.86	1394.47	110.666	56.3469	1620	0.16201
14	-0.67	0.68	-1.00	1311.82	86.3769	40.3465	1637.28	0.160647
15	-0.73	0.63	-1.00	1309.58	84.15	46.2062	1643.14	0.158576
16	-0.74	0.69	-0.59	1542.28	160.866	76.3615	1620	0.140444
17	-0.48	0.89	-1.00	1319.78	94.0588	21.99	1620	0.118047
18	-0.81	0.82	-0.01	1773.16	264.466	130.329	1620	0.091811

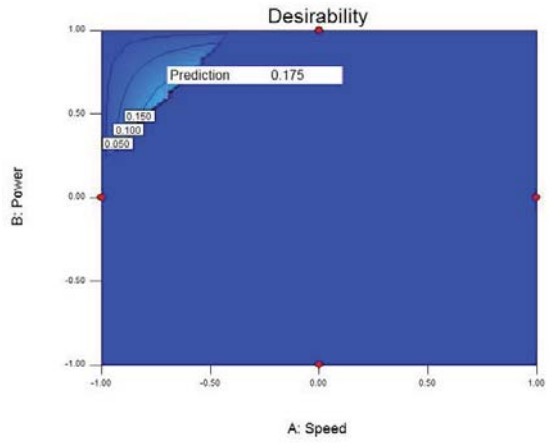

Figure 6. 44 Optimum of desirability of stack-up 0.75 mm-1.80 mm

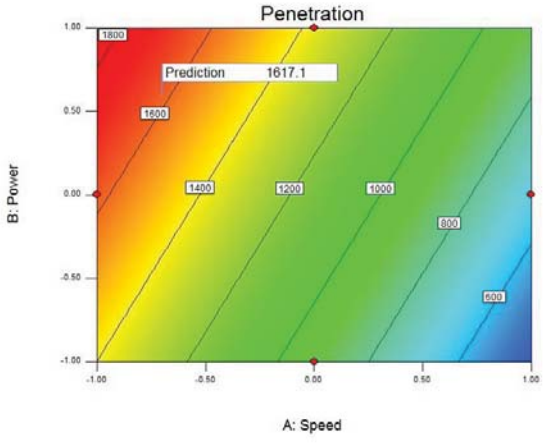

Figure 6. 45 Optimum of penetration on plane of power and speed for stack-up 0.75 mm-1.80 mm

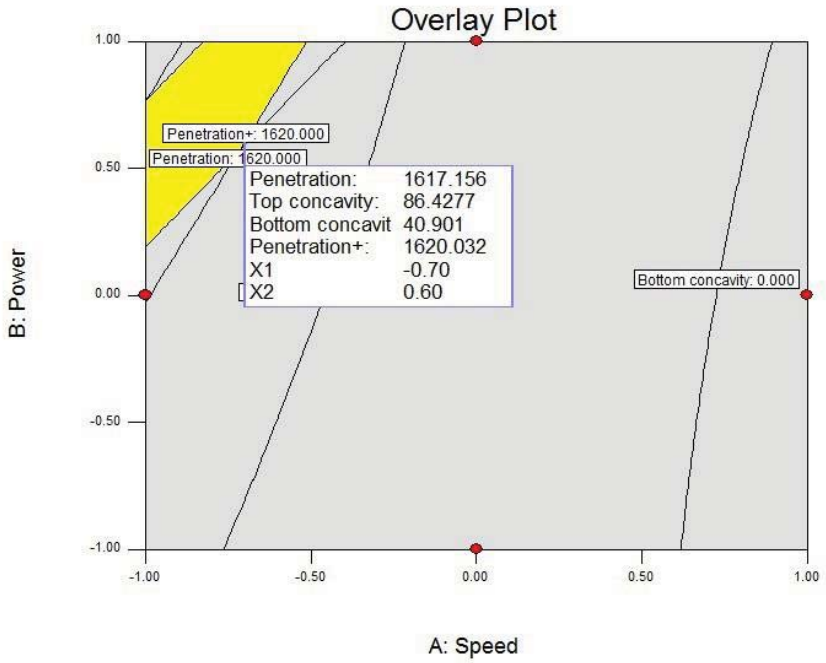

Figure 6. 46 Overlay Plot of Optimum setting gap at 0.15mm for stack-up 0.75 mm-1.80 mm

6.4.2 Optimization formulation for stack-up 0.75 mm-1.00 mm

Objectives:

$$\begin{cases}\text{Maximize speed}\\ \text{Minimize power}\end{cases}$$

Constraints:

$$\begin{cases}\text{penetration} \geq 300\ \mu\text{m};\\ \text{interface width} \geq 675\ \mu\text{m};\\ \text{top concavity} \ll 375\ \mu\text{m};\\ \text{bottom concavity} \leq 500\ \mu\text{m};\end{cases}$$

The optimum results are listed in the Table 6. 20. For example, the optimized desirability result is:

$$\begin{cases}A = -0.14\\ B = -0.62\\ C = -0.11\end{cases}$$

According to the transformation equations:

$$\begin{cases}\text{Speed} = A + 4.00 = 3.86\ \text{m/min}\\ \text{Power} = {}^{B}/_{2} + 3.50 = 3.19\ \text{kW}\\ \text{Gap} = 0.05 * C + 0.20 = 0.18\ \text{mm}\end{cases}$$

Figure 6. 47 is the contour graph of desirability function at the aforementioned point. Figure 6. 48 the contour graph with penetration as response on the plane of power and speed. Figure 6. 49 is the overlay plot of this situation on the plane of power and speed. In all these three graphs, the gap is at -0.11 or 0.18mm.

Table 6. 20 Optimization results of stack-up 0.75 mm-1.00 mm

Number	A	B	C	Interface width (μm)	Top concavity (μm)	Bottom concavity (μm)	Penetration (μm)	Desirability
1.00	-0.14	-0.62	-0.11	1583.55	305.684	0	900.001	0.59
2.00	-0.13	-0.59	-0.09	1587.21	310.164	0	900	0.59
3.00	-0.16	-0.65	-0.13	1579.95	301.42	0	900.114	0.59
4.00	-0.18	-0.69	-0.16	1573.42	294.191	0	900	0.59
5.00	-0.10	-0.53	-0.04	1594.46	319.69	0	900	0.59
6.00	-0.19	-0.71	-0.18	1570.61	291.195	0	900	0.59
7.00	-0.11	-0.56	-0.07	1590.89	314.029	0	902.125	0.59

8.00	-0.08	-0.49	-0.01	1599.3	326.666	0	900	0.59
9.00	-0.22	-0.76	-0.21	1563.91	284.328	0	900.002	0.59
10.00	-0.07	-0.47	0.01	1601.4	329.893	0	900.005	0.59
11.00	-0.24	-0.79	-0.23	1559.22	279.719	0	900.029	0.59
12.00	-0.21	-0.73	-0.21	1565.69	284.51	0	905.878	0.58
13.00	-0.19	-0.69	-0.19	1569.95	287.31	0	911.209	0.58
14.00	-0.03	-0.39	0.09	1610.28	345.432	0	900.001	0.58
15.00	-0.02	-0.37	0.10	1611.78	347.052	0	902.069	0.58
16.00	-0.09	-0.48	-0.06	1596.64	315.374	0	917.708	0.58
17.00	0.00	-0.33	0.15	1615.73	357.472	0	900	0.58
18.00	0.01	-0.31	0.17	1617.42	361.892	0	900.001	0.58

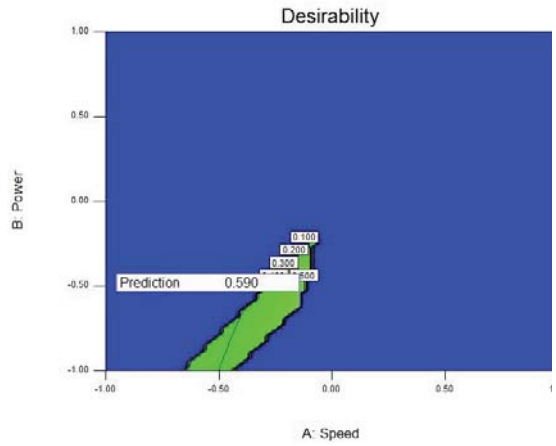

Figure 6. 47 Optimum of desirability of stack-up 0.75 mm-1.00 mm

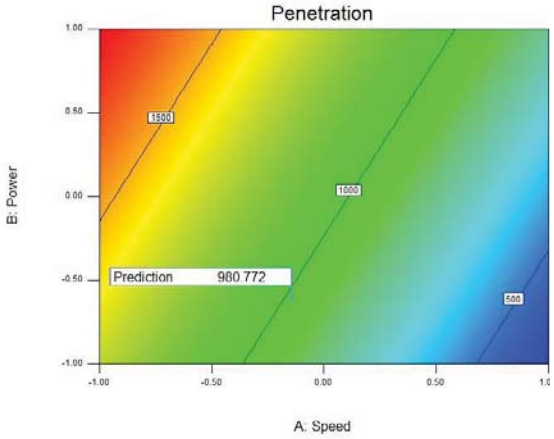

Figure 6. 48 Optimum of penetration on plane of power and speed for stack-up 0.75 mm-1.00 mm

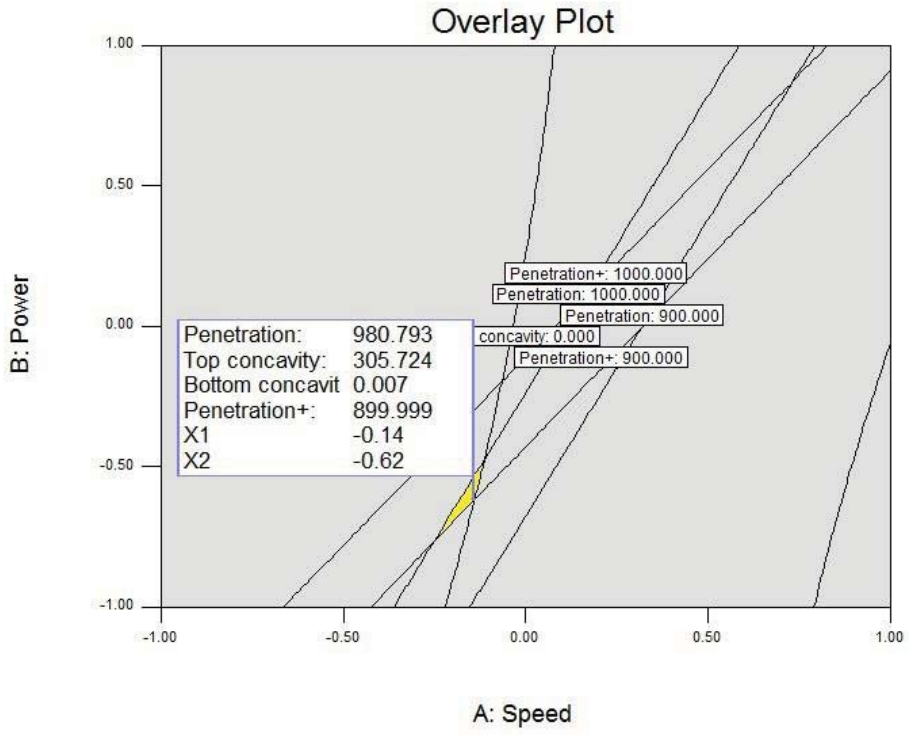

Figure 6. 49 Overlay Plot of Optimum setting gap at 0.18 mm for stack-up 0.75 mm to 1.00 mm

The predicted geometric structure dimensions are:

$$\begin{cases} \text{Top concavity} = 305.68\ \mu\text{m} \leq 375\ \mu\text{m} \\ \text{Interface width} = 1583.55\ \mu\text{m} \geq 675\ \mu\text{m} \\ Penetration = 900\ \mu m \geq 300\ \mu m \\ \text{Bottom concavity} = 0\ \mu\text{m} \leq 500\mu\text{m} \end{cases}$$

Though the results could meet the requirements, one drawback of this study is that no verification trial has been run to prove the accuracy of this model.

6.4.3 Optimization formulation for stack-up 0.75 mm-0.70 mm

Objectives:

$$\begin{cases} \text{Maximize speed} \\ \text{Minimize power} \end{cases}$$

Constraints:

$$\begin{cases} \text{penetration} \geq 210\ \mu\text{m} \\ \text{interface width} \geq 675\ \mu\text{m} \\ \text{top concavity} \leq 375\ \mu\text{m} \\ \text{bottom concavity} \leq 350\ \mu\text{m} \end{cases}$$

The optimum results are listed in the Table 6. 20. For example, the first result is:

$$\begin{cases} \text{A} = 0.65 \\ \text{B} = -0.61 \\ \text{C} = -1.00 \end{cases}$$

According to the transformation equations:

$$\begin{cases} \text{Speed} = \text{A} + 4.00 = 4.65\ \text{m/min} \\ \text{Power} = {}^{\text{B}}/_{2} + 3.50 = 3.195\ \text{kW} \\ \text{Gap} = 0.05 * \text{C} + 0.20 = 0.15\ \text{mm} \end{cases}$$

Figure 6. 50 is the contour graph of desirability function at the aforementioned optimum point. Figure 6. 51 the contour graph with penetration as response on the plane of power and speed. Figure 6. 52 is the overlay plot of this situation on the plane of power and speed. In all these three graphs, the gap is at -1.00 or 0.15 mm.

The predicted geometric structure dimensions are:

$$\begin{cases} \text{Top concavity} = 179.62\ \mu\text{m} \leq 375\ \mu\text{m} \\ \text{Interface width} = 1345.98\ \mu\text{m} \geq 675\ \mu\text{m} \\ Penetration = 675\ \mu m \geq 210\ \mu m \\ \text{Bottom concavity} = 0\ \mu\text{m} \leq 350\ \mu\text{m} \end{cases}$$

Though the results meet the requirements, however one drawback of this study is that no verification trial has been run to prove the accuracy of this model.

Table 6. 21 Optimization results of stack-up 0.75 mm- 0.70 mm

Number	A	B	C	Interface width (μm)	Top concavity (μm)	Bottom concavity (μm)	Penetration+ (μm)	Desirability
1	0.65	-0.61	-1.00	1345.98	179.616	0.00104146	675.002	0.816752
2	0.68	-0.57	-1.00	1347.28	180.676	2.40934	675.001	0.813714
3	0.66	-0.59	-0.96	1361.56	187.489	8.33401E-005	675.001	0.811909
4	0.72	-0.53	-1.00	1348.75	181.878	5.2151	675	0.809773
5	0.74	-0.49	-1.00	1349.75	182.698	7.16971	675	0.806785
6	0.66	-0.54	-1.00	1346.7	178.934	0.00136189	693.668	0.800777
7	0.66	-0.52	-1.00	1346.99	178.656	9.74508E-005	701.331	0.794075
8	0.69	-0.48	-0.85	1401.93	208.89	0.0010676	681.598	0.791749

9	0.87	-0.33	-1.00	1355	186.942	17.6768	675	0.787573
10	0.89	-0.30	-1.00	1355.82	187.657	19.7571	675	0.783273
11	0.97	-0.19	-1.00	1359.16	190.386	27.2357	675	0.76614
12	1.00	-0.15	-1.00	1360.46	191.449	30.252	675.001	0.758613
13	0.94	-0.17	-0.85	1411.03	217.463	19.4214	675.001	0.753534
14	-0.08	-1.00	0.21	1556.5	374.999	1.12425E-005	716.748	0.678954
15	-0.07	-0.94	0.21	1561.48	375	1.91996E-005	730.87	0.672601
16	-0.06	-0.92	0.21	1563.22	375	0.000452333	735.826	0.670284
17	0.97	0.09	-0.27	1545.43	325.848	3.02808E-005	675.001	0.669456
18	1.00	0.10	-0.33	1536.79	314.534	4.09298	675	0.669181
19	-0.10	-0.97	0.13	1564.1	358.559	0.0002709	747.04	0.663847

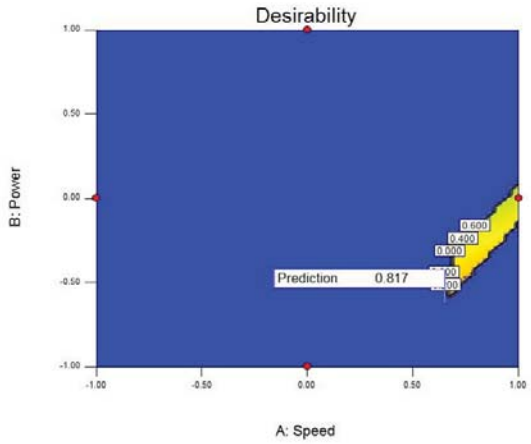

Figure 6. 50 Optimum of desirability of stack-up 0.75 mm-0.7 mm

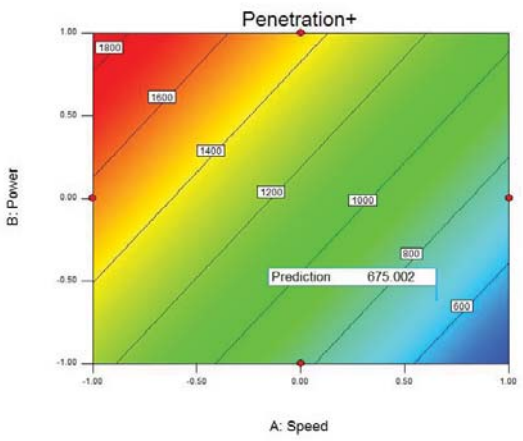

Figure 6. 51 Optimum of penetration on plane of power and speed for stack-up 0.75 mm-0.7 mm

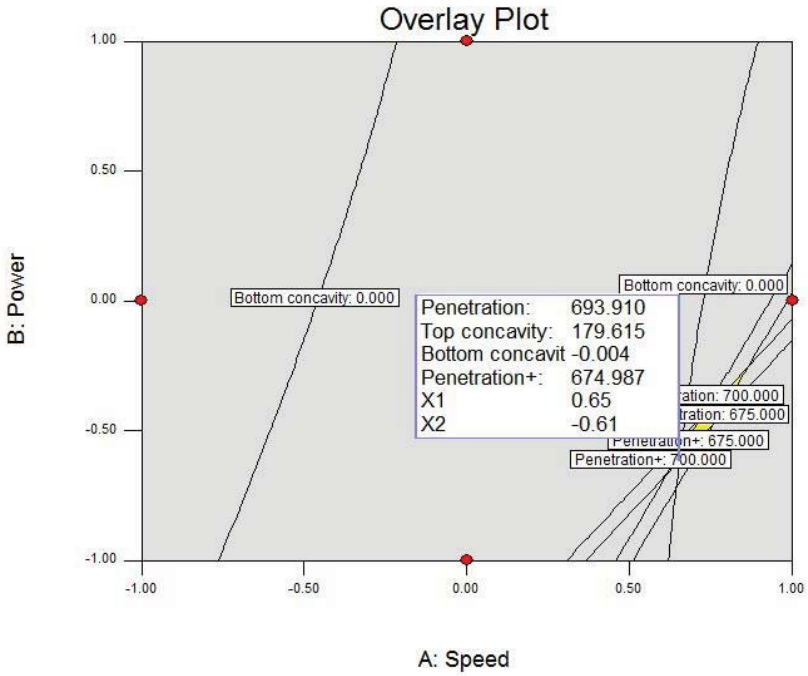

Figure 6. 52 Overlay Plot of Optimum setting gap at 0.05 mm

7. Conclusions and discussion

This chapter contains major conclusions in response to the goals of this study and discussion of limitations of this study.

7.1 Conclusions

In response to the goals of this study, several conclusions could be made based on the results of experimental campaigns.

1. As one of the two major goals of this study, the process window within which weld joints fulfilling industrial requirements are produced for stack-up DX56D+Z 1.00 mm plus DX54D+Z 1.00 mm turns out to be as follows: Power = [3.0,4.0] kW; Speed= [2.5, 5.5] m/min; Gap= [0.15, 0.30] mm. Visual inspection and cross-section microscopic inspection are the two steps of inspection of weld quality. In the visual inspection phase, defects like spatter, cut-through, burn-through and insufficient weld were observed.

2. Another purpose of this study is to maximize the speed and minimize the power and at the same time meet the cross-section geometric requirements so that optimal conditions for welding different stack-ups could be found. For stack-up of 0.75 mm-1.80 mm, an optimal frontier is available and optimized desirability result is speed= 3.30 m/min, power = 3.80 kW and gap= 0.15 mm; Similarly, for stack-up of 0.75mm-1.00mm, a frontier could be obtained and the optimized desirability result is speed=3.86 m/min, power= 3.19 kW and gap= 0.18 mm. For stack-up of 0.75 mm-0.70 mm, the optimized working condition is speed=4.65 m/min, power=3.2 kW and gap=0.15 mm.

The optimization analysis is run based on the following response models:

Top concavity=324.30+55.06 *A-15.49*B +190.19* C

Penetration=1021.73-419.02*A+312.93*B -199.19* C

No regression models could be deducted for interface width and bottom concavity. The models show speed (A) has negative effect on penetration while positive effect on top concavity, which means faster speed would reduce penetration but increase top concavity. Power (B) has positive effect on penetration and negative effect on top concavity. Gap (C) has negative effect on penetration and positive effect on top concavity.

3. In order to simplify the modelling process and avoid tedious experimental work, a paired mean hypothesis testing between stack-up of 0.75 mm-1.80 mm and stack-up of 0.75 mm-1.00 mm is done and concludes that the lower thickness is not a significant factor for the welding process. This is why the response model of stack-up 0.75mm plus 1.80 mm could be shared to optimized for other stack-ups with thinner lower thickness, assuming they are partially penetrated without bottom concavity. This conclusion is prerequisite for optimizing for different stack-ups.

7.2 Discussion

Given more time and resources, more work could have been done in improving the accuracy of the correlation model. Observing from the linear empirical models of penetration and top concavity, more experimental campaigns could have been

designed around the optimal experimental setup with smaller process windows. In this way possibly curvature models could be obtained, which could display more detailed information. Besides, the replicates of the centre points in Box-Behnken design could have bigger size, in which case the lack-of-fit testing could be more statistically reliable. Another shortcoming of this study is the lack of confirmation trials that have been run to verify the optimal results due to time and resource limitation. Given more time, the three optimum experimental points should have been run and compared to the predicted value.

It is also noticed that the interface width of all produced welded joints exceed 1000 μm which is much bigger than the required 90% of the thinner thickness (675μm). It means the constraint is losing its importance. As to the bottom concavity, in the RSM modelling phase, the models assume partial or near full penetration without bottom concavity. Nevertheless, there are actually a few weld joints with bottom concavity (trial 1, 7, 8) and to which degree they are affecting the accuracy of the correlation model of penetration is not clear. This issue could have been further investigated if time and resource are sufficient.

Another concern of this study needs to be clarified. In the phase of metallographic treatment, cross-section of the stitch is a crucial step of the study. The total length of a stitch is 25mm, and it is cut into five pieces. For the RSM analysis, the centre surface is chosen to represent the weld bead profile. However, an interesting phenomenon could be spotted if every cross-section is carefully observed. For example, when the speed is 3.00 m/min, power is 4.00 kW and gap is 0.25 mm, the five cross-sections of the stitch are shown in Figure 7. 1, Figure 7. 2, Figure 7. 3, Figure 7. 4 and Figure 7. 5. The bead profiles show some degree of similarity.

However, if measurements are taken with high resolution, the differences of the measurements are quite obvious. The differences are analysed in MATLAB, and the mean values and standard deviations of the geometric structure are calculated and shown in Figure 7. 6, Figure 7. 7, Figure 7. 8 and Figure 7. 9. The standard deviations of top surface concavity, interface width, penetration and bottom surface concavity are around 20~30 μm which are acceptable amount of errors in this experimental setting. However, under certain experimental settings, for example, when the speed is 4 m/min, power is 3 kW and gap is 0.30 mm, the cross-sections show very different landscapes (Figure 7. 10, Figure 7. 11, Figure 7. 12 and Figure 7. 13). In such case, the selection of centre data to represent the geometric structure is very risky and no countermeasure has been taken in response to such risk in this study, which might have undermined the accuracy of the established models.

However, generally speaking though variation exists within one stitch, it is controlled at acceptable level and displays the reliability and repeatability of the welding system. The cross-sections for all the BBD could be referred to in Appendix A, and the variation analysis is in Appendix B.

Figure 7. 1 Cross-section 1 of trial 1

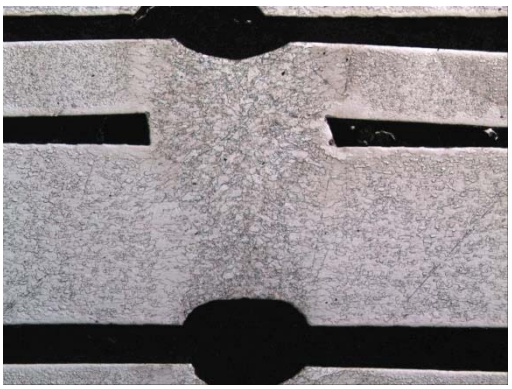

Figure 7. 2 Cross-section 2 of trial 1

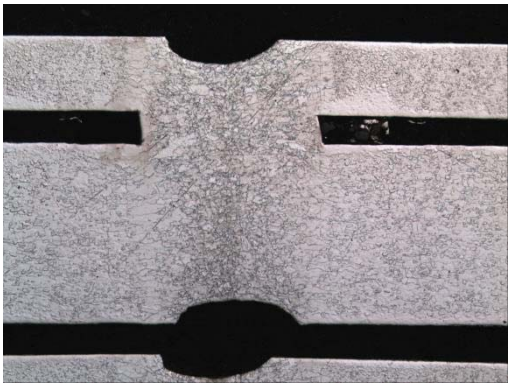

Figure 7. 3 Cross-section 3 of trial 1

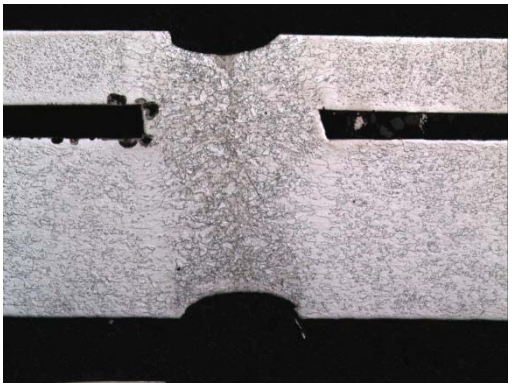

Figure 7. 4 Cross-section 4 of trial 1

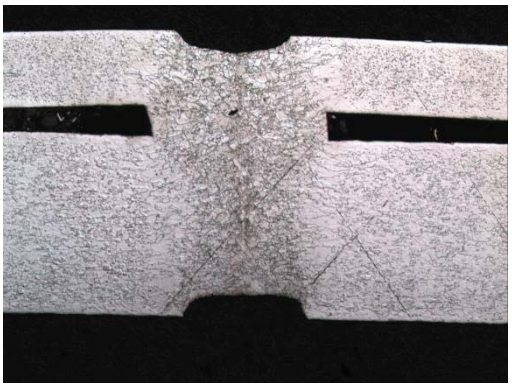

Figure 7. 5 Cross-section 5 of trial 1

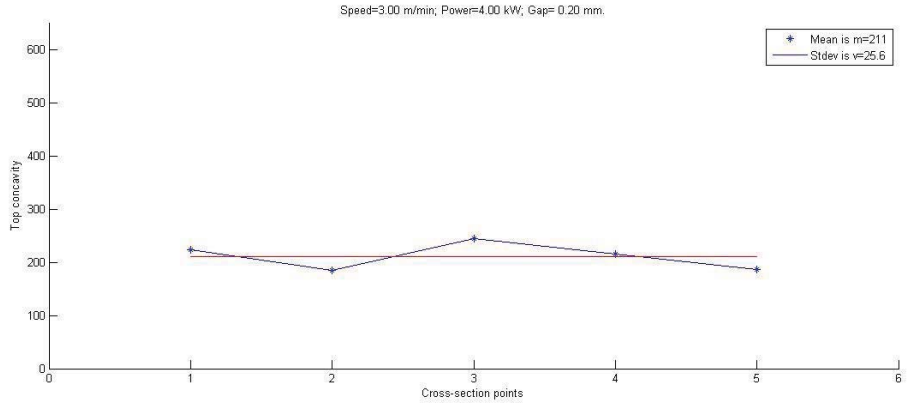

Figure 7. 6 The mean value and standard deviation of top surface concavity

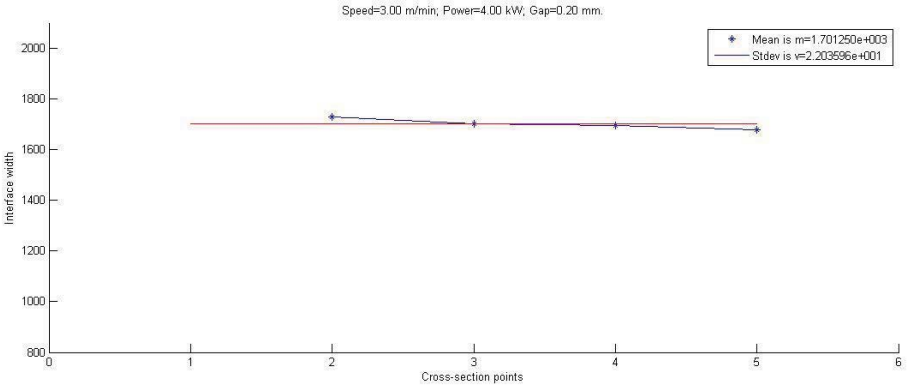

Figure 7. 7 The mean value and standard deviation of interface width

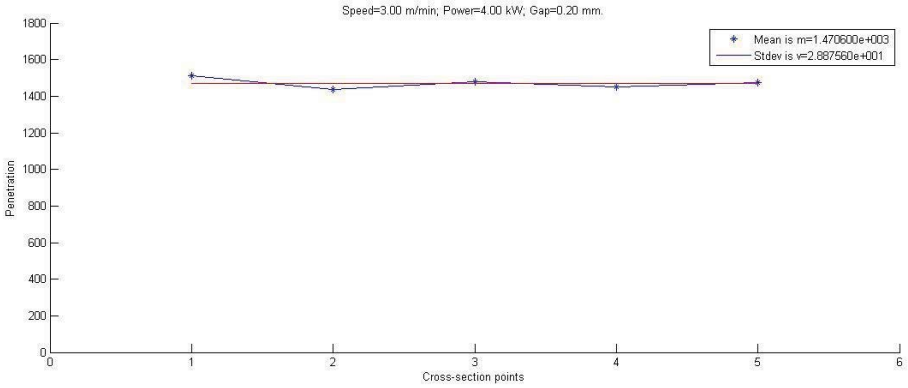

Figure 7. 8 The mean value and standard deviation of Penetration

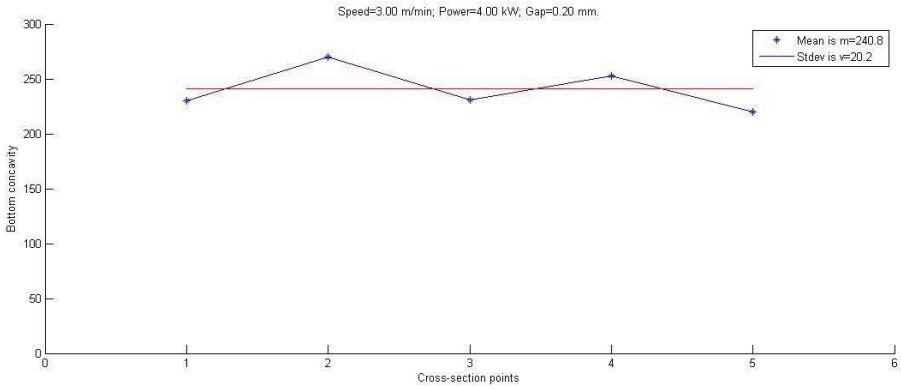

Figure 7. 9 The mean value and standard deviation of bottom surface concavity

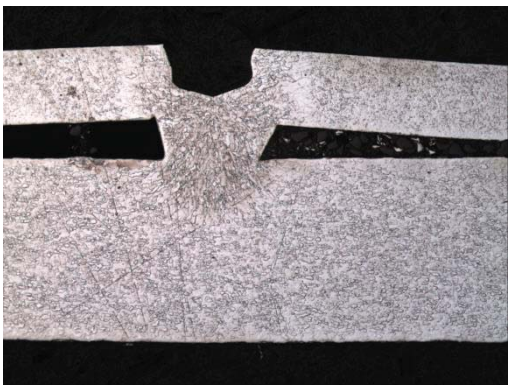

Figure 7. 10 Cross-section 1 if trial 4

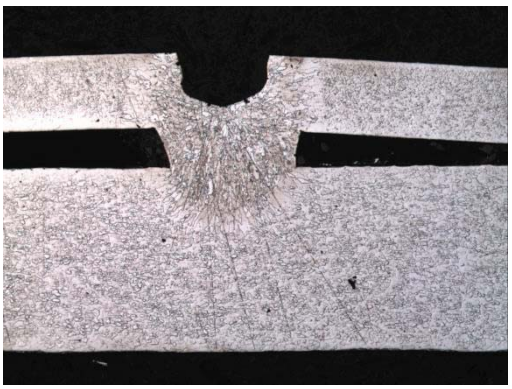

Figure 7. 11 Cross-section 2 of trial 4

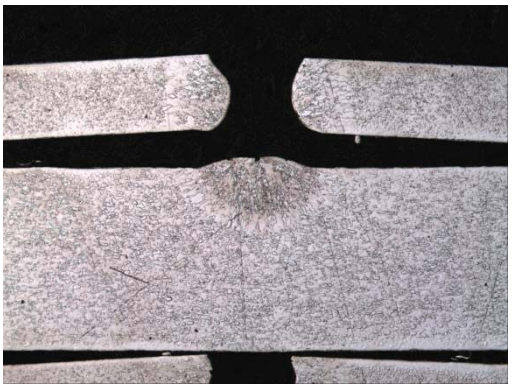

Figure 7. 12 Cross-section 3 of trial 4

Figure 7. 13 Cross-section 4 of trial 4

References

ANAWA, E. & OLABI, A.-G. 2008. Optimization of tensile strength of ferritic/austenitic laser-welded components. *Optics and Lasers in Engineering,* 46**,** 571-577.

ARROYAVE, A. O. 2012. *OPTIMIZATION OF REMOTE LASER WELDING PROCESS PARAMETERS USING DESIGN-OF-EXPERIMENTS AND ADAPTIVE SAMPLING.* MSc in Manufacturing Systems Engineering, University of Warwick

BAARDSEN, E. L. 1975. *Method of welding galvanized steel*. United States of America patent application.

BANAS, C. M. & DOYLE, B. M. 1987. *Twin spot laser welding*. United States of America patent application.

BENYOUNIS, K. & OLABI, A. 2008. Optimization of different welding processes using statistical and numerical approaches–a reference guide. *Advances in Engineering Software,* 39**,** 483-496.

BENYOUNIS, K., OLABI, A. & HASHMI, M. 2005a. Optimizing the laser-welded butt joints of medium carbon steel using RSM. *Journal of Materials Processing Technology,* 164**,** 986-989.

BENYOUNIS, K. Y., OLABI, A. G. & HASHIMI, M. S. J. 2005b. Effect of laser welding parameters on the heat input and weld-bead profile. *Journal of Materials Processing Technology,* 164-165**,** 978-985.

BILGE, U., JENUWINE, W. C. & JURCZYSZYN, C. E. 1993. *Laser welding method.* United States of America patent application.

BLEY, H., WEYAND, L. & LUFT, A. 2007. An alternative approach for the cost-efficient laser welding of zinc-coated sheet metal. *CIRP Annals-Manufacturing Technology,* 56**,** 17-20.

CEGLAREK, D. & SHI, J. 1995. Dimensional variation reduction for automotive body assembly. *Manufacturing Review,* 8.

CHEN, G., MEI, L., ZHANG, M., ZHANG, Y. & WANG, Z. 2012. Research on key influence factors of laser overlap welding of automobile body galvanized steel. *Optics & Laser Technology*.

CHEN, W., ACKERSON, P. & MOLIAN, P. 2009. CO_2 laser welding of galvanized steel sheets using vent holes. *Materials and Design,* 30**,** 245-251.

COLOMBO, D., COLOSIMO, B. M. & PREVITALI, B. 2012. Comparison of methods for data analysis in the remote monitoring of remote laser welding. *Optics and Lasers in Engineering*.

FABBRO, R., COSTE, F., GOEBELS, D. & KIELWASSER, M. 2006. Study of CW Nd-YAG laser welding of Zn-coated steel sheets. *Journal of Physics D: Applied Physics,* 39**,** 401-409.

GRUPP, M., SEEFELD, T. & VOLLERTSEN, F. Laser beam welding with scanner. Proceeding of the second international WLT-conference on lasers in manufacturing, LIM, 2003.

HIGUCHI, T. 2010. Remote laser welding–development and applications in American automotive industries. *Welding International,* 24**,** 764-767.

ISHIKAWA, K. & ISHIKAWA, K. 1982. *Guide to quality control*, Asian Productivity Organization Tokyo.

JENG, J.-Y., MAU, T.-F. & LEU, S.-M. 2000. Prediction of laser butt joint welding parameters using back propagation and learning vector quantization networks. *Journal of Materials Processing Technology,* 99**,** 207-218.

JURAN, J. M., GODFREY, A. B., HOOGSTOEL, R. E. & SCHILLING, E. G. 1999. *Juran's quality handbook*, McGraw Hill New York.

KANG, H.-S., SUH, J. & KWAK, S. J. Welding on the Fly by using Laser Scanner and Robot. Control, Automation and Systems (ICCAS), 2011 11th International Conference on, 2011. IEEE, 1688-1691.

KHAN, M., ROMOLI, L., FIASCHI, M., DINI, G. & SARRI, F. 2011. Experimental design approach to the process parameter optimization for laser welding of martensitic stainless steels in a constrained overlap configuration. *Optics & Laser Technology,* 43**,** 158-172.

LEE, H.-K., HAN, H.-S., SON, K.-J. & HONG, S.-B. 2006. Optimization of Nd: YAG laser welding parameters for sealing small titanium tube ends. *Materials Science and Engineering: A,* 415**,** 149-155.

MANONMANI, K., MURUGAN, N. & BUVANASEKARAN, G. 2007. Effects of process parameters on the bead geometry of laser beam butt welded stainless steel sheets. *The International Journal of Advanced Manufacturing Technology,* 32**,** 1125-1133.

MEI, L., CHEN, G., JIN, X., ZHANG, Y. & WU, Q. 2009. Research on laser welding of high-strength galvanized automobile steel sheets. *Optics and Lasers in Engineering,* 47**,** 1117-1124.

MIRAPEIX, J., GARCÍA-ALLENDE, P., COBO, A., CONDE, O. & LÓPEZ-HIGUERA, J. 2007. Real-time arc-welding defect detection and classification with principal component analysis and artificial neural networks. *Ndt & E International,* 40**,** 315-323.

MONTGOMERY, D. C. 1984. *Design and analysis of experiments*, Wiley New York.

MORI, K., TARUI, T., HASEGAWA, T. & YOSHIKAWA, N. 2010. Remote laser welding applications for car bodies. *Welding International,* 24**,** 758-763.

MYERS, R. H., MONTGOMERY, D. C. & ANDERSON-COOK, C. M. 2009. *Response Surface Methodology: Process and Product Optimization Using Designed Experiments*, Wiley.

OLABI, A. G. & ANAWA, E. 2006. Effects of laser welding conditions on toughness of dissimilar welded components. *Applied Mechanics and Materials,* 5**,** 375-380.

PADMANABAN, G. & BALASUBRAMANIAN, V. 2010. Optimization of laser beam welding process parameters to attain maximum tensile strength in AZ31B magnesium alloy. *Optics & Laser Technology,* 42**,** 1253-1260.

PAN, L. K., WANG, C. C., HSIAO, Y. C. & HO, K. C. 2005. Optimization of Nd: YAG laser welding onto magnesium alloy via Taguchi analysis. *Optics & Laser Technology,* 37**,** 33-42.

PENNINGTON, E. J. 1987. *Laser welding of galvanized steel*. United States of America patent application.

PETRICK, F. D. 1990. *Method of making hemmed joints utilizing laser welding*. United States of America patent application.

RITO, N., YAMADA, T., GOTOH, J. & KITAGAWA, T. 1988. *Laser welding method*. United States of America patent application.

RIZZI, D., SIBILLANO, T., CALABRESE, P., ANCONA, A. & LUGARA, P. 2011. Spectroscopic, energetic and metallographic investigations of the laser lap welding of AISI 304 using the response surface methodology. *Optics and Lasers in Engineering,* 49**,** 892-898.

SATHIYA, P., JALEEL, A., M.Y, KATHERASAN, D. & SHANMUGARAJAN, B. 2011. Optimization of laser butt welding parameters with multiple performance characteristics. *Optics & Laser Technology,* 43**,** 660-673.

SCHMIDT, M., OTTO, A. & KAGELER, C. 2008. Analysis of YAG laser lap-welding of zinc coated steel sheets. *CIRP Annals-Manufacturing Technology,* 57**,** 213-216.

SHIBATA, K. 2008. Recent automotive applications of laser processing in Japan. *The Review of Laser Engineering,* 36**,** 1188-1191.

SINGH, R. 2012. *Applied Welding Engineering: Processes, Codes, and Standards*, Butterworth-Heinemann.

SINHA, A. K., KIM, D. Y. & CEGLAREK, D. 2013. Correlation analysis of the variation of weld seam and tensile strength in laser welding of galvanized steel. *Optics and Lasers in Engineering*.

STEEN, W. M. & MAZUMDER, J. 2010. *Laser material processing*, Springer.

STOL, I. & MARTUKANITZ, R. P. 2004. *Laser welding with beam oscillation*. United States of America patent application.

VITEK, J., ISKANDER, Y., OBLOW, E., BABU, S., DAVID, S., FUERSCHBACH, P. & SMARTT, H. 1998. Neural network modeling of pulsed-laser weld pool shapes in aluminum alloy welds. Sandia National Labs., Albuquerque, NM (United States).

YIH-FONG, T. 2006. Gap-free lap welding of zinc-coated steel using plused CO_2 laser. *International Journal of Advanced Manufacturing Technology,* 29**,** 287-295.

ZHAO, Y., ZHANG, Y., HU, W. & LAI, X. 2012. Optimization of laser welding thin-gage galvanized steel via response surface methodology. *Optics and Lasers in Engineering,* 50**,** 1267-1273.

Appendix A

Referring to Table 6. 10

No.1 : speed=3.00 m/min; power= 4.00 kW; gap=0.20 mm

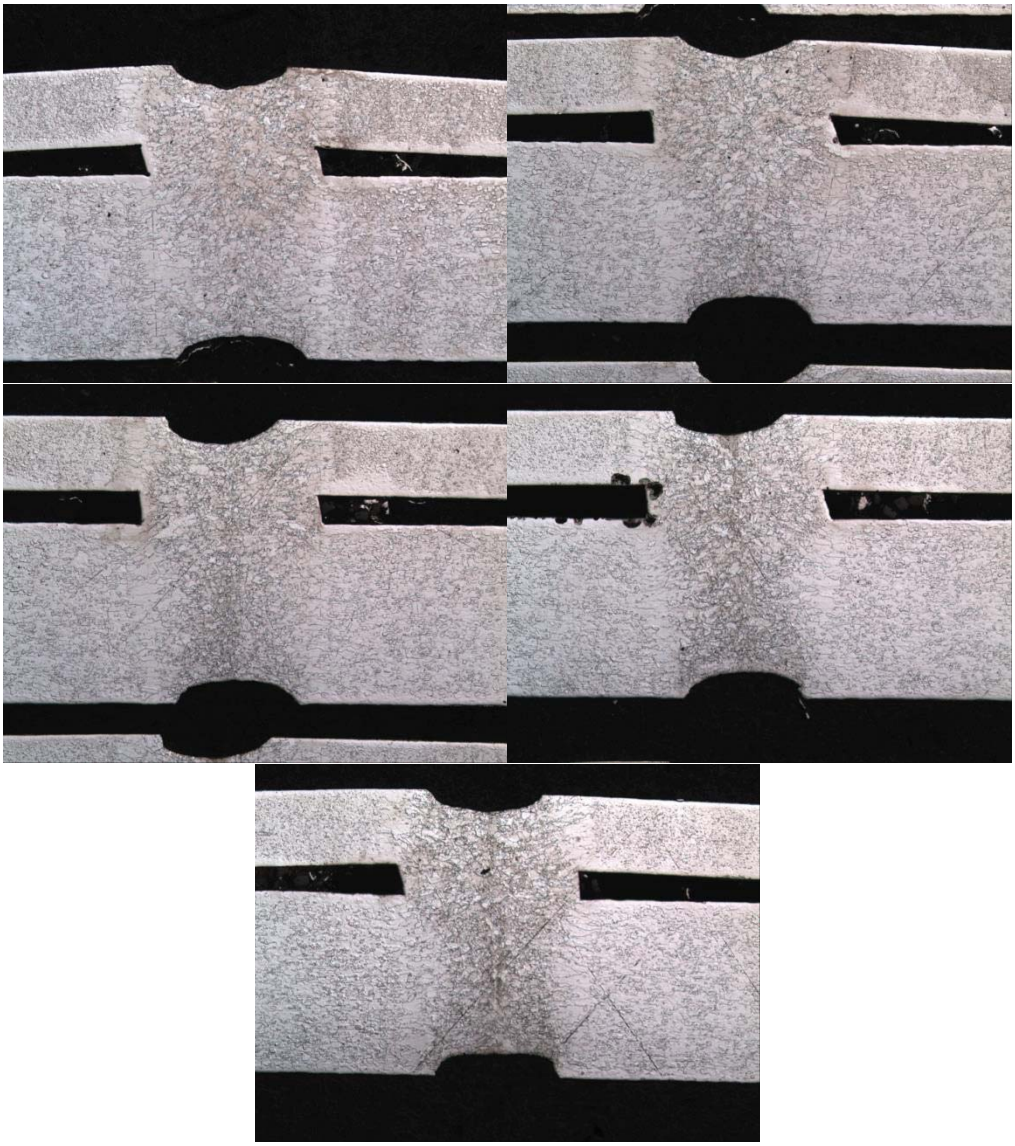

No.2: speed=5.00 m/min; power=3.00 kW; gap=0.25mm

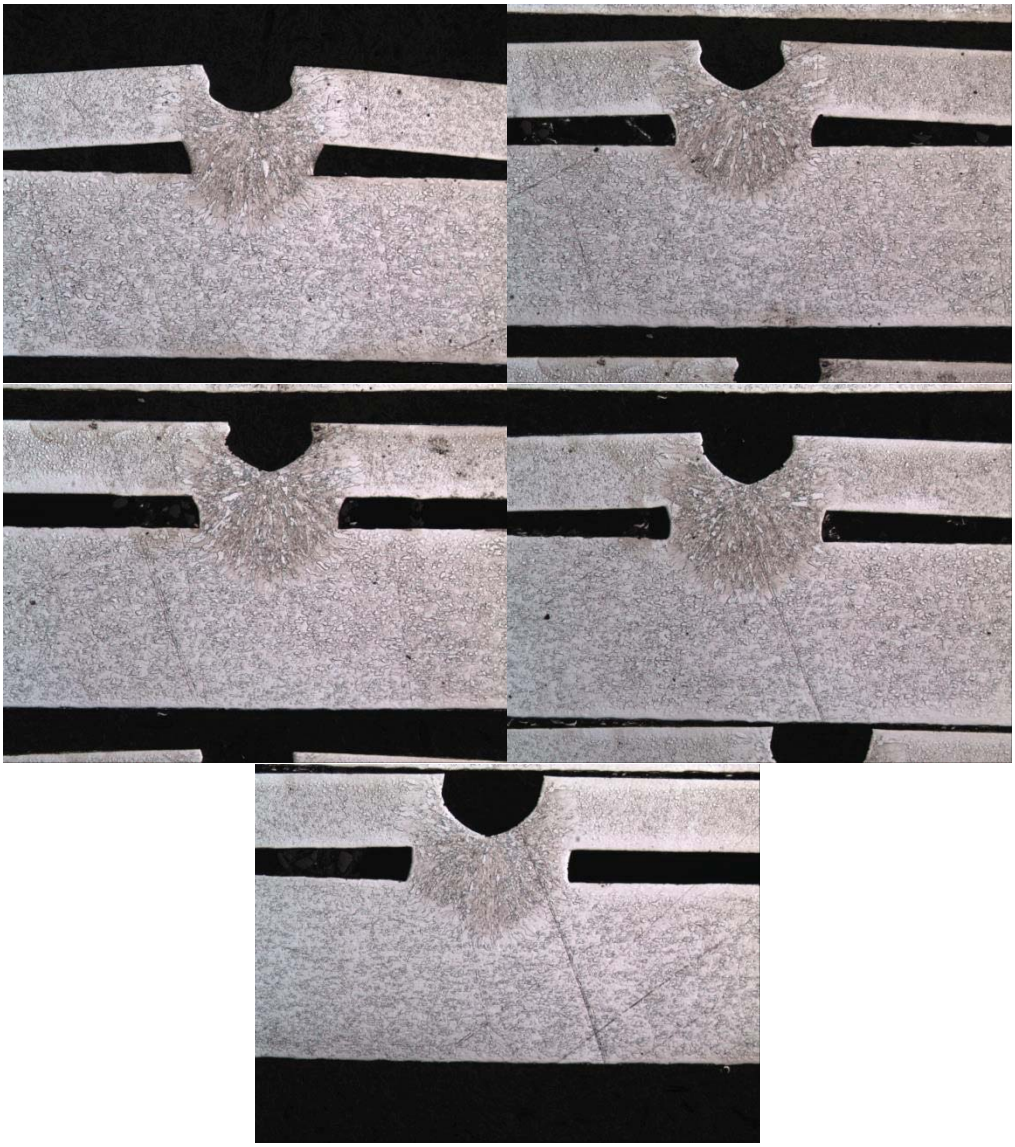

No.3 : speed=3.00 m/min; power =3.50 kW; gap=0.15 mm

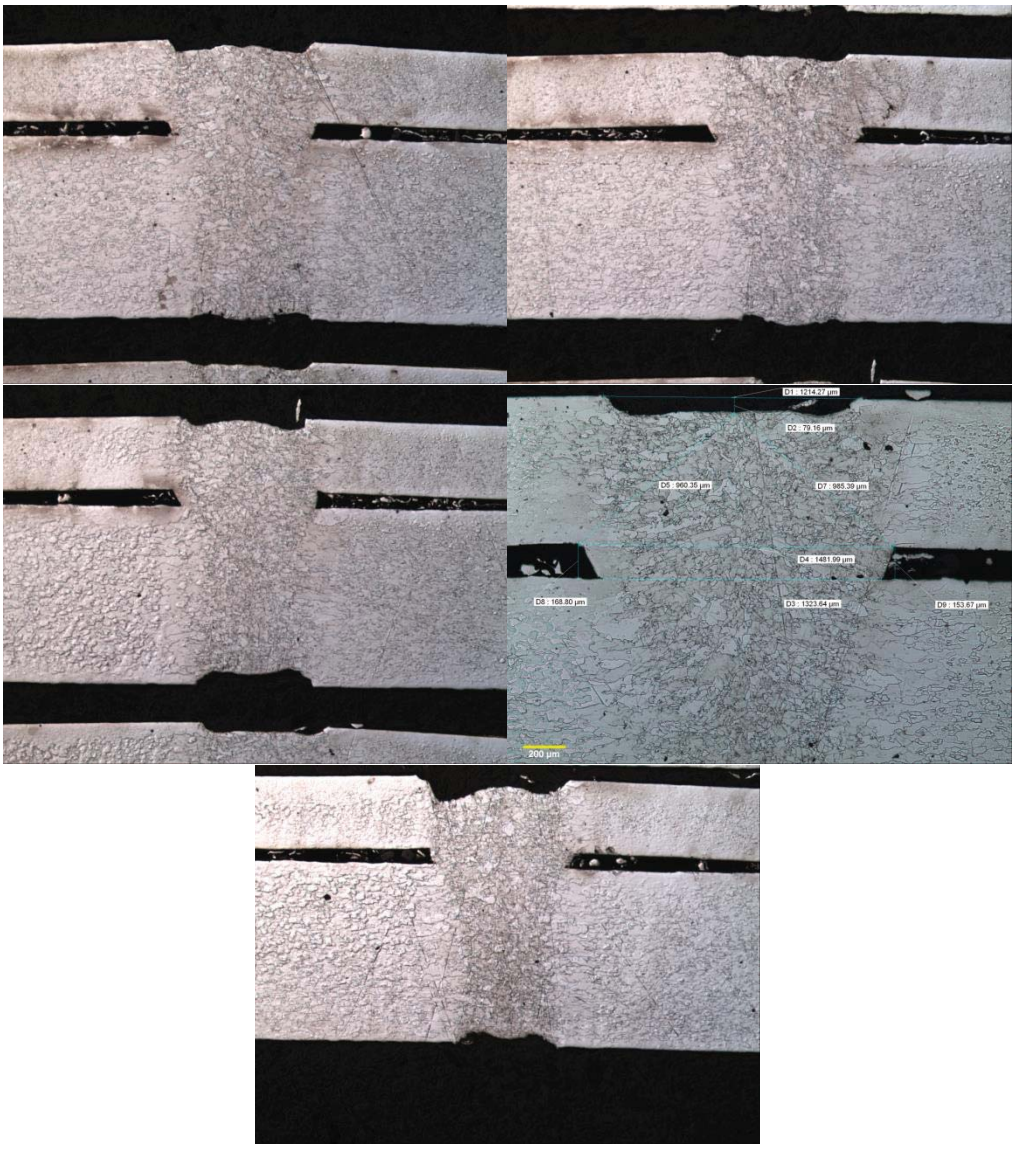

Note: the 4th picture with the same resolution is missing.

No.4 : speed=4.00 m/min; power= 3.00 kW; gap=0.25 mm

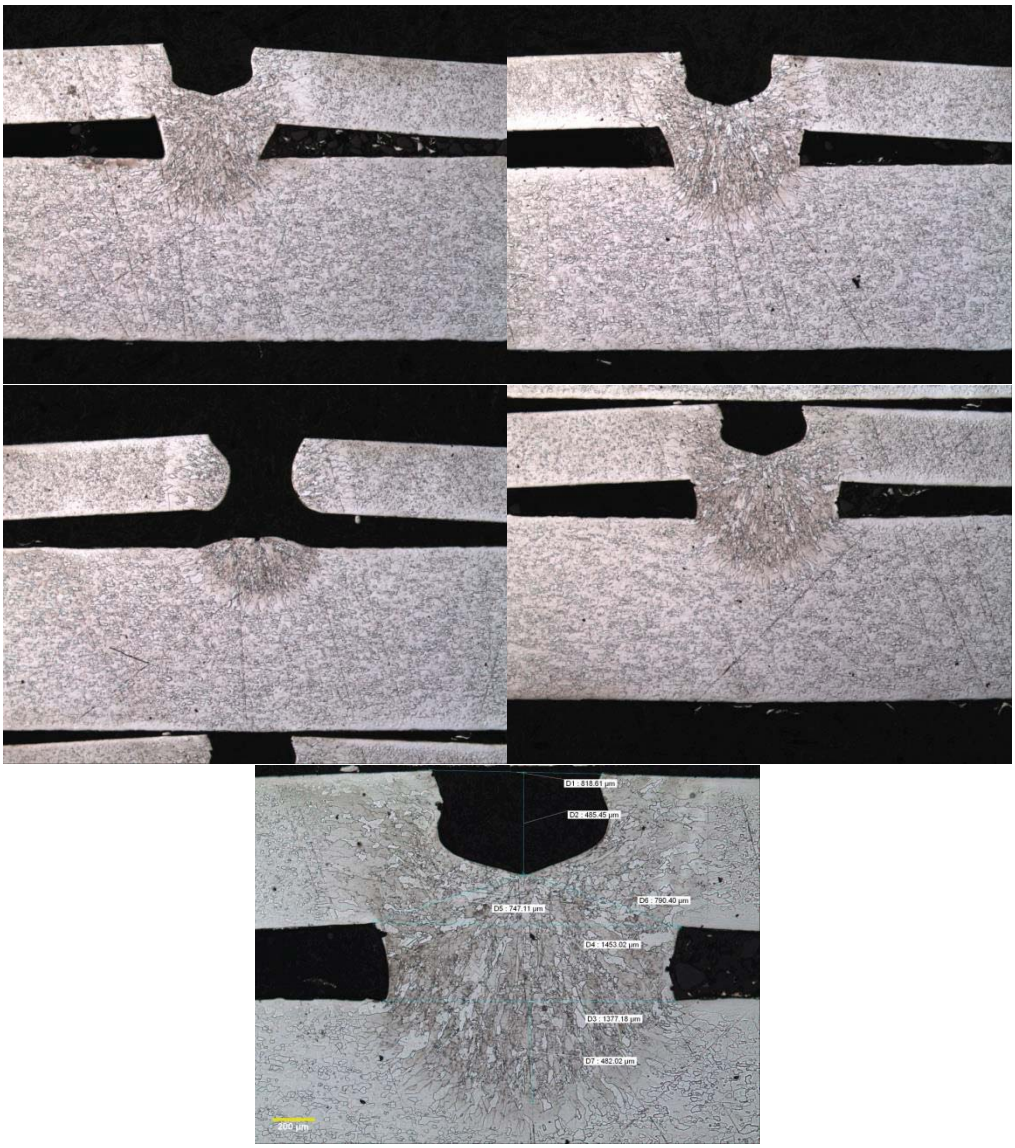

Note: the 5th picture with the same resolution is missing

No. 5: speed=4.00 m/min; power=3.50 kW; gap=0.20 mm

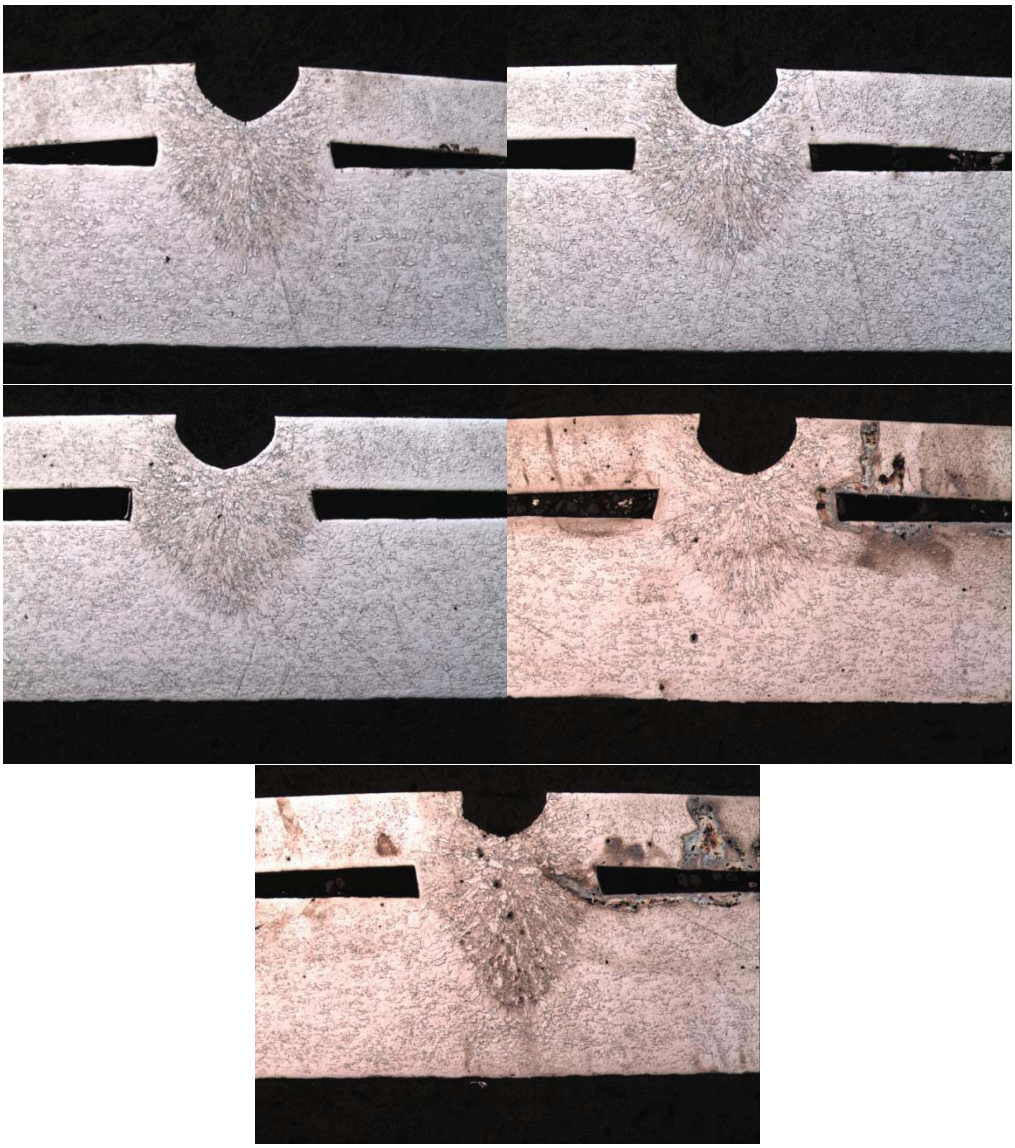

No.6 : speed=5.00 m/min; power= 4.00 kW; gap=0.20 mm

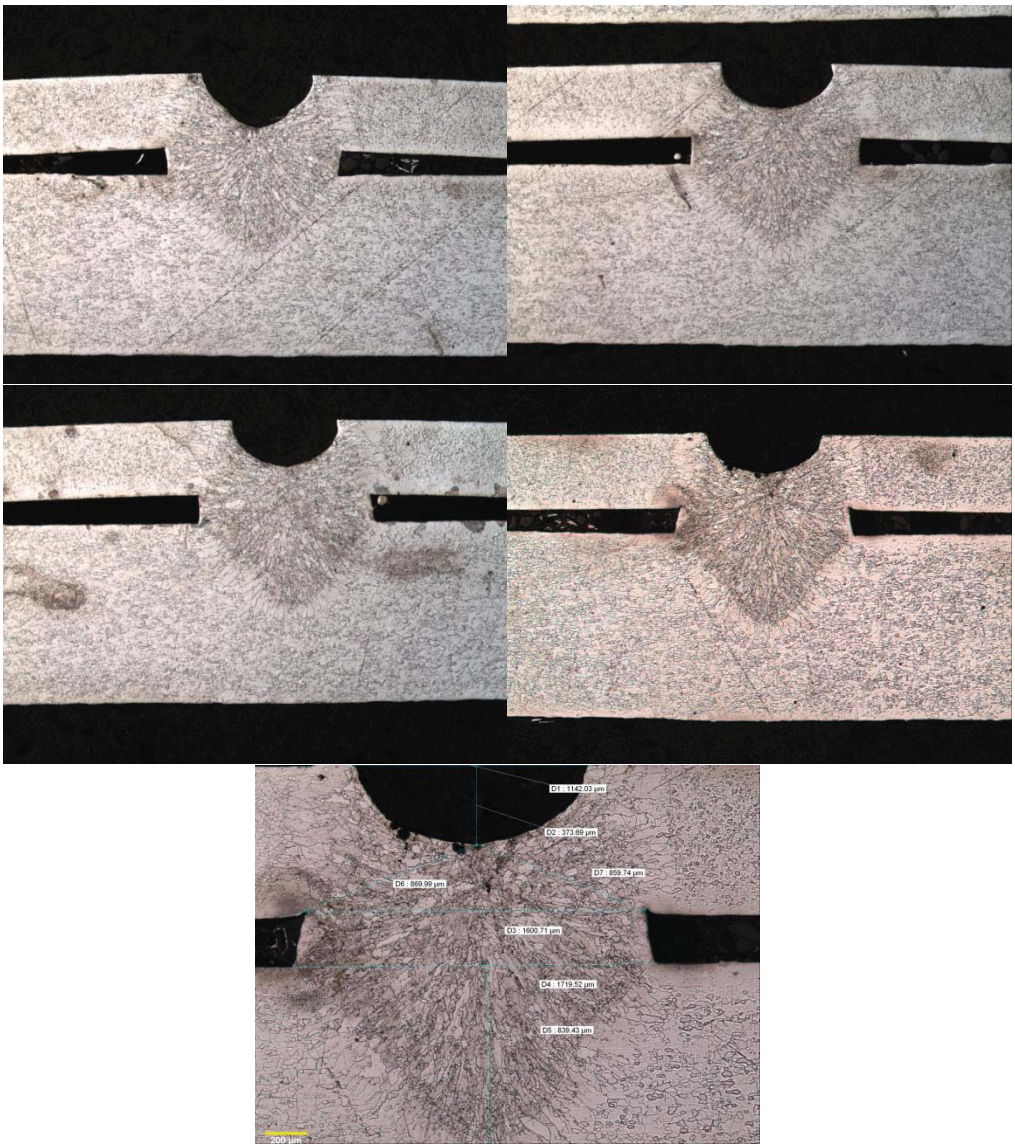

Note: the 5th picture with the same resolution is missing

No. 7: speed= 3.00 m/min; power= 3.00 kW; gap=0.20mm

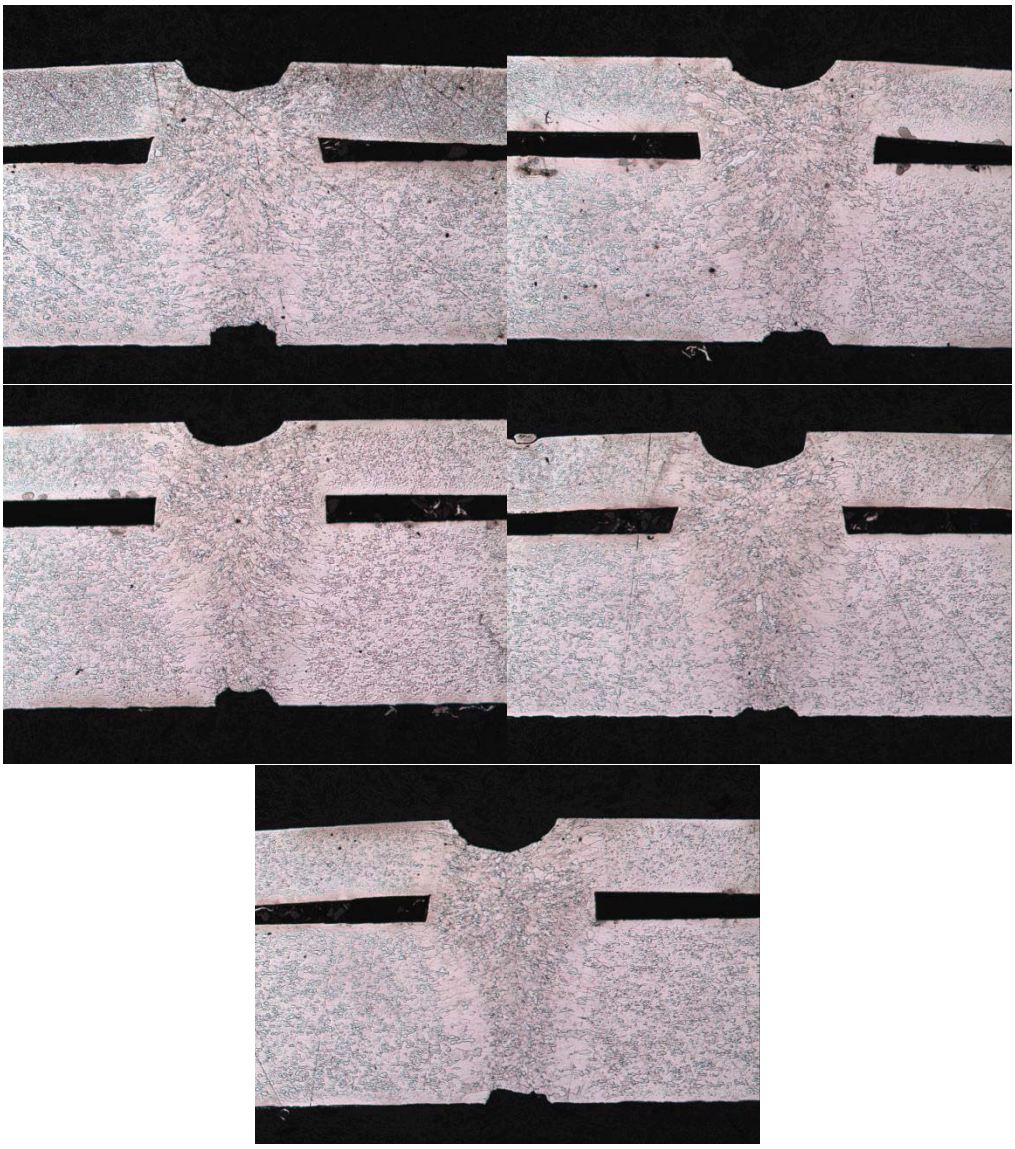

No. 8: speed= 3.00 m/min; power=3.50 kW; gap=0.25mm

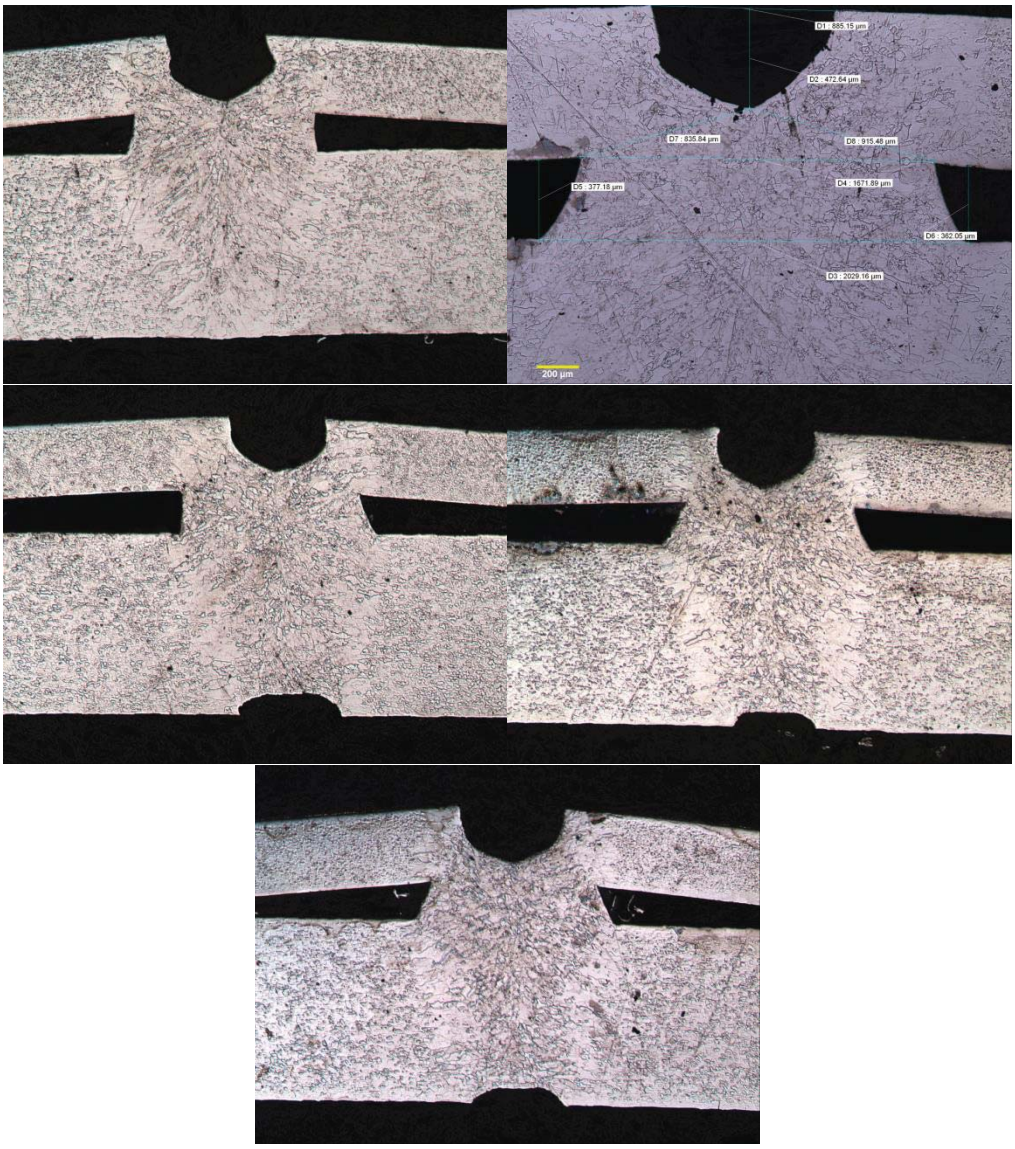

Note: the 2nd picture with the same resolution is missing

No. 9: speed=4.00 m/min; power= 3.50 kW; gap=0.20mm

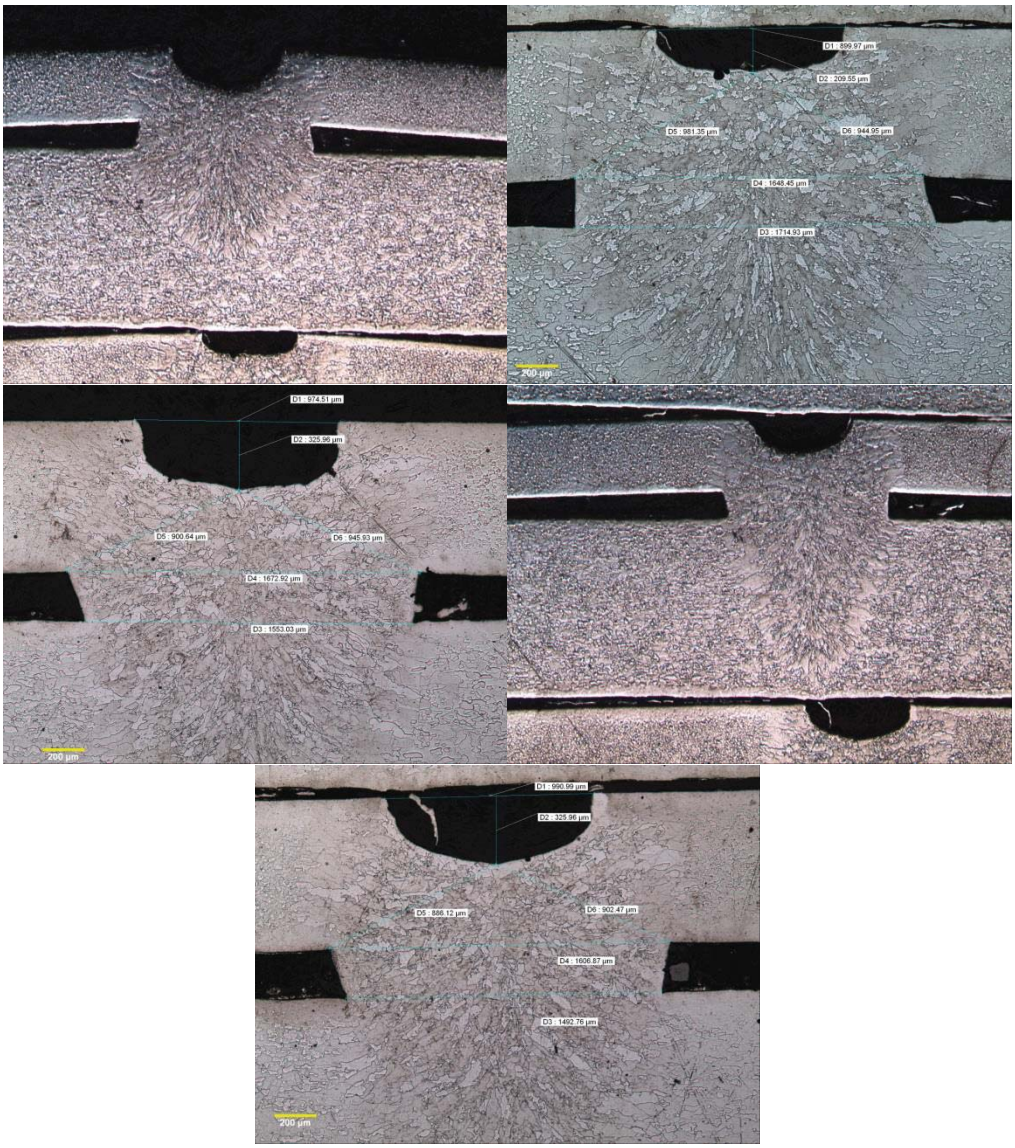

Note: the 2nd , 3rd and 5th pictures with the same resolution is missing

No. 10: speed=4.00 m/min; power= 3.50 kW; gap=0.20 mm

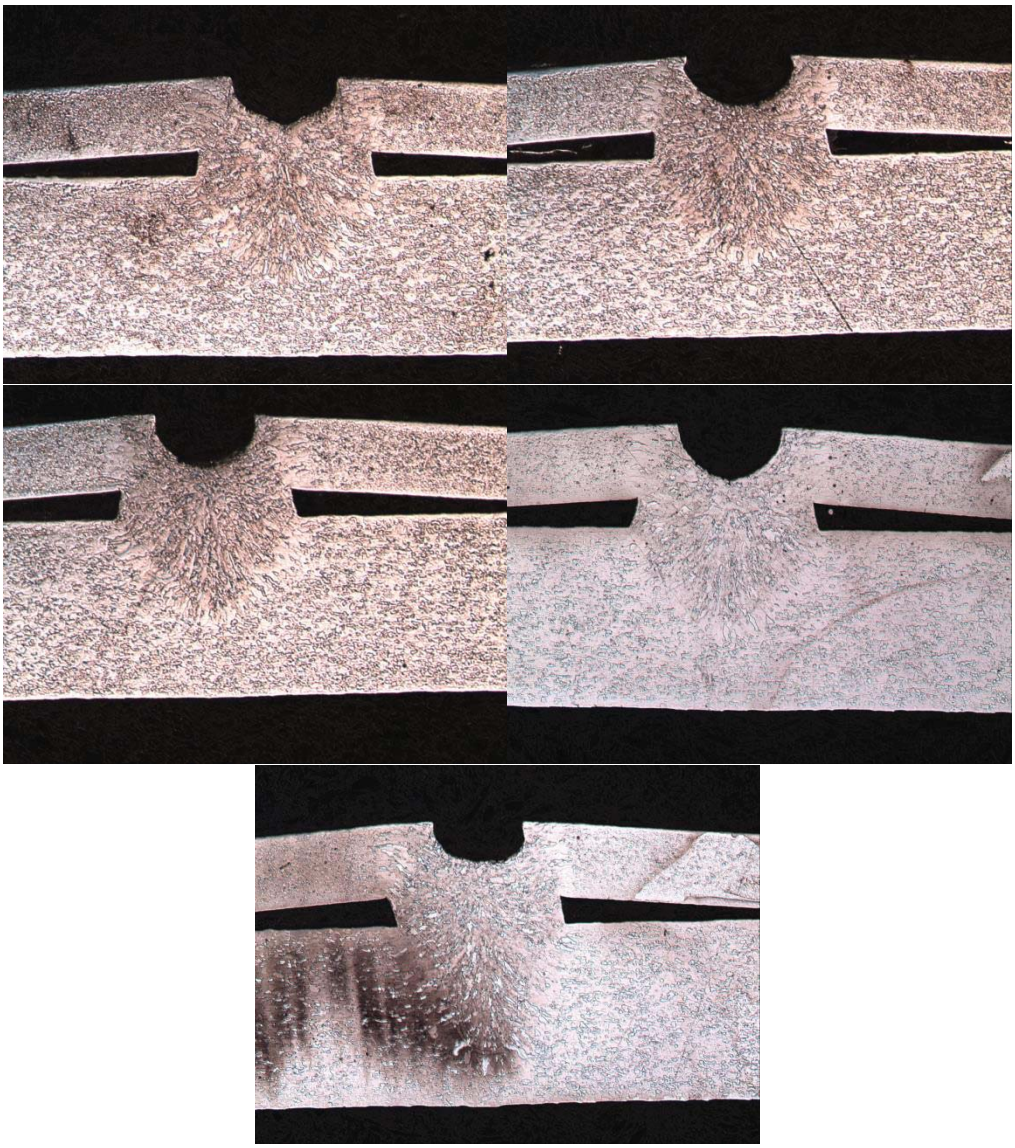

No.11: speed= 4.00 m/min; power= 3.00 kW; gap=0.15 mm

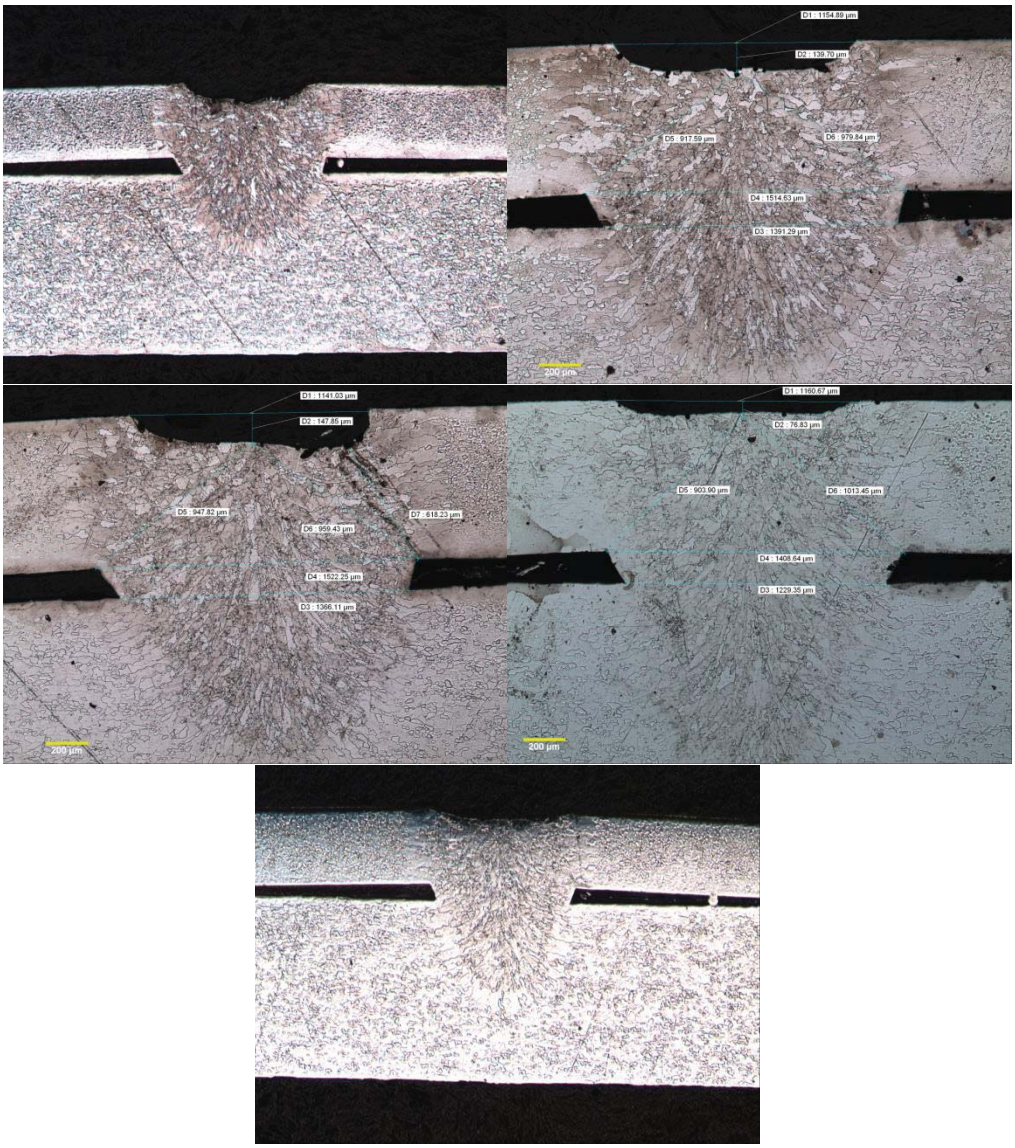

Note: the 2nd, 3rd and 4th pictures with the same resolution are missing

No. 12: speed= 5.00 m/min; power= 3.50 kW; gap=0.15 mm

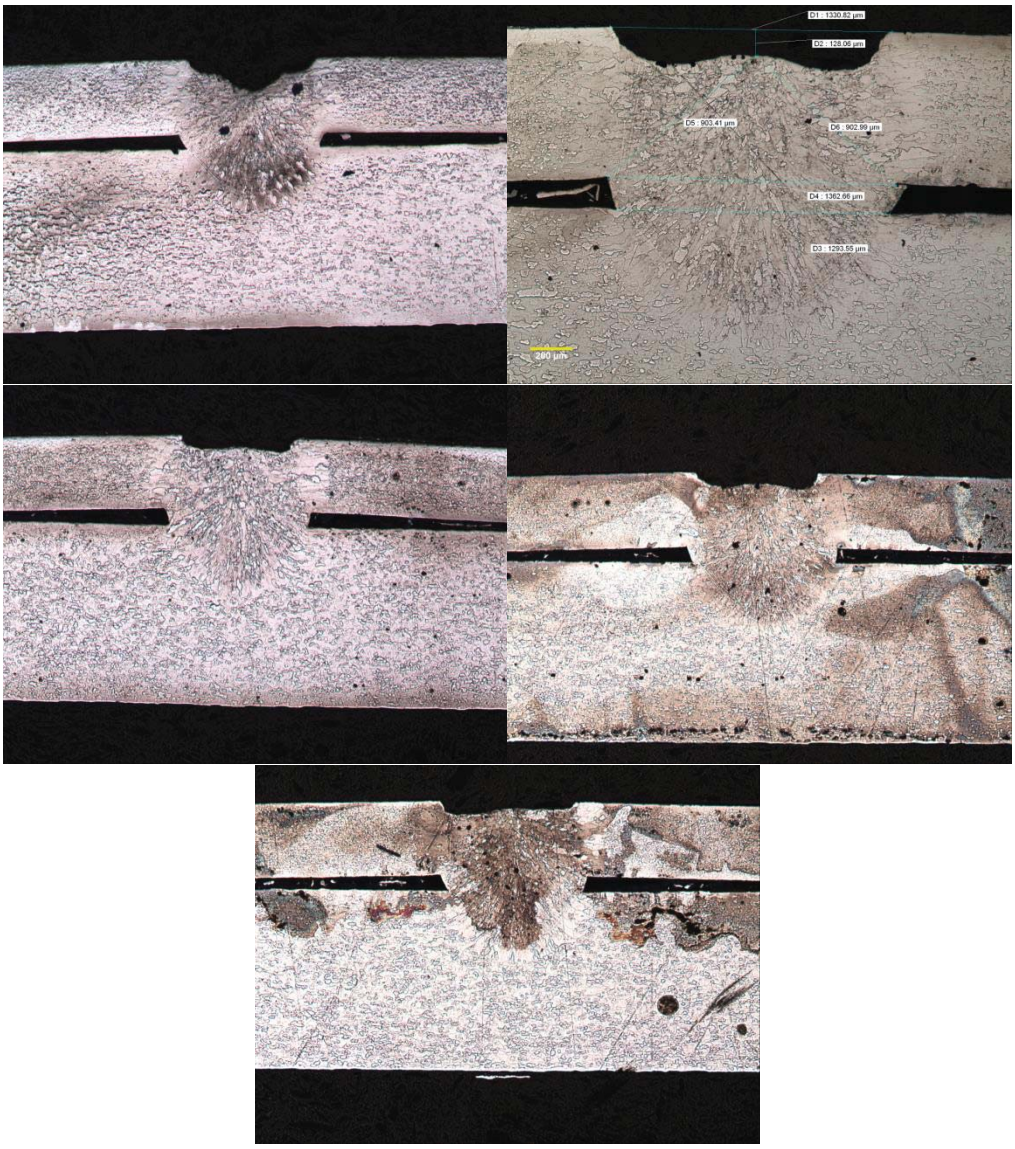

Note: the 2nd picture with the same resolution is missing

No. 13: speed= 5.00 m/min; power=3.00 kW; gap= 0.20 mm

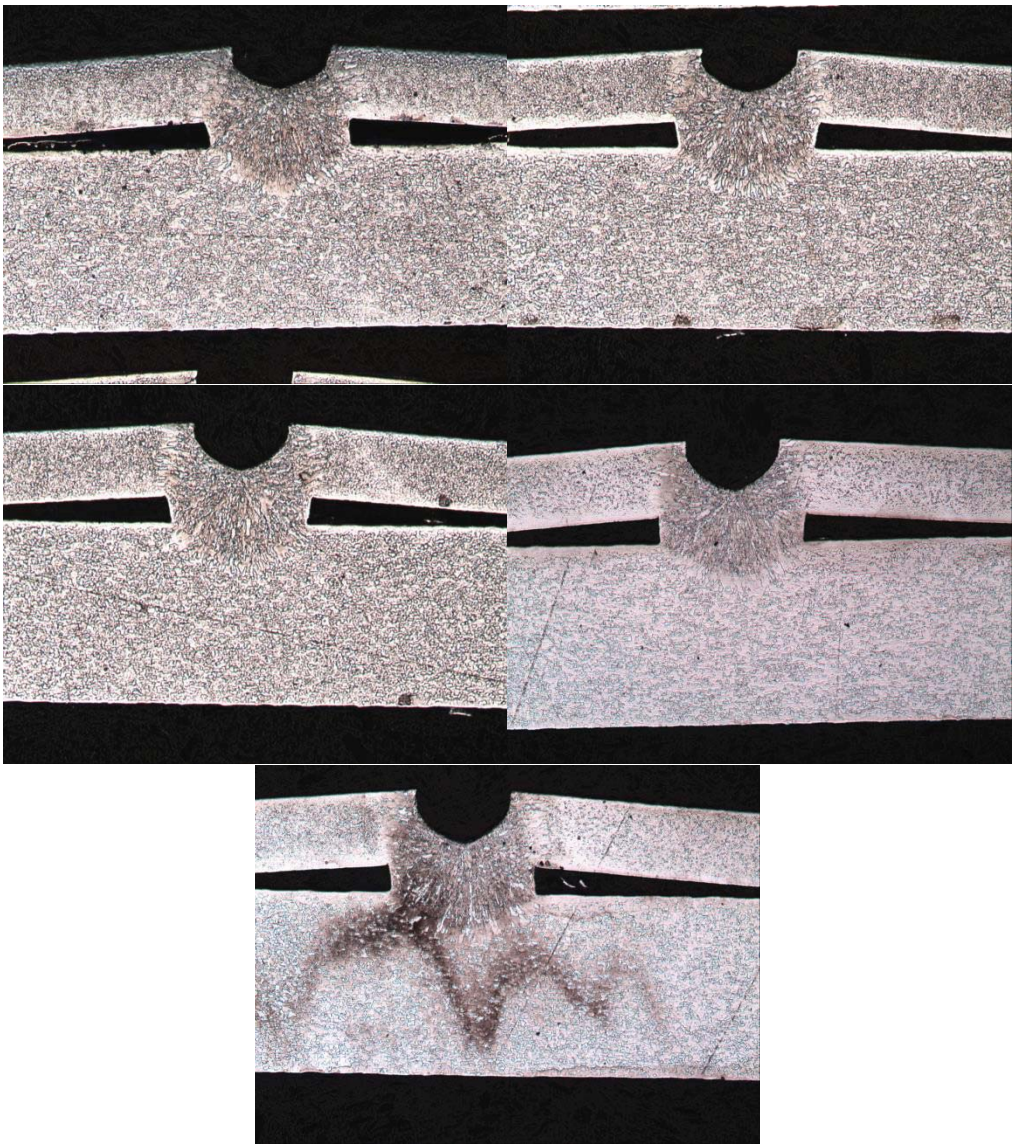

No. 14: speed=4.00 m/min; power=4.00 kW; gap= 0.15mm

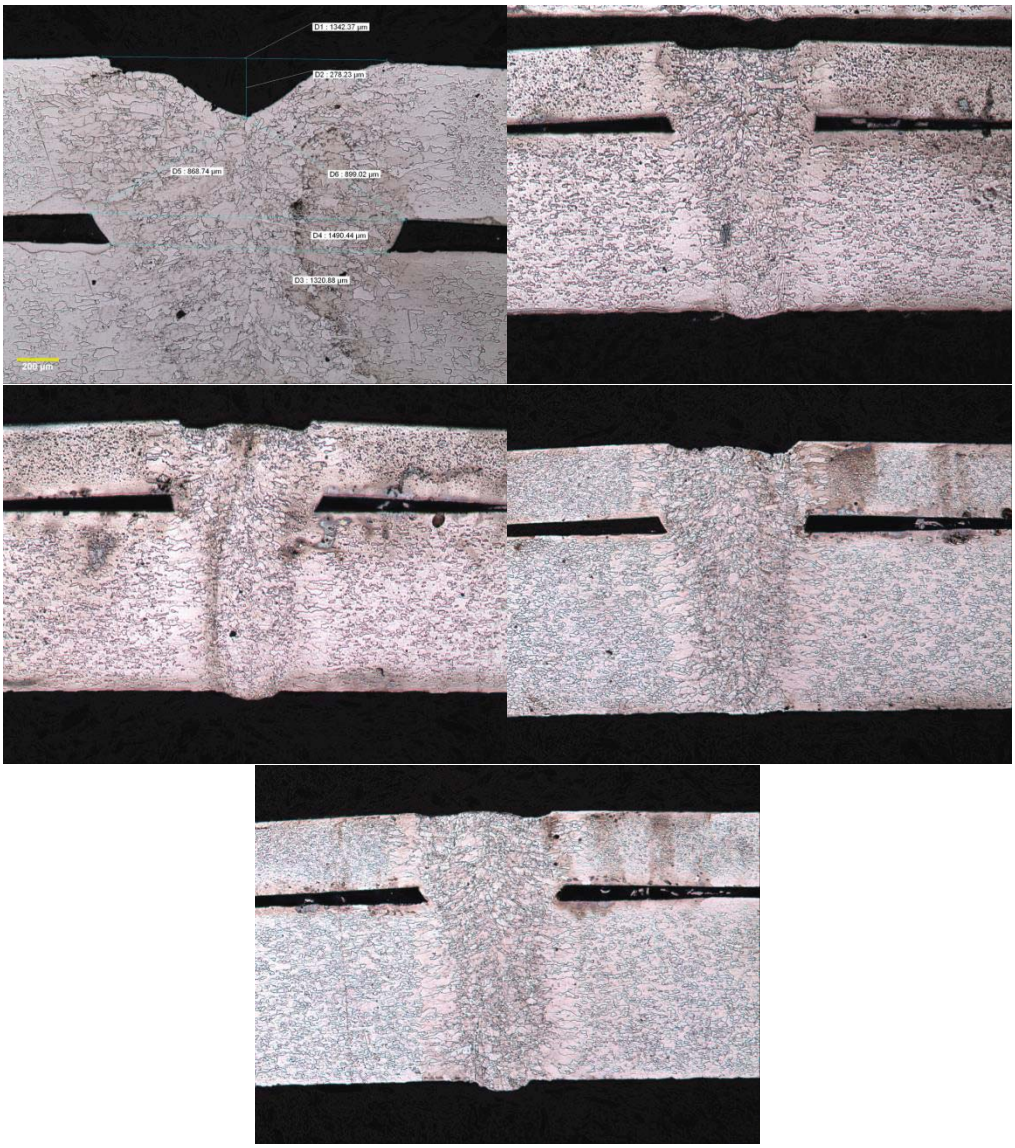

Note: the 1st picture with the same resolution is missing

No. 15: speed= 4.00 m/min; power= 4.00 kW; gap= 0.25 mm

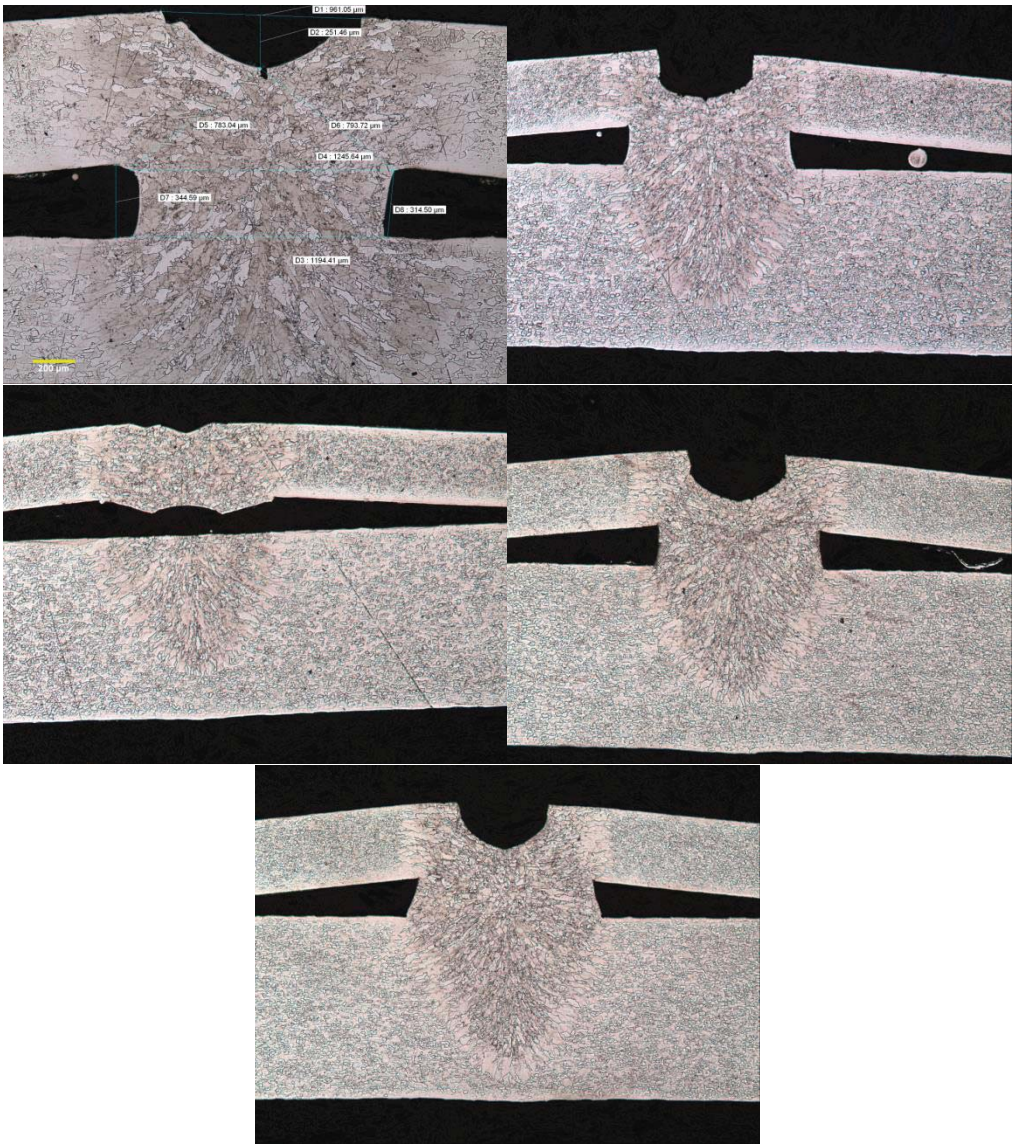

Note: the 1st picture with the same resolution is missing

Appendix B

Top concavity

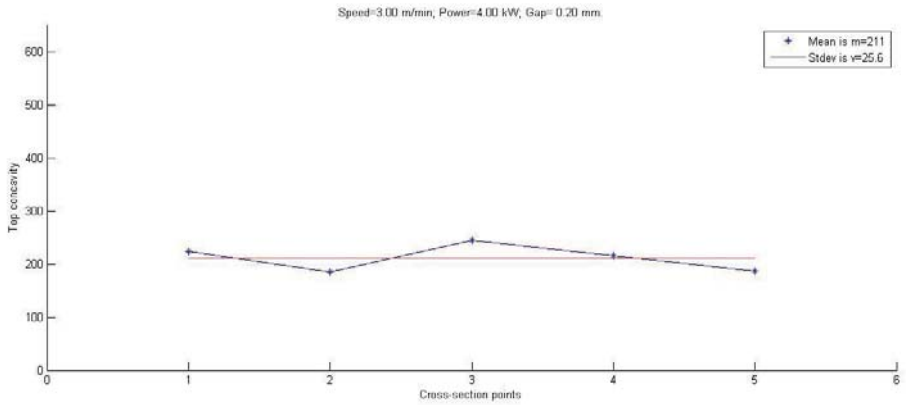

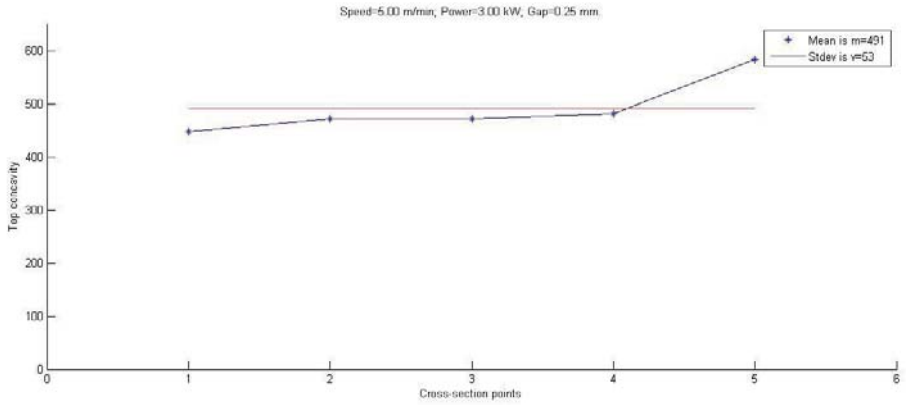

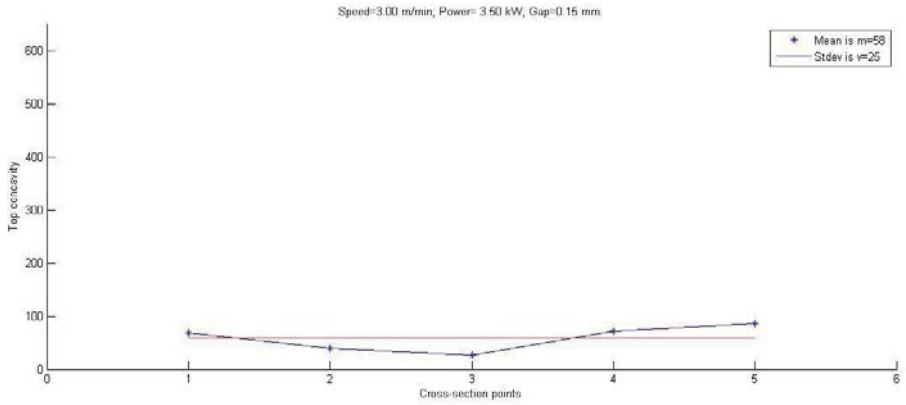

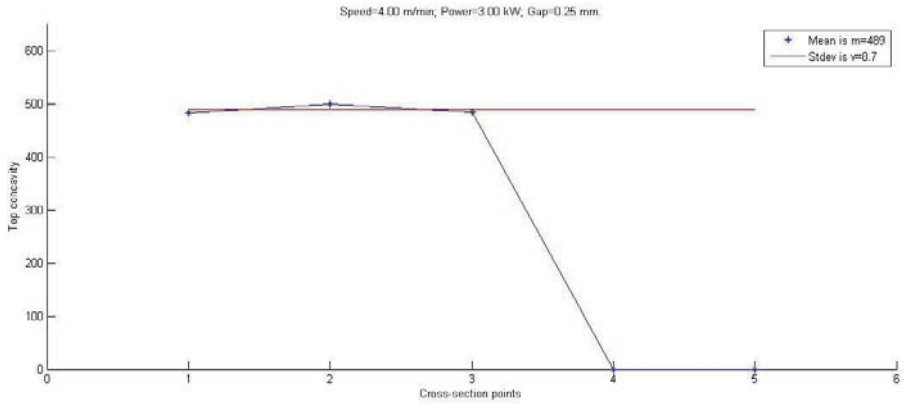
Speed=4.00 m/min; Power=3.00 kW; Gap=0.25 mm.
Mean is m=489
Stdev is v=0.7
Top concavity
Cross-section points

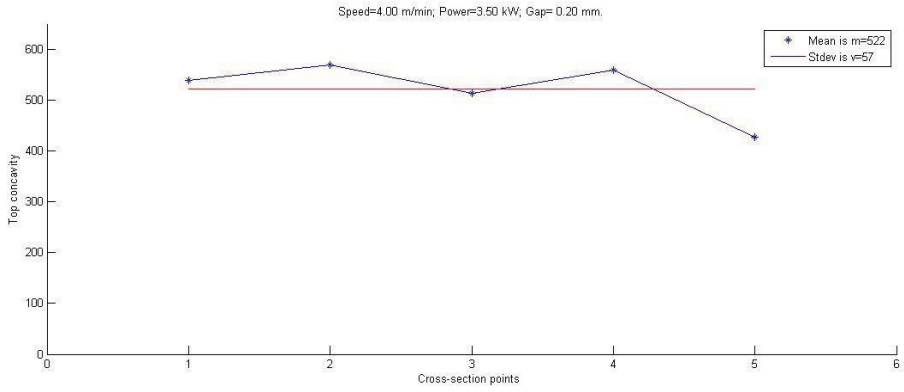
Speed=4.00 m/min; Power=3.50 kW; Gap= 0.20 mm.
Mean is m=522
Stdev is v=57
Top concavity
Cross-section points

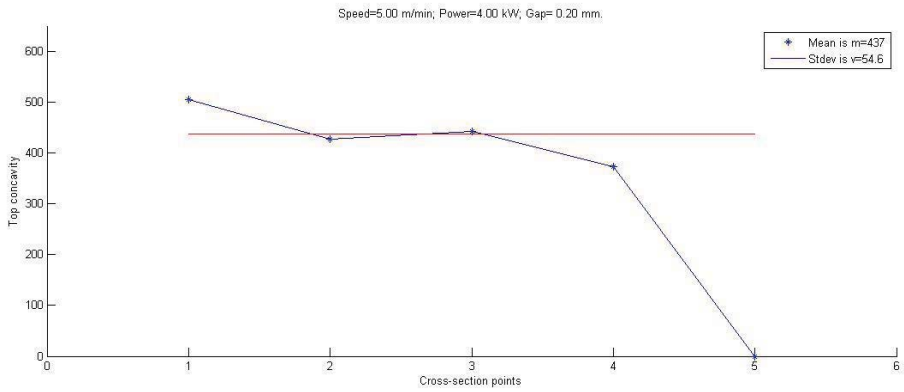
Speed=5.00 m/min; Power=4.00 kW; Gap= 0.20 mm.
Mean is m=437
Stdev is v=54.6
Top concavity
Cross-section points

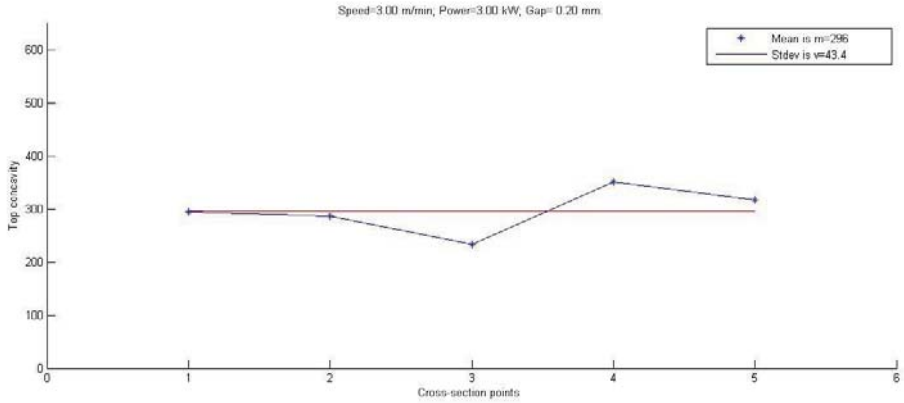
Speed=3.00 m/min; Power=3.00 kW; Gap= 0.20 mm.
Mean is m=296
Stdev is v=43.4
Top concavity
Cross-section points

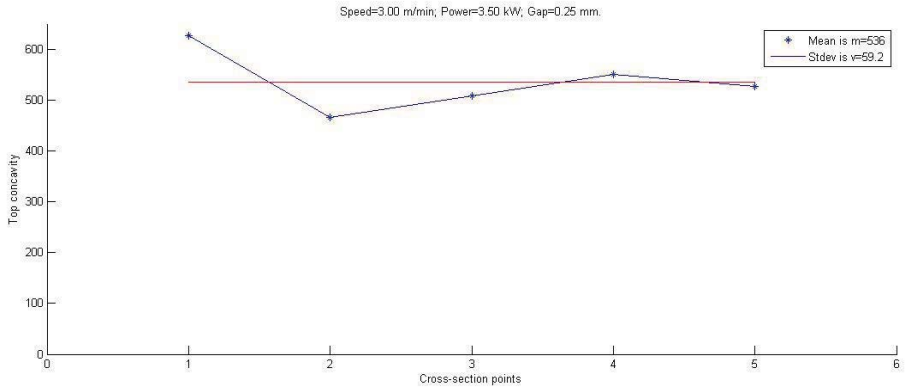
Speed=3.00 m/min; Power=3.50 kW; Gap=0.25 mm.
Mean is m=536
Stdev is v=59.2
Top concavity
Cross-section points

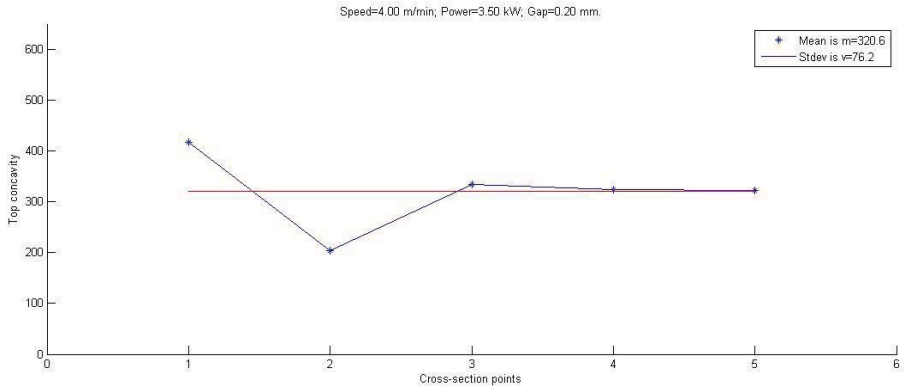
Speed=4.00 m/min; Power=3.50 kW; Gap=0.20 mm.
Mean is m=320.6
Stdev is v=76.2
Top concavity
Cross-section points

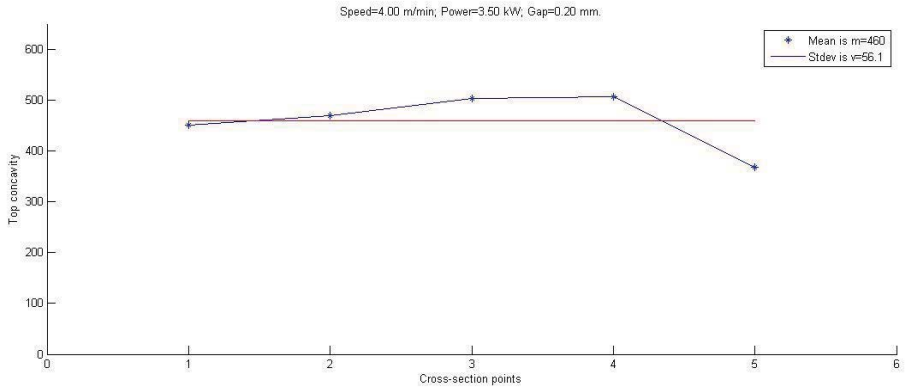
Speed=4.00 m/min; Power=3.50 kW; Gap=0.20 mm.
Mean is m=460
Stdev is v=56.1
Top concavity
Cross-section points

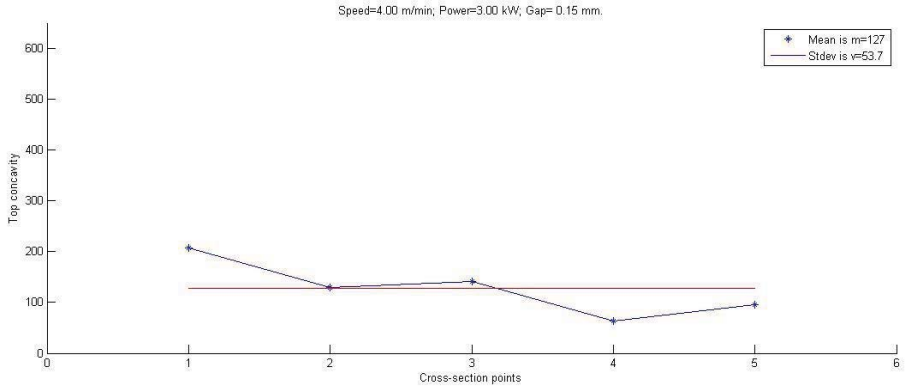
Speed=4.00 m/min; Power=3.00 kW; Gap= 0.15 mm.
Mean is m=127
Stdev is v=53.7
Top concavity
Cross-section points

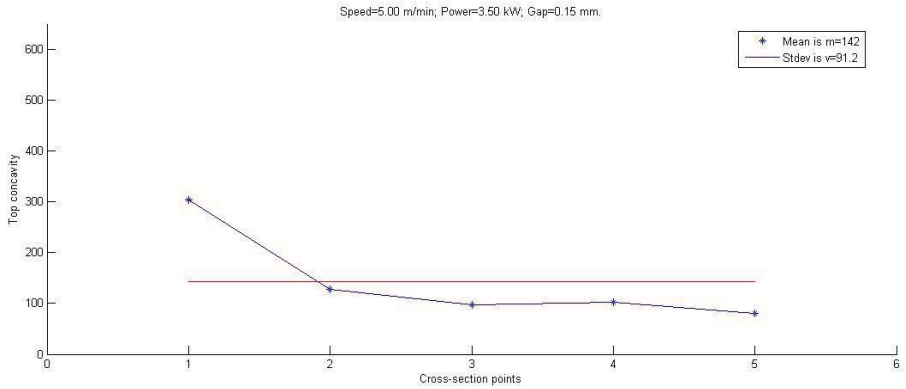
Speed=5.00 m/min; Power=3.50 kW; Gap=0.15 mm.
Mean is m=142
Stdev is v=91.2
Top concavity
Cross-section points

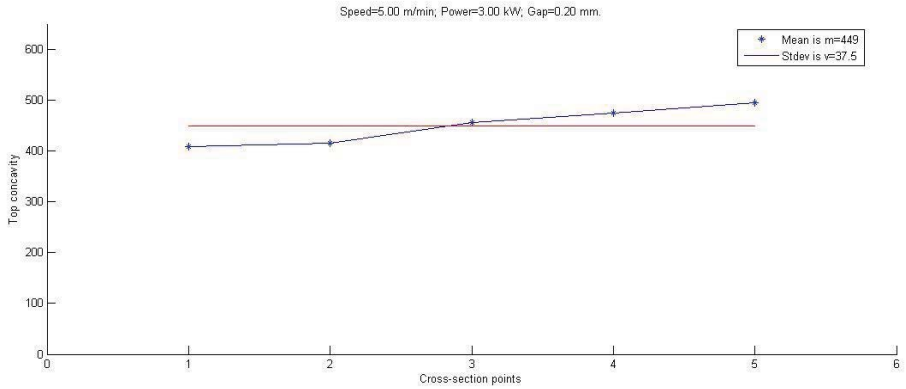
Speed=5.00 m/min; Power=3.00 kW; Gap=0.20 mm.
Mean is m=449
Stdev is v=37.5
Top concavity
Cross-section points

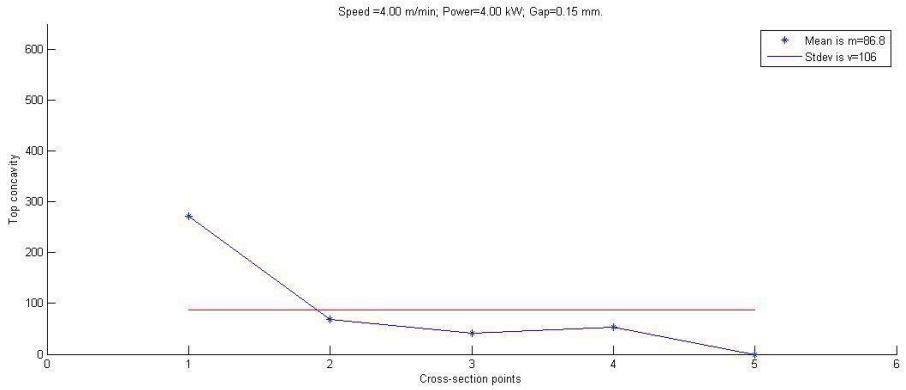
Speed =4.00 m/min; Power=4.00 kW; Gap=0.15 mm.
Mean is m=86.8
Stdev is v=106
Top concavity
Cross-section points

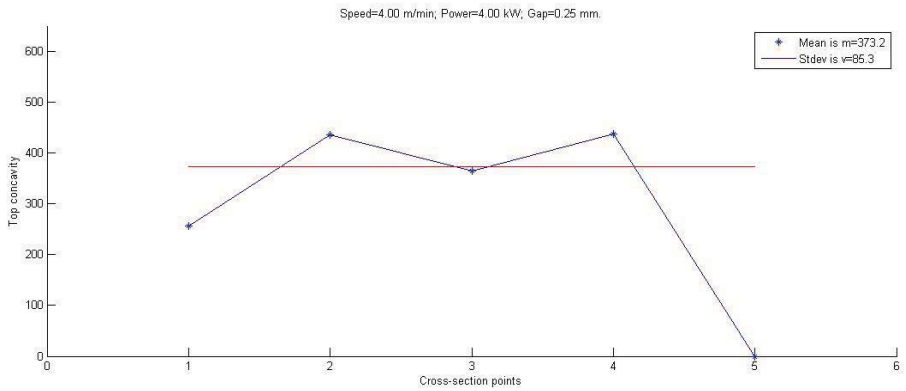
Speed=4.00 m/min; Power=4.00 kW; Gap=0.25 mm.
Mean is m=373.2
Stdev is v=85.3
Top concavity
Cross-section points

Interface width

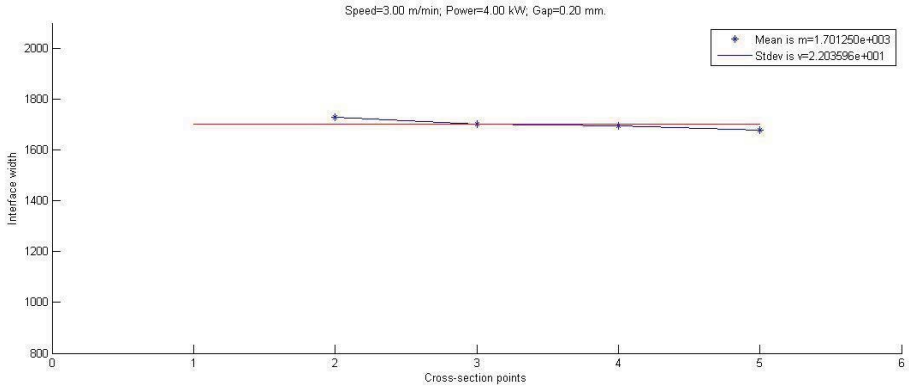

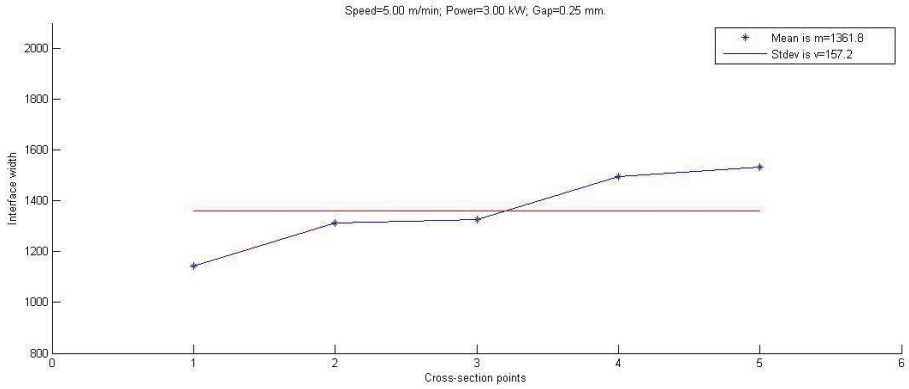

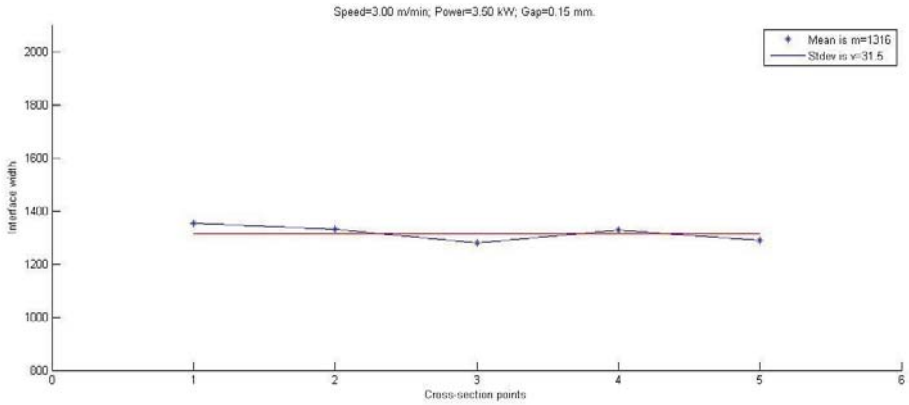

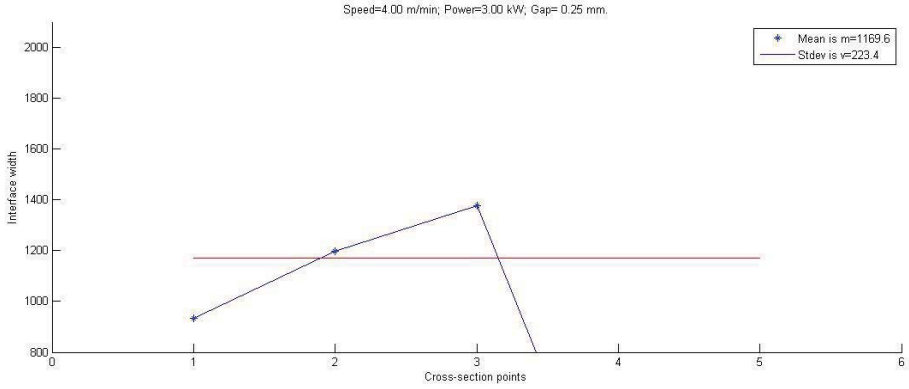

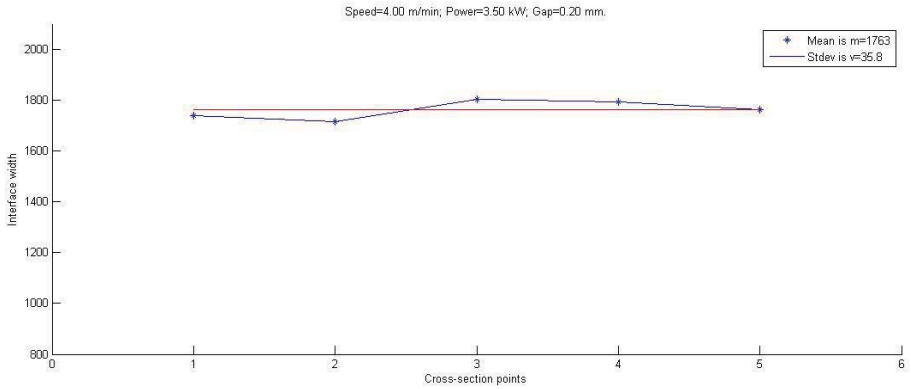
Speed=4.00 m/min; Power=3.50 kW; Gap=0.20 mm.
Mean is m=1763
Stdev is v=35.8
Interface width
Cross-section points

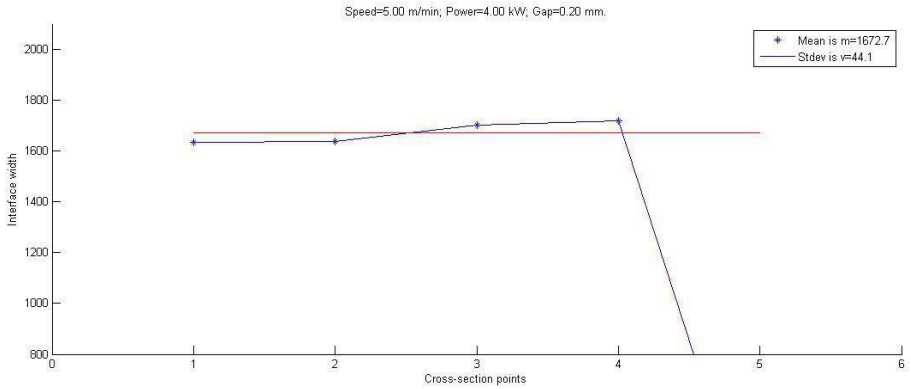
Speed=5.00 m/min; Power=4.00 kW; Gap=0.20 mm.
Mean is m=1672.7
Stdev is v=44.1
Interface width
Cross-section points

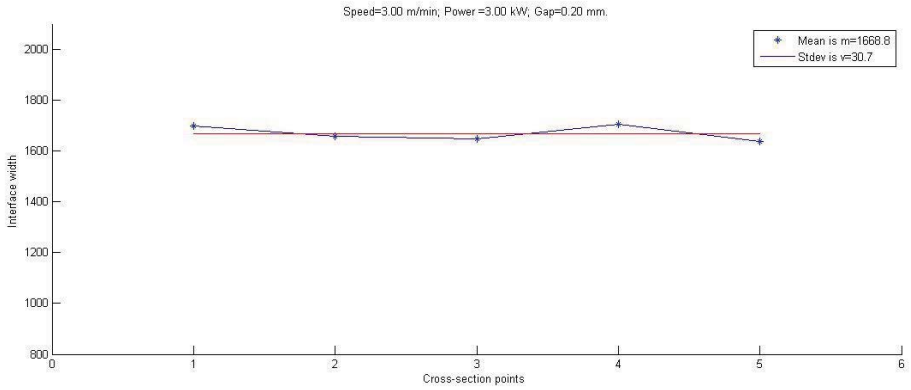
Speed=3.00 m/min; Power =3.00 kW; Gap=0.20 mm.
Mean is m=1668.8
Stdev is v=30.7
Interface width
Cross-section points

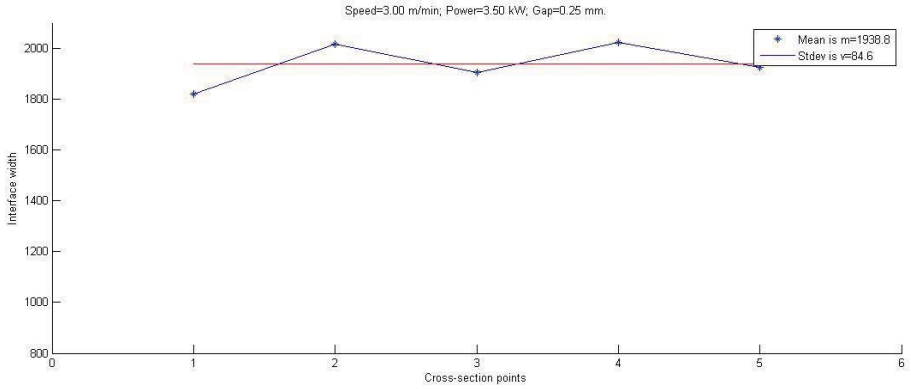
Speed=3.00 m/min; Power=3.50 kW; Gap=0.25 mm.
Mean is m=1938.8
Stdev is v=84.6
Interface width
Cross-section points

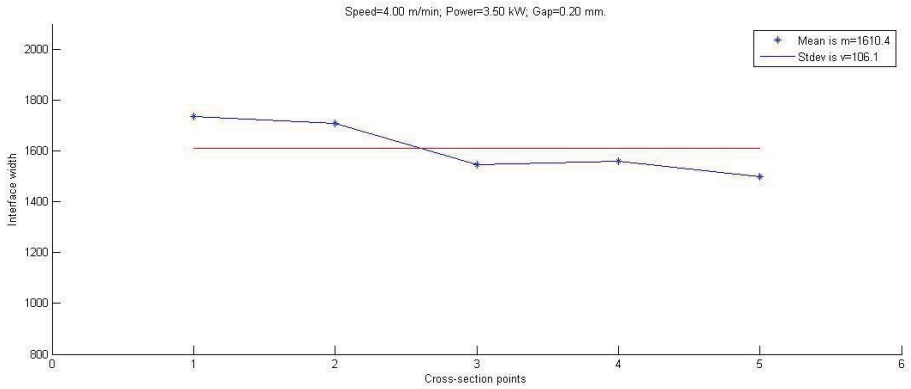
Speed=4.00 m/min; Power=3.50 kW; Gap=0.20 mm.
Mean is m=1610.4
Stdev is v=106.1
Interface width
Cross-section points

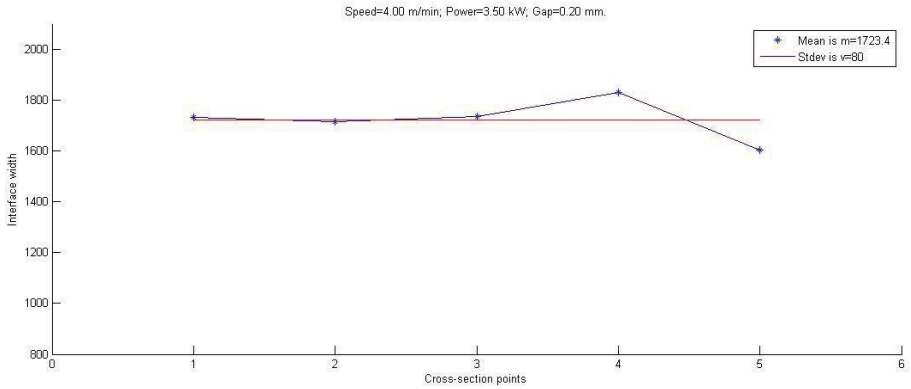
Speed=4.00 m/min; Power=3.50 kW; Gap=0.20 mm.
Mean is m=1723.4
Stdev is v=80
Interface width
Cross-section points

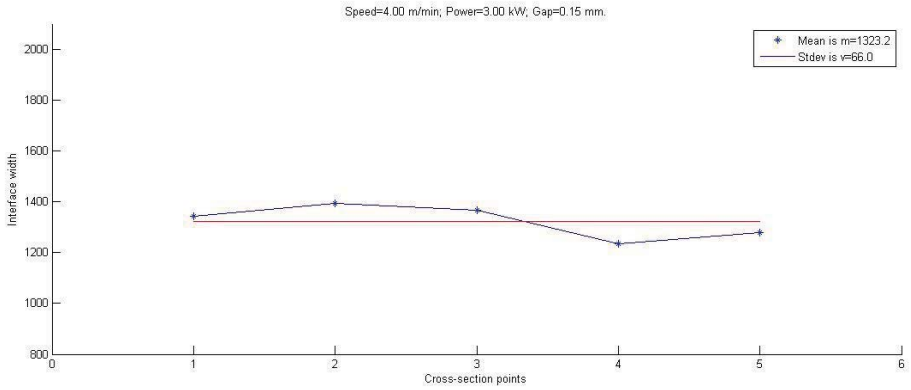
Speed=4.00 m/min; Power=3.00 kW; Gap=0.15 mm.
Mean is m=1323.2
Stdev is v=66.0
Interface width
Cross-section points

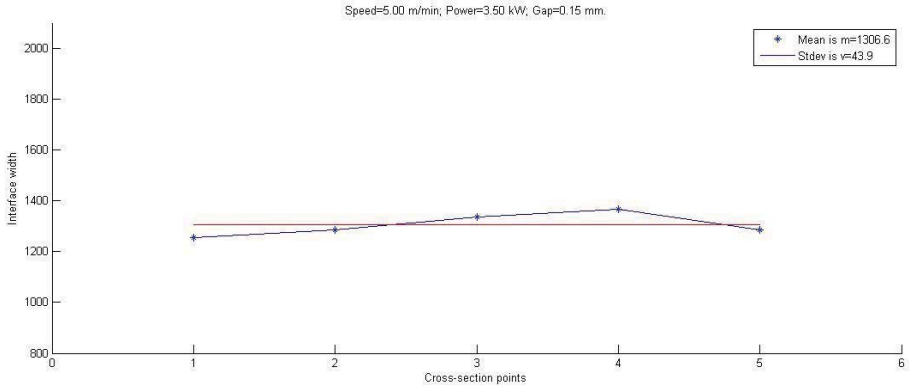
Speed=5.00 m/min; Power=3.50 kW; Gap=0.15 mm.
Mean is m=1306.6
Stdev is v=43.9
Interface width
Cross-section points

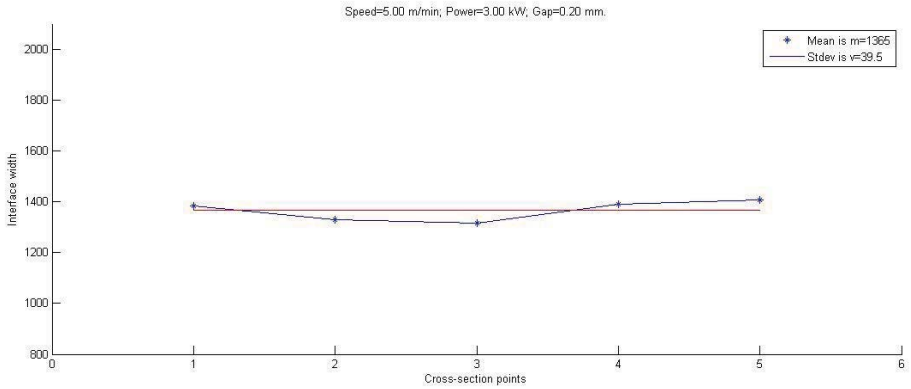
Speed=5.00 m/min; Power=3.00 kW; Gap=0.20 mm.
Mean is m=1365
Stdev is v=39.5
Interface width
Cross-section points

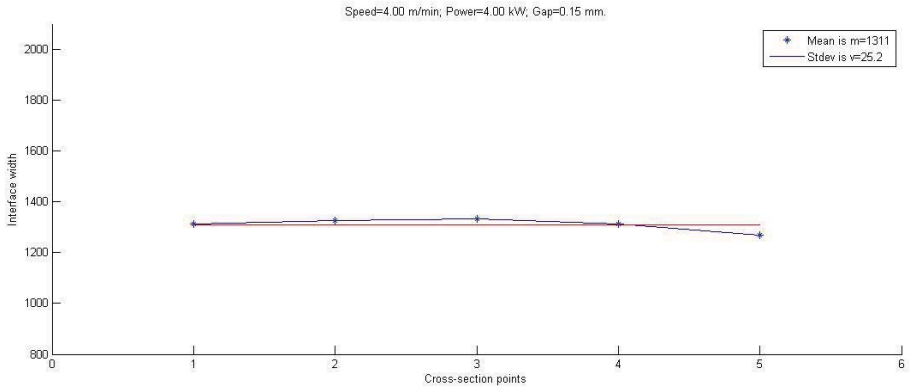
Speed=4.00 m/min; Power=4.00 kW; Gap=0.15 mm.
Mean is m=1311
Stdev is v=25.2
Interface width
Cross-section points

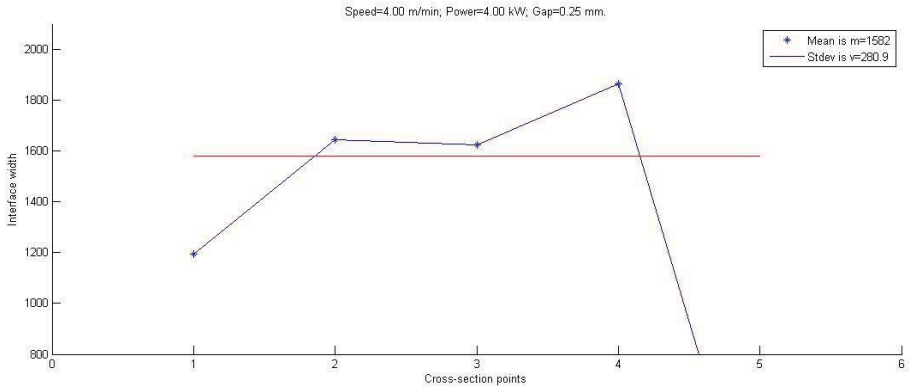
Speed=4.00 m/min; Power=4.00 kW; Gap=0.25 mm.
Mean is m=1582
Stdev is v=280.9
Interface width
Cross-section points

Penetration

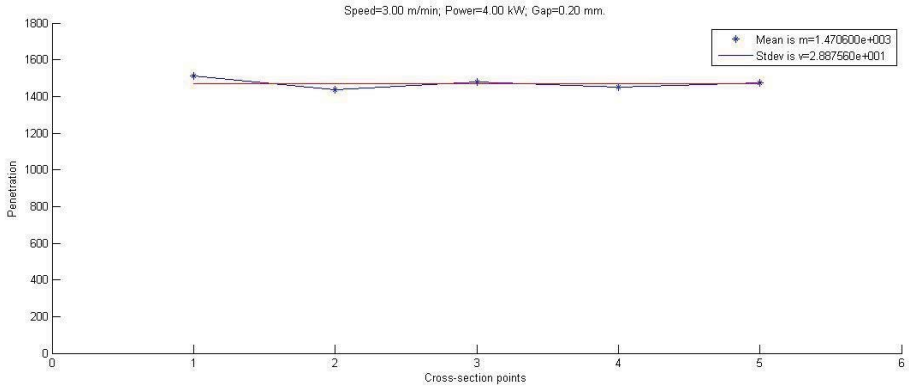

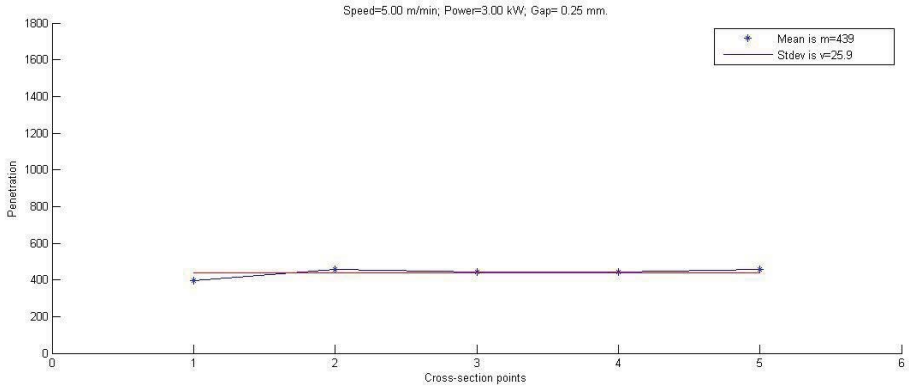

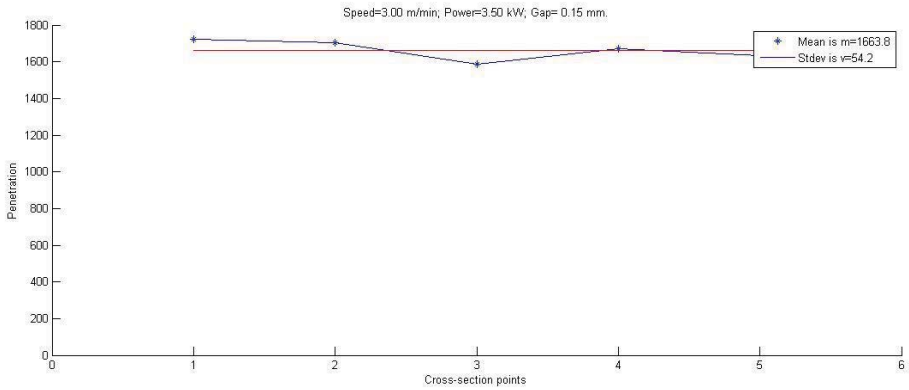

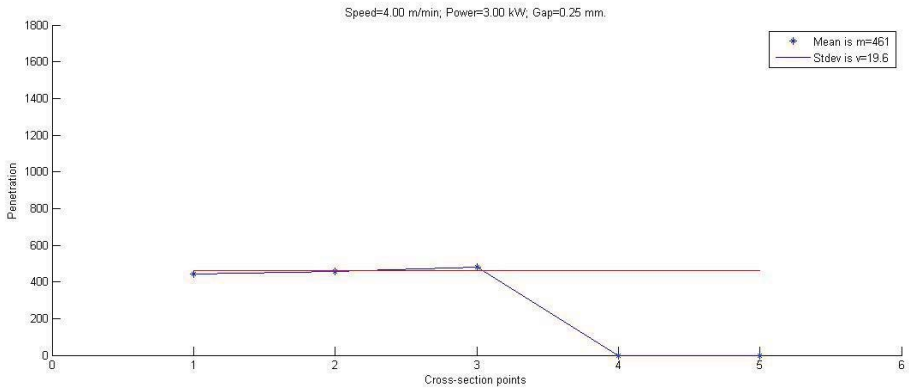

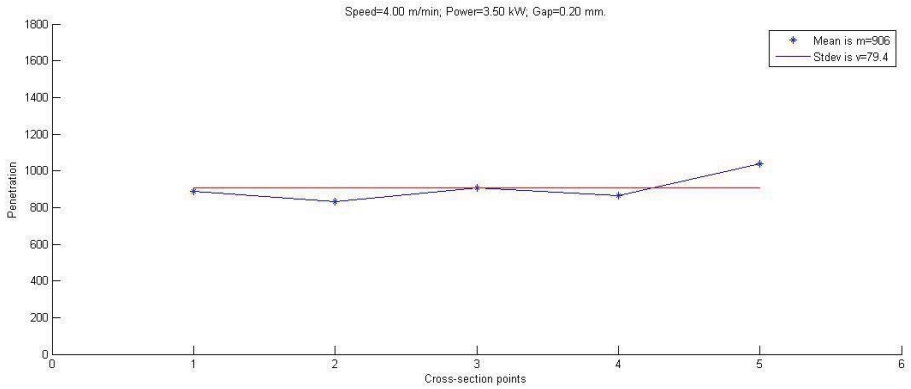
Speed=4.00 m/min; Power=3.50 kW; Gap=0.20 mm.
Mean is m=906
Stdev is v=79.4
Penetration
Cross-section points

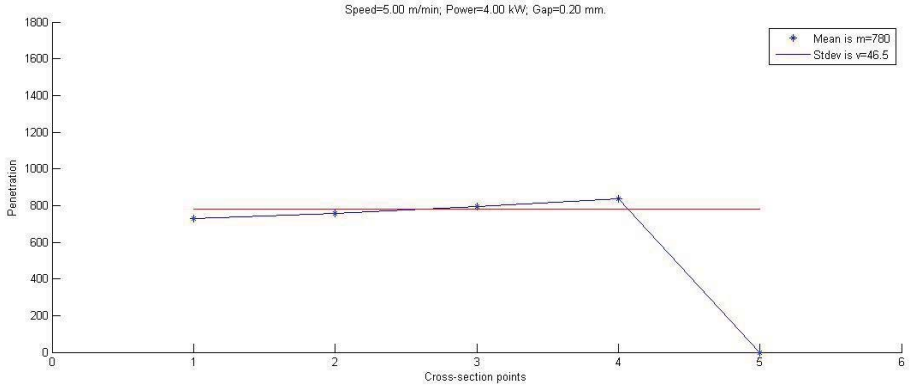
Speed=5.00 m/min; Power=4.00 kW; Gap=0.20 mm.
Mean is m=780
Stdev is v=46.5
Penetration
Cross-section points

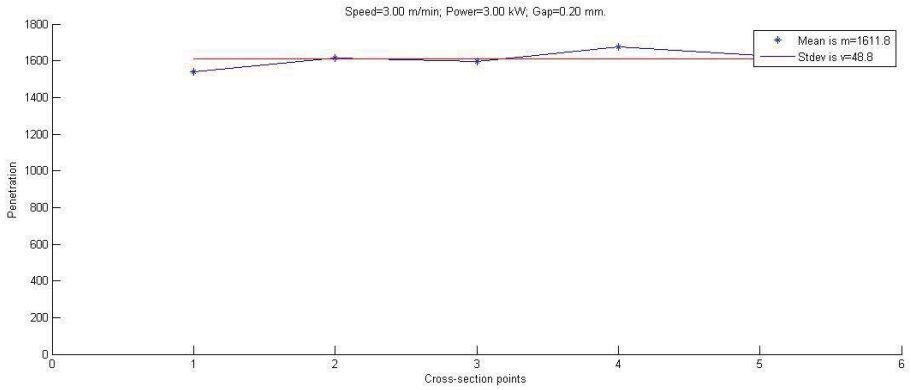
Speed=3.00 m/min; Power=3.00 kW; Gap=0.20 mm.
Mean is m=1611.8
Stdev is v=48.8
Penetration
Cross-section points

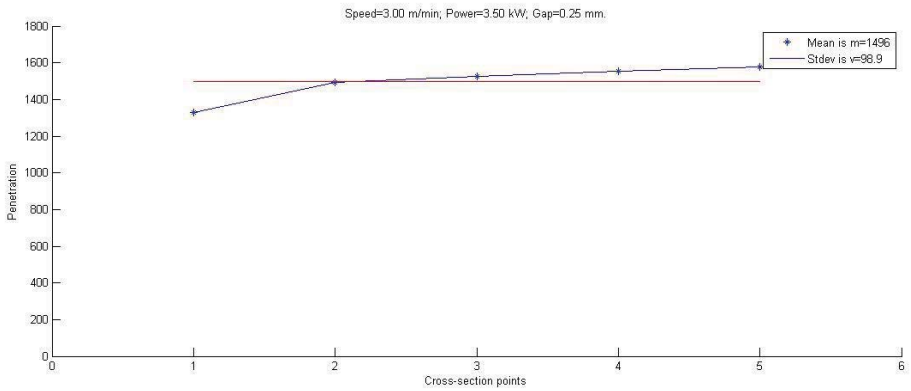
Speed=3.00 m/min; Power=3.50 kW; Gap=0.25 mm.
Mean is m=1496
Stdev is v=98.9
Penetration
Cross-section points

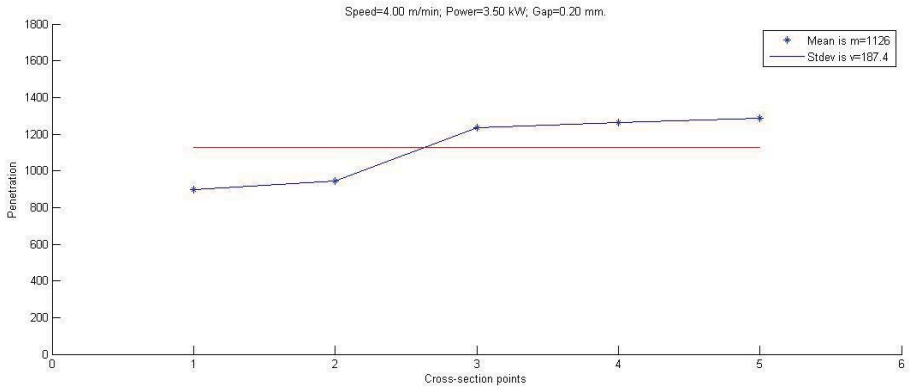
Speed=4.00 m/min; Power=3.50 kW; Gap=0.20 mm.
Mean is m=1126
Stdev is v=187.4
Penetration
Cross-section points

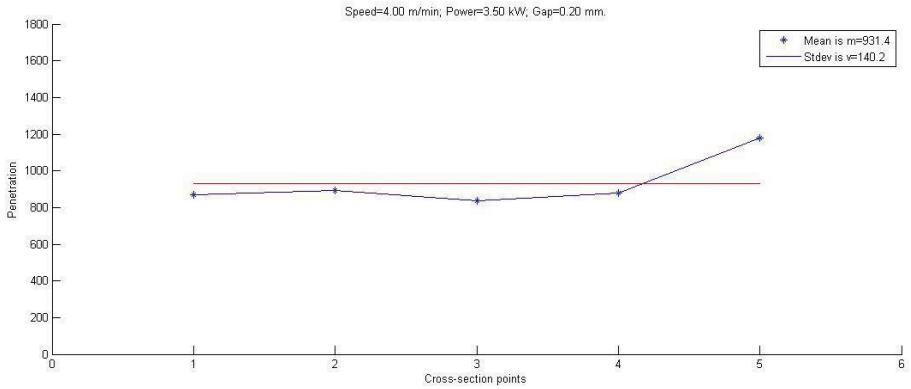
Speed=4.00 m/min; Power=3.50 kW; Gap=0.20 mm.
Mean is m=931.4
Stdev is v=140.2
Penetration
Cross-section points

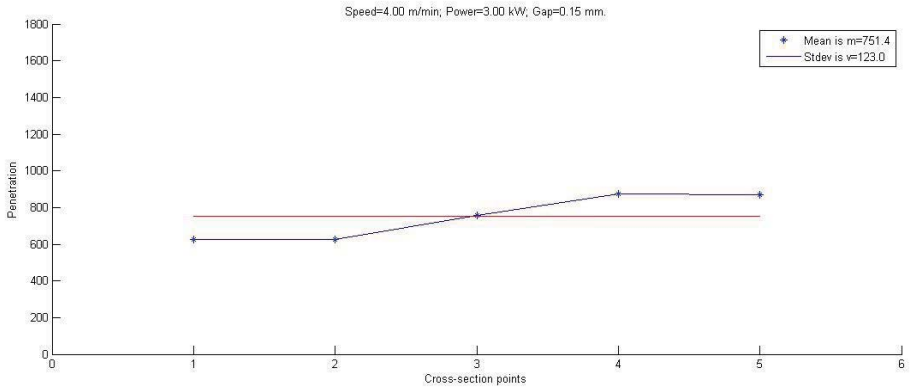
Speed=4.00 m/min; Power=3.00 kW; Gap=0.15 mm.
Mean is m=751.4
Stdev is v=123.0
Penetration
Cross-section points

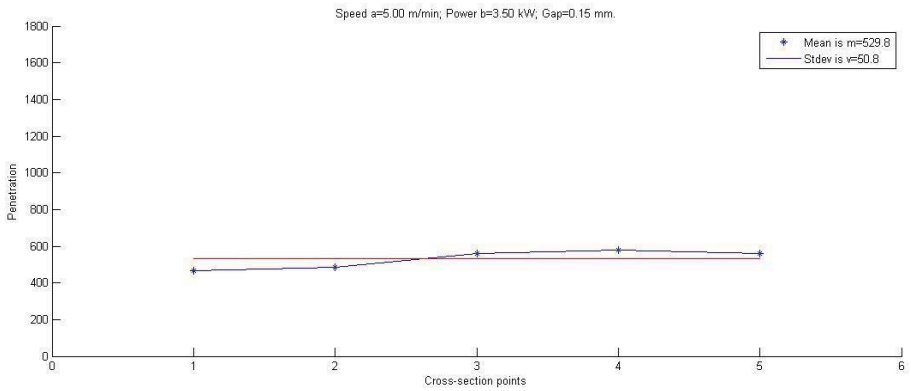
Speed a=5.00 m/min; Power b=3.50 kW; Gap=0.15 mm.
Mean is m=529.8
Stdev is v=50.8
Penetration
Cross-section points

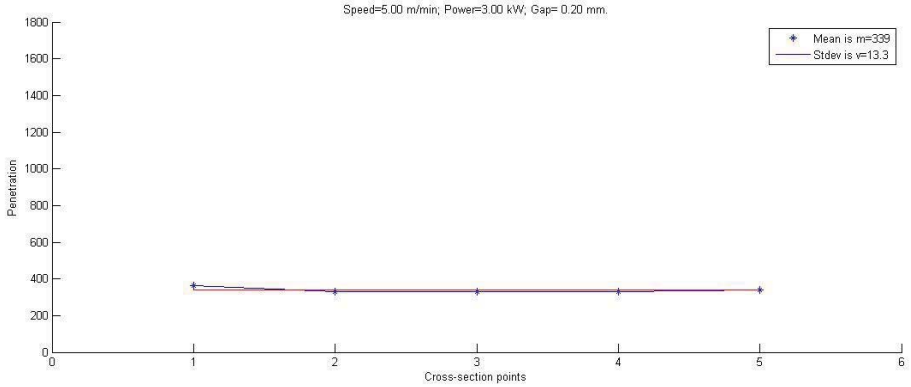
Speed=5.00 m/min; Power=3.00 kW; Gap= 0.20 mm.
Mean is m=339
Stdev is v=13.3
Penetration
Cross-section points

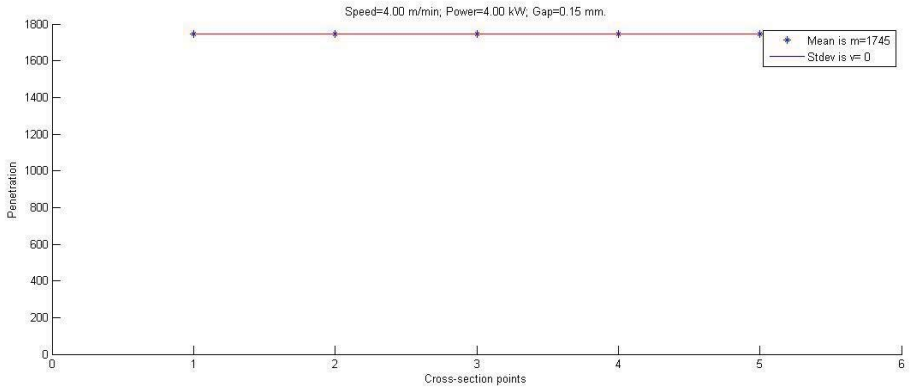
Speed=4.00 m/min; Power=4.00 kW; Gap=0.15 mm.
Mean is m=1745
Stdev is v= 0
Penetration
Cross-section points

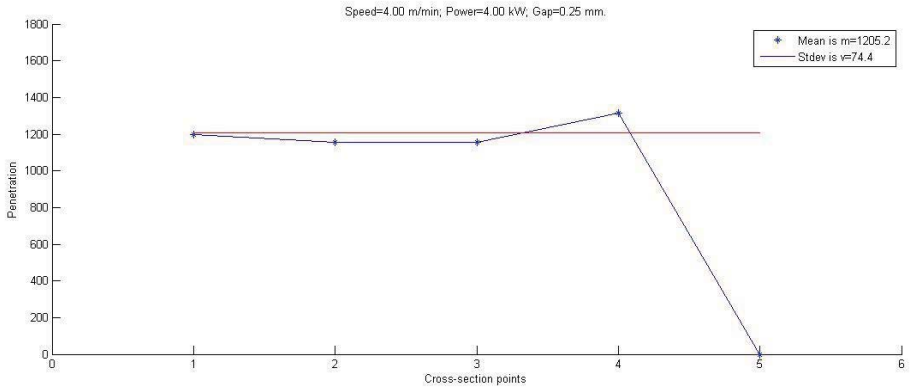
Speed=4.00 m/min; Power=4.00 kW; Gap=0.25 mm.
Mean is m=1205.2
Stdev is v=74.4
Penetration
Cross-section points

Bottom concavity

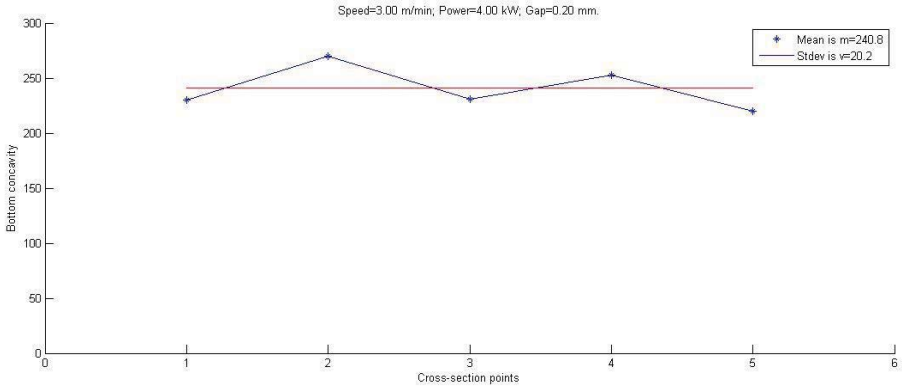

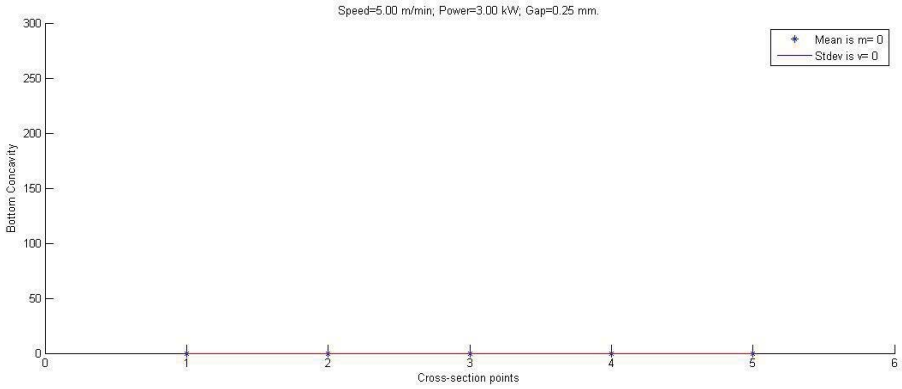

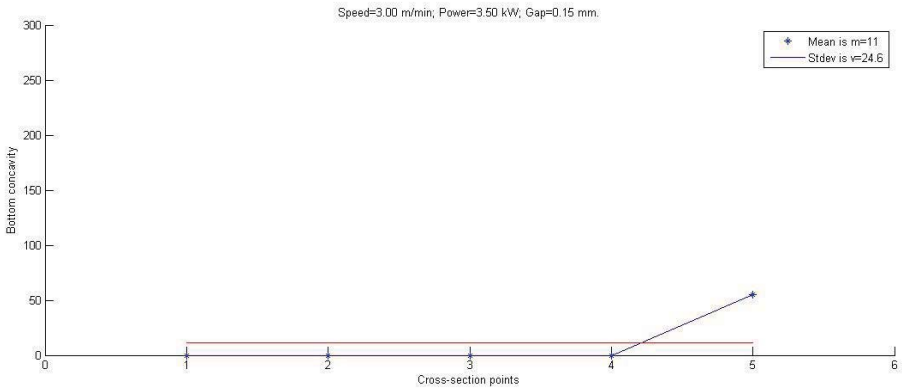

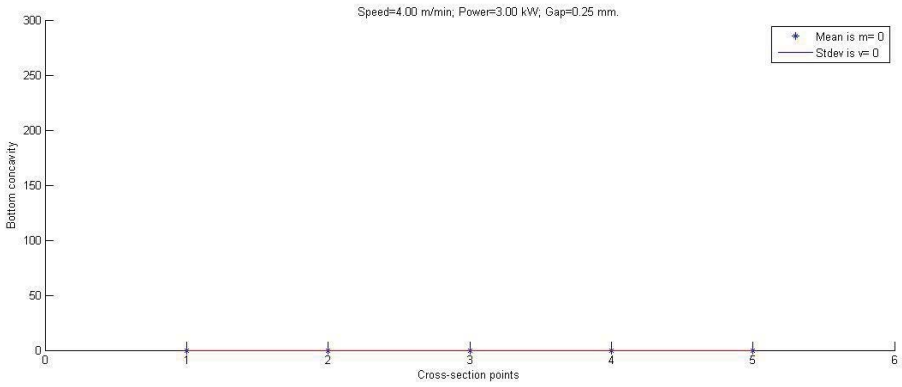

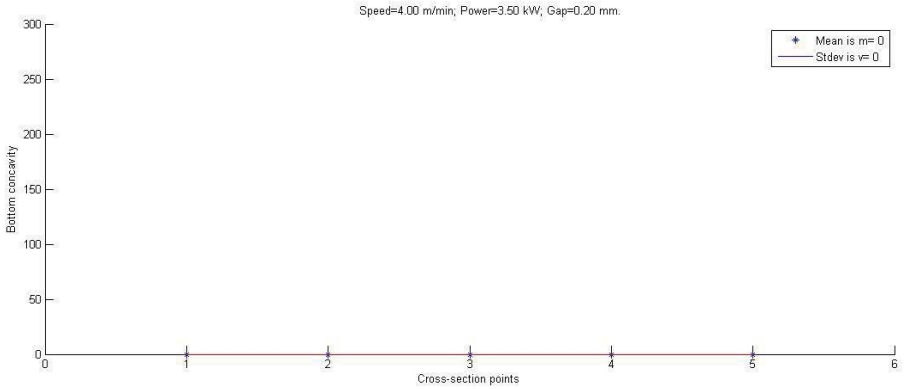
Speed=4.00 m/min; Power=3.50 kW; Gap=0.20 mm.
Mean is m= 0
Stdev is v= 0
Bottom concavity
Cross-section points

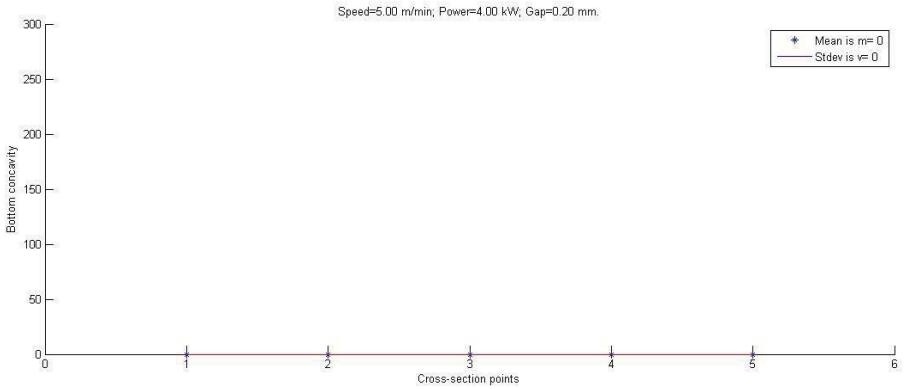
Speed=5.00 m/min; Power=4.00 kW; Gap=0.20 mm.
Mean is m= 0
Stdev is v= 0
Bottom concavity
Cross-section points

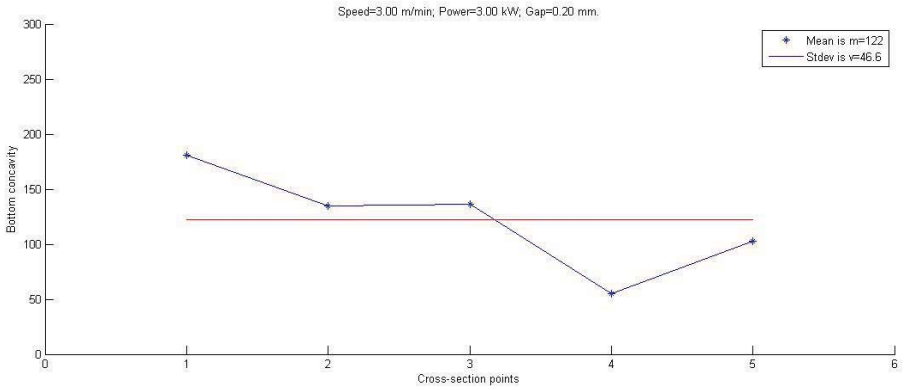
Speed=3.00 m/min; Power=3.00 kW; Gap=0.20 mm.
Mean is m=122
Stdev is v=46.6
Bottom concavity
Cross-section points

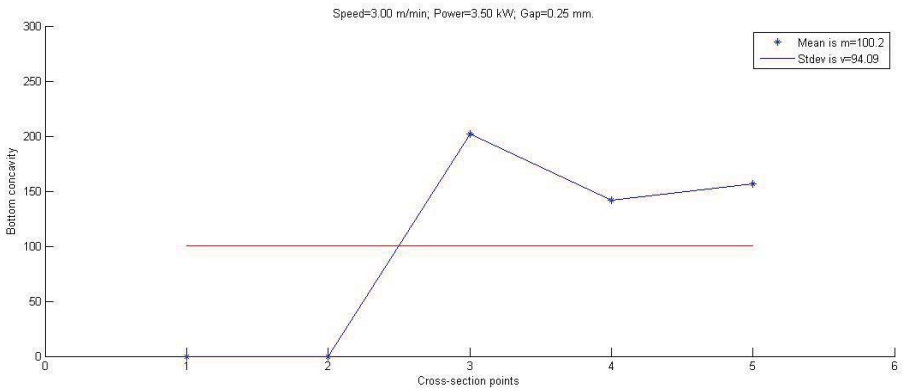
Speed=3.00 m/min; Power=3.50 kW; Gap=0.25 mm.
Mean is m=100.2
Stdev is v=94.09
Bottom concavity
Cross-section points

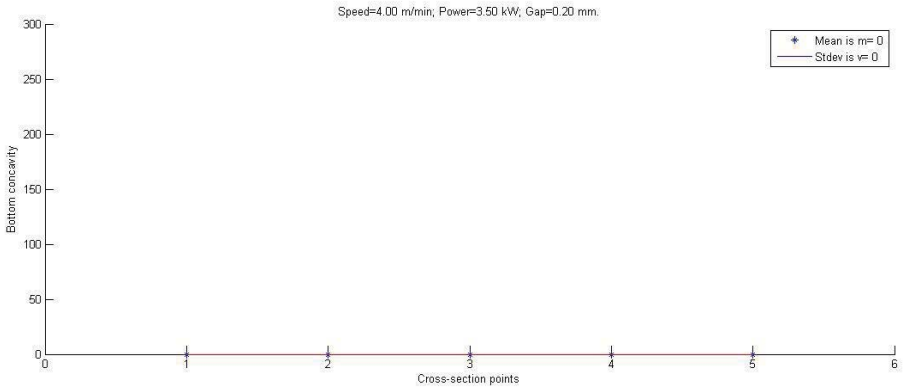
Speed=4.00 m/min; Power=3.50 kW; Gap=0.20 mm.
Mean is m= 0
Stdev is v= 0
Bottom concavity
Cross-section points

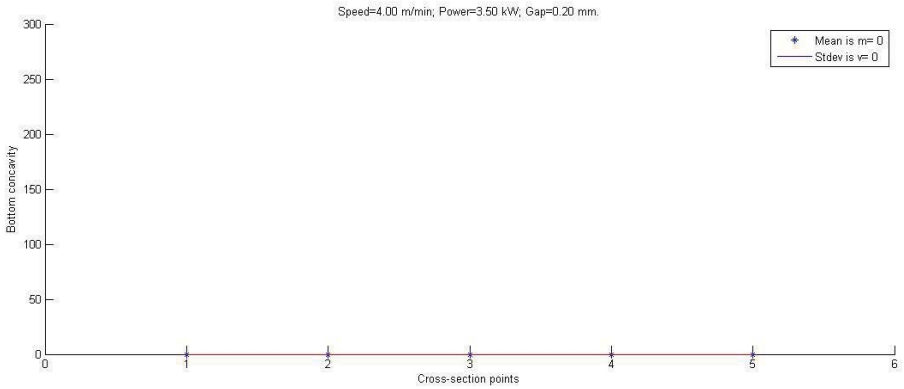
Speed=4.00 m/min; Power=3.50 kW; Gap=0.20 mm.
Mean is m= 0
Stdev is v= 0
Bottom concavity
Cross-section points

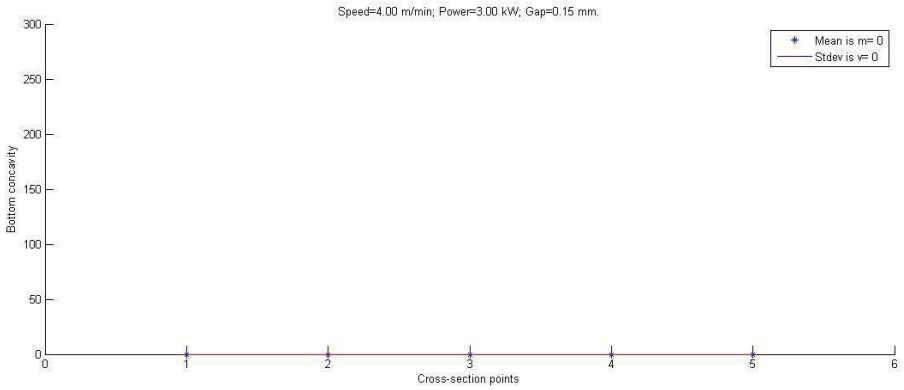
Speed=4.00 m/min; Power=3.00 kW; Gap=0.15 mm.
Mean is m= 0
Stdev is v= 0
Bottom concavity
Cross-section points

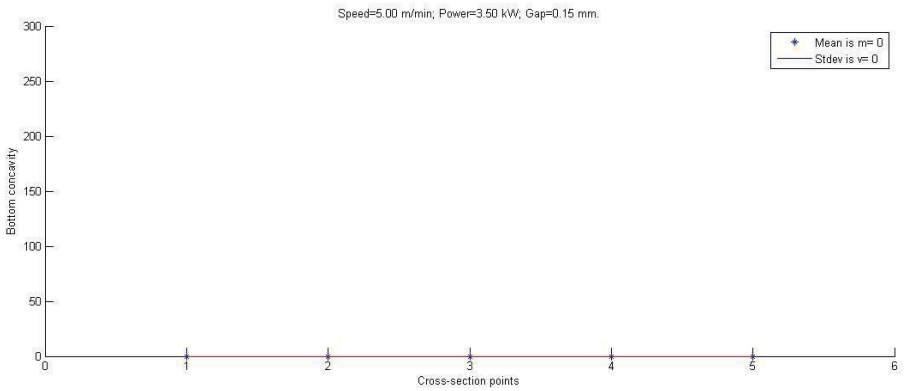
Speed=5.00 m/min; Power=3.50 kW; Gap=0.15 mm.
Mean is m= 0
Stdev is v= 0
Bottom concavity
Cross-section points

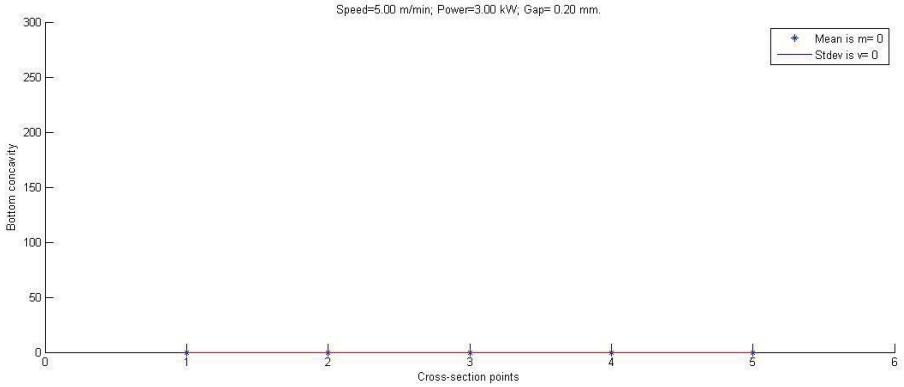
Speed=5.00 m/min; Power=3.00 kW; Gap= 0.20 mm.
Mean is m= 0
Stdev is v= 0
Bottom concavity
Cross-section points

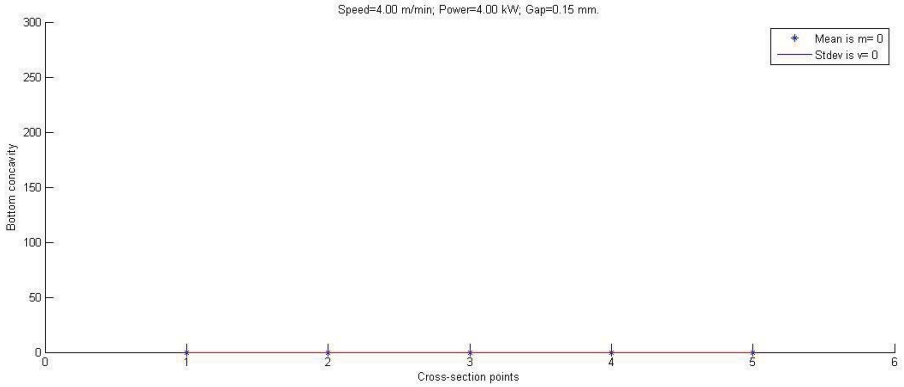
Speed=4.00 m/min; Power=4.00 kW; Gap=0.15 mm.
Mean is m= 0
Stdev is v= 0
Bottom concavity
Cross-section points

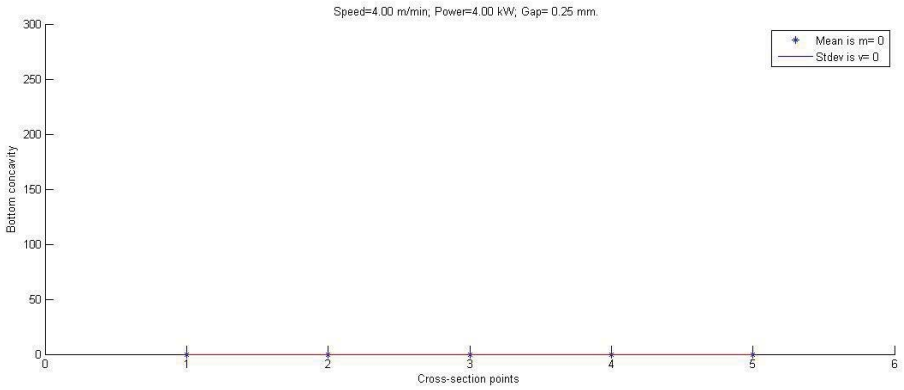
Speed=4.00 m/min; Power=4.00 kW; Gap= 0.25 mm.
Mean is m= 0
Stdev is v= 0
Bottom concavity
Cross-section points

Appendix C

This appendix is a poster of COMAU and provided by the company during RLW project. COMAU is one of the partners of this project.

EN

SmartLaser™
Remote 3D Laser Welding

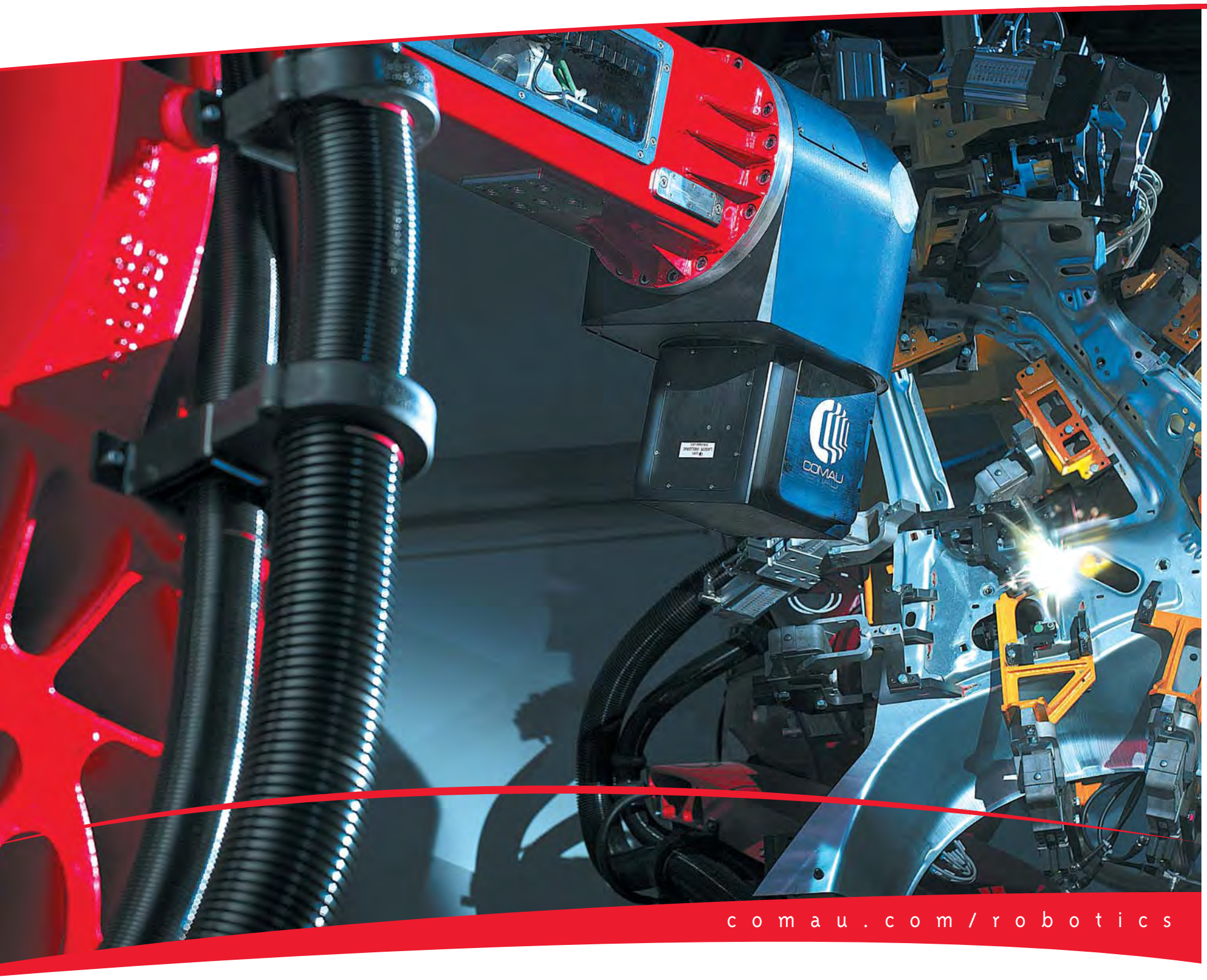

comau.com/robotics

COMAU
ROBOTICS

Remote Laser Welding to increase productivity

SmartLaser™ is the sole remote 3D laser welding robot operating worldwide. Once again Comau Robotics is offering you today the technology of tomorrow.

Compared to conventional spot welding, laser welding allows quicker and more accurate processing. Remote laser welding, in particular, offers further advantages in terms of positioning speed and reduces the criticalities of access between the robot head and tooling to achieve the joint.

Whilst a conventional focusing head moves and repositions by each welding stitch, the SmartLaser™ technology allows operation from remote areas (>750 mm). In addition the welding stitch can be modified simply by adjusting the laser beam working angle and its focal length.

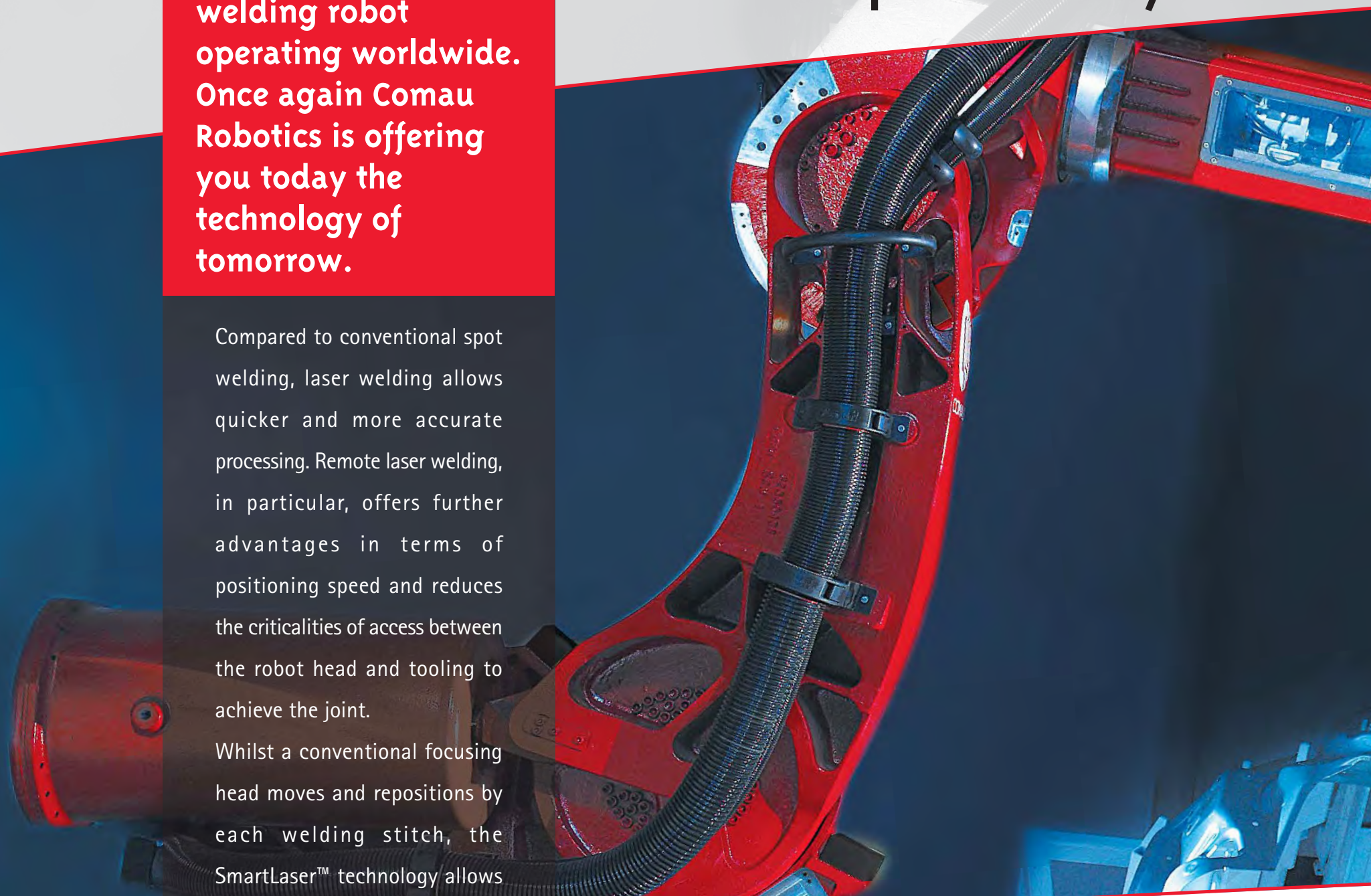

Traditional stitches laser welding

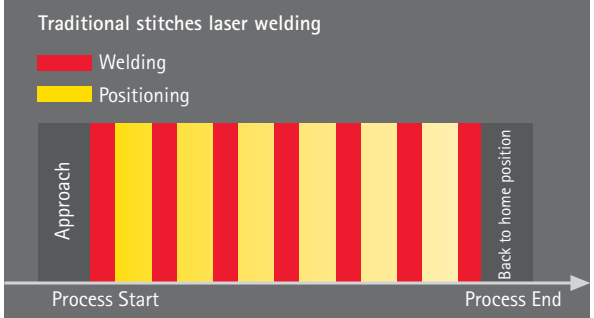

Remote stitches laser welding

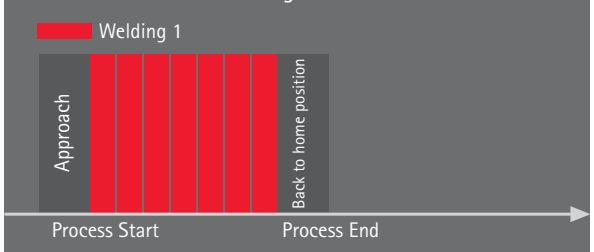

REMOTE LASER WELDING PECULIARITIES

The processing high speed enables a considerable reduction in cycle-time, number of working stations and, subsequently, also the system overall dimensions.

In case of stand-alone stations, the loading and unloading of the parts to be welded can be accomplished in hidden time, with duty cycle (Beam-On-Time) close to 100%.

From a perspective of reliability, the large stand-off between the actual welding stitch and the head of the robot eliminates contamination of the protective cover glass, resulting in improved system uptime and production performance.

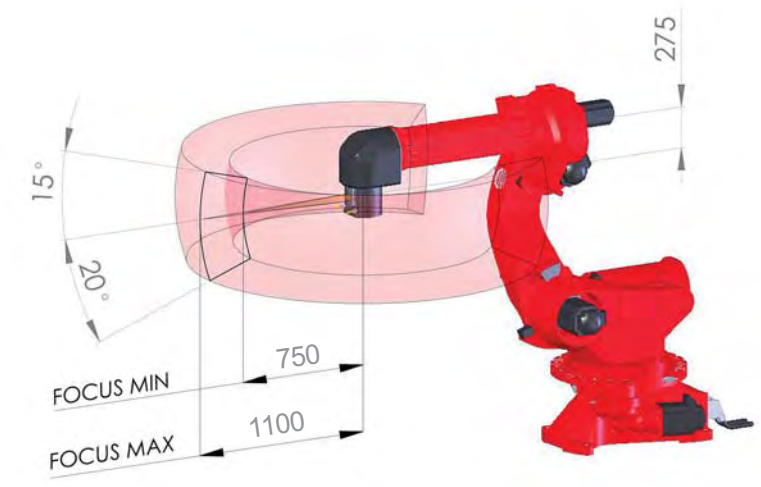

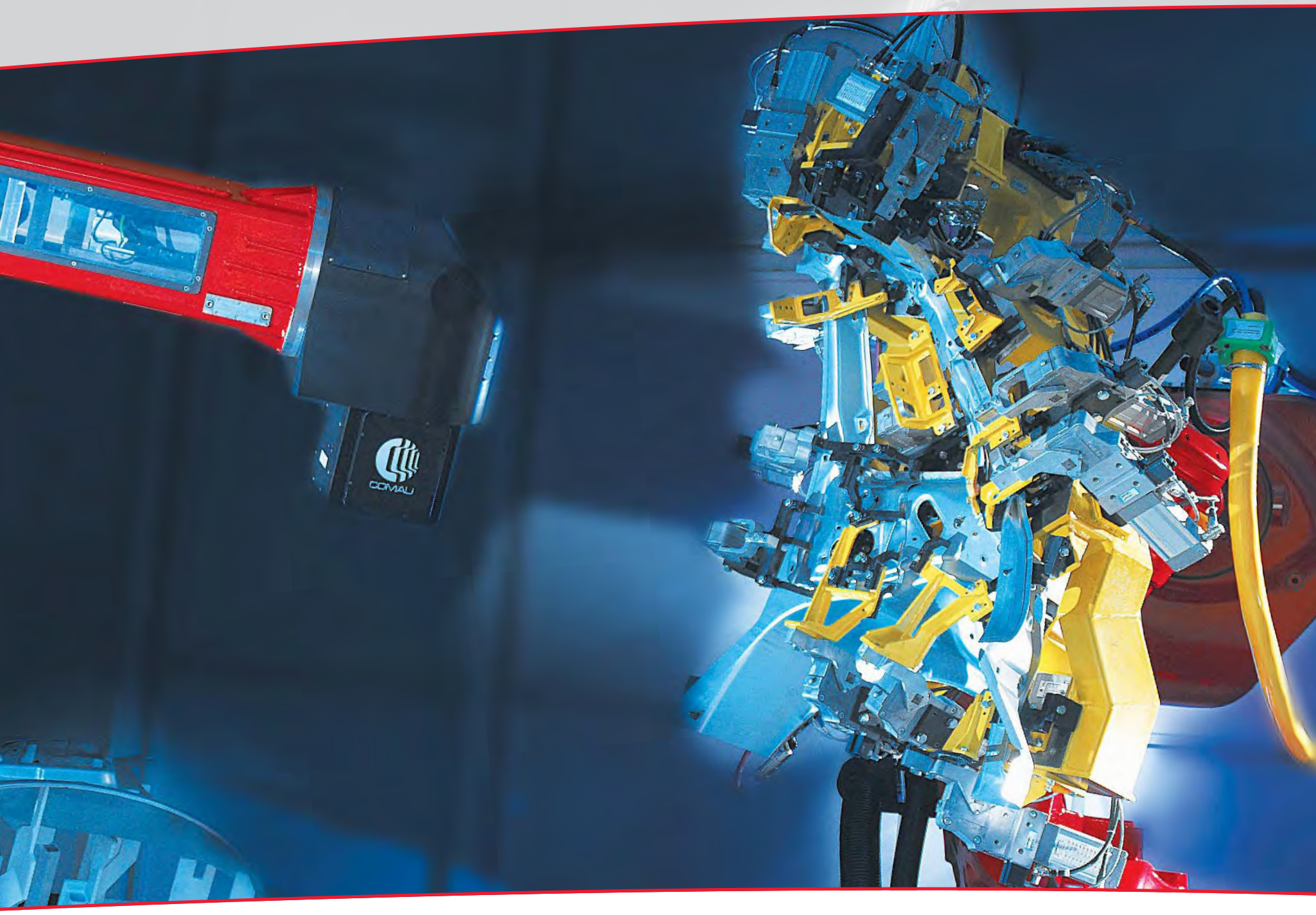

ALL THE ADVANTAGES OF A REVOLUTIONARY PROJECT

- Minimised positioning time thanks to the low inertia of the beam deflection and focalisation system
- Maximum "Beam-On-Time"
- Large working area
- Programmable working distance, from 750 to 1100 mm
- Increase in processing distance; possibility to weld also areas that are conventionally difficult to reach
- Optimised sequence of the welding stitches -> reduction of thermal distortion
- Reduction of material in overlapping flanges -> higher flexibility in the part manufacturing
- Small production lots can be processed more efficiently
- Beam deflection (X, Y) through mirror controlled by direct drive technology
- Beam positioning speed > 1000 m/min
- Focus vertical positioning (Z) through high speed linear motor > 200 m/min

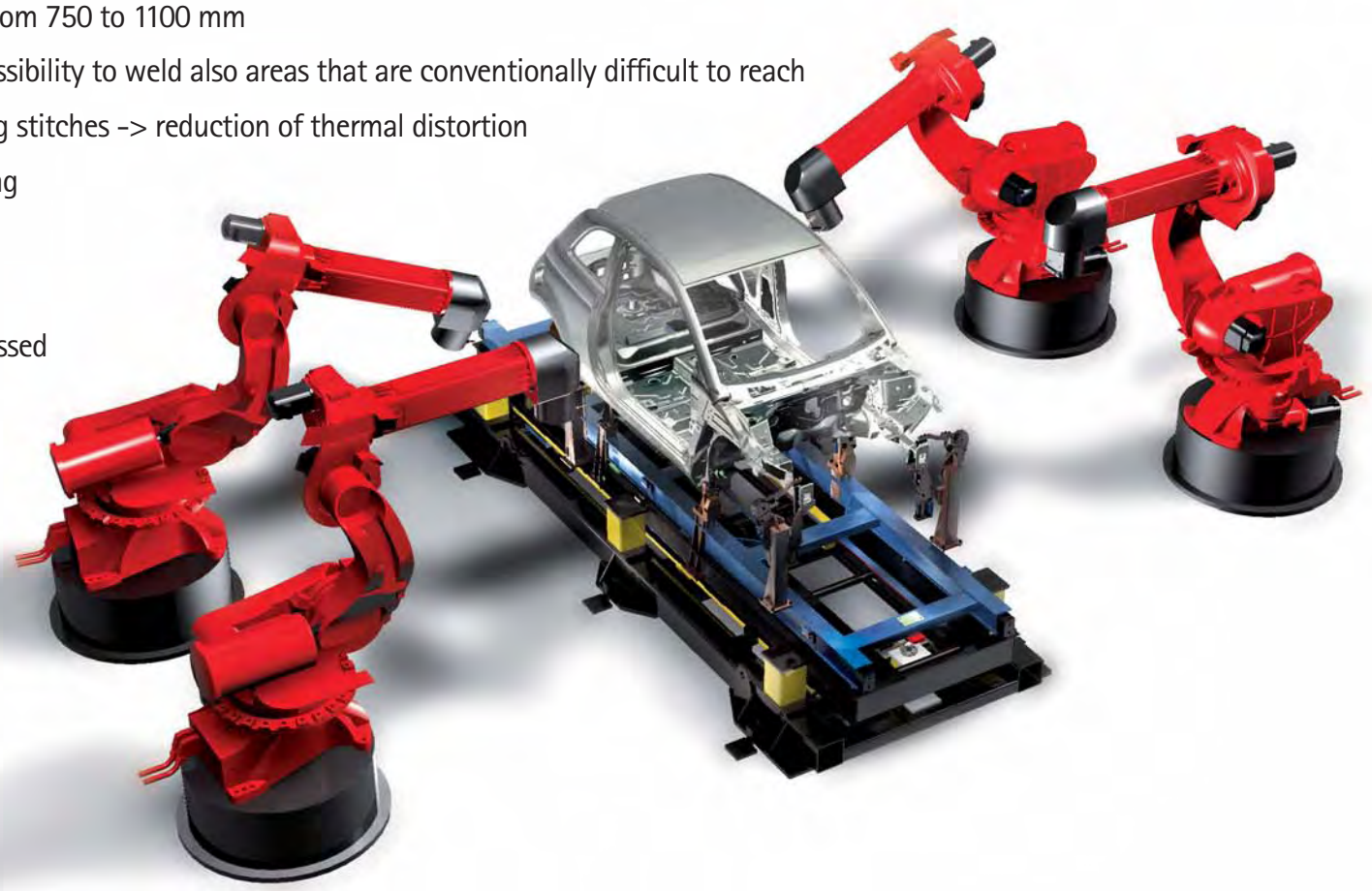

SmartLaser™: unique in the world

INTEGRATED STRUCTURE

The system is made of the integration of a remote laser focusing and addressing module with a standard anthropomorphic robot of the NH series. The result is an unprecedented laser welding system, combining robot motion versatility with the exceptional potential of the best performing, high speed and extremely accurate laser technology, all controlled through a single Control Unit: Comau Robotics C4G.

INTEGRATED DRESSING

The beam high quality laser source is positioned near the welding cell and the laser beam is transferred through an optical fibre, which matches with the robot axis 4. This solution prevents stresses on the fibre as well as all problems associated with the reliability of external robot dressing. The combination allows the reduction of mechanical stresses with a simplified offline programming functionality.

HIGHER SPEED

The 3D system features excellent dynamic properties within the entire working volume, with accelerations on the linear motor up to 8G. The repositioning speed on Z axis is 10 times higher compared that of a normal anthropomorphous robot.

AN "OFF-THE-SHELF" SPECIAL SYSTEM

The complete integration of a remote laser focalization and repositioning module with a conventional standard Comau robot offers undeniable advantages in terms of cost-efficiency and reliability. Above all in terms of flexibility and performance efficiency, the system undoubtedly provides unrivalled benefits when there are complex operations within confined space.

COMPARISON OF POSITIONING TIME IN THE SPACE

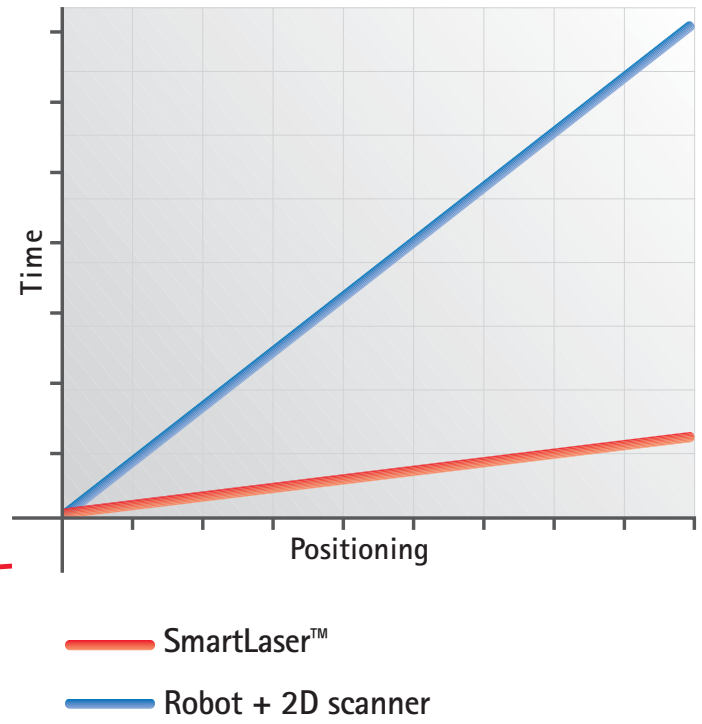

Agility, reliability, speed and ability to increase productivity dramatically: SmartLaser™ is unmatched.

The deep know-how in laser welding technology that Comau has gained over the years with the co-operation of several car-manufacturers has resulted in an unique and thoroughly innovative project: the new fully integrated robotized system SmartLaser™.

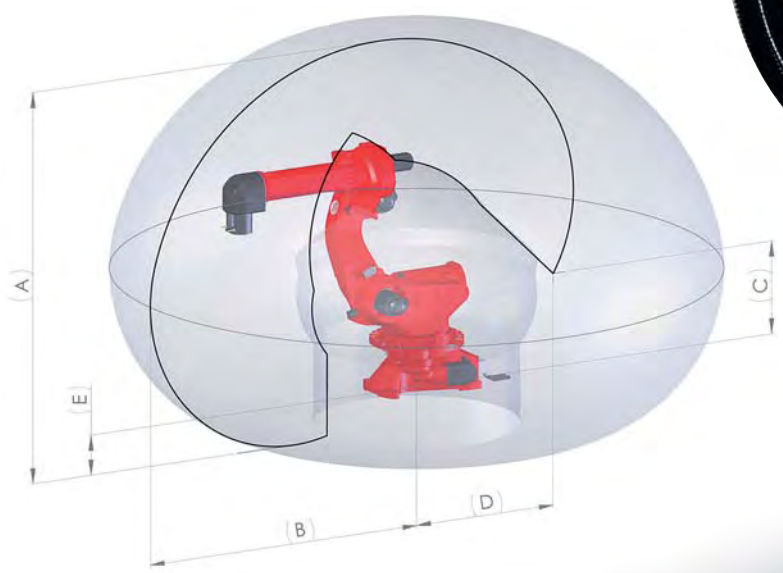

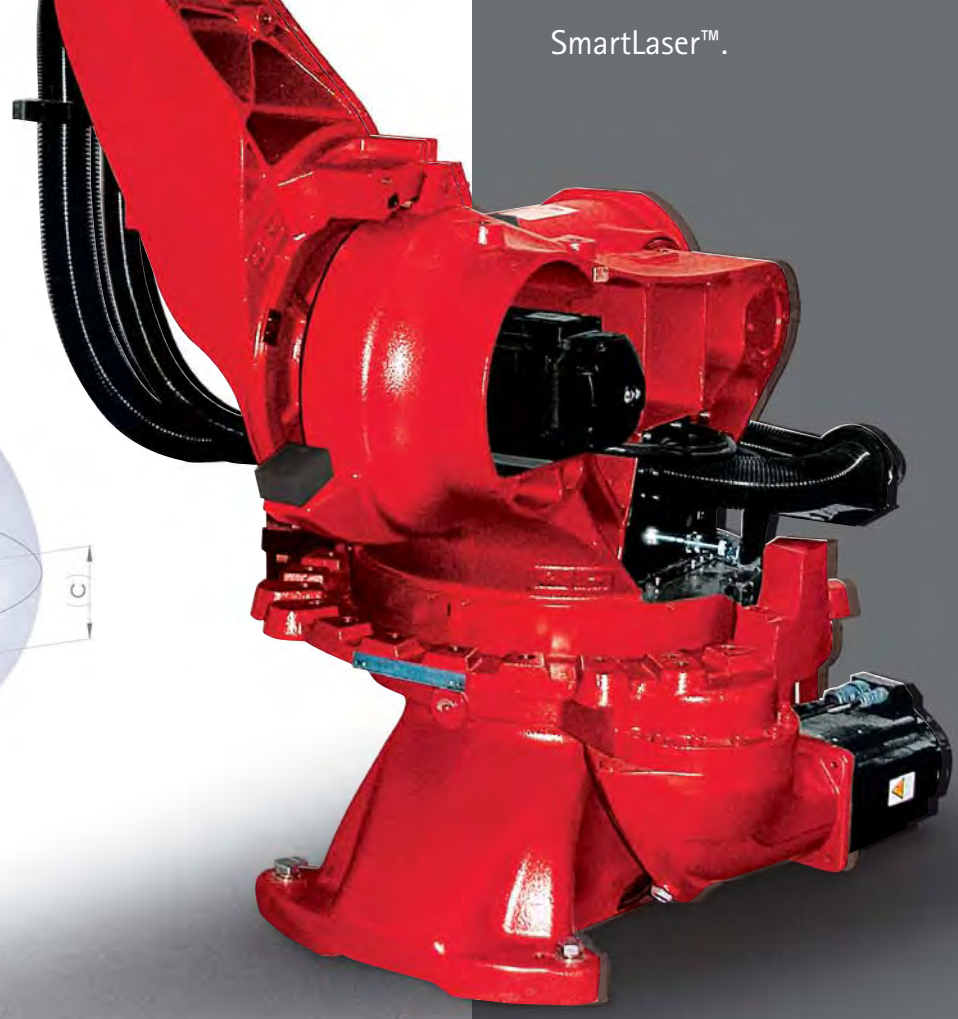

Specific Features

Number of axes		7	
Repeatability (mm)		+/-0.07	
Installation position		floor	
Protection class		IP65	
	axis 3	stroke (mm)	+0.1 to +315.0
		speed (m/s)	3
	axis 4	stroke (°)	+/- 140
		speed (°/s)	1289
	axis 5	stroke (°)	+10 / -7.5
		speed (°/s)	945

ARM1

ARM2

Operating areas

axis 1	stroke (°)	+/-180
	speed (°/s)	108
axis 2	stroke (°)	+75/-55
	speed (°/s)	104
axis 3	stroke (°)	+110/-170
	speed (°/s)	110
axis 4	stroke (°)	+/-282
	speed (°/s)	190
A	(mm)	3396.13
B	(mm)	2863.41
C	(mm)	900
D	(mm)	1686.75
E	(mm)	387.66

Freedom of movement and dedicated software

WIRELESS CONTROL

The WiTP Wireless Teach Pendant enables the robot to be programmed without the limits of movement, wear and tear due to conventional cable connections. WiTP is flexible: a single Teach Pendant can communicate with several Control Units, as well as manage the laser source and the robot at the same time.

DEDICATED SOFTWARE

The dedicated Human Machine Interface features the following functional units:

- Process management keys
- Introduction main page
- SETUP environment
- Tables with process related DATA (DATA Page)
- HELP I/O environment
- User's programs editing environment
- Technological instruction set
- Alarm management and recovery
- Multilanguage management
- Automatic configuration of the Input/Output signals to control the Laser source
- Automatic configuration of the Input/Output signals from and to external PLC

OPERATING

The SmartLaser™ is the only 3D remote welding robot that can be matched with any high quality multi-kilowatt commercial source, with wave lengths between 1030 and 1070 nanometres.

SmartLaser™ : the 3D remote laser welding robot that covers a wide operating area with slight angular adjustments of the mirrors.

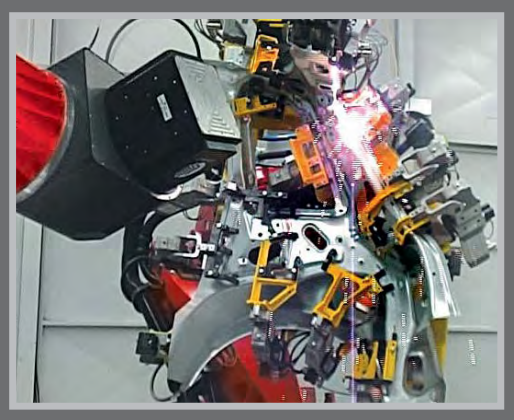

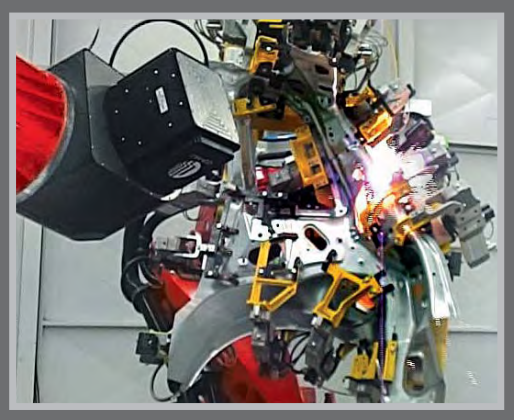

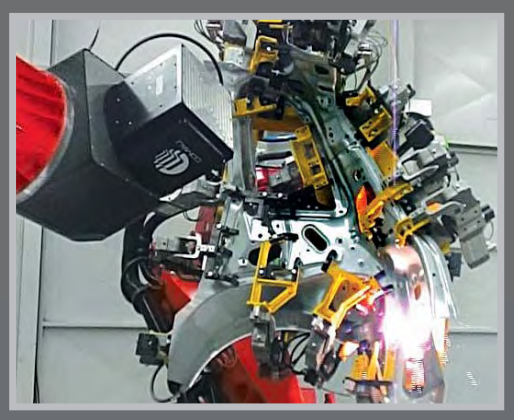

CONFIGURATION SCHEME

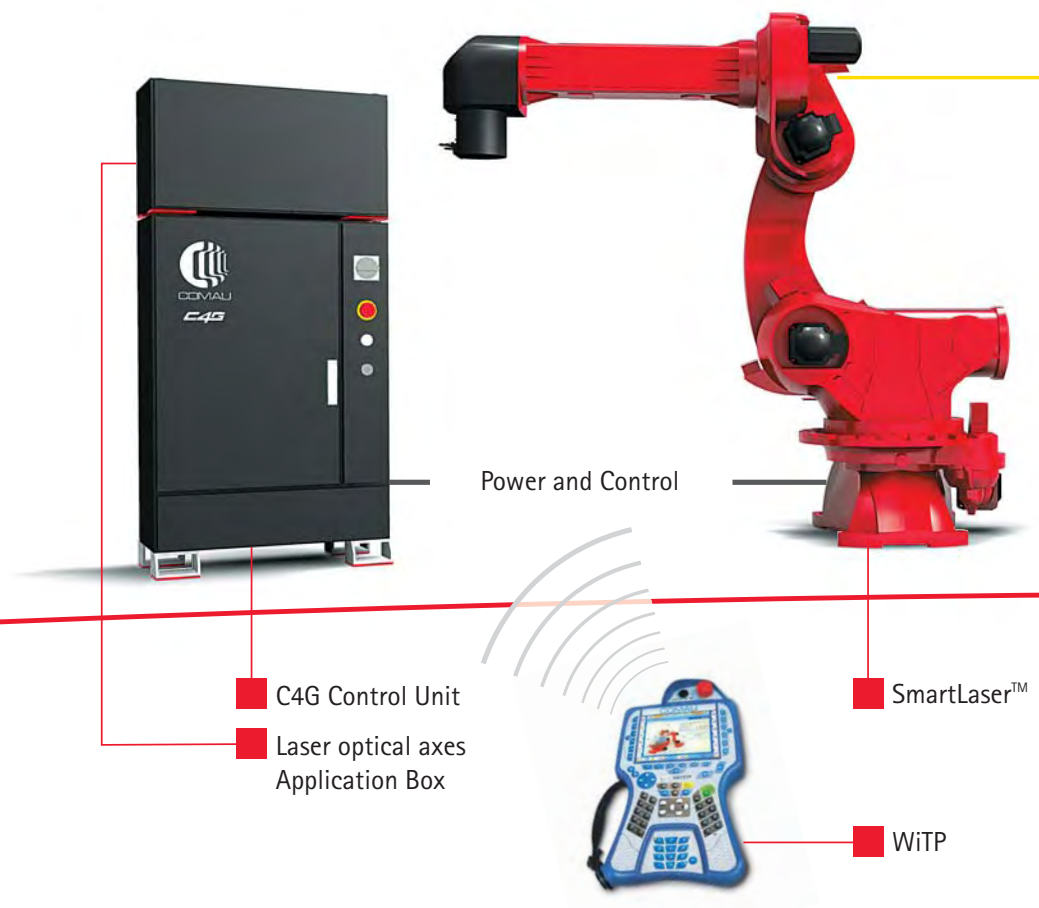

COMAU

Comau in the World

COMAU S.p.A.
Headquarters
Via Rivalta, 30
10095 Grugliasco - TO (Italy)
Tel. +39-011-0049111

COMAU S.p.A.
Powertrain Machining & Assembly
Via Rivalta, 30-49
10095 Grugliasco - TO (Italy)
Tel. +39-011-0049111
Telefax +39-011-0049688

COMAU S.p.A.
Body Welding & Assembly
Strada Borgaretto, 22
10092 Borgaretto di Beinasco - TO (Italy)
Tel. +39-011-0049111
Telefax +39-011-0048672

COMAU S.p.A.
Robotics & Service ■
Via Rivalta, 30
10095 Grugliasco - TO (Italy)
Tel. +39-011-0049111
Telefax +39-011-0049773

COMAU S.p.A.
Dies Business Line
Corso Unione Sovietica, 460
10035 Torino (Italy)
Tel. +39-011-0045876
Telefax +39-011-0045884

Comau France S.A.S ■
5-7, rue Albert Einstein
78197 Trappes Cedex (France)
BP 107
Tel. +33-1-30166100
Telefax +33-1-30166149

Comau Estil ■
10, Midland Road
Luton, Bedfordshire LU2 0HR (UK)
Tel. +44-1582-817600
Telefax +44-1582-817700

Comau Deutschland GmbH ■
Monzastrasse 4D
D-63225 Langen (Germany)
Tel. +49-6103-31035 -0
Telefax +49-6103-31035-29

Mecaner S.A.
Calle Aita Gotzon 37
48610 Urduliz - Vizcaya (Spain)
Tel. +34-94-6769100
Telefax +34-94-6769132

Comau Poland Sp.Z.O.O. ■
Ul. Turyńska 100
43-100 Tychy (Poland)
Tel. +48-32-2179404
Telefax +48-32-2179440

Comau Romania S.r.l.
P.ta Ignatie Darabant, 1
410235 oradea, Bihor
(Romania)
Tel. +40-259-414769
Telefax +40-259-479840

Comau Russia S.R.L.
Tower B / 17 floor
18 Krasnopresnenskaya emb.,
Moscow - 123317
(Russian Federatiom)
Tel. +7-495-7885265
Telefax +7-495-7885266

Comau Inc. ■
21000 Telegraph Road
Southfield, MI 48034 (USA)
Tel. +1-248-3538888
Telefax +1-248-3682531

Comau Pico Mexico S. de R.L. de C.V. ■
Av. Acceso Lotes 12 y 13
Col. Fracc. Ind. El Trébol 2° Secc.
C.P. 54610, Tepotzotlan (Mexico)
Tel. +11-52-5 8760644
Telefax +11-52-5 8761837

Comau Canada Inc.
4325 Division Road Unit # 15
Ontario N9A 6J3 (Canada)
Tel. +1-519-9727535
Telefax +1-519-9720809

Comau do Brasil Ind. e Com. Ltda. ■
Rodovia Fernão Dias Km 429
Distrito Industrial Paulo Camilo
Pena - CEP.: 32.530.970
Betim / MG (Brasil)
Tel. +55-31-21236306
Telefax +55-31-21233349

Comau Argentina S.A. ■
Ruta 9, Km 695
5020 - Ferreyra
Córdoba (Argentina)
Tel. +54-351-4503996
Telefax +54-351-4503909

Comau (Shanghai) Automotive Equipment Co., Ltd. ■
1353 Jiu Gan Road,
Sijing Town, Songjiang District
201601 Shanghai (P.R.China)
Tel. +86-21-37616222
Telefax +86-21-57617386

Comau India Pvt.Ltd. ■
34Km Milestone
Pune - Negar Road
Shikrapur,
Pune - 412208 (India)
Tel. +91-2137-678100
Telefax +91-2137-678110

■ Comau Robotics After Sales Service

Appendix D

This appendix is the original executive results of TSB project and provided by the project manager.

Process Engineering Guidelines

Remote Fibre Laser Welding - Overlap welding of Steels

Weld nomenclature

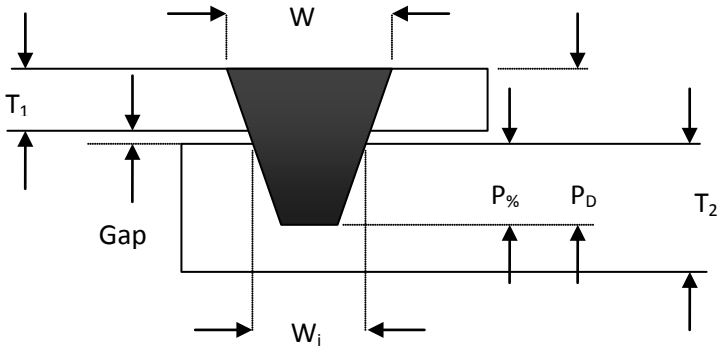

Key:

	T_1	Top sheet material thickness
	T_2	Bottom sheet material thickness
	W	Weld bead top width
	W_i	Weld interface width
	P	Weld penetration depth
	$P_{\%}$	Weld penetration into back sheet (% of T_2)

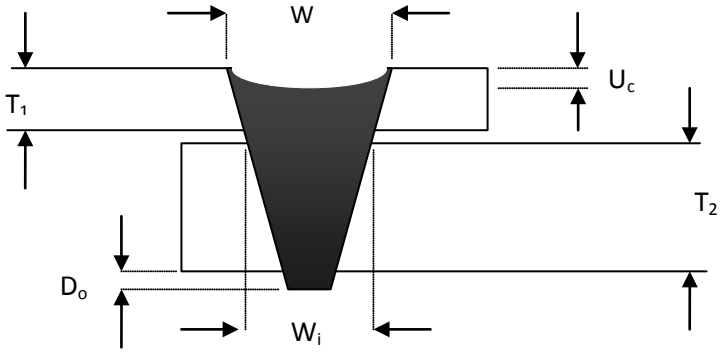

Key:

	T_1	Top sheet material thickness
	T_2	Bottom sheet material thickness
	W	Weld bead top width
	W_i	Weld interface width
	U_c	Depth of weld bead undercut
	D_0	Depth of drop out

Technology description

Overview

Remote Fibre Laser Welding (RFLW) is a welding technique that utilises a laser beam and beam delivery system with a long focal length (typically +1m) which is manipulated across the work piece via scanning optics mounted onto a 'large-area' manipulation system, such as a 6-axis industrial robot. Typically lasers in excess of 4kW are used for RFLW. RFLW produces a weld with attributes similar to those made using close-coupled laser welding technologies (the welds feature high aspect ratios, deep penetration and narrow heat effected zones). Unlike close coupled welding, the RFLW process will not usually apply an inert shielding gas to the weld zone / weld keyhole. An RFLW system will however utilize nozzle systems mounted to the beam delivery system to direct compressed air onto the weld area to remove generated fumes, but this will have no shielding effect or influence on the suppression of the laser generated plasma plume. Mounting the fume suppressing air jets on the beam delivery system ensures that the air jets track over the work piece as the beam delivery system is manipulated. The beam delivery system will also utilise an air-knife to blow ejected weld material and weld fume away from the output optics / aperture. RFLW does not utilise filler wires which may limit the application of the technology for certain materials and material combinations.

Equipment

Equipment required (see Fig. 1.):

1. High power, 'high brightness' laser source (~1070nm Yr-Fibre laser source or ~1060nm diode-pumped Nd:YAG laser source).
2. Laser scanning head (beam delivery system) with 2-axis (X and Y) or preferably 3-axis (X,Y, Z)
3. Large-area manipulation system (6-axis robot)
4. Optical fibre link between laser source and beam-delivery system
5. Safety enclosure
6. Part work holding
7. Services for the above (electrical supply, chilled water supplies, clean, compressed air, etc)

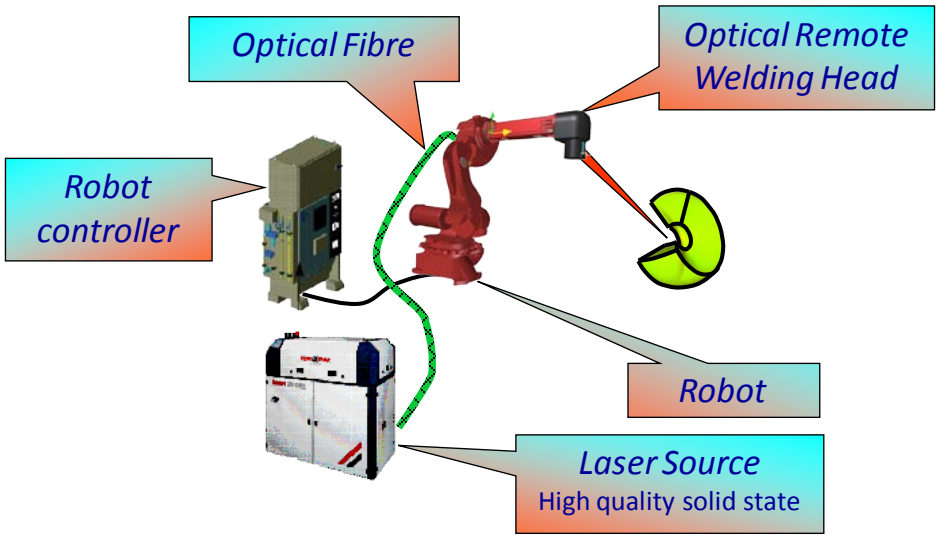

Fig.1. Equipment layout for Remote Laser Welding, excluding tooling (courtesy Comau S.p.a.)

The high beam quality (or 'brightness') of the laser source enables a focal spot appropriate for welding applications to be made with a long focal length (typically 1m+). This in turn permits large stand-off distances between the beam delivery system and the work piece. Laser scanning systems

have very low inertia and can manipulate the laser beam over the work piece at very high speeds (circa 700m/min). The working volume of scanning systems is relatively small however, ranging from approximately 350mm X 350 mm x 150mm up to 500mm x 500mm x 400mm. This constrains not only the maximum part size which may be processed but also the number of planes in which the part may be processed. Early RFLW systems featured CO_2 lasers running through static scanners, limiting the process to planar parts. In contemporary systems the scanning head is mounted onto, or incorporated into, the final axis of a second, large-area manipulation system, typically a 6-axis industrial robot. This allows larger, non-planar parts to be processed. By integrating the motion of both the robot and the scanning system, large areas may be covered with the time taken to traverse between individual stitches reduced by a factor of ten when compared to conventional, discrete joining technologies such as RSW and SPR. The welding speed with the laser is still governed by the energy density available in the focussed spot and the type and thickness of material to be welded, but the reduction in non-productive time (the time to move between each required weld) can allow significant reductions in part cycle time over conventional, discrete joining processes.

For remote laser welding applications, laser sources operating in the near-IR spectrum, such as Nd:YAG or Fibre lasers, are preferred. This is based on two key factors - firstly the wavelength of these lasers is short enough to allow transmission via optical fibres, simplifying the integration of the laser system with the beam delivery system. Secondly, the wavelength of light produced by these sources is not influenced by the plasma plume generated by the welding process. Like the diode-pumped solid state lasers, CO_2 lasers produce a high produce a high quality (or high 'brightness') beam but at a wavelength which is incompatible with fibre optic delivery, meaning that beam transport between the laser and the beam delivery system must be achieved via a network of tubes and mirrors. This adds complications and reliability issues when integrating into a conventional industrial robot. The beam wavelength is also readily absorbed by the plasma plume, and this necessitates the use of plasma suppression gases. This adds costs to the process from both gas delivery systems and the gas itself (typically helium).

Tooling

Unlike conventional, discreet joint process (such as RSW and SPR) the RFLW process applies no force to the work piece, and the long focal lengths employed significantly reduces the potential of collision between the manipulation systems and the work-piece / tooling. As a consequence, it may be possible to construct required tooling using lighter materials and less investment intensive techniques. Increased productivity may also allow more joints to be produced per time cycle, meaning more work can be undertaken per tool with an associated reduction of the total number of tools required.

As RFLW applies no force to the work-piece the tooling must be used to affect panel closure where welds are to be sited. Further to this, if zinc-coated steels are employed a small gap (0.1mm to 0.2mm) must be maintained between the overlapping sheets at the weld site to allow generated zinc vapours to exhaust away from the weld. Failure to include a gap will result in unacceptable levels of material ejection and welds of unacceptable quality. A gap of up to 0.3mm between the sheets is readily acceptable. Lager gaps will result in a reduced performance under peel loads, and excessive top-sheet undercut, reducing fatigue life and corrosion performance.

For uncoated steels, a zero gap is preferable, but a gap of up to 0.25mm is readily acceptable. Lager gaps will result in a reduced performance under peel loads, and excessive top-sheet undercut, reducing fatigue life and corrosion performance

Process cycle times

Process time - theoretical example
Joint: Overlap weld in a stack of 1mm DX54 and 1mm DX54*
Laser source: 4kw Fibre laser
Weld speed (from actual data) = 3.8 m/min (63 mm/s)
Weld length = 25mm (equivalent to 8rt RSW)
Approximate welding time = 0.4s (25mm @ 63mm/s)
Transport time to next stitch = 0.3s
Total time per stitch = 0.7s

Accepted synthetic cycle time for geometry joint (RSW) = 3.6s
Accepted synthetic cycle time for re-spot joint (RSW) = 2.4s

Time saving per geometry stitch = 2.9s
Time saving per re-spot stitch = 1.7s

Time cycle from actual application development
Part: rear cross member for small SUV
Material stack: 1.8mm galvanised steel to 1.8mm galvanised steel
Number of welds: 57
Weld length: 25mm
Approximate total weld length: 1425mm
Weld speed: 1.8 m/min (29 mm/s)
Total weld time: 49s
Total cycle time (robot home to robot home): 59s
Mean time between stitches: 0.18s

*A pre-process ('nubbing') and additional loading operation will be applied when welding galvanised materials, for purposes of zinc-degassing and needs to be accounted for in calculations of total system process time

Typical weld

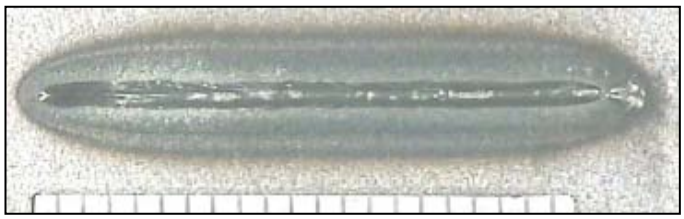

Fig. 2. Top bead made by remote laser welding in an overlap joint: 1.2mm to 1.2mm, DC05

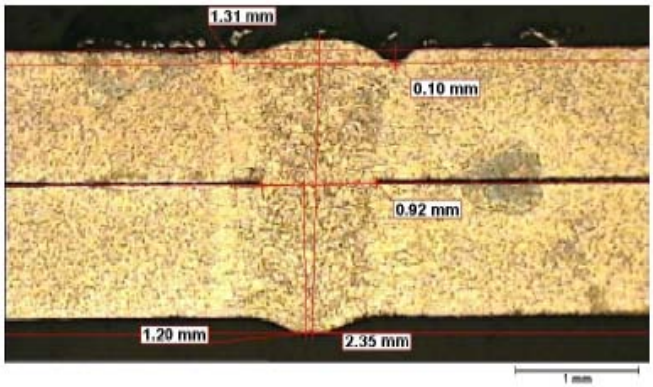

Fig.3. Microsection:Remote laser weld in an overlap joint: 1.2mm to 1.2mm, DC05

The above figures (Fig.2. and Fig.3.) show the ideal laser made in an overlap of two 1.2mm thick sheets of DC05 (an un-coated, plain carbon steel). The weld length shown in Fig.2. is 25mm. Of importance to note is the width of the both the weld top surface and the interface zone when compared to the depth of the weld pentration (in this case full pentration of both upper and lower sheet). The high aspect ratio (depth to width) of the weld is indicative of the laser welding process. The upper sheet and weld top bead should be free from spatter, craters and cracks. The surface should be consistant and show little undercut and the underside of the weld should show no droping out of the weld material. The weld should also be free of pores and cracks.

The below figures (Fig.4. and Fig.5.) show the ideal laser made in an overlap of two 1.0mm thick sheets of DX54 (a zinc coated, DC02 grade, plain carbon steel). When welding zinc coated materials, the rapid boiling of the zinc coating at the interface of the two sheets creates a high-pressure vapour. Unless exhausted, this vapour will vent explosively through the weld zone. To prevent this phenomenon it is typical to force a gap between the two sheets at the interface, thus providing an exhaust volume for the zinc vapours. This gap (approximately 0.2mm thick) is shown in the micrograph (Fig.5) below. As with the DCO5 grade materials, it is expected that the material surface and weld top bead are from spatter , craters and cracks. The surface should be consistant and show little undercut and the underside of the weld should show no droping out of the weld material. The weld should be free of pores and cracks.

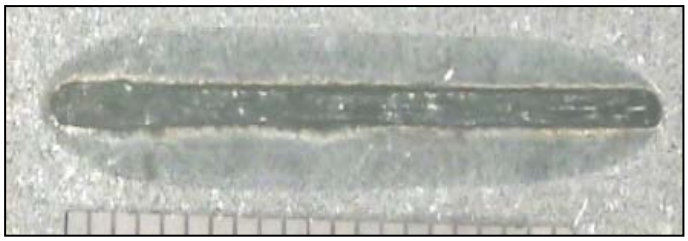
Fig.4. Remote fibre laser weld top bead in an overlap joint: 1.0mm to 1.0mm, DX54, 0.2mm gap

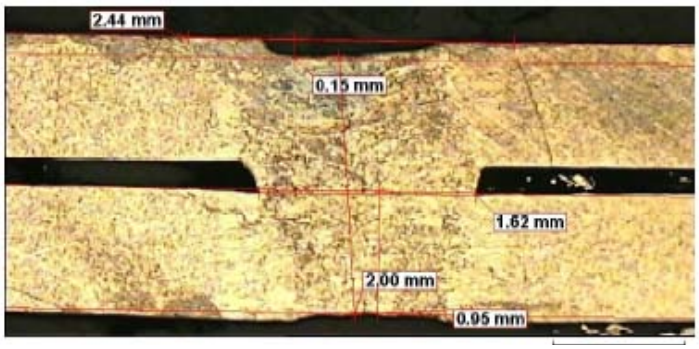

Fig.5. Microsection: Remote laser weld in an overlap joint: 1.0mm to 1.0mm, DX54, 0.2mm gap

Typical failure modes

Undercut

Identification

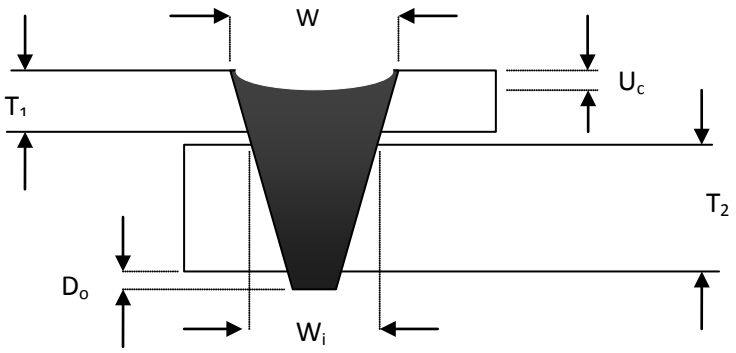

Key:

	T_1	Top sheet material thickness
	T_2	Bottom sheet material thickness
	W	Weld bead top width
	W_i	Weld interface width
	U_c	Depth of weld bead undercut
	D_0	Depth of drop out

Fig.6. Schematic: Annotated weld cross-section

Cause

1. Material ejection (spatter evident around joint and local tooling) (see Fig.7: top bead.)
    a. Zero gap with coated steels (see micrograph Fig.7: microsection.)
    b. Adhesive contamination at interface (top bead appearance as shown in photograph Fig.7: top bead.)
2. Excessive gap between sheets (see Fig.8: micrograph) (undercutting is present without evidence of material ejection - see photograph Fig.8: top bead)
3. Excessive weld penetration - excessive heat input per unit length per unit time for the given thickness of material (associated with *Drop-out*, see below)

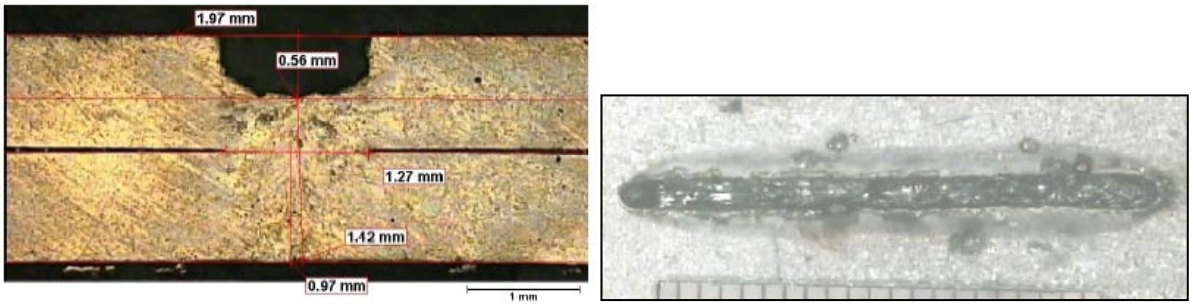

Fig.7. Microsection and top bead: overlap weld 1.0mm to 1.0mm DX54, 0mm gap

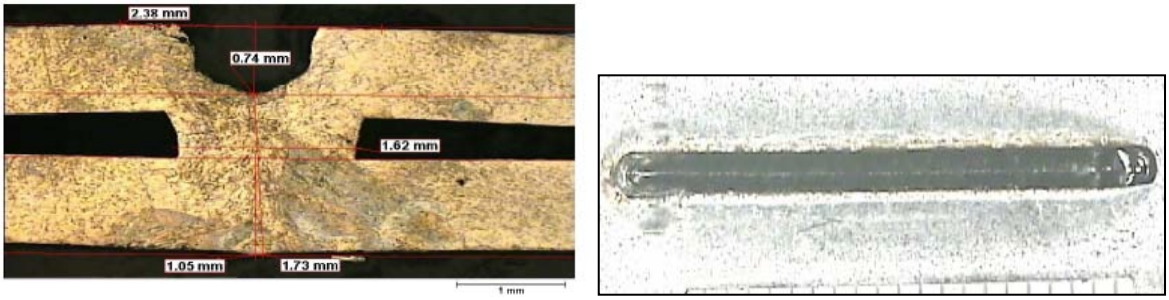

Fig.8. Microsection and top bead: overlap weld 1.0mm to 1.0mm DX54, 0.4mm gap

Drop-out

Identification

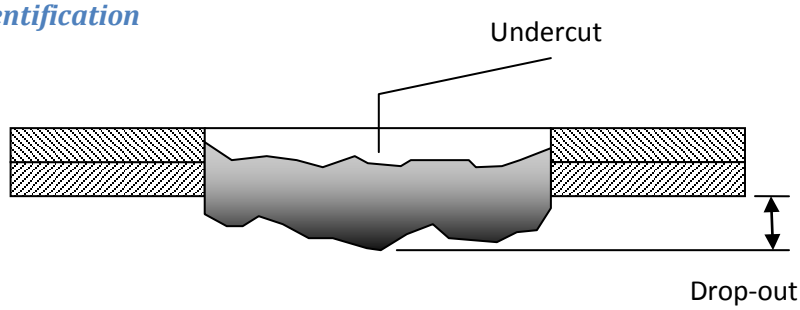

Fig.9. Schematic: Longitudinal weld section showing undercut and drop-out

Cause

- Excessive power per unit length per unit time.
    a. Weld speed too low.
    b. Laser power too high.
    c. Material too thin.

Interface width

Identification

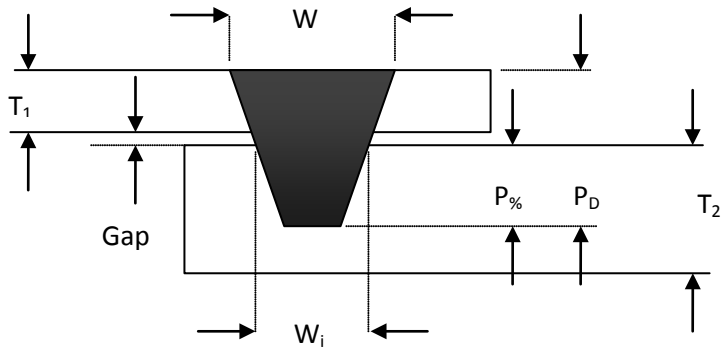

Key:

	T_1	Top sheet material thickness
	T_2	Bottom sheet material thickness
	W	Weld bead top width
	W_i	Weld interface width
	P	Weld penetration depth
	$P_{\%}$	Weld penetration into back sheet (% of T_2)

Fig.10. Schematic: Annotated weld cross-section

Cause

- Lack of penetration
    a. Reduced power per unit length per unit time.
        i. Laser power too low.
        ii. Weld speed too high.
        iii. Laser out of focus (increased spot size).
            1. Contaminated optics
            2. Relationship between laser beam and material surface has changed
            3. Issue with laser source
        iv. Impingement angle too steep
            1. Increased reflection of laser radiation
            2. Increased spot size
            3. Increase in effective thickness of material
        v. Masking of the beam
    b. Material too thick.
- Narrow weld
    a. Reduced laser spot size

Penetration

Identification

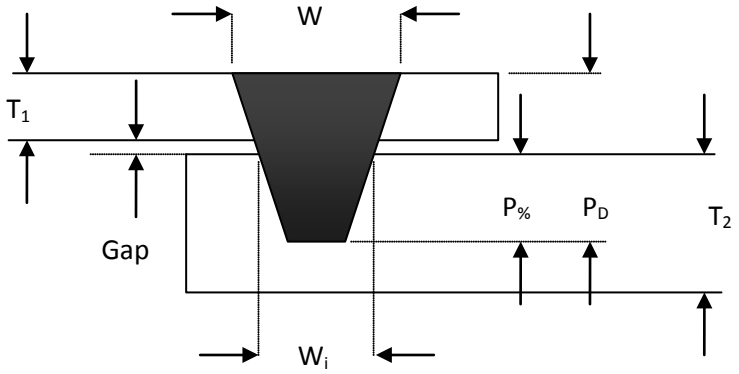

Key:
T_1	Top sheet material thickness
T_2	Bottom sheet material thickness
W	Weld bead top width
W_i	Weld interface width
P	Weld penetration depth
$P_{\%}$	Weld penetration into back sheet (% of T_2)

Fig.11. Schematic: Annotated weld cross-section

Cause

1. Reduced power per unit length per unit time.
    a. Laser power too low.
    b. Weld speed too high.
    c. Laser out of focus (reduced energy density).
    d. Impingement angle too steep (increased reflection of laser radiation).
2. Increased material thickness.

Porosity

Identification

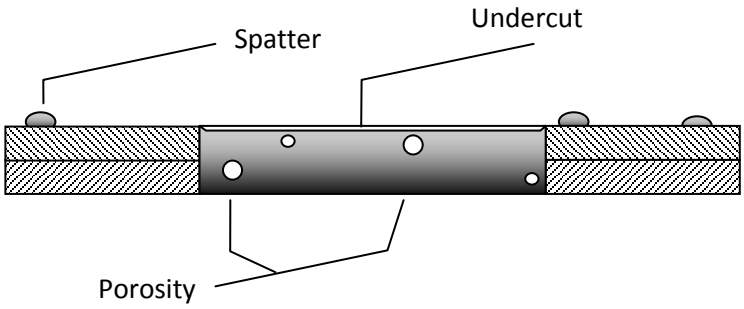

Fig.12. Schematic: Longitudinal weld section showing porosity, undercut and spatter

Cause

1. Material ejection (spatter evident around joint and local tooling)
    a. Zero gap with coated steels
    b. Adhesive contamination at interface

Holes

Identification

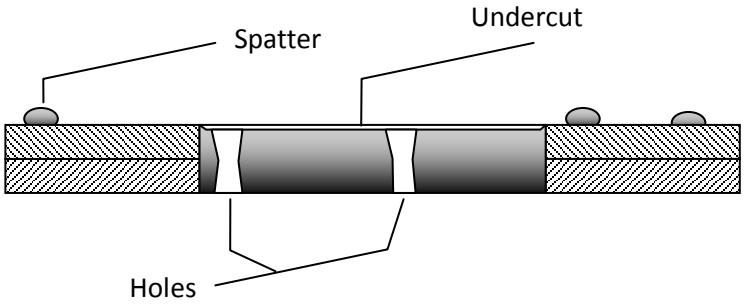

Fig. 13.a. Schematic: Longitudinal weld section showing holes and spatter

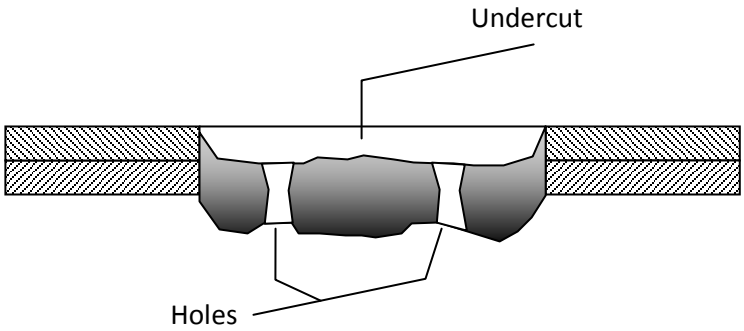

Fig.14.b. Schematic: Longitudinal weld section showing undercut, dropout and holes

A hole is a discrete discontinuity in the weld that extends to a depth below the interface. A hole does not have to fully penetrate the weld material. Some standards class blind holes (holes that do not fully penetrate the weld material) as ‘top surface cut-through’. The classification of a hole presented here is applicable to welds that both fully penetrate and partially penetrate the lower sheet. Both through-holes and ‘top surface cut-through’ share common causes.

Cause

1. Material ejection (spatter evident around joint and local tooling) (see Fig.13.a.)
    a. Zero gap with coated steels
    b. Adhesive contamination at interface
2. Excessive interface gap (the weld will also feature undesirable levels of undercutting)
3. Reduced focus spot (remote cutting)
4. Excessive energy input per unit length per unit time (the weld will also demonstrate over-penetration and drop-out) (see Fig.13.b.)
    a. Weld speed too low
    b. Laser power too high
    c. Reduced material thickness

Cracks

Identification

Cracking was not detected in any of the samples produced for the data in the document.

Cause

1. Excessive cooling rates
2. Material contraction upon cooling

Missing weld

Identification

Fig.15.a. Typical laser weld stitch on DX54

Fig.15b. Typical missing weld on DX54

A location on the part where a weld stitch is expected (refer to master part or master documentation) but remains unaffected by laser output (no witness marks on the workpiece). A witness mark on the material surface indicates different failure modes.

Cause

First off parts:

- Incorrect programming of part
- Complete masking of the weld location by tooling or the workpiece
- Software failure within the programme or control system
- Masking of weld zone
- Malfunction of communication within the cell
- Incorrect operation of the welding cell

Serial parts:

- Modification of the part programme
- Software failure within the programme or control system
- Malfunction of communication within the cell
- Incorrect operation of the welding cell
- Intermittent failure of the laser source

Stitch shape

Identification

The overall length or the shape of the welded stitch is not as described on the master part on in the master document.

Cause

Stitch length:

- Incorrect part programming- an incorrect stitch shape was programmed, or selected by the robot programme.
- Masking of the weld zone by tooling or the workpiece.
- Software failure within the programme or control system
- Malfunction of communication within the cell
- Incorrect operation of the welding cell
- Intermittent failure of the laser source

Stitch shape:

- Incorrect part programming - an incorrect stitch shape was programmed, or selected by the robot programme.

Stitch location

Identification

The laser stitch will not be in the location defined on the master part or within the master document.

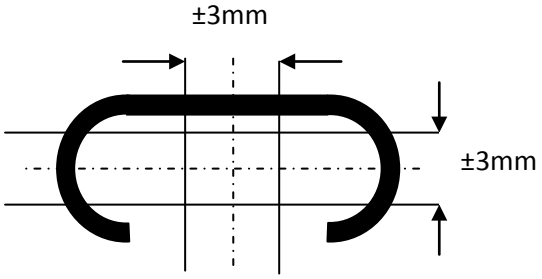

Fig.16: Schematic: Positional tolerance for a laser stitch

Cause

First-off parts:

- Incorrect location programmed.
- Parts located incorrectly, change of master location
- Incorrect parts

Serial parts:

- Modification to programme.
- Modification to part / master location
- Parts located incorrectly, change of master location

- Incorrect parts
- Failure of robot / scanning sytem

Process Engineering Guidelines

Applicable joint types

These guidelines are only applicable to joints made in steel sheet in an overlapping configuring.

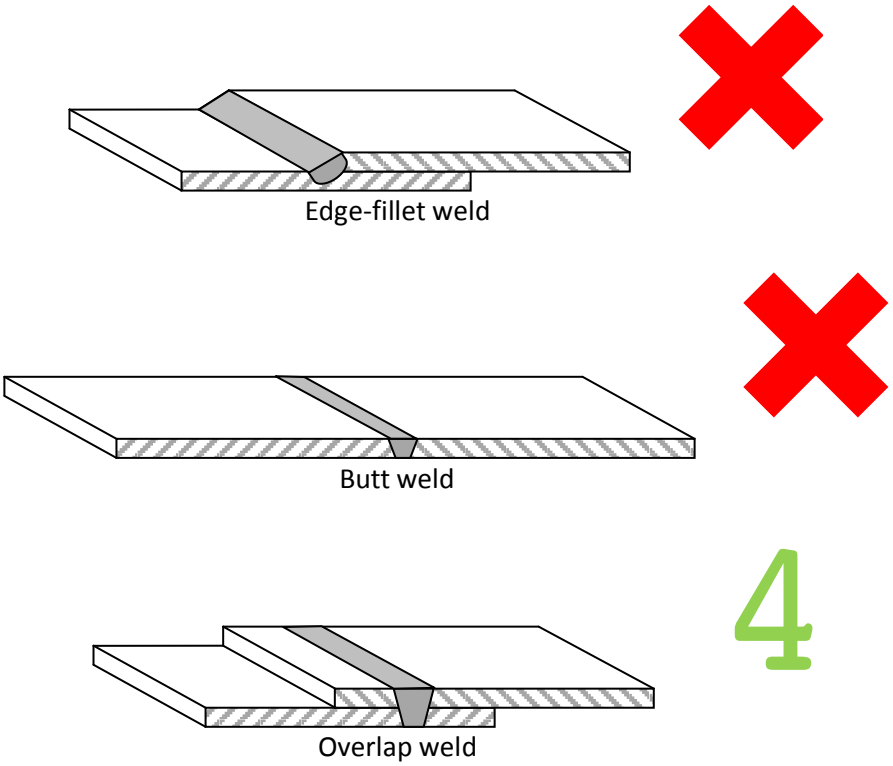

Fig.17. Schematic: Permissible joint configurations for remote laser welding

Material stacks: thickness and thickness combinations

Thickness

Steel alloy stacks of up to 6mm total thickness (2 x 3mm) can be acceptably laser welded providing neither sheet exceeds 3mm thickness.

Robust and repeatable welds have been made on material stack combinations up to, and including 3mm to 3mm overlap welds. Results are shown below for joint stacks of 1mm -1mm, 2mm - 2mm and 3mm - 3mm.

Thickness combinations (thin/thick, thick/thin)

Two-sheet stack combinations with thickness differentials of up to 1.3mm (e.g. 0.7mm to 2.0mm sheet) have been proved in both thin/thick and thick/thin orientations.

Material Capability: DX54: Expected Lap shear strength / Weld Speed								
		Top						
		0.7	1	1.5	1.7	2	2 (boron)	3
Bottom	0.7	4.6 / 4.4	5.1 / 4.2		5.8 / 3.4	5.8 / 3.4	6.0 /	
	1	5.1 / 4.2	7.4 / 3.8	7.7 / 3.8		6.2 / 3.2		
	1.5		7.8 / 3.8	11.4/3.2				
	1.7	5.5 / 3.4			12.7/2.6			
	2	5.8 / 3.6	8.2 / 3.4			17.8 / 2.2		
	2 (boron)	6.0 /	9.4 / 3.8					
	3							17.2 / 0.8

Fig.18. Table: Lap shear strength and weld speed for permissible material stack combinations: DX54

Stack combinations up to 0.7 to 2.0mm (1.3mm thickness differential) have been tested in both thin/thick and thick/thin orientations with acceptable performance from the resulting joints. Weld speed will require tailoring to suit the specific top sheet thickness of any presented stack combination.

Material stacks: grades and combinations

Material grades

Any combination of the following grades of steel can be readily and acceptably welded: DC04, DC05, DX54, DX55, HSLA, BH (up to 260), XF (up to 350), DP (up to 600), boron steels (up to 1200), 304, EN8 EN16, EN3

The above steels may be uncoated or galvanised (HDG, EZ). Tested Boron steels were aluminised coated. For stack combinations that include zinc coated steels, refer to the rules on interface gap control.
Mixed thickness combinations tested to date are specified in Fig.19. below. For plain carbon steels, the weld speed is dependent on the material thickness and not the grade of the steel alloy processed.

Material Capability: DX54 Permissable stack combinations								
		Top						
		0.7	1	1.5	1.7	2	2 (boron)	3
Bottom	0.7							
	1							
	1.5							
	1.7							
	2							
	2 (boron)							
	3							

Fig.19. Table: Permissible material stack combinations: DX54

Thickness combinations (thin/thick, thick/thin)

With appropriate changes to weld speed, the steel alloys tested can be welded regardless of stack orientation

Stack combinations up to 0.7 to 2.0mm (1.3mm thickness differential) have been tested in both thin/thick and thick/thin orientations with acceptable performance from the resulting joints. Weld speed will require tailoring to suit the specific top sheet thickness of any presented stack combination.

i. For conventional steel materials, stack combinations of up to 6mm total thickness (3mm+3mm) have been successfully welded.
ii. The plain carbon steel alloys tested demonstrate no sensitivity (in terms of mechanical performance) to stack orientation. Stack combinations up to 0.7 to 2.0mm (1.3mm thickness differential) have been tested in both thin/thick and thick/thin orientations and joint performance is unaffected. Weld speed will require tailoring to suit the specific top sheet thickness of any presented stack combination, as indicated in the table below.

Material Stacks: Mixed materials

Material stack combinations containing both steel and aluminium alloys cannot be welded.

Material stacks that include both aluminium and steel alloys are non-viable material combinations for the laser welding processes. Alternative joining technologies must be sought.

Material stacks: Three sheet stacks

Uncoated steels

Uncoated steels are readily welded in stacks of three sheets.

Coated steels

Material stack combinations including three sheets where some or all of the sheets are coated with zinc are readily weldable if a suitable interface gap (optimum 0.18mm) is maintained at any interfaces where zinc will be present.

Cycle time

Process time - theoretical example

Joint: Overlap weld in a stack of 1mm DX54 and 1mm DX54
Laser source: 4kw Fibre laser
Weld speed (from actual data) = 3.8 m/min (63 mm/s)
Weld length = 25mm (equivalent to 8rt RSW)
Approximate welding time = 0.4s (25mm @ 63mm/s)
Transport time to next stitch = 0.3s
Total time per stitch = 0.7s

Accepted synthetic cycle time for geometry joint (RSW) = 3.6s
Accepted synthetic cycle time for re-spot joint (RSW) = 2.4s

Time saving per geometry stitch = 2.9s
Time saving per re-spot stitch = 1.7s

Process time: example

Time cycle from actual application development

Part: rear cross member for small SUV
Material stack: 1.8mm galvanised steel to 1.8mm galvanised steel
Number of welds: 57
Weld length: 25mm
Approximate total weld length: 1425mm
Weld speed: 1.8 m/min (29 mm/s)
Total weld time: 49s
Total cycle time (robot home to robot home): 59s
Non-productive time: 10s
Mean time between stitches: 0.18s (10s / 57 stitches)

For further cycle time calculations refer to Fig.20. below, showing expected weld speeds for a range of two-sheet material stacks.

Material Capability: DX54: Expected Weld Speed								
		Top						
		0.7	1	1.5	1.7	2	2 (boron)	3
Bottom	0.7	4.4	4.2		3.4	3.4		
	1	4.2	3.8	3.8		3.2		
	1.5		3.8	3.2				
	1.7	3.4			2.6			
	2	3.6	3.4			2.2		
	2 (boron)		3.8					
	3							0.8

Fig.20. Table: Weld speeds for permissible stack combinations: DX54

Flange requirement / opportunity

RFLW can be applied to panels featuring a flange width of 8mm

Adhesive requirements

Adhesive products (structural, sealant or anti-flutter) must not be present at the weld location. Weld stitches must be 10mm away from the location of any adhesive bead or product (pumpable, tape, pre-form etc)

Lubricant tolerance

Wet lubricant coatings of up to 6gm/m^2 can be readily tolerated. Heavier lubricant coatings have not been tested.

Weld attributes

Undercut

Undercutting of the weld top surface must not exceed 25% of the top sheet thickness (evidence)

Drop-out

Standards do not specify limits for material drop-out, however drop-out is always associated with undercutting of the top-bead surface, therefore limits on drop out can be defined by the undercutting (maximum undercut of 25% T_1), providing the underside of the material stack:

- is neither a Class A of Class B surface (drop out and complete penetration would be unacceptable).
- Does not interfere with interfacing surfaces from further or subsequent assembly (drop out would be unacceptable).

Interface width

Interface width must exceed the width of the thinnest material in the welded stack.

Penetration

A laser weld must penetrate at least 30% into the lower material sheet

Porosity

The must be no more than one visible surface pore (exceeding 0.2mm diameter) per 5mm of weld stitch.

On sectioned samples, the interface width must be free from porosity.

Holes

One hole, not exceeding 1.0mm diameter per 10mm of weld length unless complete sealing of the weld is specifically specified, in which case holes are unacceptable in welds that fully penetrate both sheets.

Stitch Length

A laser weld stitch, if being used as a direct substitute for a resistance spot weld, should be at least 25mm in length.

A laser weld stitch, if being used as a direct substitute for a resistance spot weld, should be at least 25mm in length. This length can include the weld start and finish. For joint stack combinations consisting of thinner gauges of DX54 and DC05 materials (0.7mm to 3mm), a laser weld stitch requires a sound weld length of between 14mm and 18mm to match the lap-shear performance of an acceptable spot weld ($4rt_1$), regardless of the shape of the stitch.

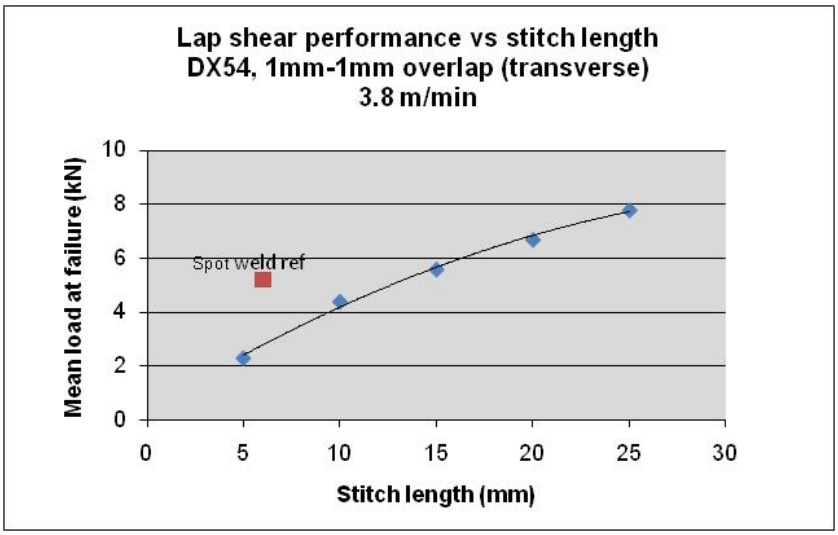

Fig.21. Graph: Lap shear strength vs stitch length: 1.0mm to 1.0mm, DX54, 0.2mm gap

The reference spot weld (6 mm measured diameter) failed at a load of 5.2kN, equating to a weld stitch length of 13.33mm

Gap requirements:

Uncoated steels

For material stack combinations that include only uncoated steels, interface gaps must not exceed 0.3mm.

The optimum interface gap for material stack combinations featuring only uncoated steels (DC04, DC05, XF350 etc) is 0mm gap. Gaps of up to 0.2mm can be readily tolerated. Larger gaps will result in reducing quasi-static and dynamic performance, particularly where peel is a factor in loading. With 0mm gap, top sheet undercut is 0mm. An interface gap larger than 0.2mm will result in a top bead undercut exceeding 20%t_1

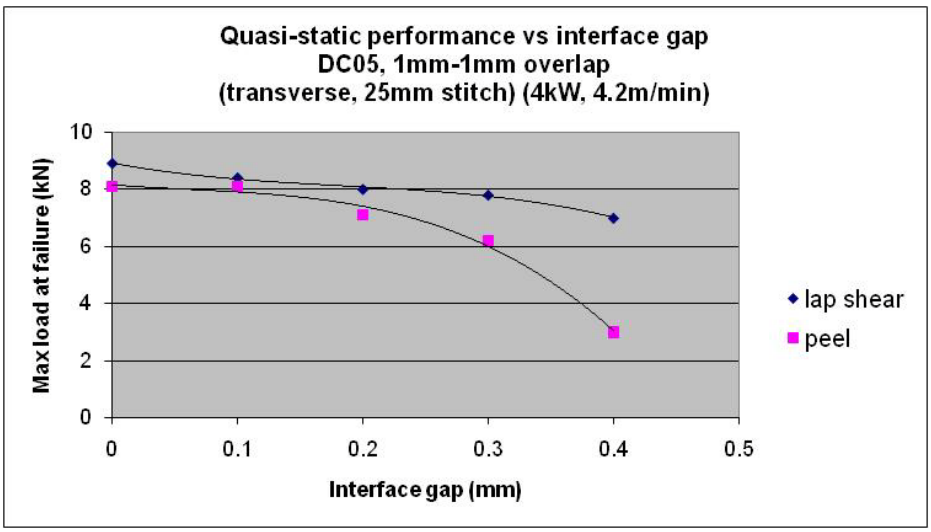

Fig.22. Graph: Weld strength vs interface gap: 1.0mm to 1.0mm, DC05, 0mm gap

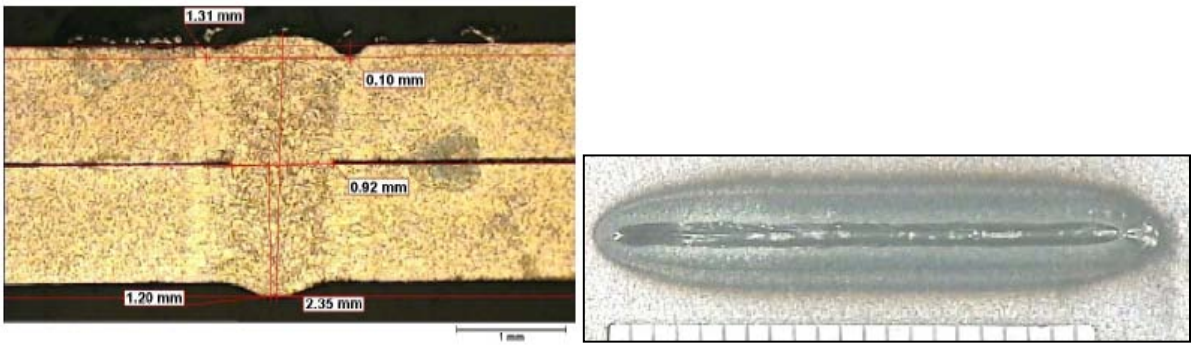

Fig.23. Microsection and top bead: overlap weld:1.2mm to 1.2mm DC05, 0mm gap.
NB: Minimal undercutting

Coated steels

Material stack combinations that include zinc coated steels will require an interface gap between 0.1 and 0.25mm

Stack combinations that include zinc coated steels (such as DX54, DP600GI etc) require an interface gap to enable the exhausting of zinc vapours that will be generated at the interface of the stack sheets. The optimum gap is approx 0.18mm, and this provides optimum weld strength under both quasi-static and dynamic loading.

Influence of gap on weld quality

Joint stack combinations featuring zinc coated steels and interface gaps of less than 0.1mm gap will demonstrate increased material ejection (spatter), increased weld bead top surface disruption, increased undercutting of the weld bead and reduced / inconsistent weld strength (see table below). Neighbouring parts and fixturing will also be subject to contamination with spatter

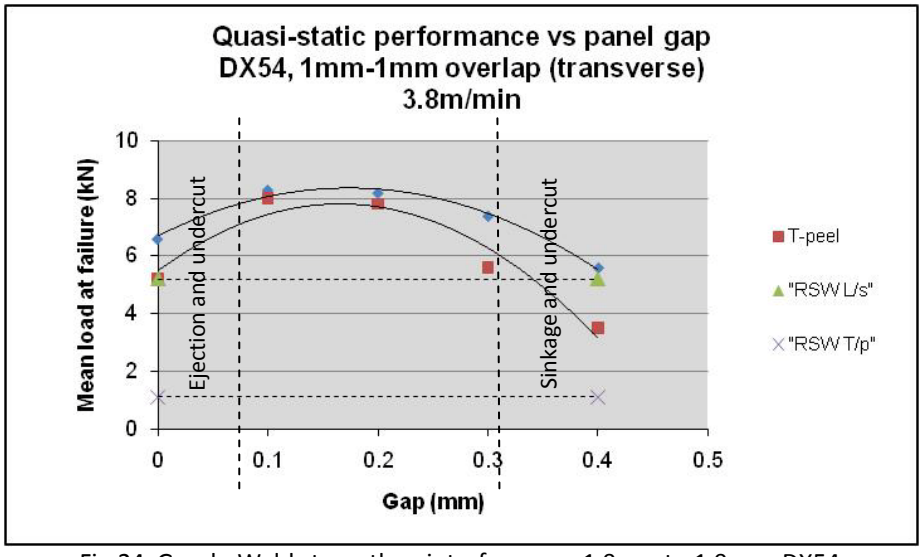

Fig.24. Graph: Weld strength vs interface gap: 1.0mm to 1.0mm, DX54

Welds made in stack combinations that include zinc coated steels and feature no interface gap will demonstrate high levels of spatter and undercut, as well as potentially high levels of porosity. All of these attributes will result in rejection of the weld.

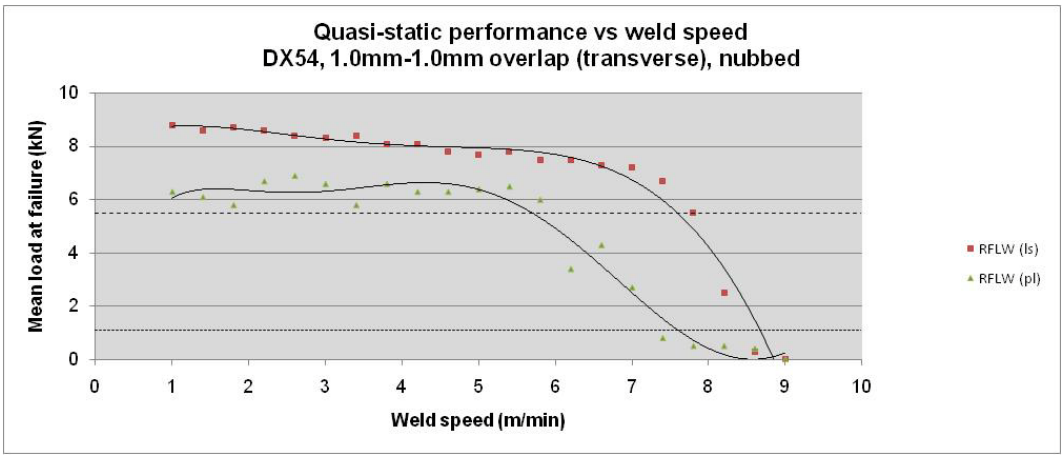

Fig.25. Graph: Weld strength vs weld speed: 1.0mm to 1.0mm, DX54 nubbed gap

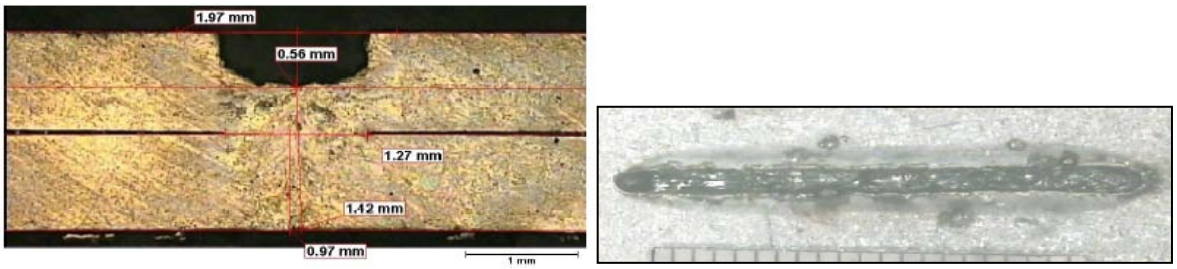

Fig.26. Microsection and top bead: 1.0mm to 1.0mm, DX54, 0mm gap. Undercut = 56%t_1

In Fig.26. spatter is clearly visible on the parent material and the top bead surface appears uneven. Weld undercutting is excessive because of the ejection of weld material. This weld will be rejected: spatter, top bead undercutting exceeds 20%t_1

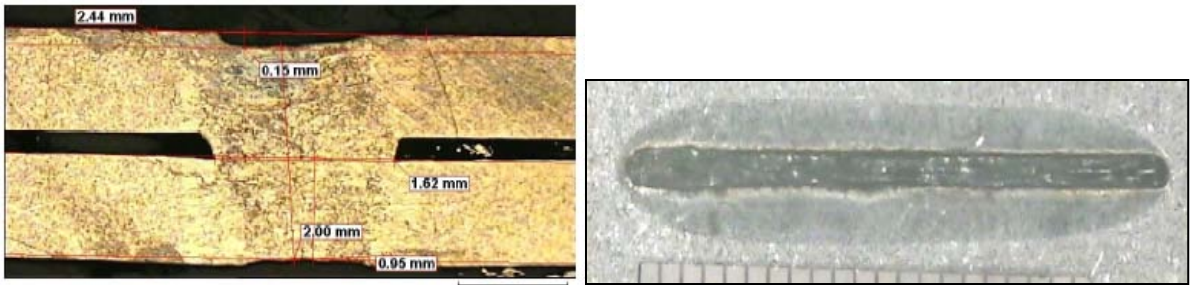

Fig.27. Microsection and top bead: 1.0mm to 1.0mm, DX54, 0.2mm gap. Undercut = 15%t_1

In Fig.27. the weld top surface appears consistent and smooth, and the weld shows minimal undercutting (material lose at the top and bottom surface is mostly attributable to the weld material filling the interface gap).

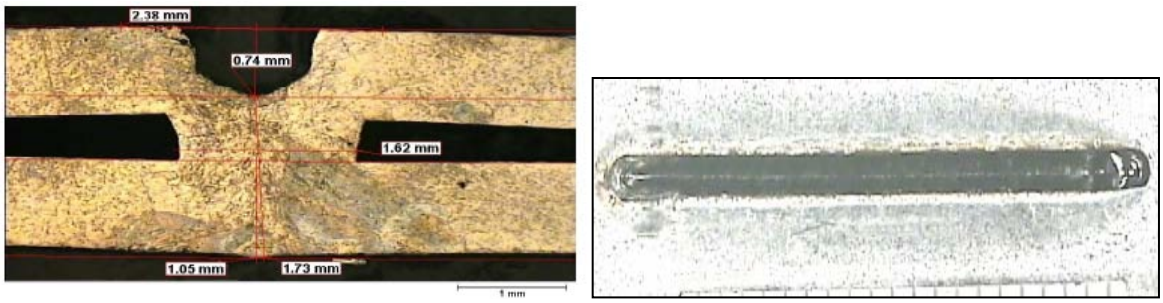

Fig.28. Microsection and top bead: 1.0mm to 1.0mm, DX54, 0.4mm gap. Undercut = 74%t_1

In Fig.28. the weld features excessive undercutting of the top bead and will be rejected on these grounds. The quasi-static strength of the weld will be acceptable because the weld material has flowed into the interface gap and created a wider effective weld interface, however under dynamic loading this joint will perform poorly.

Nub requirements

Nub attributes

0.12 - 0.18mm high

Distribution per stitch

Three nubs - one start, one finish and one offset in the middle (for straight stitches). For elliptical stitches, three nubs equi-spaced along the centreline of the end radii (see picture)

Nub cycle time

Clamp requirements

Strength

Stitch length

A laser weld stitch, if being used as a direct substitute for a resistance spot weld, should be at least 25mm in length.

A laser weld stitch, if being used as a direct substitute for a resistance spot weld, should be at least 25mm in length. This length can include the weld start and finish. For joint stack combinations consisting of thinner gauges of DX54 and DC05 materials (0.7mm to 3mm), a laser weld stitch requires a sound weld length of between 14 and 18mm of to match the lap-shear performance of an acceptable spot weld ($4rt_1$), regardless of the shape of the stitch.

Proof by weld performance (maximum load at lap shear failure)

The reference spot weld (6 mm measured diameter) failed at a load of 5.2kN, equating to a weld stitch length of 13.33mm

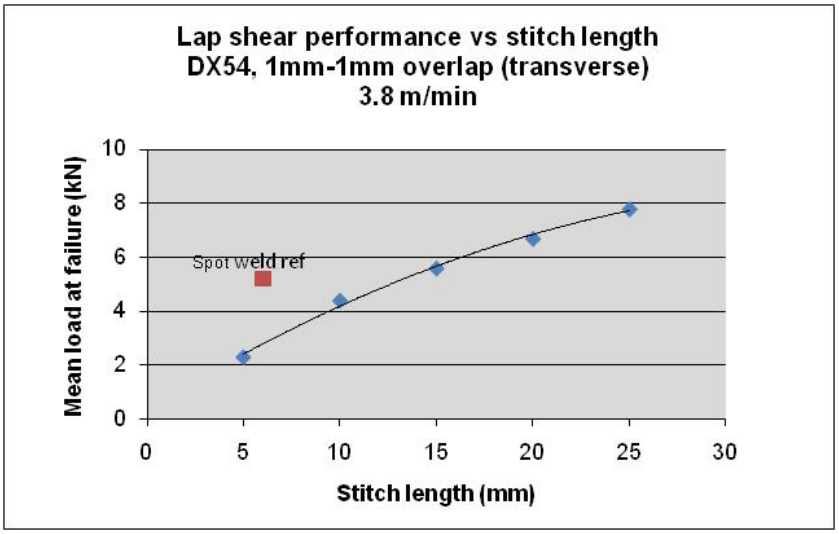

Fig.29. Graph: Lap shear strength vs stitch length: 1.0mm to 1.0mm, DX54, 0.2mm gap

Proof by weld interface area:

Weld performance, with respect to maximum load before failure can be considered a function of the area of welded interface.

Assumptions:
Material stack: 1mm / 1mm DX54
Laser weld interface width: 1.6mm (see micrograph below)

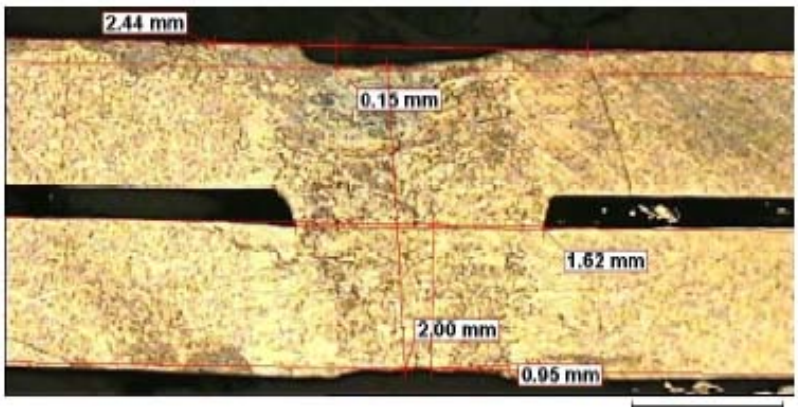

Fig.30. Microsection: Remote laser weld: 1.0mm to 1.0mm, DX54, 0.2 mm gap

Accepted spot diameter: $4rt_1$
Spot weld diameter ($4rt_1$) = 4mm
Spot weld interface area (πr^2) = 25mm^2
Equivalent length of laser stitch = 16mm

Strength vs stitch shape

Mechanical performance (failure modes etc)(fatigue)

Process window

Weld speed tolerance

Material stacks: thickness and thickness combinations

Thickness

> Steel alloy stacks of up to 6mm total thickness (2 x 3mm) can be acceptably laser welded.

Robust and repeatable welds have been made on material stack combinations up to, and including 3mm to 3mm overlap welds. Results are shown below for joint stacks of 1mm -1mm, 2mm - 2mm and 3mm - 3mm (see figures 31, 32 and 33 below).

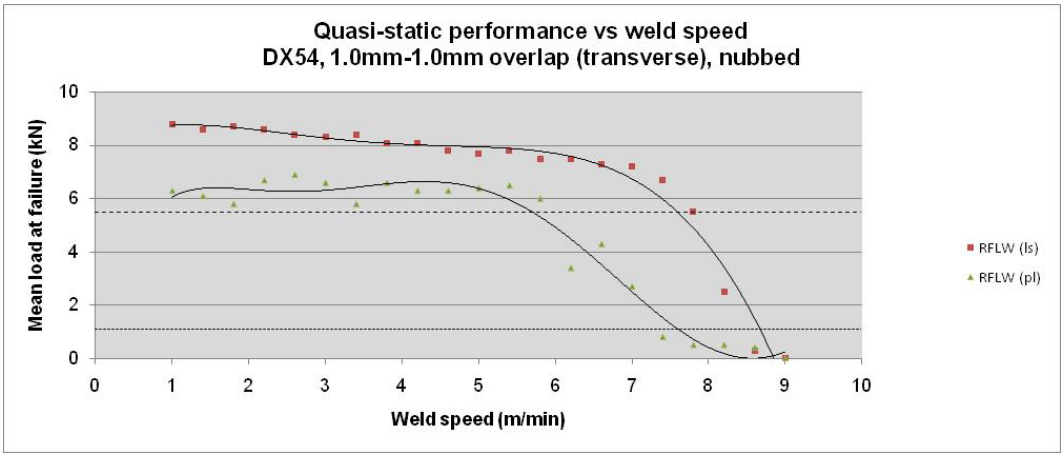

Fig.31. Graph: Weld strength vs weld speed: 1.0mm to 1.0mm, DX54. Nubbed gap

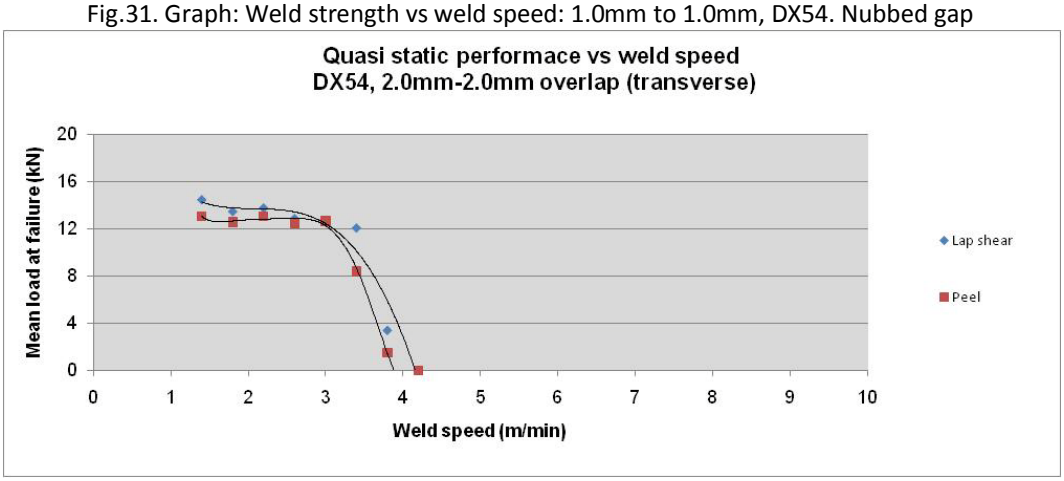

Fig.32. Graph: Weld strength vs weld speed: 2.0mm to 2.0mm, DX54, 0.2mm gap

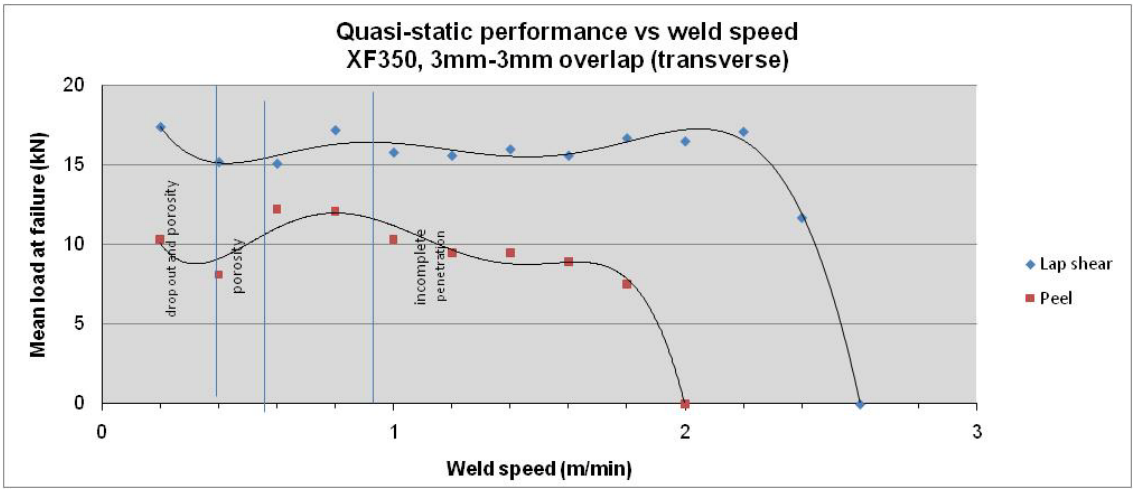

Fig.33. Graph: Weld strength vs weld speed: 3.0mm to 3.0mm, XF350

Thickness combinations

The steel alloys tested demonstrate no sensitivity to stack orientation.

Stack combinations up to 0.7 to 2.0mm (1.3mm thickness differential) have been tested in both thin/thick and thick/thin orientations and joint performance is acceptable in both orientations. Weld speed will require tailoring to suit the specific top sheet thickness of any presented stack combination (see Fig.34. below).

Material Capability: DX54 Permissable stack combinations								
		Top						
		0.7	1	1.5	1.7	2	2 (boron)	3
Bottom	0.7							
	1							
	1.5							
	1.7							
	2							
	2 (boron)							
	3							

Fig.34. Table: Permissible material stack combinations: DX54

The steel alloys tested demonstrate no sensitivity (in terms of mechanical performance) to stack orientation. Stack combinations up to 0.7 to 2.0mm (1.3mm thickness differential) have been tested in both thin/thick and thick/thin orientations and joint performance is unaffected. Weld speed will require tailoring to suit the specific top sheet thickness of any presented stack combination, as indicated in the table below.

Material Capability: DX54: Expected Lap shear strength / Weld Speed								
		Top						
		0.7	1	1.5	1.7	2	2 (boron)	3
Bottom	0.7	4.6 / 4.4	5.1 / 4.2		5.8 / 3.4	5.8 / 3.4	6.0 /	
	1	5.1 / 4.2	7.4 / 3.8	7.7 / 3.8		6.2 / 3.2		
	1.5		7.8 / 3.8	11.4/3.2				
	1.7	5.5 / 3.4			12.7/2.6			
	2	5.8 / 3.6	8.2 / 3.4			17.8 / 2.2		
	2 (boron)	6.0 /	9.4 / 3.8					
	3							17.2 / 0.8

Fig.35. Table: lap shear stregnth and weld speed for permissible material stack combinations: DX54

Material stacks: grades and combinations

Material grades

Any combination of the following grades of steel can be readily and acceptably welded: DC04, DC05, DX54, DX55, HSLA, BH (up to 260), XF (up to 350), DP (up to 600), boron steels (up to 1200), 304, EN8 EN16, EN30

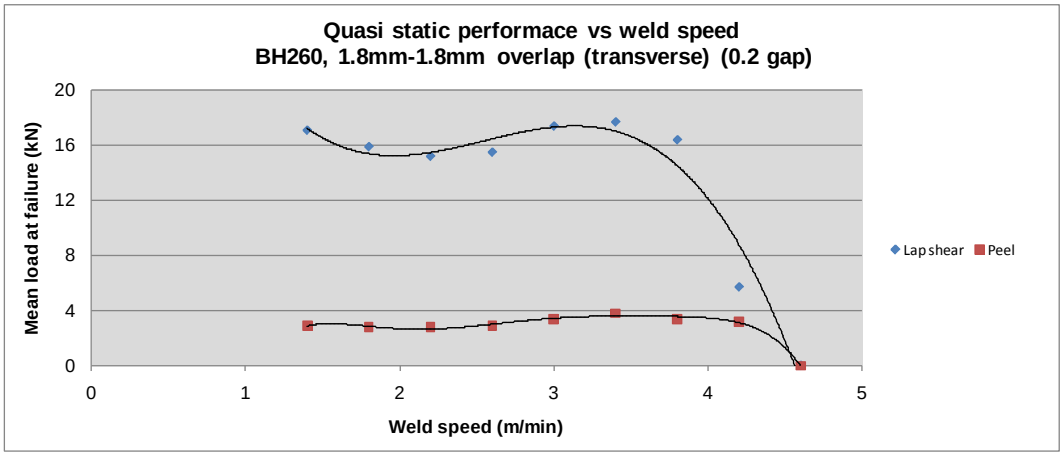

Fig.36. Graph: Weld strength vs weld speed: 1.8mm to 1.8mm, BH260, 0.2mm gap

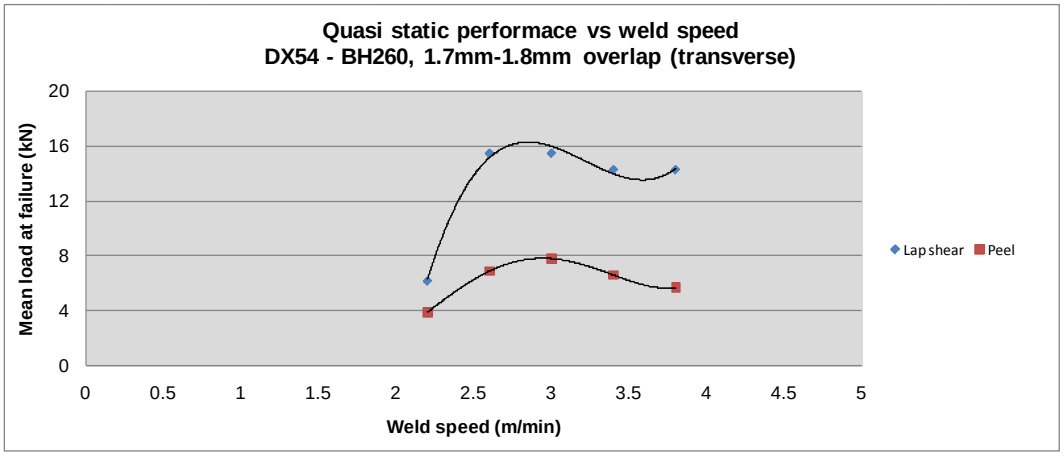

Fig.37. Graph: Weld strength vs weld speed: 1.7mm DX54 to 1.8mm BH260, 0.2mm gap

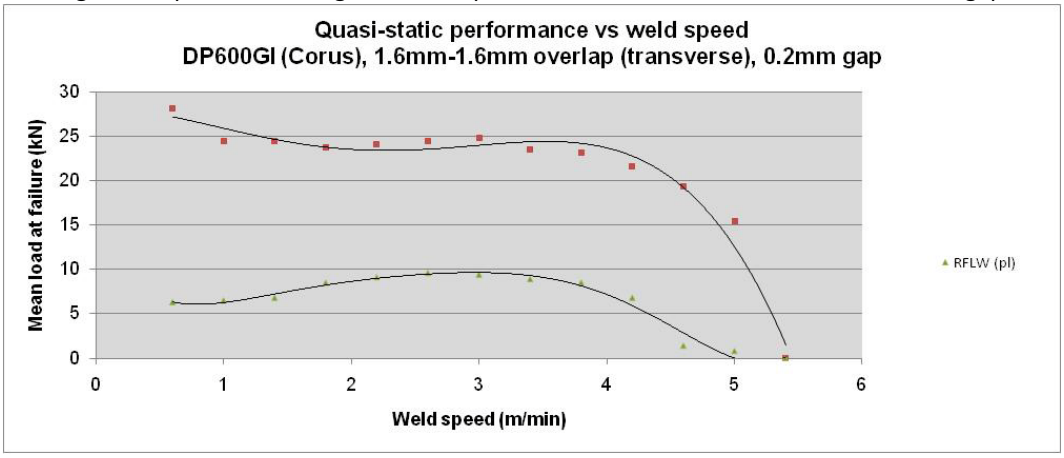

Fig.38. Graph: Weld strength vs weld speed: 1.6mm to 1.6mm, DP600GI, 0.2mm gap

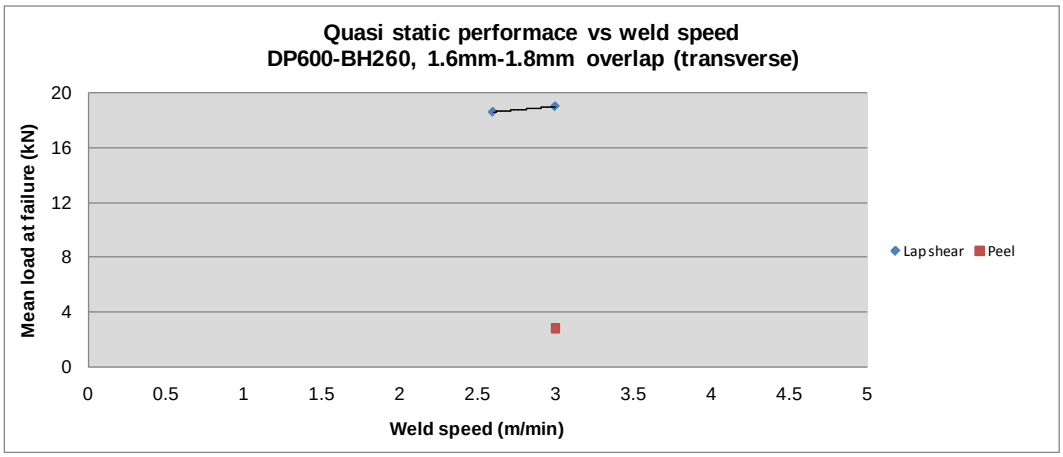

Fig.39. Graph: Weld strength vs weld speed: 1.6mm DP600 to 1.8mm BH260, 0.2mm gap

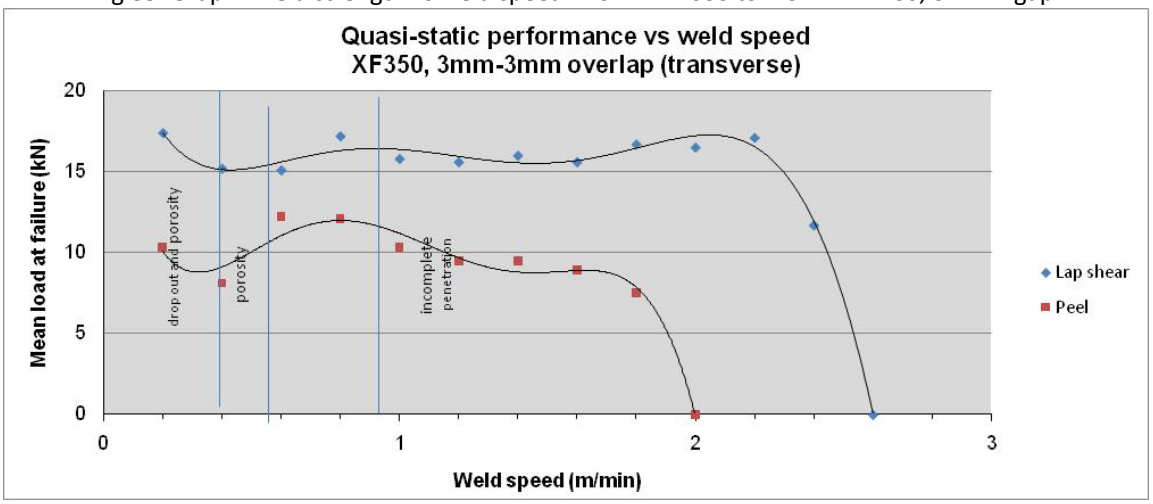

Fig.40. Graph: Weld strength vs weld speed: 3.0mm to 3.0mm, XF350, 0mm gap

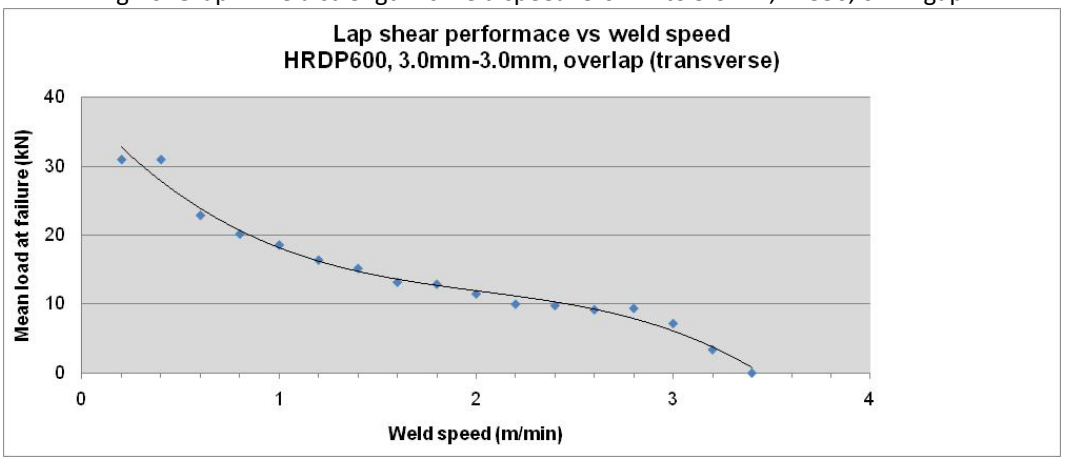

Fig.41. Graph: Lap shear strength vs weld speed: 3.0mm to 3.0mm, HRDP600, 0mm gap

i. Above steels may be uncoated or galvanised (HDG, EZ). Tested Boron steels were aluminised coated. For stack combinations that include zinc coated steels, refer to rules on interface gap control.

ii. Mixed thickness combinations tested to date are specified in Fig.42. below. For plain carbon steels, the weld speed is dependent on the material thickness and not the grade of the steel alloy processed.

Material Capability: DX54 Permissable stack combinations								
		Top						
		0.7	1	1.5	1.7	2	2 (boron)	3
Bottom	0.7							
	1							
	1.5							
	1.7							
	2							
	2 (boron)							
	3							

Fig.42. Table: Permissible material stack combinations: DX54

Thickness combinations (thin/thick, thick/thin)

With appropriate changes to weld speed, the steel alloys tested can be welded regardless of stack orientation

Stack combinations up to 0.7 to 2.0mm (1.3mm thickness differential) have been tested in both thin/thick and thick/thin orientations with acceptable performance from the resulting joints. Weld speed will require tailoring to suit the specific top sheet thickness of any presented stack combination.

Material Capability: DX54: Expected Lap shear strength								
		Top						
		0.7	1	1.5	1.7	2	2 (boron)	3
Bottom	0.7	4.6	5.1		5.8	5.8	6	
	1	5.1	7.4	7.7		6.2		
	1.5		7.8	11.4				
	1.7	5.5			12.7			
	2	5.8	8.2			17.8		
	2 (boron)	6	9.4					
	3							17.2

Fig.43. Table: Lap shear strength for permissible material stack combinations: DX54

iii. For conventional steel materials, stack combinations of up to 6mm total thickness (3mm+3mm) have been successfully welded. For stainless steels, stack combinations of up to 12mm have been successfully welded

iv. The plain carbon steel alloys tested demonstrate no sensitivity (in terms of mechanical performance) to stack orientation. Stack combinations up to 0.7 to 2.0mm (1.3mm thickness differential) have been tested in both thin/thick and thick/thin orientations and joint performance is unaffected. Weld speed will require tailoring to suit the specific top sheet thickness of any presented stack combination, as indicated in the table below.

Material Capability: DX54: Expected Weld Speed								
		Top						
		0.7	1	1.5	1.7	2	2 (boron)	3
Bottom	0.7	4.4	4.2		3.4	3.4		
	1	4.2	3.8	3.8		3.2		
	1.5		3.8	3.2				
	1.7	3.4			2.6			
	2	3.6	3.4			2.2		
	2 (boron)		3.8					
	3							0.8

Fig.44. Table: Weld speeds for permissible material stack combinations: DX54

For the plain carbon steels tested, the weld speed is dependent on the material thickness and not the grade of the steel alloy processed.

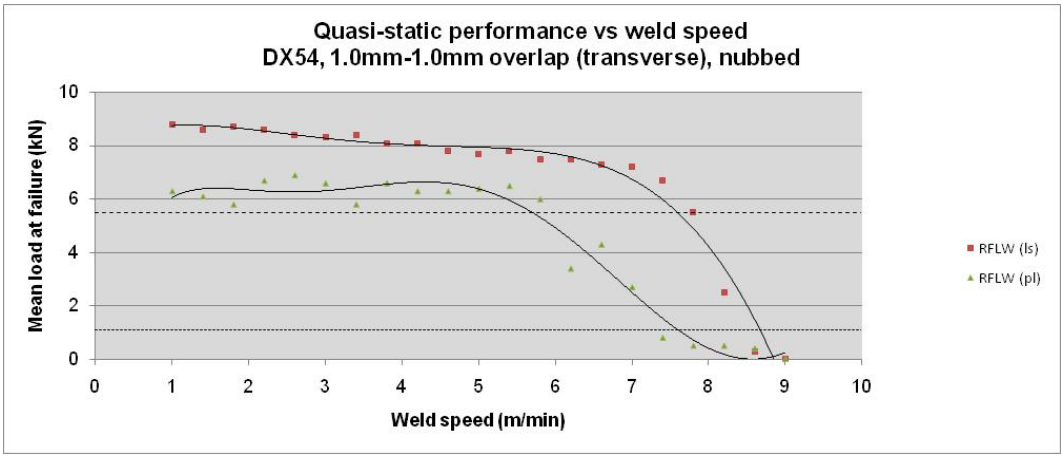

Fig.45. Graph: Weld strength vs weld speed: 1.0mm to 1.0mm, DX54, nubbed gap

Material stacks: Mixed materials

Material stack combinations containing both steel and aluminium alloys cannot be welded.

Material stacks that include both aluminium and steel alloys are non-viable material combinations for the laser welding processes. Alternative joining technologies should be sought.

Material stacks: Three sheet stacks

Uncoated steels

Uncoated steels are readily welded in stacks of three sheets, without gaps.

Coated steels

Material stack combinations including three sheets where some or all of the sheets are coated with zinc are readily weldable if a suitable interface gap (optimum 0.18mm) is maintained at the interfaces where zinc will be present.

Fig.46. below shows the lap shear results attained from 3-sheet stacks of 1mm DX54 material. The top surfaces of the lower sheets were nubbed to maintain gaps at both interfaces. Two sets of samples were manufactured in the orientations shown in Fig.47a. and Fig.47b.

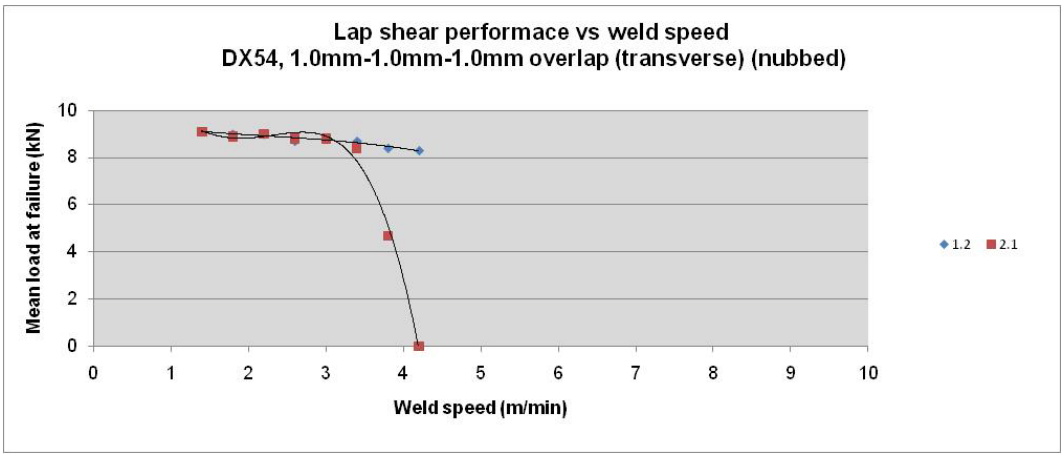

Fig.46. Graph: Lap shear strength vs weld speed: 1.0mm to 1.0mm to 1.0mm, DX54, nubbed gap

Fig.47a. 3-sheet stack combination '1.2'

Fig.47b. 3-sheet stack combination '2.1'

Impingement angle

For plain carbon steels, the laser beam can impinge the material at a perpendicular angle ±30° (see Fig.48.)

At greater angles, the welding process becomes unreliable due to high levels of beam reflection and reduced effective penetration.

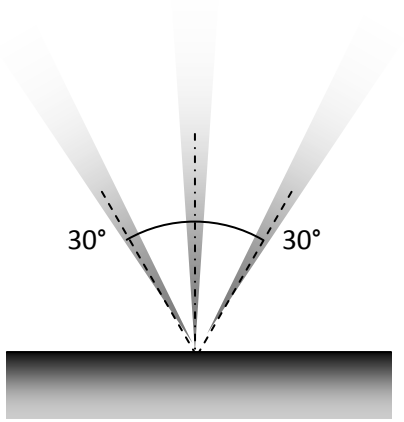

Fig.48. Permissible beam impingement angle envelope

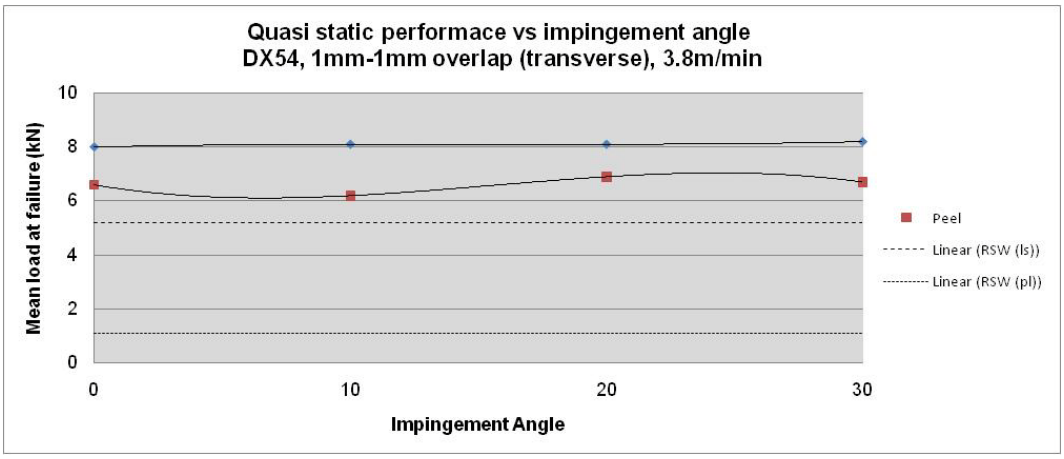

Fig.49. Graph: Weld strength vs impingement angle: 1.0mm to 1.0mm, DX54, 0.2mm gap

Focus tolerance

For acceptable welding the beam must be focussed onto the surface of the material ±20mm (see Fig.50.)

If the focal stand-off exceeds ±20mm then an unacceptable weld will be produced.

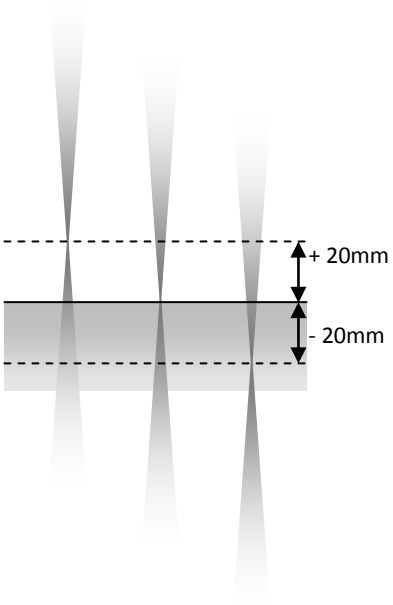

Fig.50. Schematic: Laser beam focus envelope

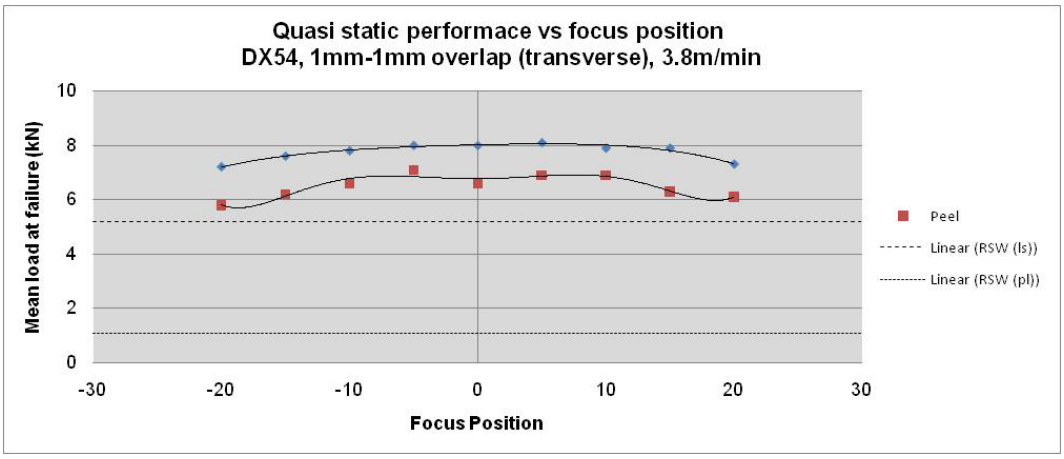

Fig.51. Graph: Weld strength vs beam focus position: 1.0mm to 1.0mm, DX54, 0.2mm gap

Adhesive requirements

> ***Adhesive products (structural, sealant or anti-flutter) must not be present at the weld location. Weld stitches must be 10mm away from the location of any adhesive bead or product (pumpable, tape, pre-form etc)***

Adhesive products (structural, sealant or anti-flutter) must not be present at the weld location. If adhesive is present at the weld location, the adhesive will reduce the joint strength by approximately 55% (under static load). The stitch will also demonstrate excessive undercutting as a consequence of material ejection. Weld stitches must be 10mm away from the location of any adhesive bead or product (pumpable, tape, pre-form etc). Adhesives perform poorly under conditions of peel load and it is conventionally expected that welded joints provide a 'peel stopping' agent for the joined seam. Where the welded stitch has been subject to adhesive contamination, the capability of the stitch to protect the adhesive from peel loading is significantly compromised.

Locating the welded stitch 10mm away from a bead of adhesive will ensure the adhesive bead cannot contaminate the weld area, providing the parts of the assembly are adequately clamped (sliding of the surfaces of the parts is eliminated). However, carless parts handling may still permit limited contamination of the weld zone with a wet adhesive product.

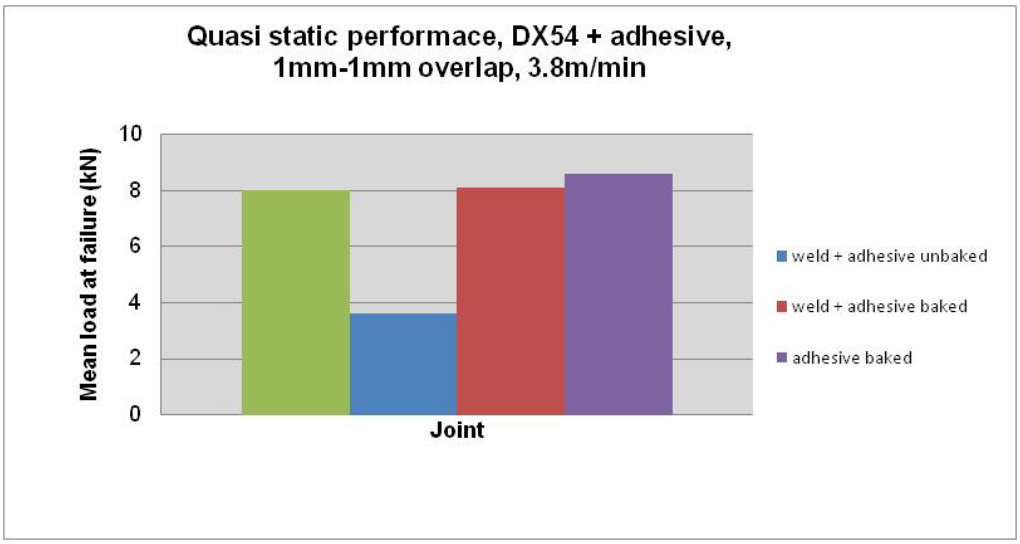

Fig.52. Graph: Lap shear of welded joints with adhesive: 1.0mm to 1.0mm, DX54, 0.2mm gap, 0mm offset

For Fig.52. the adhesive (Dow Betamate 4601) was applied in a single button to the lower, nubbed coupon. The adhesive was centred on the midpoint of the weld stitch. The coupons were then clamped together to distribute the adhesive. Samples A were then removed from the fixture and subject to a paint-bake cycle (180deg, 20mins). Samples B and C were both welded at 3.8m/min. Samples B were subject to a paint bake cycle (as before) and Sample set C left unbaked. Sample sets A,B and C were then subject to lap shear testing. The results are shown in the graph above, which includes the lap shear result for a 1mm, 1mm DX54 overlap weld without adhesive for reference.

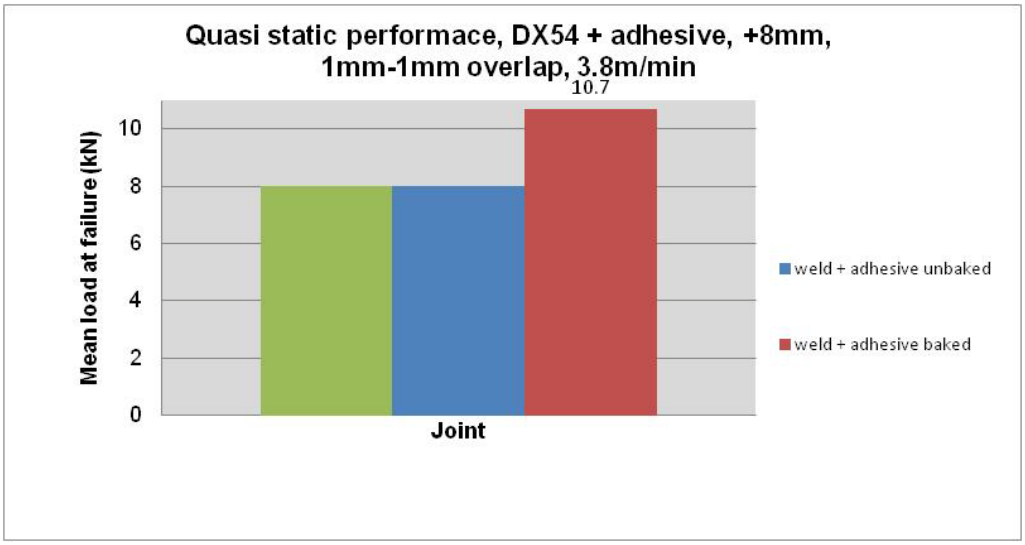

Fig.53. Graph: Lap shear of welded joints with adhesive: 1.0mm to 1.0mm, DX54, 0.2mm gap, +8mm offset

For Fig.53. the area of the coupons associated with the weld was covered with a single strip of 16mm PVC tape. The adhesive (Dow Betamate 4601) was applied to the lower, nubbed sheet below the tape strip and on the coupons longitudinal axis. The coupons were then assembled in an overlap configuration and clamped, ensuring distribution of the adhesive. The samples were unclamped, separated and the PVC tape strip removed, including any adhesive they may have been squeezed onto the tape. In theory, the adhesive would now a minimum of 8mm away from the weld stitch. The coupons were then reassembled in the fixture, clamped and welded at 3.8m/min. After welding half the samples were subjected to a paint-bake cycle (180deg, 20 mins) prior to testing. The other samples were left unbaked and tested. The comparative results of the two sets of samples (compared with a baseline RFLW sample) are shown in the graph above.

Lubricant tolerance

Wet lubricant coatings of up to 6gm/m^2 can be readily tolerated. Heavier lubricant coatings have not been tested.

Weld test have been undertaken with a range of levels of panel lubricant present at the interface, ranging from 0gm/m^2 up to 6gm/m^{2+} (see Fig.54.). The presence of lubricant on the surface made no significant difference to either welding process or the performance of the resulting joint. The quasi-static performance of the weld for increasing weights of lubricant coating is shown in the graph below. Other attributes of the weld were evaluated (material ejection, undercutting etc) and these were unaffected by the presence of lubricating oils.

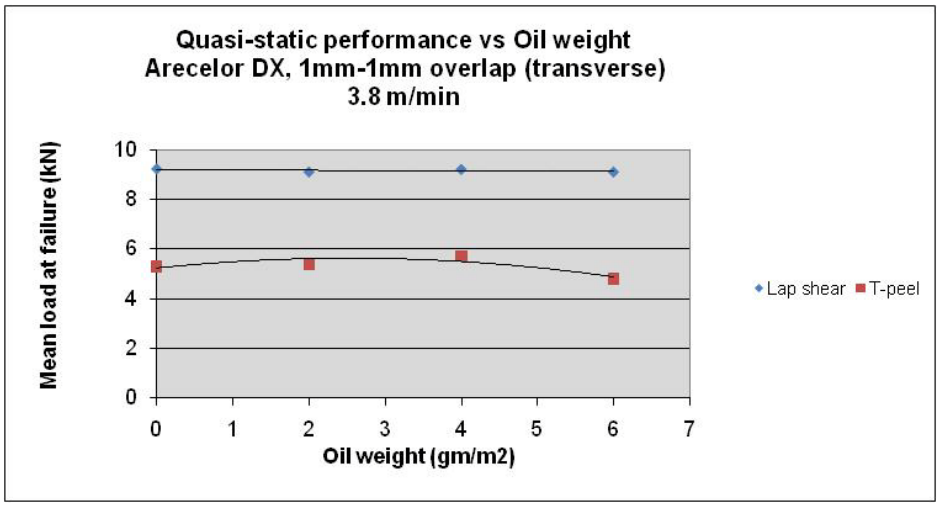

Fig.54. Graph: Weld strength vs oil contamination weight: 1.0mm to 1.0mm, DX54, 0.2mm gap

Quality Assurance: Acceptable weld

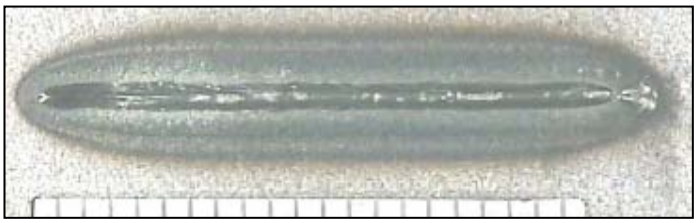

Fig.55. Top bead: made by remote fibre laser welding in an overlap joint, 1.2mm to 1.2mm DC05

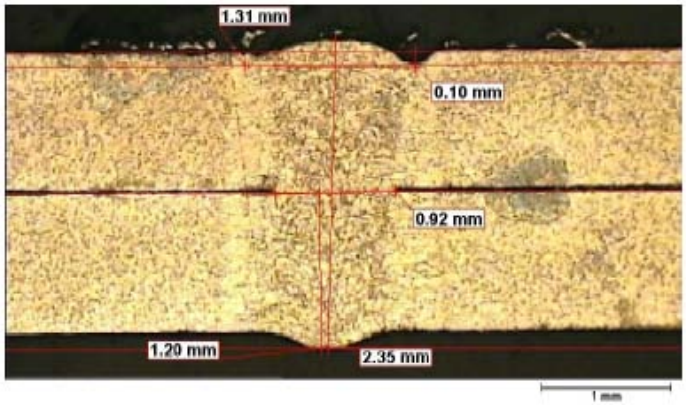

Fig.56. Microsection: remote fibre laser weld in an overlap joint: 1.2mm to 1.2mm DC05.

The above figures (55. and 56.) show the ideal laser made in an overlap of two 1.2mm thick sheets of DC05 (an un-coated, plain carbon steel). The weld length shown in Fig.55. is 25mm. Of importance to note is the width of the both the weld top surface and the interface zone when compared to the depth of the weld pentration (in this case full pentration of both upper and lower sheet). The high aspect ratio (depth to width) of the weld is indicative of the laser welding process. The upper sheet and weld top bead should be free from spatter, craters and cracks. The surface should be consistant and show little undercut and the underside of the weld should show no droping out of the weld material. The weld should also be free of pores and cracks.

The below figures (57. and 58.) show the ideal laser made in an overlap of two 1.0mm thick sheets of DX54 (a zinc coated, DC02 grade, plain carbon steel). When welding zinc coated materials, the rapid boiling of the zinc coating at the interface of the two sheets creates a high-pressure vapour. Unless exhausted, this vapour will vent explosively through the weld zone. To prevent this phenomenon it is typical to force a gap between the two sheets at the interface, thus providing an exhaust volume for the zinc vapours. This gap (approximately 0.2mthick) is clearly shown in the micrograph Fig.58. below. As with the uncoated, DCO5 grade materials, it is expected that the material surface and weld top bead are from spatter , craters and cracks. The surface should be consistant and show little undercut and the underside of the weld should show no droping out of the weld material. The weld should be free of pores and cracks.

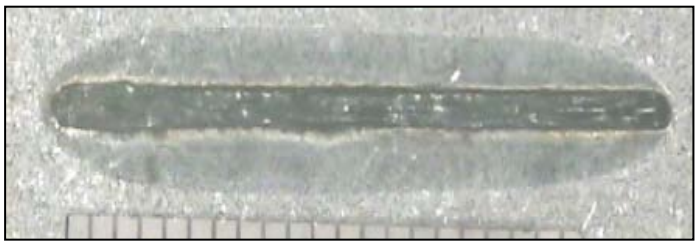

Fig.57. Top bead: remote laser weld in an overlap joint: 1.0mm to 1.0mm DX54

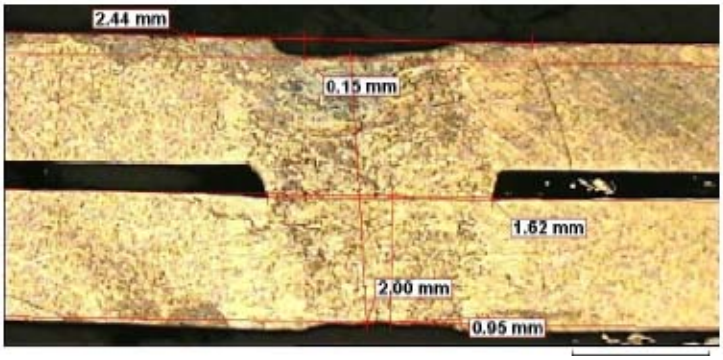

Fig.58. Microsection: remote laser weld in an overlap joint: 1.0mm to 1.0mm DX54.

Typical load test examples

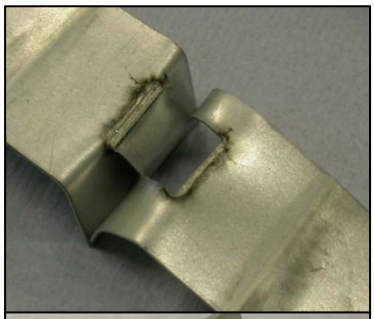

Fig.59. Test result: Lap shear of a linear stitch: 1.0mm to 1.0mm, DX54, 0.2mm gap

Fig.60. Test result: Lap shear of an elliptical stitch: 1.0mm to 1.0mm, DX54, 0.2mm gap

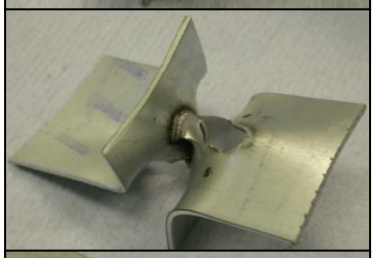

Fig.61. Test result: Peel test of a longitudinal elliptical stitch: 1.5mm to 1.5mm, DX54. 0.2mm gap

Fig.62. Test result: Lap shear of a linear stitch: 1.6mm to 1.6mm, DP600GI, 0.2,, gap

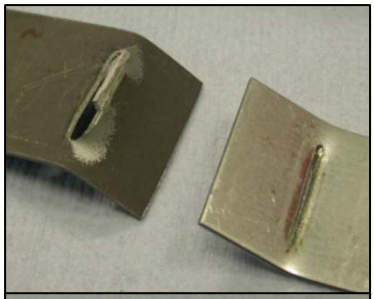

Fig.63. Test result: Lap shear of a linear stitch: 1.6mm DP600GI to 1.6mm boron steel, 0.2mm gap

Fig.64. Test result: Lap shear of a linear stitch: 0.7mm DX54 to 2.0mm boron steel, 0.2 gap

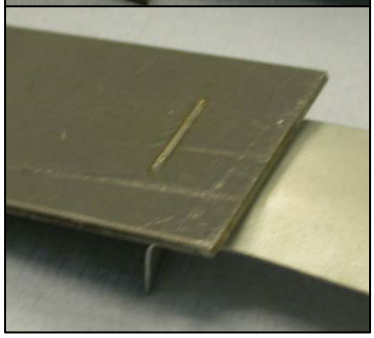

Fig.65. Test result: Lap shear of a linear stitch: 2.0mm to 0.7mm, DX54, 0.2mm gap

Quality Assurance: Weld failure modes

Undercut

Identification

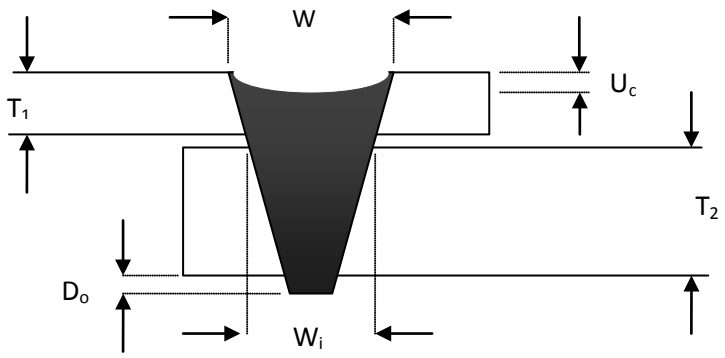

Key:

	T_1	Top sheet material thickness
	T_2	Bottom sheet material thickness
	W	Weld bead top width
	W_i	Weld interface width
	U_c	Depth of weld bead undercut
	D_0	Depth of drop out

Fig.66. Schematic: annotated weld cross-section

Limits

Undercutting of the top sheet must not exceed 25% of the top sheet thickness. Increased undercut may not reduce joint strength under static loads (lap shear or peel) but it will significantly reduce joint performance under dynamic loads.

Cause

1. Material ejection (spatter evident around joint and local tooling) (see Fig.67: top bead.)
    a. Zero gap with coated steels (see Fig.67: microsection.)
2. Adhesive contamination at interface (top bead surface as Fig.67: top bead)
3. Excessive gap between sheets (see Fig.68: microsection) (undercutting is present without evidence of material ejection -see Fig.68: top bead.)
4. Excessive weld penetration - excessive heat input per unit length per unit time for the given thickness of material (associated with *Drop-out*, see below)

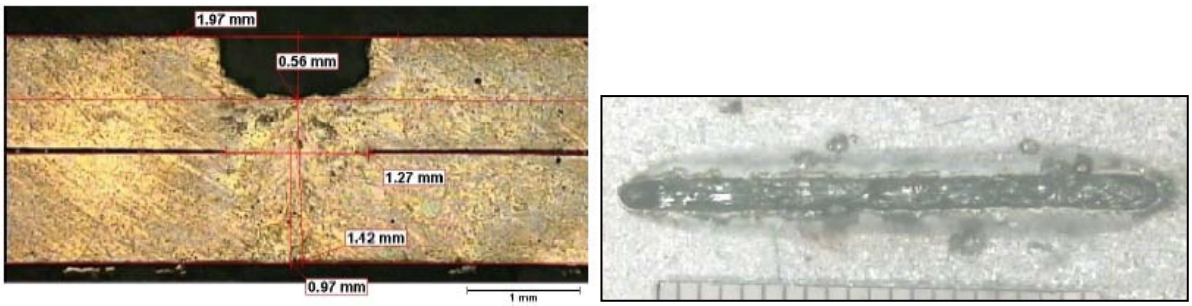

Fig.67. Microsection and top bead: Overlap weld: 1.0mm to 1.0mm, DX54, 0mm gap, showing undercut and surface spatter

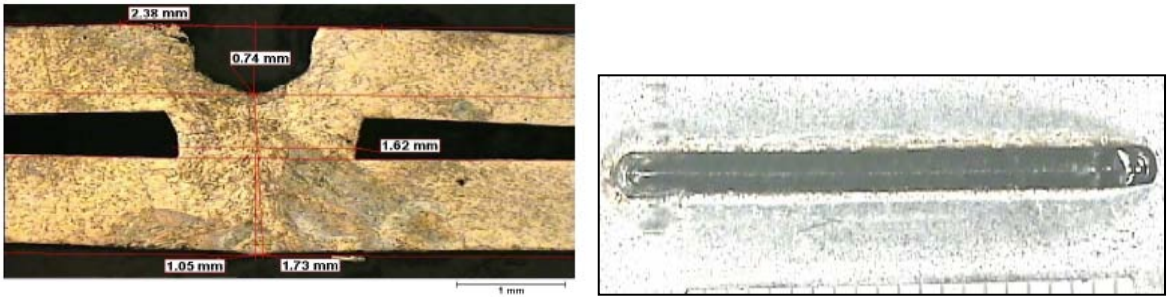

Fig.68. Microsection and top bead: Overlap weld: 1.0mm to 1.0mm, DX54, 0.4mm gap, showing large interface gap, undercut and no spatter

Drop-out

Undercutting of the weld top bead is often associated with the gap condition between the two sheets, particularly if no drop-out is present on the underside of the weld. If there is apparent material ejection around the weld, then this is an indication that the there was insufficient gap between the sheets to allow the exhausting of zinc vapours. The undercutting indicates the volume of material ejected with the boiling zinc. Gap is not only related to the stand-off distance between the panels - if there is contamination between the two panels, such as an interlayer of adhesive, then this effectively reduces the gap between the sheets to 0mm. This can exacerbate any material ejection witnessed - not only will the zinc at the interface vaporise, but any contaminant is likely to also vaporise and require exhausting.

If there is no apparent ejected material surrounding the weld then this indicates that the gap between the sheets was too big. The weld top bead will slump into the volume created by a gap and this will cause some undercutting of the top bead, even with an optimal gap of 0.10mm to 0.25mm. If the gap is too large, not only will the molten material slump into the gap, but it will also be drawn into the volume of space directly around the weld seem, exacerbating the undercutting witnessed. This phenomenon serves to increase the width of the weld at the interface zone and promotes acceptable joint strength under static loads (lap shear and peel), however, the effective thinning of material on the top sheet at the weld zone will cause a significant reduction of dynamic performance.

Recovery

Stabilise the gap between the sheets. For coated steels this gap must be between 0.1 mm and 0.25mm. (hyperlink?). Gaps smaller than 0.1mm do not allow sufficient exhausting of zinc vapours. Gaps greater than 0.25mm will result in increasing undercut as the molten weld material flows to fill the missing volume.
Ensure the weld area is free from adhesive contamination; either remove the adhesive from the area, or move the weld away the location of the adhesive bead (hyperlink?).
If drop-out is also witnessed on the underside of the weld, then either increase the weld speed to reduce heat input per unit length, per unit of time, or reduce the laser power (see *Drop-out,* below).

Drop-out

Identification

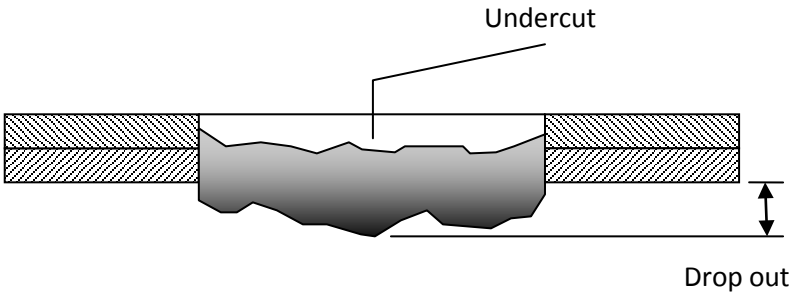

Fig.69. Schematic: longitudinal weld section showing undercut and drop-out

Limits

Standards do not specify limits for material drop-out, however drop-out is always associated with undercutting of the top-bead surface, therefore limits on drop out can be defined by the undercutting (maximum undercut of 25% T_1), providing the underside of the material stack:

- is neither a Class A of Class B surface (drop out and complete penetration would be unacceptable).
- Does not interfere with interfacing surfaces from further or subsequent assembly (drop out would be unacceptable).

Cause

- Excessive power per unit length per unit time.
    a. Weld speed too low.
    b. Laser power too high.
    c. Material too thin.

It is typical for a laser weld to fully penetrate both sheets of material in the stack. The molten metal is held in place within the weld zone by the effects of source tension (a function of the narrow nature of the laser weld, and the fluid dynamics of the steel material. If excessive energy is input to the weld, for the thickness of the material stack (termed 'over penetration'), a greater width of material is melted than can be sustained by the surface tension of the material. Under these circumstances, the molten material begins to sag out of the bottom of the material stack. This is the phenomenon termed 'drop-out'. The effect of drop-out on joint performance is similar to that of undercut. The wider weld interface caused by over-penetration can increase joint strength under static loads (lap shear and peel, however the effective thinning of the top sheet caused by the material dropping out significantly reduces the performance of the joint under dynamic loads.
Laser welding parameters are based on a simple balance of laser energy input to the part, per unit length, per unit time (laser power and weld speed) for a given thickness combination of material. The effective width of the weld will be increased if one or more of the following occurs:

- the laser power increases
- the weld speed reduces
- the material is reduced in thickness.

If laser power increases too much and/or there is a reduction of weld speed or material thickness decreases then over-penetration will result and drop-out will be experienced.

Recovery

Increase weld speed in order to reduce the laser energy input to the material per length per unit time or if weld speed is at the machine maximum and drop-out still occurs, reduce the weld power until penetration decreases.

Check the thickness of material for conformity to the accepted design. If a thickness reduction is noted, and is intended, then adjust the weld speed and laser power parameters to suit the new material stack thickness combination.

Interface width

Identification

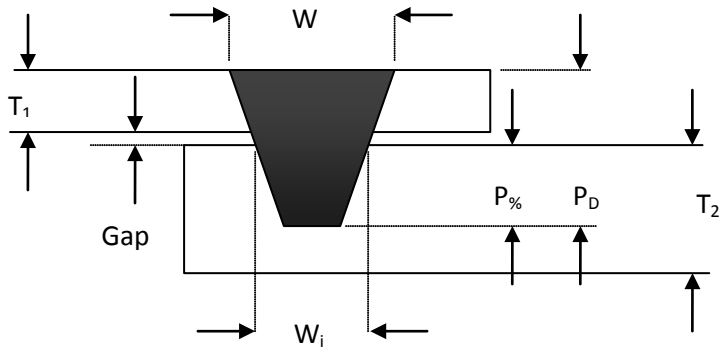

Key:

	T_1	Top sheet material thickness
	T_2	Bottom sheet material thickness
	W	Weld bead top width
	W_i	Weld interface width
	P	Weld penetration depth
	$P_{\%}$	Weld penetration into back sheet (% of T_2)

Fig.70. Schematic: annotated weld cross-section

There is no obvious process for externally determining the interface width of an overlap laser weld. The interface width can be ascertained using NDT techniques including X-ray/CT scan and ultrasonic scanning (multi-phase arrays and scanning systems) or the weld can be sectioned. The use of eddy current based inspection systems for measuring the weld interface width is currently unproven.

Limits

Graph required of optimum joint thickness for material stack

Cause

- Lack of penetration
    a. Reduced power per unit length per unit time.
        i. Laser power too low.
        ii. Weld speed too high.
        iii. Laser out of focus (increased spot size).
            1. Contaminated optics
            2. Relationship between laser beam and material surface has changed
            3. Issue with laser source
        iv. Impingement angle too steep
            1. Increased reflection of laser radiation
            2. Increased spot size
            3. Increased effective thickness of material
        v. Masking of beam
    b. Material too thick.
- Narrow weld
    a. Reduced laser spot size

The strength of a welded interface is a direct function of the interface area, therefore, with a remote laser weld stitch, the wider the interface, the better the weld will perform under static and dynamic loading. It is also true that the longer a weld is, for a given weld width the stronger the weld is also, as shown in the graph below:

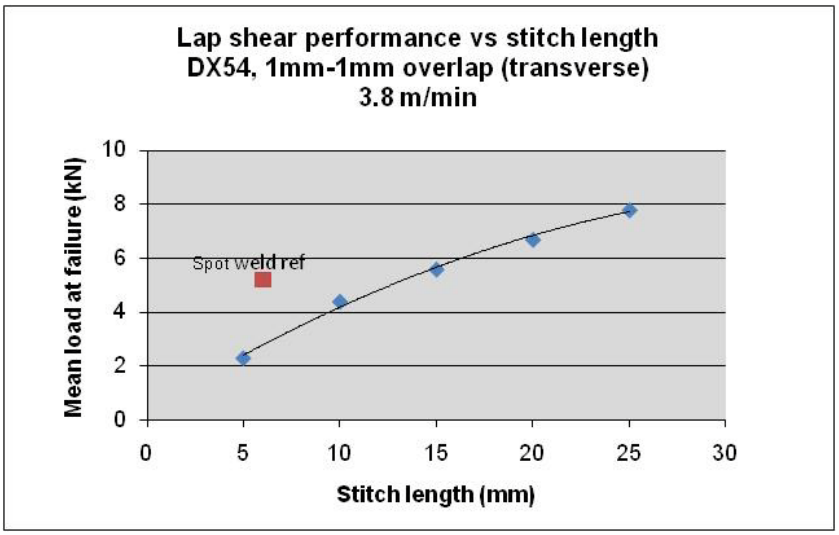

Fig.71. Graph: Lap shear strength vs stitch length: 1.0mm to 1.0mm DX54, 0.2mm gap

The width of laser weld can be controlled, within limits, by selection of the welding parameters. It can be shown that as a consequence of the shape of the weld cross-section, as the depth of penetration of the weld decreases, so the weld interface width will also reduce.

Laser welding parameters are based on a simple balance of laser energy input to the part, per unit length, per unit time (laser power and weld speed) for a given thickness combination of material. The effective width of the weld will reduce if one or more of the following occurs:

- the weld speed increases
- the laser power decreases
- the energy density of the laser spot decreases
- the impingement angle of the beam on the workpiece increases
- the top-sheet material thickness increases

If the weld speed increases, the depth of penetration decreases, and consequently the weld interface width will also decrease - there is less energy input to the workpiece per unit length per unit time.

Changes in laser power can be affected by requesting lower laser powers on the laser source (either on the laser source directly or via a second party controller such as the robot etc). However there other factors that can influence the power of the laser beam that impinges onto the work piece. And these are discussed in detail below

If the path of the laser beam between the beam delivery system and the workpiece is interrupted, a percentage of the beam will be absorbed and /or scattered. Typically this can either be as a consequence of contaminated output optics in the beam delivery system or by the masking of the beam by tooling etc (the weld zone may be 'in the shadow' of some tooling, or another part of the workpiece). As with contaminated optics, this will reduce the power of the laser impinging on the workpiece.

Typically, laser welds will be made with the laser beam at, or close to, the point of focus of the laser beam. This provides the smallest focused spot and consequently maximises the energy density within that spot. If the point of focus changes the effective power of the spot decreases and this can result in reduced weld penetration and reduced interface width. Further to this however, if the focused spot is too small, the weld produced will be too narrow to form a weld of appropriate strength and it is sometimes required for welds to be made lower weld speeds with the laser beam defocused at the point of impingement on the workpiece. The reduced weld speed compensates for

the reduced energy density of the spot, but the wider spot will produce a wider weld width, and consequently a wider weld interface.

There are a number of reasons why the point of focus may change. Firstly, the relationship between the workpiece and the beam delivery output may change (tooling may move, there may significant distortion of the workpiece, or the programmed point of the robot may have moved. If the diameter of the focussed spot is considered to have reduced in diameter, then it is expected to be as a result of a change in stand-off between the laser and the workpiece or a change in the programmed point of focus of the laser beam. Contaminated optics may also cause focussing changes with the laser beam - if contamination results in the heating of an optical element, the optical properties of that element will change, altering the focal characteristics of the beam in a phenomenon known as 'thermal lensing'. It is expected that thermal lensing etc will reduce the effective laser power in the spot and therefore penetration / weld interface will reduce. It is not expected for optical contamination / thermal lensing to reduce the diameter of the focal spot, even if the laser beam was already defocused. Thirdly, there may be fault within the laser source that affects the divergence properties of the beam and this will change the focus characteristics of the beam.

As the angle of impingement of the beam on the workpiece increases, an increasing amount of laser energy is reflected from the workpiece Also, as the impingement angle increases area of the focussed spot, resulting in a lower effective laser power. Typically on steel, an ideal impingement angle is perpendicular to the material surface, with an acceptable window of ±25° without degradation to the acceptability of the resulting weld. Beyond 25° the reduced effectiveness of the beam results in an unacceptable weld.

A final factor that will affect weld penetration and thusly the width of the weld interface, is the thickness of the top sheet. If the top sheet is thicker than expected, then the weld interface width decreases. Although the total weld penetrations remains unchanged, the percentage penetration into the back sheet will be reduced.

Recovery

For first-off parts:

- Increase the programmed laser power if more power is available. This will impart more energy into the workpiece per unit length per unit time without sacrificing cycle time.
- Reduce the programmed weld speed in order to increase the energy input to the material per unit time per unit length. This will result in a wider weld but will also increase the cycle time per stitch, and consequently, per part.
- Ensure that the beam path between beam delivery output and workpiece is unobstructed (a key indicator can be the presence of thermal damage on any tooling or other parts of the workpiece).
- Ensure the output optics are undamaged and free from contamination
- Check for issues with the laser source
- Check the thickness of material for conformity to the accepted design. If a thickness reduction is noted, and is intended, then adjust the weld speed and laser power parameters to suit the new material stack thickness combination.
- Check for programmed location of weld stitch / point of focus for the laser beam
- Ensure that the angle of impingement of the laser beam is within the accepted tolerance (perpendicular ±30°).
- If laser based parameters and material thickness are in accord with required settings then the beam will need to be checked against a calibrated standard. This will indicate the stability of the laser output and if anything has changed that may not be externally apparent.

- Ensure that the alignment beam used for programming etc is coincident with the working beam - do both beams focus at the same distance?

For serial parts:

- Ensure that the programmed laser power is in accordance with the master document
- Ensure that the weld speed is in accordance with that specified by the master document
- Ensure the output optics are undamaged and free from contamination
- Check for programmed location of weld stitch / point of focus for the laser beam
- Check for any change in dimensions / shape of components or changes in master locations
- Check for issues with the laser source
- Check the thickness of material for conformity to the accepted design. If a thickness reduction is noted, and is intended, then adjust the weld speed and laser power parameters to suit the new material stack thickness combination.
- If laser based parameters and material thickness are in accord with required settings then the beam will need to be checked against a calibrated standard. This will indicate the stability of the laser output and if anything has changed that may not be externally apparent.

Penetration

Identification

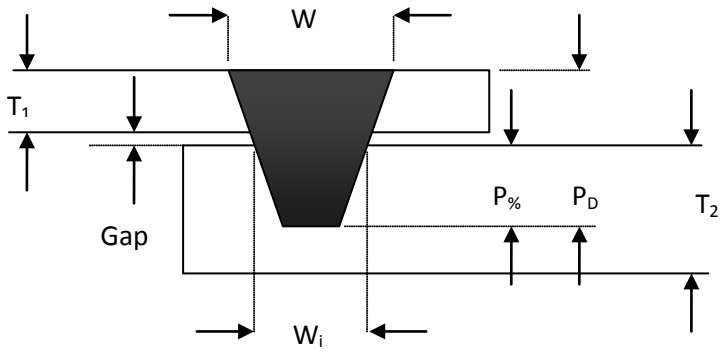

Key:
- T_1 Top sheet material thickness
- T_2 Bottom sheet material thickness
- W Weld bead top width
- W_i Weld interface width
- P Weld penetration depth
- $P_{\%}$ Weld penetration into back sheet (% of T_2)

Fig.72. Schematic: annotated weld cross-section

Unless welds were intended to fully penetrate the back sheet then there is no NDT method for assessing the depth to which the weld has penetrated the material. NDT technologies such as ultrasonic inspection, eddy-current inspection or X-ray/ CT scanning will only detect the external shape of the weld interface and porosity within the weld - the weld material is same density as the parent material therefore is no internal boundary for such test methods to recognize. Reduced penetration will externally manifest as reduced joint strength or reduced durability, but sectioning is required in order to measure the depth to which the weld has penetrated the back sheet.

Limits

The weld must penetrate the lower material sheet to at least a depth of 30% sheet thickness. Lower penetration figures result in unacceptable joint strength and durability.

Cause

3. Reduced power per unit length per unit time.
    a. Laser power too low.
    b. Weld speed too high.
    c. Laser out of focus (reduced energy density).
    d. Impingement angle too steep (increased reflection of laser radiation).
4. Increased material thickness.

The strength of a welded interface is a direct function of the interface area, therefore, with a remote laser weld stitch, the wider the interface, the better the weld will perform under static and dynamic loading. The depth of penetration (and consequently the weld interface width) of a laser weld can be controlled, within limits, by selection of the welding parameters. It can be shown that as a consequence of the shape of the weld cross-section, as the depth of penetration of the weld decreases, so the weld interface width will reduce

Laser welding parameters are based on a simple balance of laser energy input to the part, per unit length, per unit time (laser power and weld speed) for a given thickness combination of material. The depth of penetration (and the effective weld width) will reduce if one or more of the following occurs:

- the weld speed increases
- the laser power decreases

- the energy density of the laser spot decreases
- the impingement angle of the beam on the workpiece increases
- the top-sheet material thickness increases

If the weld speed increases, the depth of penetration decreases, and consequently the weld interface width will also decrease - there is less energy input to the workpiece per unit length per unit time.

Changes in laser power can be affected by requesting lower laser powers on the laser source (either on the laser source directly or via a second party controller such as the robot etc). However, other factors can influence the power of the laser beam that impinges onto the work piece. Firstly, the beam, path may be interrupted, causing a percentage of the beam to absorbed, or scattered. Typically this can be a consequence of contaminated output optics on the beam delivery system. Another cause can be the masking of the beam by tooling etc - the weld zone may be 'in the shadow' of some tooling, or another part of the workpiece. As with contaminated optics, this will reduce the power of the laser impinging on the workpiece.

Typically, laser welds will be made with the laser beam at, or near, it's point of focus. This provides the smallest focused spot and consequently maximises the energy density within that spot. If the point of focus changes the effective power of the spot decreases and this can result in reduced weld penetration and reduced interface width. There are a number of reason why the point of focus may change. Firstly, the relationship between the workpiece and the beam delivery output may change (tooling may move, there may significant distortion of the workpiece, or the programmed point of the robot may have moved. Contaminated optics may also cause focussing discrepancies with the laser beam - if contamination results in the heating of an optical element, the optical properties of that element will change, altering the focal characteristics of the beam in a phenomenon known as 'thermal lensing'. As before, this will reduce the effective laser power in the spot and penetration / weld interface will reduce. Thirdly, there ma y be fault within the laser source that effects the divergence properties of the beam and this will change the focus characteristics of the beam.

As the impingement angle of the beam on the workpiece increases, an increasing amount of laser energy is reflected from the workpiece Also, as the impingement angle increases area of the focussed spot, resulting in a lower effective laser power. Typically on steel, an ideal impingement angle is perpendicular to the material surface, with an acceptable window of ±25° without degradation to the acceptability of the resulting weld. Beyond 25° the reduced effectiveness of the beam results in an unacceptable weld.

A final factor that will affect weld penetration and thusly the width of the weld interface, is the thickness of the top sheet. If the top sheet is thicker than expected, then the weld interface width decreases. Although the total weld penetration remains *unchanged*, the percentage penetration into the back sheet will be reduced.

Recovery

For first-off parts:

- Increase the programmed laser power if more power is available. This will impart more energy into the workpiece per unit length per unit time without sacrificing cycle time.
- Reduce the programmed weld speed in order to increase the energy input to the material per unit time per unit length. This will result in a wider weld but will also increase the cycle time per stitch, and consequently, per part.

- Ensure that the beam path between beam delivery output and workpiece is unobstructed (a key indicator can be the presence of thermal damage on any tooling or other parts of the workpiece).
- Ensure the output optics are undamaged and free from contamination
- Check for issues with the laser source
- Check the thickness of material for conformity to the accepted design. If a thickness reduction is noted, and is intended, then adjust the weld speed and laser power parameters to suit the new material stack thickness combination.
- Check for programmed location of weld stitch / point of focus for the laser beam
- Ensure that the angle of impingement of the laser beam is within the accepted tolerance (perpendicular ±30°).
- If laser based parameters and material thickness are in accord with required settings then the beam will need to be checked against a calibrated standard. This will indicate the stability of the laser output and if anything has changed that may not be externally apparent.
- Ensure that the alignment beam used for programming etc is coincident with the working beam - do both beams focus at the same distance?

For serial parts:

- Ensure that the programmed laser power is in accordance with the master document
- Ensure that the weld speed is in accordance with that specified by the master document
- Ensure the output optics are undamaged and free from contamination
- Check for programmed location of weld stitch / point of focus for the laser beam
- Check for any change in dimensions / shape of components or changes in master locations
- Check for issues with the laser source
- Check the thickness of material for conformity to the accepted design. If a thickness reduction is noted, and is intended, then adjust the weld speed and laser power parameters to suit the new material stack thickness combination.
- If laser based parameters and material thickness are in accord with required settings then the beam will need to be checked against a calibrated standard. This will indicate the stability of the laser output and if anything has changed that may not be externally apparent.

Porosity

Identification

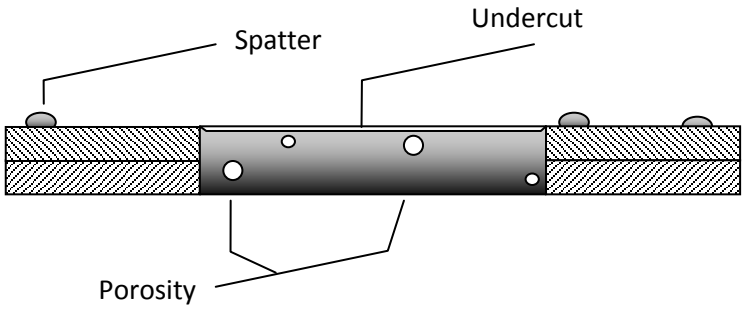

Fig.73. Schematic: longitudinal weld section showing porosity, undercut and spatter

Limits

The must be no more than one visible surface pore (exceeding 0.2mm diameter) per 5mm of weld stitch.
On sectioned samples, the interface width must be free from porosity.

Cause

2. Material ejection (spatter evident around joint and local tooling)
    a. Zero gap with coated steels
    b. Adhesive contamination at interface

Recovery

For zero-gap weld interface

- Ensure the interface gap is between 0.1mm and 0.3mm to allow exhausting of zinc vapours.

For adhesive contamination

- Ensure weld location is free from adhesive material (welds must be sited at least 10mm away from any adhesive bead) or,
- Move the weld to a location where adhesive will not be present

Holes

Identification

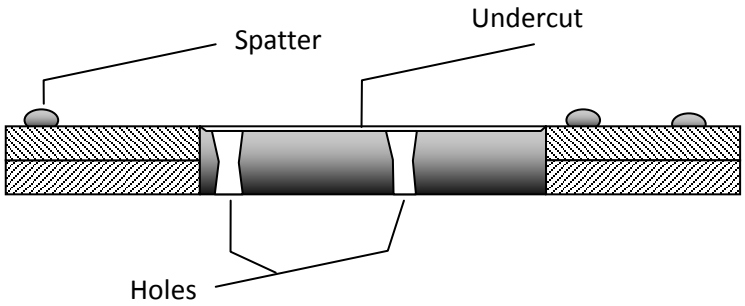

Fig.74a. Schematic: longitudinal weld section showing holes and spatter

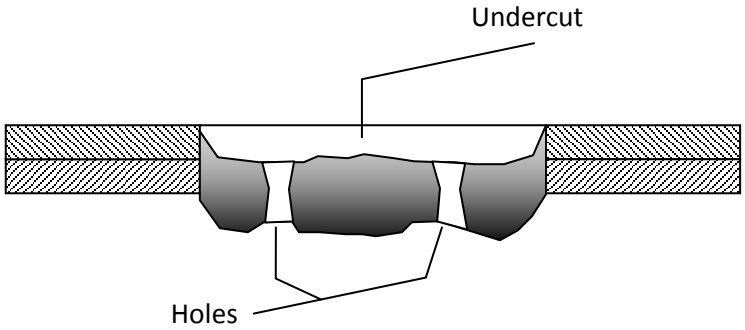

Fig.74b. Schematic: longitudinal weld section showing undercut, dropout and holes

A hole is a discrete discontinuity in the weld that extends to a depth below the interface. A hole does not have to fully penetrate the weld material. Some standards class blind holes (holes that do not fully penetrate the weld material) as 'top surface cut-through'. The classification of a hole presented here is applicable to welds that both fully penetrate and partially penetrate the lower sheet. Both through-holes and 'top surface cut-through' share common causes.

Limits

One hole, not exceeding 1.0mm diameter per 10mm of weld length unless complete sealing of the weld is specifically specified, in which case holes are unacceptable in welds that fully penetrate both sheets.

Cause

1. Material ejection (spatter evident around joint and local tooling) (see Fig.74a.)
    a. Zero gap with coated steels
    b. Adhesive contamination at interface
2. Excessive interface gap (the weld will also feature undesirable levels of undercutting)
3. Reduced focus spot (remote cutting)
4. Excessive energy input per unit length per unit time (the weld will also demonstrate over-penetration and drop-out) (see Fig.74b.)
    a. Weld speed too low
    b. Laser power too high
    c. Reduced material thickness

Holes in the weld bead can be associated with the gap condition between the two sheets. If there is apparent material ejection around the weld, then this is an indication that the there was insufficient gap between the sheets to allow the exhausting of zinc vapours. Top bead undercutting and the presence of holes indicate the volume of material ejected with the boiling zinc. Panel gap is not only

related to the stand-off distance between the panels - if there is contamination between the two panels, such as an interlayer of adhesive, then this effectively reduces the gap between the sheets to 0mm. This can exacerbate any material ejection witnessed - not only will the zinc at the interface vaporise, but any contaminant is likely to also vaporise exhaust explosively through the weld.

If there is no apparent ejected material surrounding the weld then this indicates that the gap between the sheets was too big. The weld top bead will slump into the volume created by a gap and this will cause some undercutting of the top bead, even with an optimal gap of 0.10mm to 0.25mm. With larger gaps, not only will the molten material slump into the gap, but it will also be drawn into the volume of space directly around the weld seem, exacerbating the undercutting witnessed. This phenomenon serves to increase the width of the weld at the interface zone and promotes acceptable joint strength under static loads (lap shear and peel), however, the effective thinning of material on the top sheet at the weld zone will cause a significant reduction of dynamic performance. For extreme gaps the volume of molten material is insufficient to fill the resulting void and this can cause holes to be formed in the weld top bead.
It is typical for a laser weld to fully penetrate both sheets of material in the stack. The molten metal is held in place within the weld zone by the effects of source tension (a function of the narrow nature of the laser weld, and the fluid dynamics of the steel material. If excessive energy is input to the weld, for the thickness of the material stack (termed 'over penetration'), a greater width of material is melted than can be sustained by the surface tension of the material. Under these circumstances, the molten material begins to sag out of the bottom of the material stack (a phenomenon termed 'drop-out') and holes may be formed. The effect of drop-out on joint performance is similar to that of undercut. The wider weld interface caused by over-penetration can increase joint strength under static loads (lap shear and peel), however the effective thinning of the top sheet caused by the material dropping out and from any holes that have formed significantly reduces the performance of the joint under dynamic loads.
Laser welding parameters are based on a simple balance of laser energy input to the part, per unit length, per unit time (laser power and weld speed) for a given thickness combination of material. The effective width of the weld will be increased if one or more of the following occurs:

- the laser power increases
- the weld speed reduces
- the material is reduced in thickness.

If laser power increases too much and/or there is a reduction of weld speed or material thickness decreases then over-penetration will result and drop-out will be experienced.

Recovery

- Stabilise the gap between the sheets. For coated steels this gap must be between 0.1 mm and 0.25mm. (hyperlink?). Gaps smaller than 0.1mm do not allow sufficient exhausting of zinc vapours, causing expulsion and increasing the likelihood of holes being formed. Gaps greater than 0.25mm will result in increasing undercut (hyperlink) as the molten weld material fills the missing volume. Ensure the weld area is free from adhesive contamination; either remove the adhesive from the area, or relocate the weld away from the adhesive bead (hyperlink?).
- Check the thickness of material for conformity to the accepted design. If a thickness reduction is noted, and is intended, then adjust the weld speed and laser power parameters to suit the new material stack thickness combination.

Cracks

Identification

Limits

Cause

Recovery

Missing weld

Identification

Fig.75.a. Typical laser weld stitch

Fig.75.b. Typical missing weld

A location on the part where a weld stitch is expected (refer to master part or master documentation) but remains unaffected by laser output (no witness marks on the workpiece). A witness mark on the material surface indicates different failure modes.

Limits

All welds must be present, in the locations specified on the master part or the master process documents. A missing weld is unacceptable.

Cause

First off parts:

- Incorrect programming of part
- Complete masking of the weld location by tooling or the workpiece
- Software failure within the programme or control system
- Masking of weld zone
- Malfunction of communication within the cell
- Incorrect operation of the welding cell

If a weld, or welds, are missing then the relevant weld stitch/stitches may have been disabled or deleted in the robot or laser programme. It may also be that the laser source has stopped responding to the instructions to operate, either because software errors or a hardware failure with the laser. For the later however, it is expected that all welds after the time of failure would be missing. If all welds missing after a certain point then it is also indicative of an e-stop issue within the cell system and the laser has been excluded from operating.
It may be possible that a weld zone has been masked entirely by an item of tooling, or another part of the workpiece.

Serial parts:

- Modification of the part programme
- Software failure within the programme or control system
- Malfunction of communication within the cell
- Incorrect operation of the welding cell
- Intermittent failure of the laser source

For serial parts, a missing weld is a significant failure mode because it will not be as a consequence of the welding process; instead it is indicative of an issue within the control system of the welding

system. If a weld, or welds, are missing then the relevant weld stitch/stitches may have been disabled or deleted in the robot or laser programme. It may also be that the laser source has stopped responding to the instructions to operate, either because software errors or a hardware failure with the laser. For later however, it is expected that all welds after the time of failure would be missing. If all welds missing after a certain point then it is possible that there has been an e-stop issue within the cell system and the laser has been excluded from operating.
If the weld zone has been masked entirely by an item of tooling, or another part of the workpiece, the missing weld will be apparent on every component made on that fixture, or with that tooling. If the failure however is intermittent then it is unlikely that masking is the root cause, unless the tooling or workpiece has been modified.

Recovery

First-off parts:

- Ensure that the part programme is complete and that all modules / steps are set to run as appropriate.
- Check for software error messages and alert codes.
- Check laser for error messages and alert codes.
- Check cell PLC for error messages and alert codes.
- Check that the laser stitch is programmed in accordance with the maser part / master document (ensure it has been programmed and that it is in the correct location), including beam focus.
- Ensure that the beam path between beam delivery output and workpiece is unobstructed (a key indicator can be the presence of thermal damage on any tooling or other parts of the workpiece).
- Ensure that the angle of impingement of the laser beam is within the accepted tolerance (perpendicular ±30°).
- Ensure cell interlocks are functioning as appropriate.

Serial parts:

- Ensure that the part programme is complete and that all modules / steps are set to run as appropriate.
- Check for software error messages and alert codes
- Check laser for error messages and alert codes.
- Check cell PLC for error messages and alert codes.
- Ensure cell interlocks are functioning as appropriate.

Stitch shape

Identification

The overall length or the shape of the welded stitch is not as described on the master part on in the master document.

Limits

The weld length and shape must be as defined on the master part or in the master document. For steel alloys, the laser welded stitch must have a total effective length of at least 25mm, regardless of stitch shape.

Stitch length:

The strength of the welded joint is a function of the interface area - the greater the interface area, then the greater the load that can be supported by that weld. The length of the welded stitch will therefore influence the joint strength. Fig.76 below shows the relationship of the length of a linear, transverse stitch and the expected joint performance under lap-shear loading.

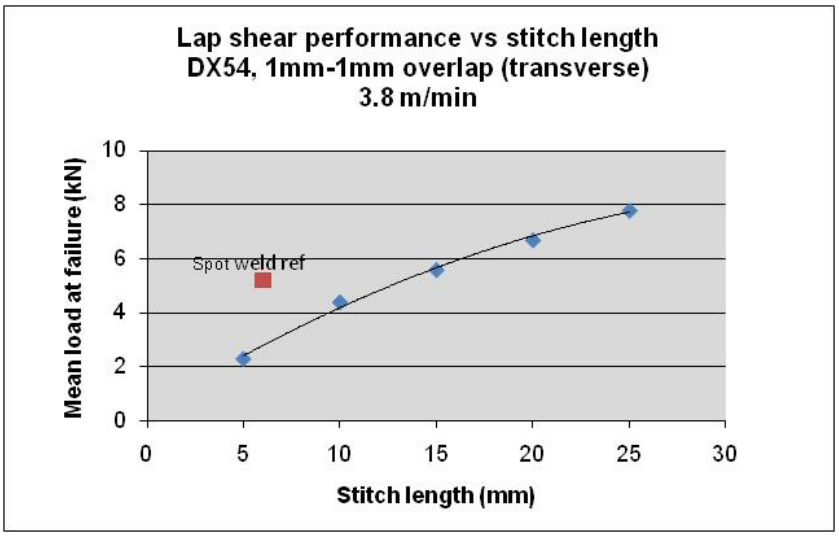

Fig.76. Graph: lap shear performance vs linear stitch length: 1.0mm to 10.mm DX54, 0.2mm gap

Typically, a laser welded stitch must have an effective length 25mm. The above graph indicates that a 15mm stitch length provides equivalent strength to a 6mm diameter resistance spot weld. However, accepted weld convention, developed via arc welding techniques requires that the first 5mm and the last 5mm of the weld stitch are not counted in calculations of weld length as they are considered unstable areas of weld with unreliable strength attributes. The validity of this assumption is not discussed by this document.

Stitch shape:

The strength of a weld is directly proportional to the area of the weld interface; the greater the interface area, the greater the load it can support in lap shear. However, the shape of the weld can significantly affect the performance of the joint under static and dynamic peel loading. Fig.77. shows three shapes of laser welded stitches (linear, 'staple' and circular), each stitch shape having the same weld interface area (1.6mm interface width and an effective 25mm weld length). The graphs in Fig.78. and Fig.79. below, show the joint strengths achieved for the range of stitch shapes in an overlap joint of 1mm to 1mm DX54 material. Each stitch shape was tested under both transverse and longitudinal loading conditions, in both lap shear and peel. For reference, the performance of a comparable, 6mm diameter, spot weld is also included on the graphs. It can be seen in Fig.78. that under lap shear load the orientation of the stitch has little influence over the performance of the stitch. Further to this, as all laser welded stitches had the same interface area, the different stitch

shapes show comparable weld strength. Under peel loading however the shape and orientation of the weld becomes a critical factor and it is shown that the greater the width of the weld that is presented to the direction of load the greater the load that can be supported.

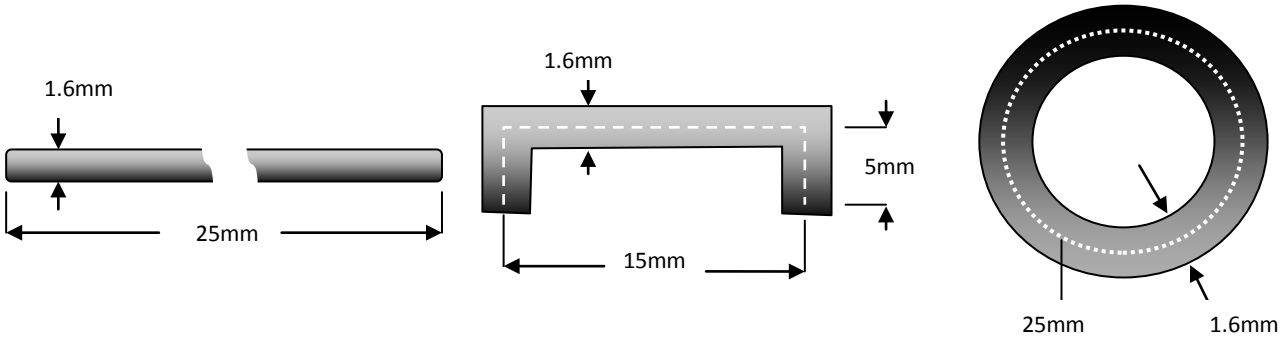

Fig.77. Schematic: laser welded stitch shapes - Linear, staple and circle (not to scale)

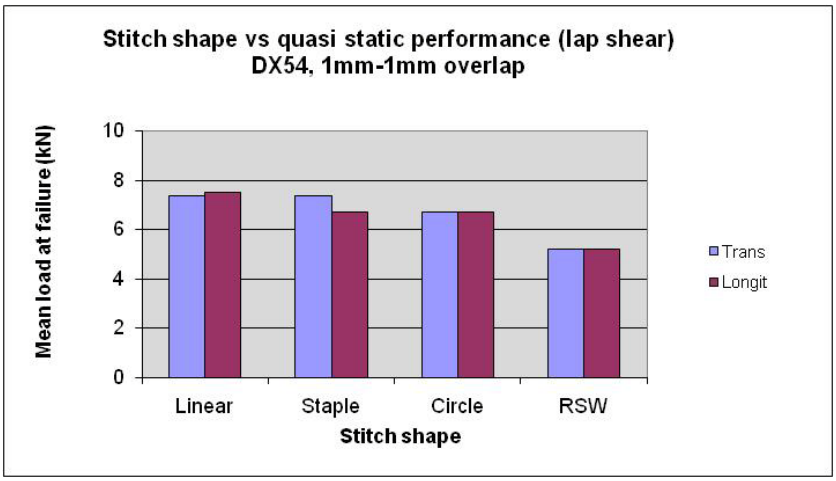

Fig.78. Graph: lap shear strength vs stitch shape and orientation: 1.0mm to 1.0mm DX54, 0.2mm gap

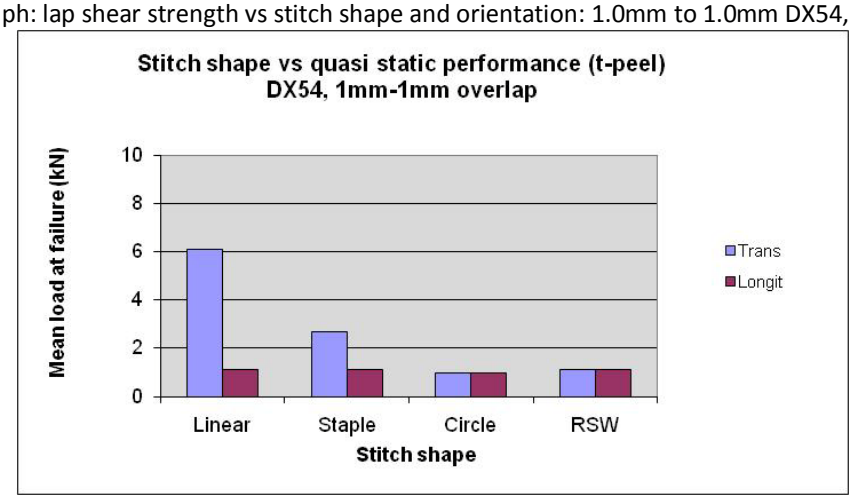

Fig.79. Graph: peel strength vs stitch shape and orientation: 1.0mm to 1.0mm DX54, 0.2mm gap

Cause

Stitch length:

- Incorrect part programming- an incorrect stitch shape was programmed, or selected by the robot programme.
- Masking of the weld zone by tooling or the workpiece.
- Software failure within the programme or control system

- Malfunction of communication within the cell
- Incorrect operation of the welding cell
- Intermittent failure of the laser source

If the weld zone has been masked entirely by an item of tooling, or another part of the workpiece, the missing weld will be apparent on every component made on that fixture, or with that tooling. If the failure however is intermittent then it is unlikely that masking is the root cause, unless the tooling or workpiece is being modified.
A missing length of weld can also be indicative of an issue within the control system of the welding system. If a length of weld is missing then it may be that the laser source has stopped responding to the instructions to operate, either because software errors or a hardware failure with the laser. For later however, it is expected that all welds after the time of failure would be missing.
If all welds missing after a certain point then it is possible that there has been an e-stop issue within the cell system and the laser has been excluded from operating.

Stitch shape:

- Incorrect part programming - an incorrect stitch shape was programmed, or selected by the robot programme.

Recovery

Stitch length:

- Amend the robot programme to produce the required stitch shape.
- Ensure that the beam path between beam delivery output and workpiece is unobstructed (a key indicator can be the presence of thermal damage on any tooling or other parts of the workpiece).
- Check for software error messages and alert codes.
- Check laser for error messages and alert codes.
- Check cell PLC for error messages and alert codes.
- Ensure cell interlocks are functioning as appropriate.

Stitch shape:

- Amend the robot programme to produce the required stitch shape.

Stitch location

Identification

The laser stitch will not be in the location defined on the master part or within the master document.

Limits

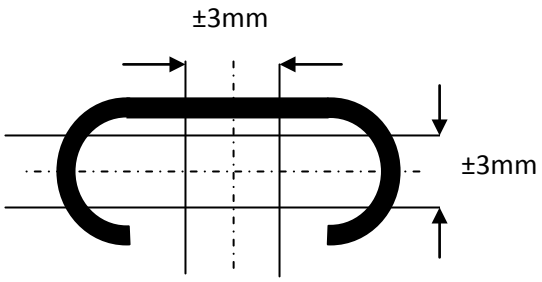

Fig.80. Schematic: positional tolerance for a laser stitch

Every laser stitch (for overlap joints) material must be within ±3.0mm of its location in lateral planes, as described on the master part, or in the master document.

Cause

First-off parts:

- Incorrect location programmed.
- Parts located incorrectly, change of master location
- Incorrect parts

Serial part:

- Modification to programme.
- Modification to part / master location
- Parts located incorrectly, change of master location
- Incorrect parts

Recovery

First-off and serial part:

- Ensure correct location of the workpiece (re-locate the part or fixture to the correct position)
- Ensure weld stitch has been correctly programmed (reprogram the stitch to location indicated on the maser part or master document)
- Ensure parts conform to the master part or master document

Non-destructive testing

Ultrasonic evaluation (AMsTech ultrasonic scanning system)

Background

Cost effective and quick track-side test of weld quality are often used for spot-checking part quality. For joints made using resistance spot welding (RSW) the 'chisel' test has historically been applied and accepted. For more detailed evolutions of weld quality, ultrasonic probes have been applied. Using this technique, a skilled operator can determine key attributes of the weld (diameter, presence of porosity etc) and these can be used a key indicators of weld quality.

Traditional single and multi-phase ultrasonic systems display data as a trace of the ultrasonic signal, requiring a skilled operator to both set and interpret the presented data. Intelligent systems are in development but these are not widely accepted at this time.

AMSTech have developed an ultrasonic NDT system that presents data in a pictorial form. The AMSTech system uses a proprietary probe system, where the transducer is both rotated eccentrically and traversed within the scanner body (see fig.81 below). The system software then presents the data as a topologically corrected colour map of the scanned area (see fig. 82 below). A trained operator will set a range of signal gates, and the colour range of the displayed maps, but then a semi-skilled operator can scan the required welds and readily interoperate the displayed images. Fig.83 is a graphical representation of the signal interpretation and gating funtionaility.

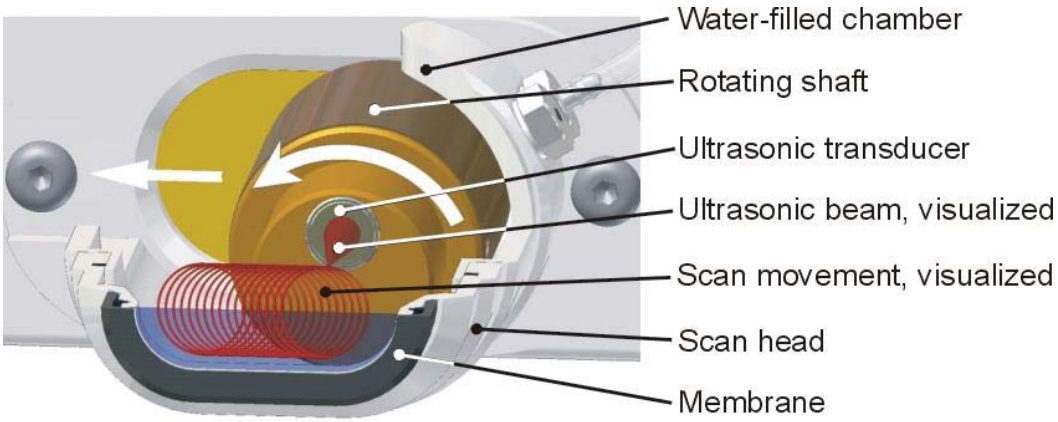

Fig.81. Operating mechanics of the AMSTech ultrasound probe. Note the relative motions of the probe

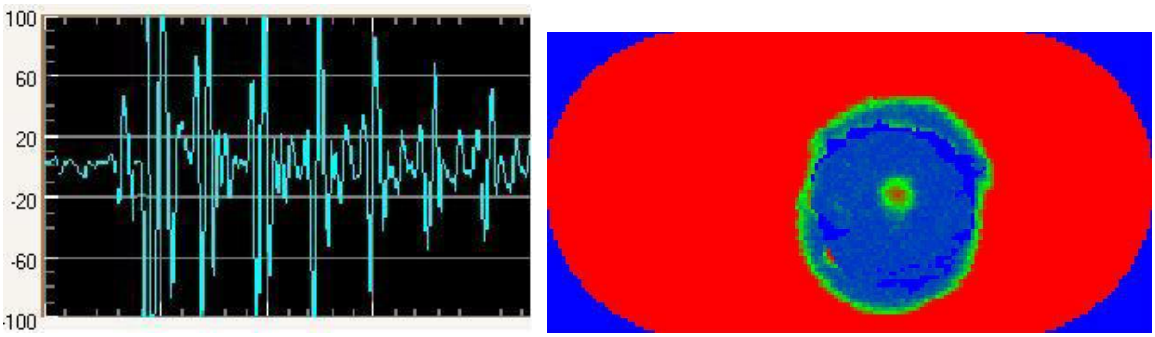

Fig:82. Traditional ultrasound data display (left) and AMSTech scanner output display (right)

In the scanner image shown in fig.82 (right) the boundary of the spot weld can be clearly identified. Two pores can also be seen within the spot weld.

To establish the suitability of the scanning system for interrogating linear laser welds a series of welds were made in overlapping sheets of 1.0mm thick DX54. Welds were made with interface gaps of 0mm, 0.1mm, 0.2mm, 0.3mm and 0.4 mm. Welds were also made with the lower sheet dimpled using a laser pre-process. Welds were made and inspected in batches of three (labelled A, B and C) apart from welds with 0mm gap, where six samples were made. The weld did not fully penetrate the back sheet and scans were made on both the top and bottom sheet. Figs 84 through 104 show the results for each weld. The left and right side of the figs show the scan from the top bead (left and the bottom bead right). Accompanying each scan is a photograph of the top bead and the image of the scan has been scaled and positioned to indicate the position of the scan in relation to the weld top bead.

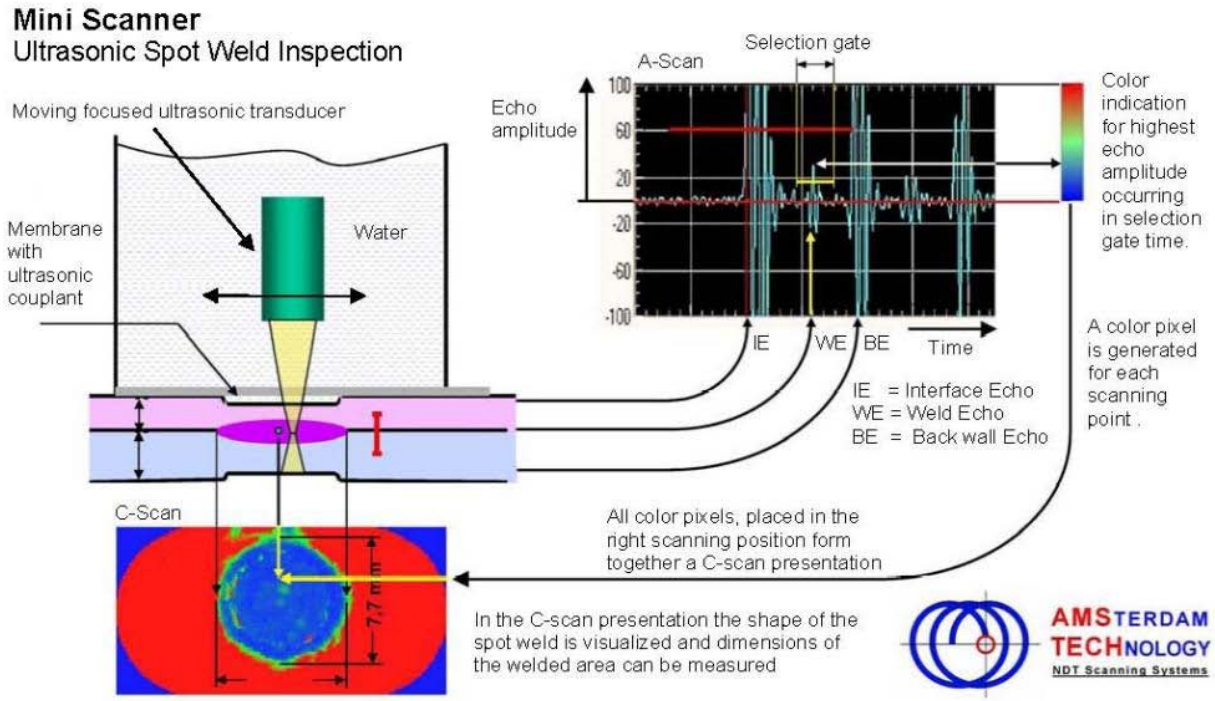

Fig.83. Operating principle of the AMSTech 'AT MIniscanner'

0mm gap

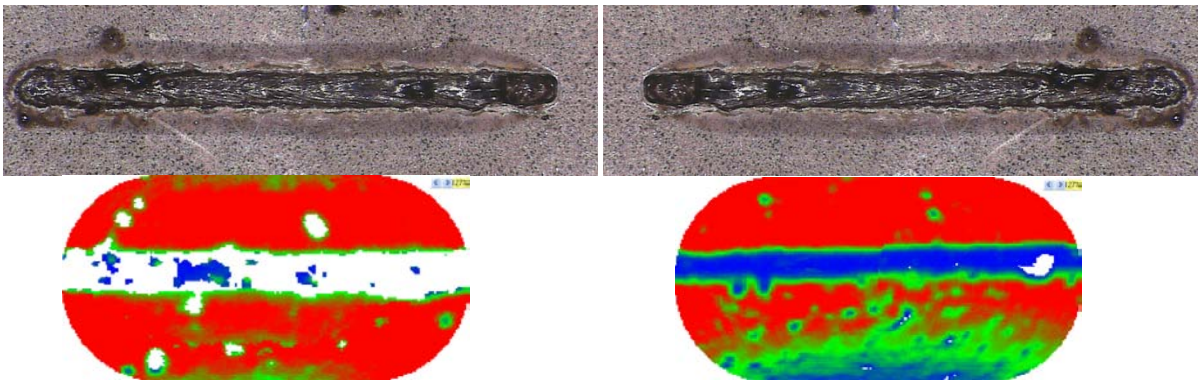

Fig.84. Weld top bead (0mm gap, sample A) and Amstech result from top bead (L) and bottom bead (R)

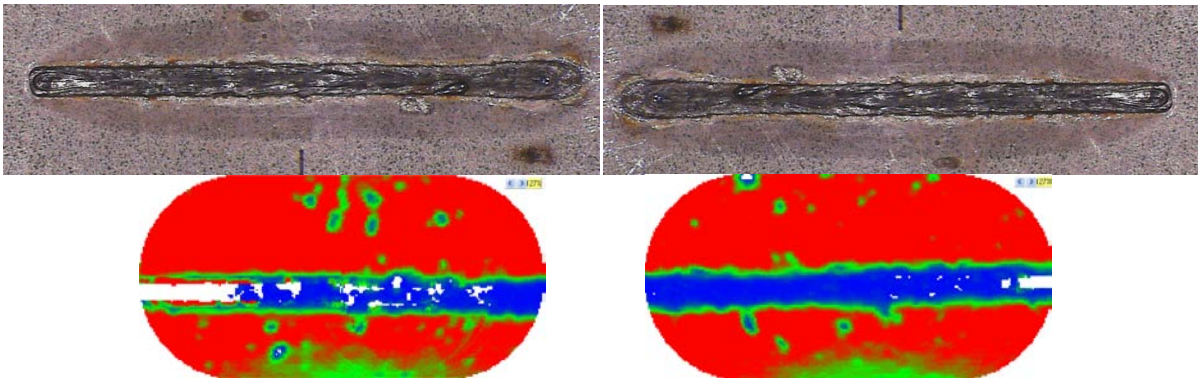

Fig.85. Weld top bead (0mm gap, sample B) and Amstech result from top bead (L) and bottom bead (R)

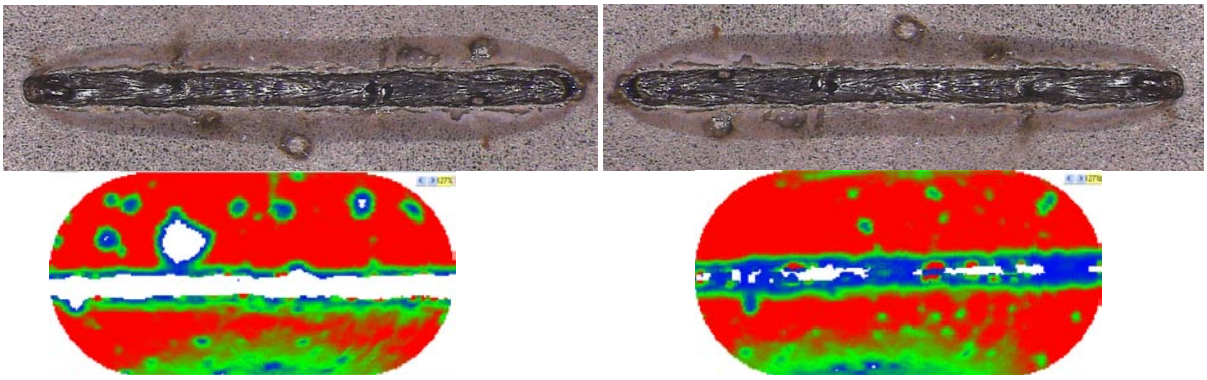

Fig.86. Weld top bead (0mm gap, sample C) and Amstech result from top bead (L) and bottom bead (R)

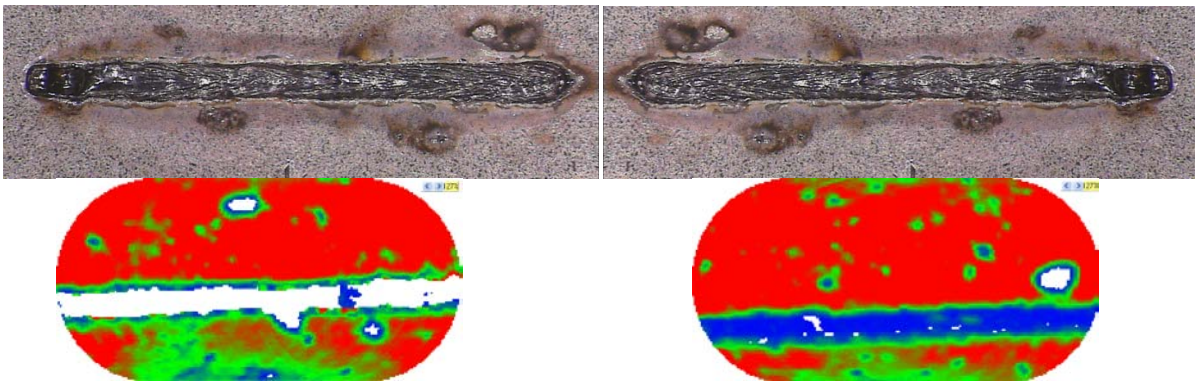

Fig.87. Weld top bead (0mm gap, sample D) and Amstech result from top bead (L) and bottom bead (R)

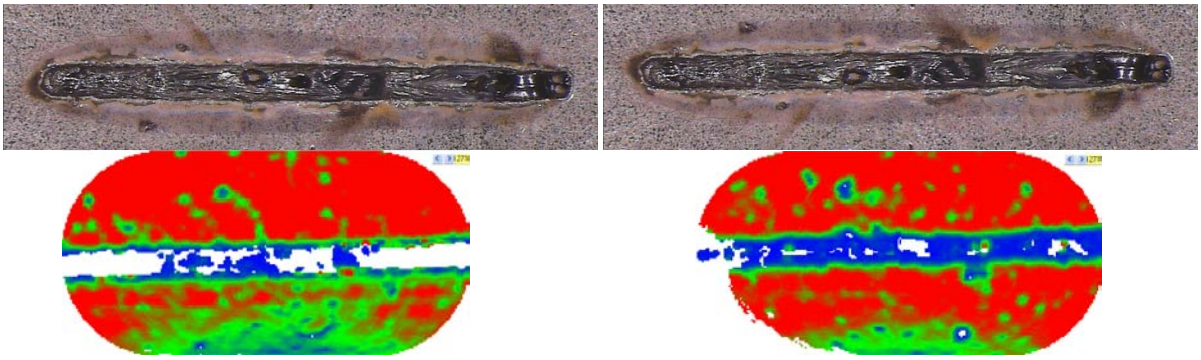

Fig.88. Weld top bead (0mm gap, sample E) and Amstech result from top bead (L) and bottom bead (R)

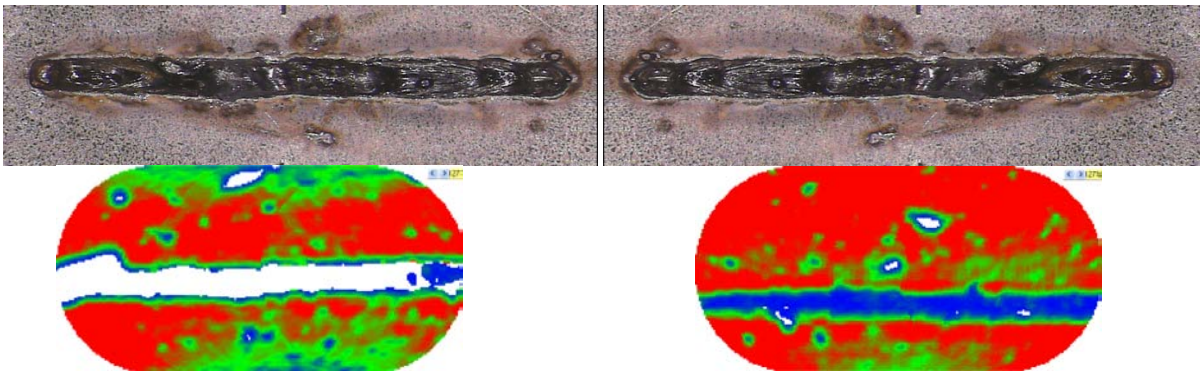

Fig.89. Weld top bead (0mm gap, sample F) and Amstech result from top bead (L) and bottom bead (R)

0.1mm Gap

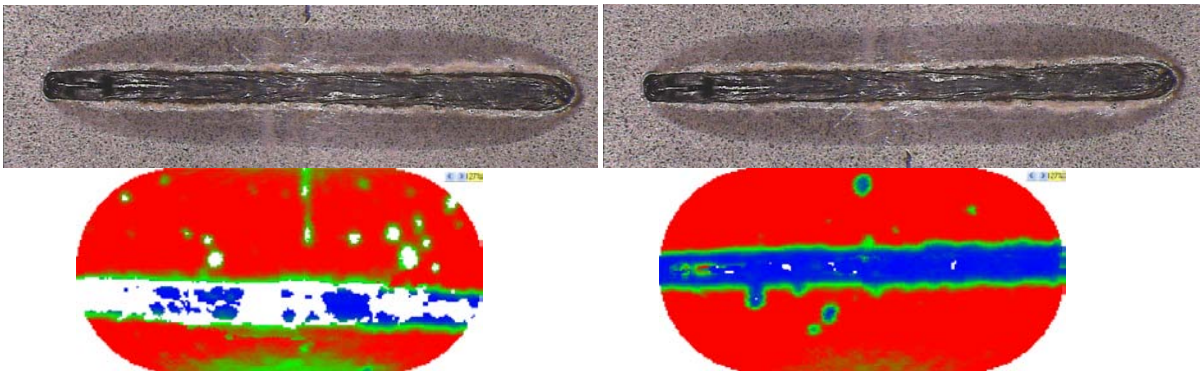

Fig.90. Weld top bead (0.1mm gap, sample A) and Amstech result from top bead (L) and bottom bead (R)

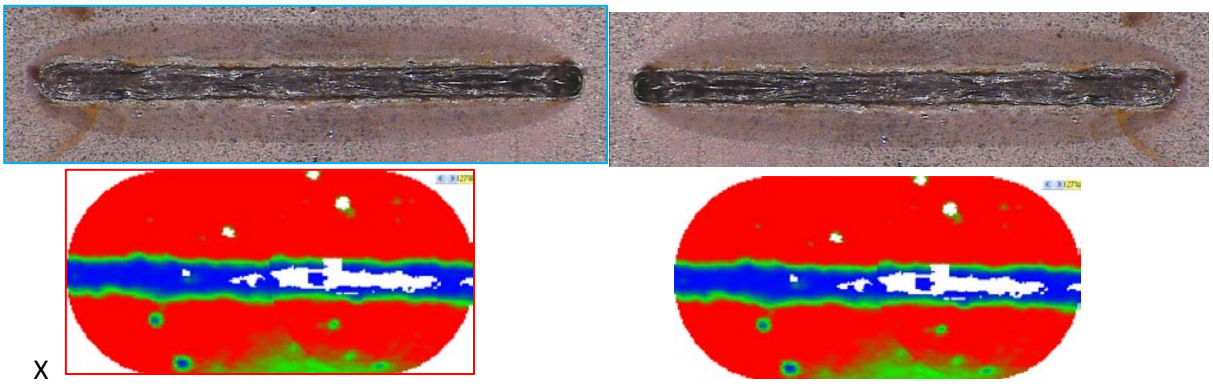

X

Fig.91. Weld top bead (0.1mm gap, sample B) and Amstech result from top bead (L) and bottom bead (R)

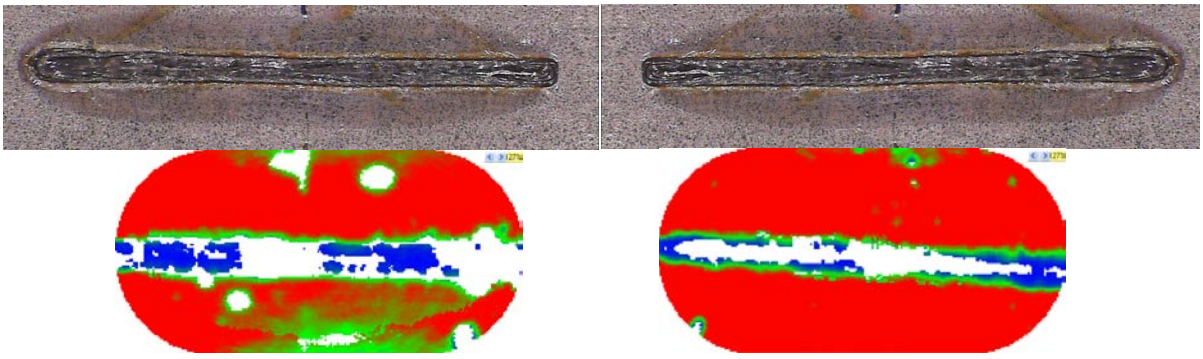

Fig.92. Weld top bead (0.1mm gap, sample C) and Amstech result from top bead (L) and bottom bead (R)

0.2mm gap

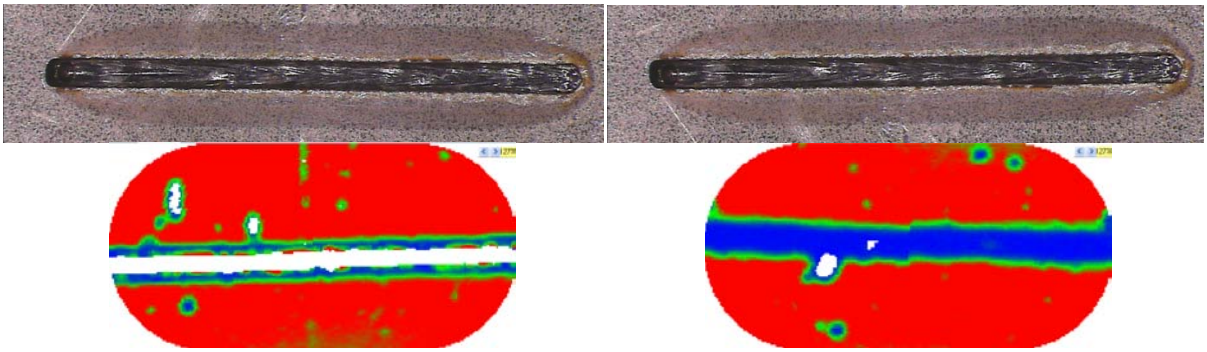

Fig.93. Weld top bead (0.2mm gap, sample A) and Amstech result from top bead (L) and bottom bead (R)

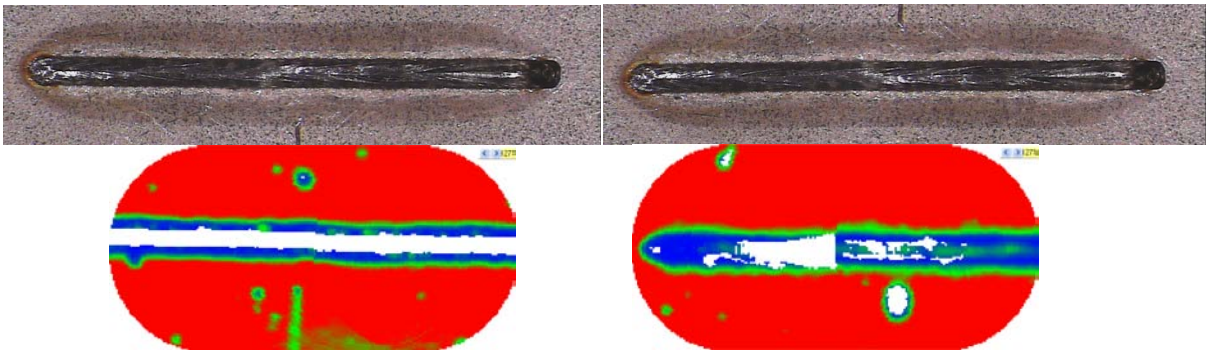

Fig.94. Weld top bead (0.2mm gap, sample B) and Amstech result from top bead (L) and bottom bead (R)

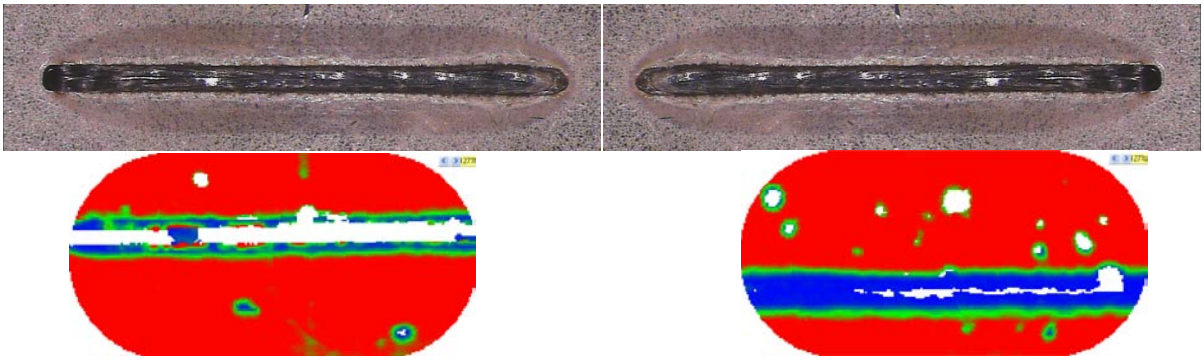

Fig.95. Weld top bead (0.2mm gap, sample C) and Amstech result from top bead (L) and bottom bead (R)

0.3mm gap

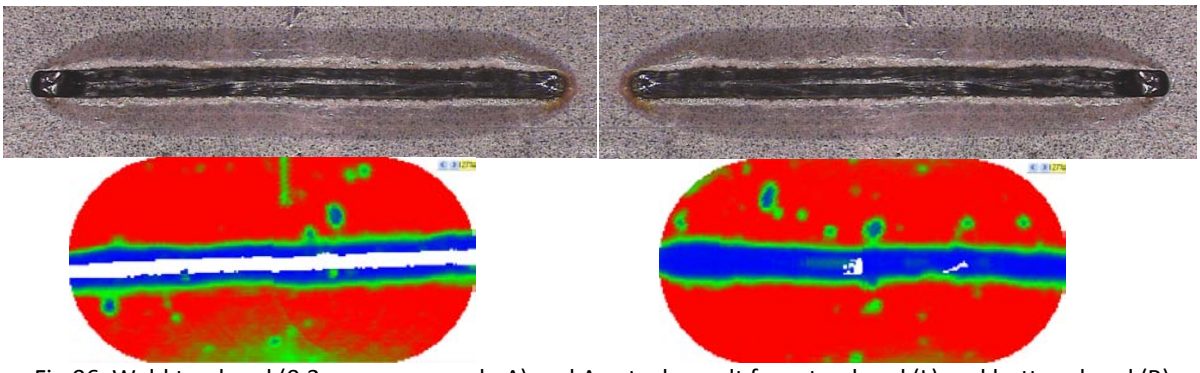

Fig.96. Weld top bead (0.3mm gap, sample A) and Amstech result from top bead (L) and bottom bead (R)

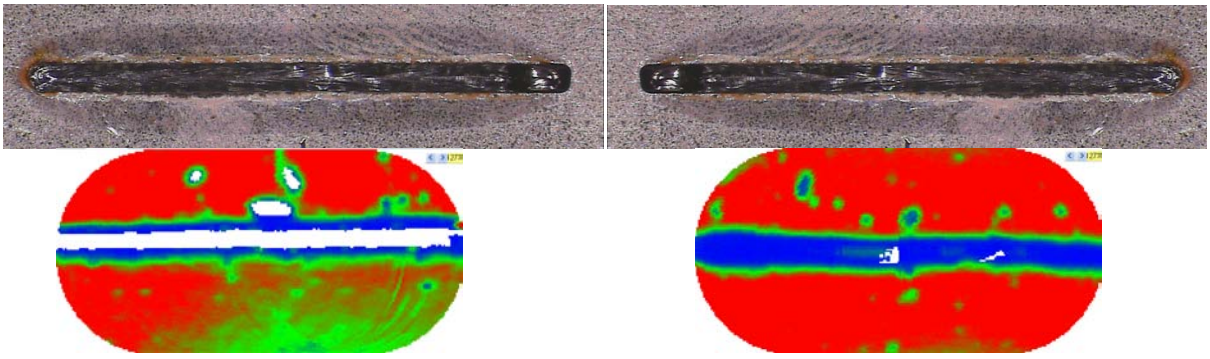

Fig.97. Weld top bead (0.3mm gap, sample B) and Amstech result from top bead (L) and bottom bead (R)

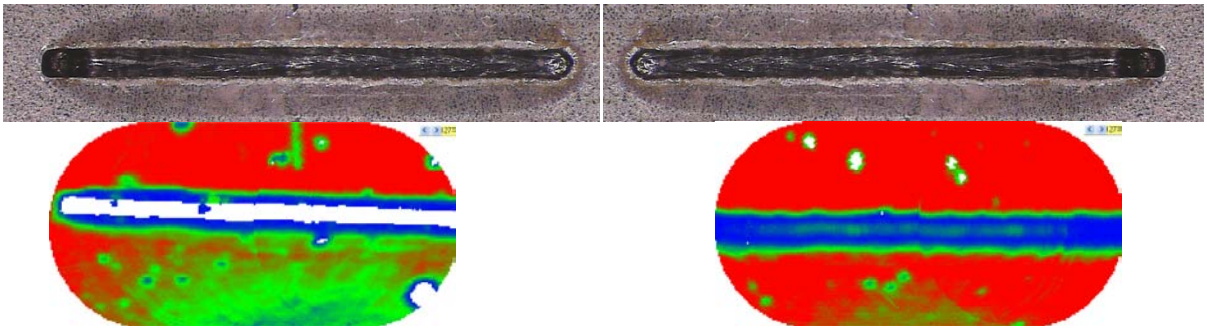

Fig.98. Weld top bead (0.3mm gap, sample C) and Amstech result from top bead (L) and bottom bead (R)

0.4mm gap

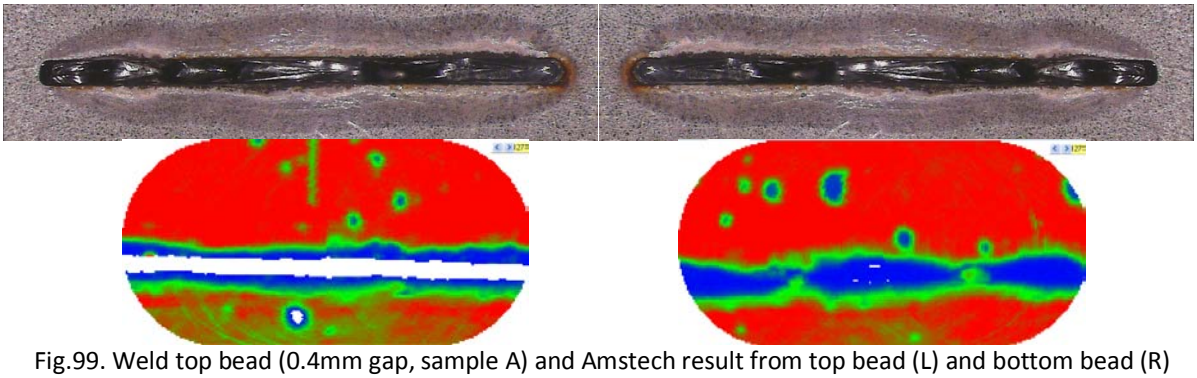

Fig.99. Weld top bead (0.4mm gap, sample A) and Amstech result from top bead (L) and bottom bead (R)

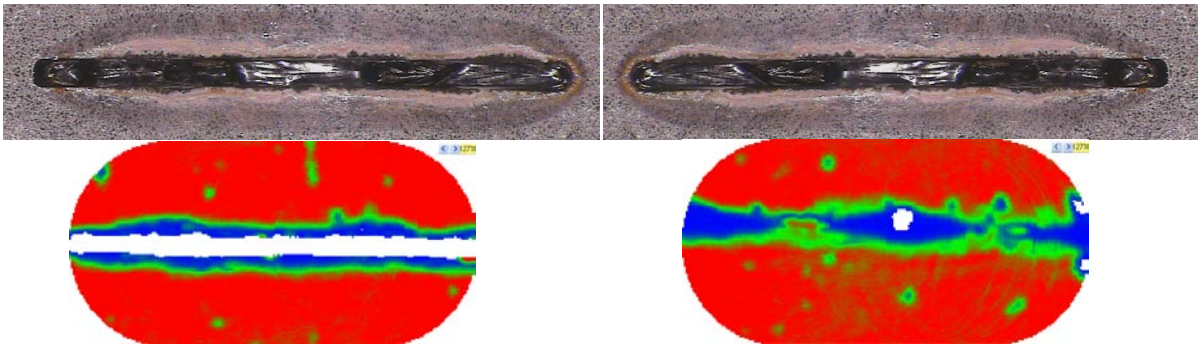

Fig.100. Weld top bead (0.4mm gap, sample B) and Amstech result from top bead (L) and bottom bead (R)

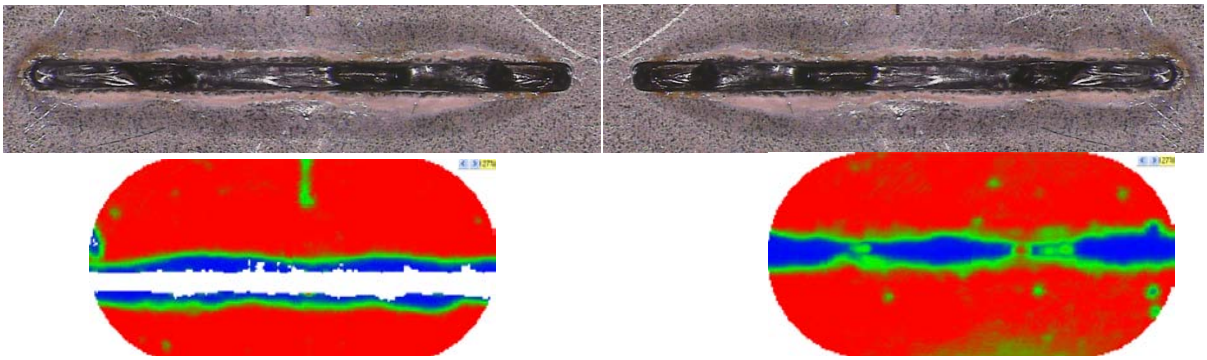

Fig.101. Weld top bead (0.4mm gap, sample C) and Amstech result from top bead (L) and bottom bead (R)

Nubbed

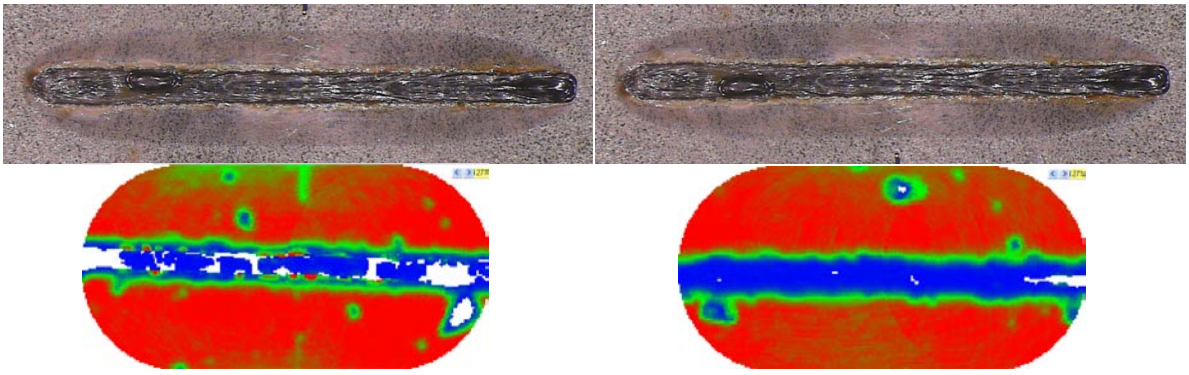

Fig.102. Weld top bead (nubbed, sample A) and Amstech result from top bead (L) and bottom bead (R)

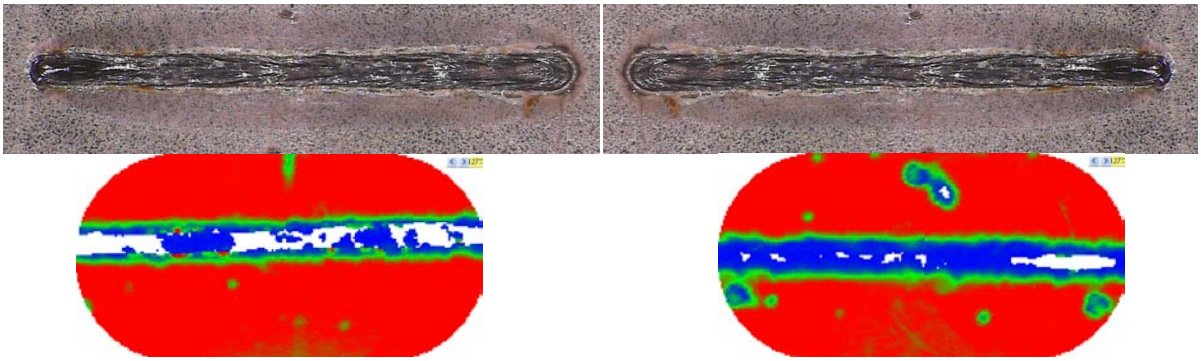

Fig.103. Weld top bead (nubbed, sample B) and Amstech result from top bead (L) and bottom bead (R)

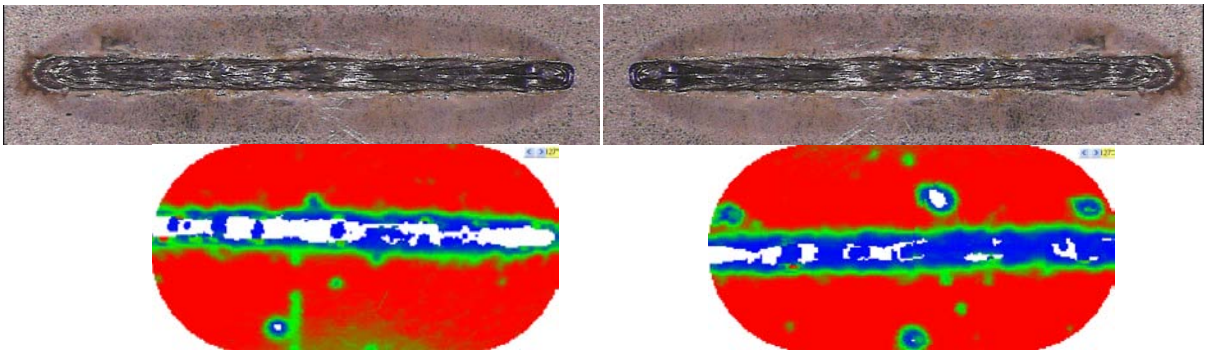

Fig.104. Weld top bead (nubbed, sample C) and Amstech result from top bead (L) and bottom bead (R)

Comments

The quality of the result from the scanning system is dependent on the probe head having unbroken contact with the material surface. Areas where the probe could detect no signal are coloured white. The undercut naturally present in most laser welds in clearly shown in many of the above samples, especially in samples with gaps over 0.1mm (figs.93. through 104.). A more reliable scan was attained when the underside of the weld was scanned (where undercutting of the weld would not be apparent). As the system cannot couple with the surface at the undercut, the system cannot provide a measure of undercut from a scan of the top bead.

Measurement of the top bead undercut may be possible if the sample is canned from the underside of the weld but further exploration of the gating parameters etc are required. The sample in fig.98. shows a green stripe along the centre line of the weld bead when evaluated from the weld underside, indicating a signal reflection at a distance corresponding to the interface of the sheets.

Samples shown manufactured with gaps of 0.1mm to 0.3mm gap (including nubbed samples), shown in figs. 96-98 and 102-104, show consistent width and edge form in the weld area (the blue band surrounded by the green border). For samples with made with 0mm gaps and 0.4mm gaps (figs. 84-89 and 99-101 respectively), the boundary of the weld interface appears inconsistent. Weld boundary shape can be identified from the scans of the top bead, despite the lack of coupling along the centreline of the weld. Therefore it may be possible to develop a system for assessing weld quality based on the shape/consistency of the weld interface boundary. Also, as the weld interface boundary can be identified, an assessment can be made of weld interface width

From the sample scans presented above, porosity was not evident. It is readily feasible may be that none of the samples generated for this test exhibit any porosity, even in the 0mm samples (typically, the material ejection typically associated with 0mm gap welding of coated steels manifests as significant undercut and open holes, as opposed to porosity). From the conducted tests it is therefore not possible to determine the effectiveness of the Amstech system for identifying porosity within the weld, although it is understood that Volvo use the Amstech system for this purpose.

Undercut measurement

Background

Cost effective and quick track-side test of weld quality are often used for spot-checking part quality. For joints made using resistance spot welding (RSW) the 'chisel' test has historically been applied and accepted. For this test, a blade is inserted between the adjoining panels and leverage is applied until failure is initiated at the weld site. If the weld breaks in an interfacial manner is considered a poor weld. An initiation of failure through the parent material (typically through the HAZ or the solid/liquid material boundary) indicates an acceptable weld. Fundamentally however, once tested the joined area is defective as a failure site has been initiated. Although the 'chisel' test is considered non-destructive, there is evidence to suggest that this is not the case. There is also anecdotal evidence that the 'chisel' test is susceptible to human influence - i.e. the test can be manipulated in such a way to present false positives etc.

For laser welding a good or bad weld can be categorised in the same manner (i.e. interfacial failure = bad weld), however it is desirable to undertake a test that does not damage the weld itself. As is the case with any welding technique, a laser weld has a number of success criteria that must be satisfied for a weld to be classed as good. Weld standards typically state the rules that each criteria must satisfy and this information is based on data comparing the performance of a weld and its relative attributes (strength vs interface width etc), although this data is not usually presented in the standards documents. A 'quick and dirty' trackside test needs to establish one or a number of the weld attributes easily and repeatedly and without inflicting damage to the weld itself. Sectioning and micro-inspection of the weld is the optimum technique for evaluating a weld and the cross section can be identified, the interface width measured and the porosity levels measured. But this is not possible at the trackside. Work is still ongoing to establish the performance of ultrasonic and eddy current based NDT systems with respect to laser welds but these techniques often require skilled operators.

One attribute that can be measured without sectioning is the undercut of the weld bead. The graph below demonstrates the relationship between weld strength and weld undercut for quasi-static lap shear tests. A study of fatigue performance would provide an indication of weld durability, but this work is yet to be undertaken.

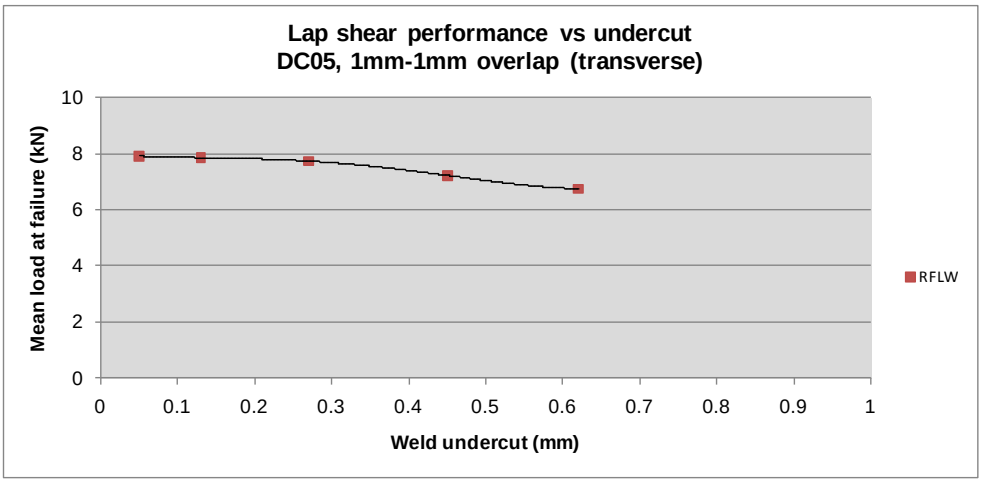

Fig.78. Graph: lap shear strength vs stitch shape and orientation: 1.0mm to 1.0mm DX54, 0.2mm gap

A pin-anvil micrometer can be used to measure the relevant dimensions of the weld, as the pin is narrow enough to probe to the weld surface it the weld is undercut, however this limits testing to

weld located on accessible flanges. An issue is apparent with this concept: does the result from the micrometer/ tread gauge reading represent a real figure for weld surface undercut?

Proceedure

A short test was undertaken to investigate the relationship between a micrometer measurement of undercut and the actual undercut measured from microsections of the welds.

Two coupons of 1mm DCO5 material (uncoated equivalent of DX55 material) replicated a current manufacturing condition) were then assembled in the fixture and welded in an overlap condition, with a 25mm long linear laser weld. This was repeated for our welds. Three of the welded coupons were subject to lap shear testing and the fourth, selected randomly, was kept for microsection analysis. The experiment was repeated using material stock in the as-delivered condition (the oil on the coupons was that applied by the home mill), but this time with gaps of 0.1mm, 0.2mm, 0.3mm and 0.4mm in consecutive sets and with 0mm and 0.2mm gaps featuring heavy oil contamination. Gaps were maintained with shims. Again welds were subject to lap shear testing and microsection analysis.

Prior to sectioning, each weld to be evaluated was measured in three locations using a pin micrometer. The features measured were:

1. Top sheet thickness (t^1)
2. The complete material stack thickness (t^t), close to the midpoint of the weld.
3. The thickness of the weld zone (t^w) at the centre of the weld.

For simplicity, it was assumed that there would be no significant undercutting or drop out on the underside of the weld. Calculating t^t-t^w would give a theoretical measurement of top sheet undercut (u) in mm. All published weld standards that quote top sheet undercut present this figure as a % of the thinnest sheet in the welded stack, and this is invariably assumed to be the upper sheet of any welded combination (although not necessarily true). Therefore using $(100/t^1)\ x\ u$ would present the measured undercut as a % of the top sheet thickness.

Following micrometer measurement the samples were sectioned as close to the midpoint of the weld as possible. The weld dimensions were then measured using a microscope based measuring system.

Results

Data from the micrometer measurement.

Interface gap (mm)	t^1 (mm)	t^w (mm)	t^t (mm)	u (mm)	u (%t^1)
0	1.05	2.07	2.12	0.05	4.8
0.1	1.04	2.12	2.25	0.13	12.5
0.2	1.04	2.06	2.33	0.27	26.0
0.3	1.06	1.96	2.41	0.45	42.5
0.4	1.06	1.90	2.52	0.62	58.5
0 (oiled)	1.05	2.04	2.11	0.07	6.7
0.2 (oiled)	1.06	2.14	2.33	0.20	19.1

Fig.78. Graph: lap shear strength vs stitch shape and orientation: 1.0mm to 1.0mm DX54, 0.2mm gap

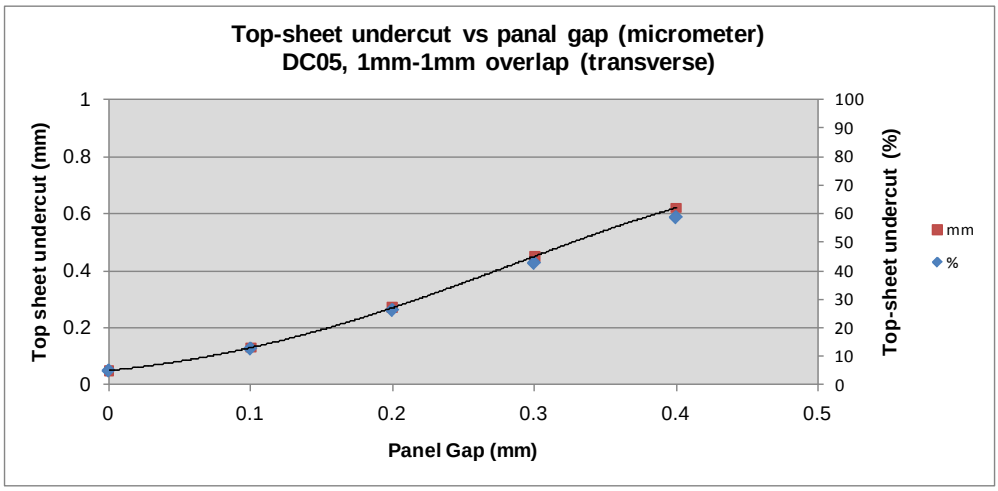

Fig.78. Graph: lap shear strength vs stitch shape and orientation: 1.0mm to 1.0mm DX54, 0.2mm gap

Data from the microsection measurement.

Interface gap (mm)	t^1 (mm)	t^w (mm)	t^t (mm)	u (mm)	u (%t^1)
0	1.05	-	-	0	0
0.1	1.05	-	-	0.14	13.3
0.2	1.05	-	-	0.17	16.2
0.3	1.06	-	-	0.47	44.3
0.4	1.07	-	-	0.61	54.7
0 (oiled)	1.05	-	-	0.09	6.7
0.2 (oiled)	1.05	-	-	0.18	17.1

Fig.78. Graph: lap shear strength vs stitch shape and orientation: 1.0mm to 1.0mm DX54, 0.2mm gap

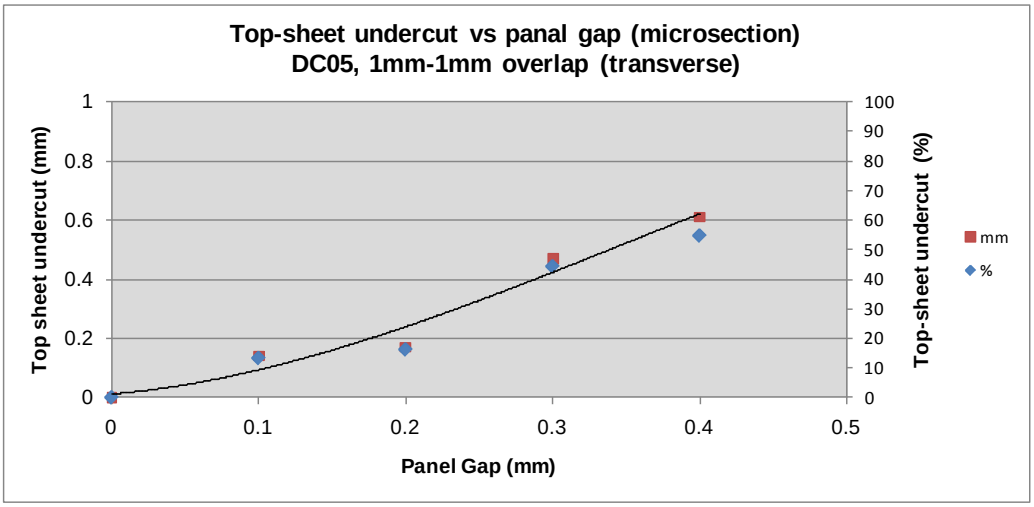

Fig.78. Graph: lap shear strength vs stitch shape and orientation: 1.0mm to 1.0mm DX54, 0.2mm gap

Microsections

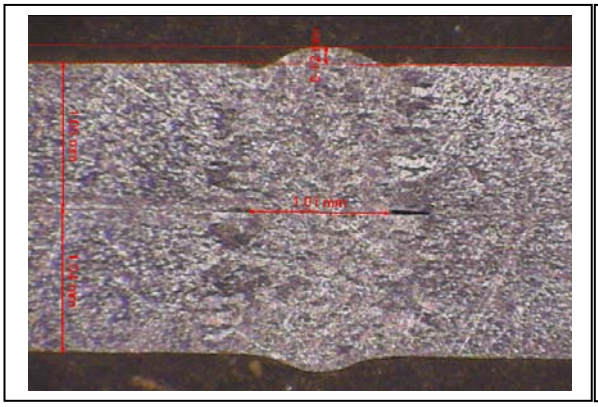

0mm gap, no additional oil

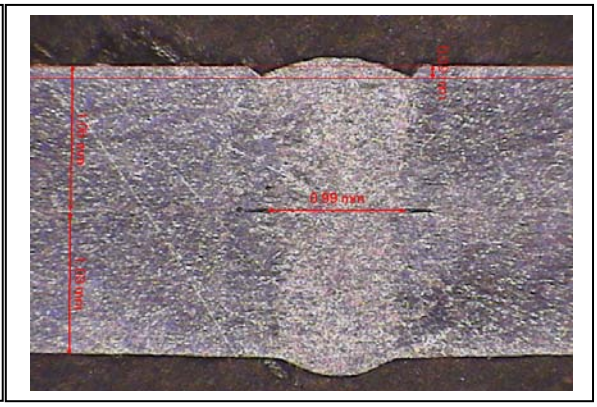

0mm gap, oiled coupons

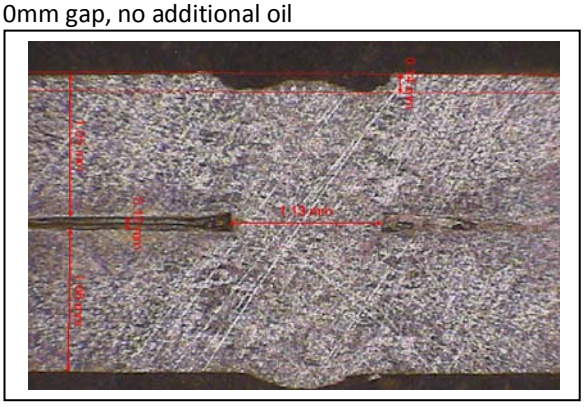

0.1mm gap, no additional oil oil

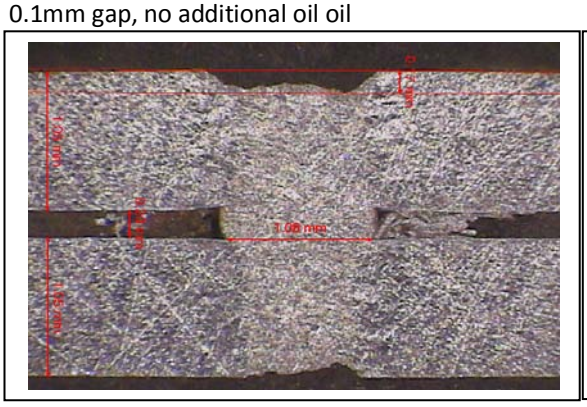

0.2mm gap, oiled coupons

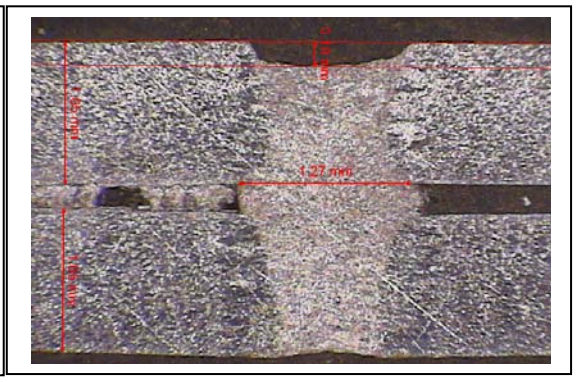

0.2mm gap, no additional

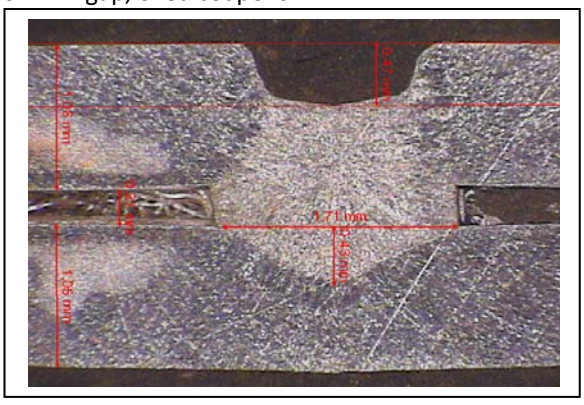

0.3mm gap, no additional oil

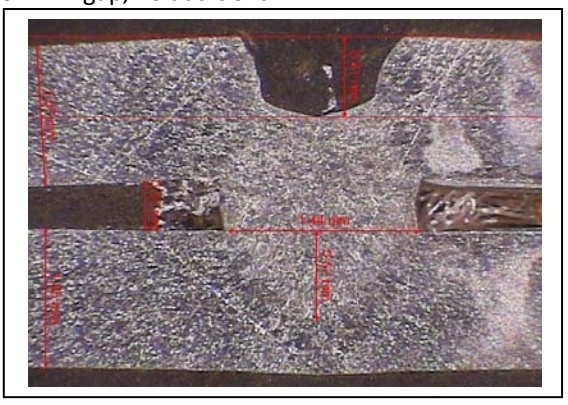

0.4mm gap, no additional oil

Fig.78. Graph: lap shear strength vs stitch shape and orientation: 1.0mm to 1.0mm DX54, 0.2mm gap

Comments

There is little observable difference between the samples welded with additional oil and those welded without. Weld penetration and weld interface width are the same and there is no evidence of porosity in either of the welds.

As panel gap increases the top surface undercut also increases. With a gap of 0.2mm the undercut is acceptable - it is less than 25% top-sheet thickness (t_1). A gap 0.3mm however, creates an undercut exceeding 25% t_1 and so would be considered a bad weld under many quality standards. The lap shear strength for the weld indicates that a weld made with a 0.3mm gap has acceptable strength however, it has been historically proven that undercuts exceeding 25% t_1 can significantly reduce the fatigue life of the weld.

There is a marginal difference between the measurements made using the micrometer and made directly for samples with gaps 0f 0mm, 01.mm, 03mm and 0.4mm, indicating an acceptable measurement can be made using the pin micrometers as an NDT technique. At 0.2mm there is a significant difference in the measurements (0.17mm compared to 0.27mm). This may be as a consequence of a disparity between where the initial measurement was made and where the weld was sectioned. If this is the case then it is also clear that the undercut of the weld may vary along the length of the weld, and that a single measurement may not present sufficient information for assessing the undercut of the weld.

The use of a pin micrometer to measure weld dimensions limits the welds that can be assessed to those located close to panel edges on flanges (the micrometer has a small throat depth and requires access to both sides of the weld. A preferred solution could be a 'tyre tread depth gauge' as this requires only single sided access and often features a pin-type probe (significant panel form may still limit access to certain welds). Unlike a pin micrometer, a tread gauge will not require the operator to know the thickness of the welded stack (including any interface gaps) as the undercut measurement is made from, and relative to, the top surface of the material stack. A simple statement sheet in the quality plan that outlines the maximum depth permitted for each weld to be tested will provide sufficient information upon which to make the measurements with the gauge (material thickness should only vary by a maximum of 10% nominal thickness). In this fashion, the only reliance on the operator is to use the gauge correctly (no calculations are required and the output requires no specialist interpretation, unlike some ultrasound based techniques.)

Appendix E

This appendix is an original process document from Ford and it is provided by RLW project partner- Jaguar and Land Rover with Ford's permission.

Engineering Specification

PART NAME	PART NUMBER
Laser Beam Welding – Stitch Welds	**ESAU5A-1B313-AA**

DATE	LET	FR	REVISIONS	DR	CK
April 23, 2010	A	ALL	Initial Release of Global Engineering Specification		
			AB00-E-12310257-003		

REFERENCES

ES7L1A-7861019-B

PREPARED/APPROVED BY

J. Hover (FoE) / T. Coon (FNA)

CHECKED BY	CHECKED BY
A. Wexler (FNA)	J. Larsson (Volvo)
S. Morgans (FNA)	G. Mueller (FoE)

CONCURRENCE/APPROVAL SIGNATURES ***Ford of Europe***

Design Engineering Management

R. Severlich 7.12.09

Manufacturing Engineering

M. Messler 3.3.10

VO Quality Office

M. Steinhaeuser

CONCURRENCE/APPROVAL SIGNATURES ***Ford North America***

PD Body Chief Engineer

B. Barthelemy

VO BCE Chief Engineer

P. Temple

CONCURRENCE/APPROVAL SIGNATURES ***Volvo Cars***

Engineering Standards Manager

U. Malmberg

PD
May 1988 **3947a1e** (Previous editions may **NOT** be used)

OUTLINE **FRAME**

I. GENERAL

I.1 Scope of Engineering Specification, General Statement

This Engineering Specification is issued to define design factors and tolerances applicable to the laser-beam welding of sheet steel

- having a minimum of 0.5 mm and a maximum thickness of 3 mm for individual sheets and
- up to a maximum of 6 mm in total joint thickness,
- comprising up to two thicknesses of steel of the same or different gauge,
- comprising up to three thicknesses of steel of the same or different gauge *on a case-by-case basis*,
- executed in various shapes such as circular, staple or linear stitches defined by having a length of less than 50 mm
    - with or without filler metal for
    - two types of generic joints
        - overlap joints (executed as edge or overlap welds) and
        - single Flare V-Groove Weld (covered by this spec, but not recommended)

used in the fabrication of body structure assemblies (including hang-on parts) so that product quality and appearance may be controlled to an acceptable degree. It harmonizes the requirements globally for Ford Motor Company and is applicable to new model programs.

Notes:

A. The laser-beam welding of steel body components to form a multi-piece blank (e.g. Tailor Welded Blanks) is covered by Engineering Specification ES-1U5A-1710064-A for Ford and VCS 5605,5179 for VCC.*

B. Continuous laser welds - defined as individual weld having a length of at least 50 mm - are covered by Engineering Specification ES-AU5A-1B312-A.*

This Engineering Specification is a supplement to the released drawing part, and all requirements herein must be met in addition to all other requirements of the part drawing. Each section specifies the minimum measures necessary for documenting compliance to this specification.

This Engineering Specification is intended to evaluate specific characteristics as a supplement to normal material inspections, dimensional checking, and in process controls and should in no way adversely influence other inspection operations.

Preparation and submission of an acceptable Control Plan are the responsibility of the manufacturing source. The manufacturing source will retain the original control plan and any later revisions per Section 7.3 in FAP02-001 and provide a copy to the design responsible Product Engineering activity.

I.2 Process Description

The laser-beam welding process, shown in Figure 1 for a lap joint condition, uses a laser beam as the source for the energy required to melt parent sheet metal. The main settings and parameters that influence the process are:

- Laser power
- Spot size and shape
- Welding speed
- Shielding gas composition and flow (if applicable)
- Filler wire size and feed rate (if applicable)

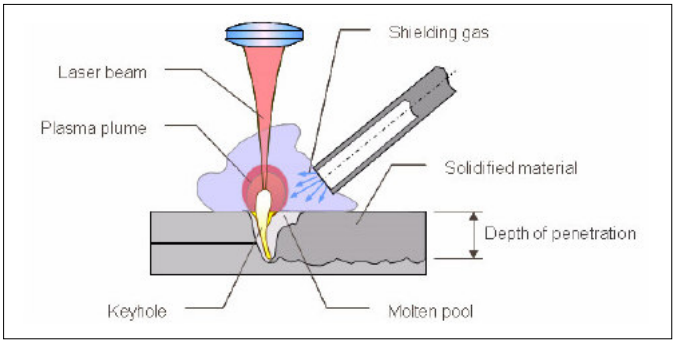

Figure 1: Laser Welding Set Up

I.3 Design Guidelines

The following design guidelines describe the generic conditions for a laser-beam welding application. Any deviation from these guidelines shall be analyzed jointly between the relevant Body and Manufacturing Engineering departments.

I.3.1 Generic Joint Design and Seam Locations

Figure 2 shows three typical stitch weld shapes. Figures 3, 4 and 5 illustrate the generic joint types used in the fabrication of body structure assemblies and hang-on parts.

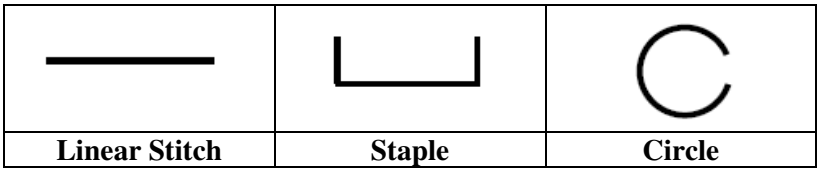

Linear Stitch	Staple	Circle

Figure 2: Typical Shapes of Stitch Welds

.

Overlap Joint, Seam Weld	
Typical Application	**Remarks**
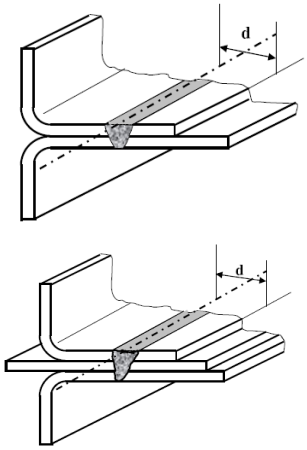	• Common joint geometry for body-in-white assembly • Can comprises up to three thicknesses • In the case of zinc-coated sheet steel, a controlled gap between the two sheets is necessary to allow zinc-gases to escape. The gap can be achieved in a number of ways, for example with an angle to the sheets or with clamping devices. • In the case of zinc-coated sheet steel there are limits to the total thickness of the zinc-coating in the interface between the sheets, details are defined in Section I.4 • The dimension distance-to-edge "d" is measured from the cut edge of the top sheet to the centerline of the weld, as shown in the figures on the left-hand side. The distance to edge dimension typically should be at least o 3 mm for a 2T joint and o 4 mm for a 3T joint to allow for variations in robot tracking and repeatability, part stamping and trimming. Note: Applications involving high or ultra high strength steels may require larger distance to edge dimensions than listed above. These applications require the approval of Body and Manufacturing Engineering. • The flange design including the minimum flat overlap depends on the equipment used (e.g. pressure wheel or fixturing system). It should consider sufficient access for the welding head and shall therefore be jointly determined with the relevant Manufacturing Departments. • Cannot be combined with structural adhesive application between the sheets

Figure 3: Overlap Joint Geometry

Overlap Joint, Seam Weld At Edge	
Typical Application	**Remarks**
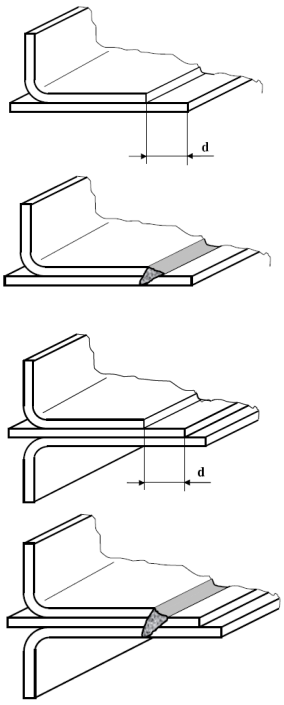	• Special joint geometry for body shop assembly • Can comprises up to three thicknesses • In the case of zinc-coated sheet steel, a controlled gap between the two sheets is necessary to allow zinc-gases to escape. The gap can either be achieved with an angle to the sheets or with clamping devices • Beneficial in the case of zinc-coated sheet steel as there is less risk of weld and zinc-gases to get trapped in the molten metal • Higher demands regarding accuracy of laser head positioning and edge tracking - position of the beam needs to be within 0.2 mm from the edge • The flange design including the minimum flat overlap depends on the equipment used (e.g. pressure wheel or fixturing system). It should consider sufficient access for the welding head and shall therefore be jointly determined with the relevant Manufacturing Departments. • The dimension distance-to-edge "d" is measured from the cut edge of the top sheet to the cut edge of the adjacent sheet, as shown in the figures on the left-hand side. The distance to edge dimension typically should be at least o 3 mm for a 2T joint and o 4 mm for a 3T joint to allow for variations in robot tracking and repeatability, part stamping and trimming. *Note:* *Applications involving high or ultra high strength steels may require larger distance-to-edge dimensions than listed above. These applications require the approval of Body and Manufacturing Engineering.* *Note:* *Lower d-values shall be checked for feasibility during the design phase and require the approval of Body and Manufacturing Engineering.*

Figure 4: Overlap Joint Geometry, Seam Weld At Edge

Flanged Butt Design, Single Flare V-Groove Weld Joint	
Generic Joint Geometry	**Remarks**
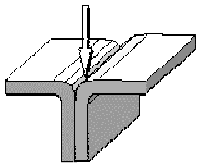	• **Not a recommended joint type for body–in-white assembly due to critical joint fit-up condition – should be avoided** • Requires special fixtures / clamping devices • Would require filler wire to properly execute in order to avoid undercut conditions

Figure 5: Flanged Butt Design, Single Flare V-Groove Weld Joint

I.3.2 Applicability to Surface Classes

Surface Class Ford	Surface Class VCC	Application	Permissible Weld Type and Material Stack Up
N/A	**Class 1**	No laser-weld application permitted in visible areas	N/A
Class 1	**Class 2**	Welds covered by visual sealing on external surfaces	Edge weld on 2-sheet combination
Class 2	**Class 3**	Welds covered by visual sealing, exposed with doors or enclosure lids in open position	Edge weld on 2-sheet combination
Class 3	**Class 4 or 5**	Welds with/without sealer hidden by trim	Edge or overlap weld on 2- or 3- sheet combination

Table I.3.2: Applicability to Surface Classes as defined in ES-F75B-11007-AA

Deviations from these rules require the approval of the relevant Body and Manufacturing Engineering departments.

I.3.3 Specific Joint Design

Gap Conditions

Laser welding of zinc coated steel requires a controlled gap of at least 0.1 mm to allow zinc-gases to escape. A touch condition of the panels leads to unstable welding conditions and porosity in the seam. Maintaining a specific gap is difficult since required tolerances cannot be obtained with normal sheet stamping procedures. *Therefore, edge weld geometries (see Figure 5) are preferred when laser welding in zinc-coated materials.*

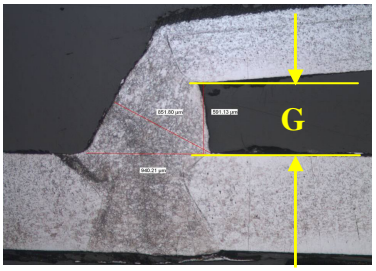

Maximum gaps as described below must be maintained for both weld geometries between the sheets at the weld location during the welding process to ensure joint integrity and appearance:

- 0.25 * t not to exceed 0.3 mm for edge or lap joint applications without filler wire
- 0.5 * t not to exceed 0.5 mm for edge joint applications with filler wire (Figure 6).

Figure 6: Gap Conditions, Edge Weld

Filler Wire

Filler wire should only be used in exceptional cases.

Design for Process Stability

At welding with full penetration it is important that the welding process is not disturbed by reflected laser light from adjacent details. Therefore the distance to the bottom sheet should not be below 3 mm, see Figure 7.

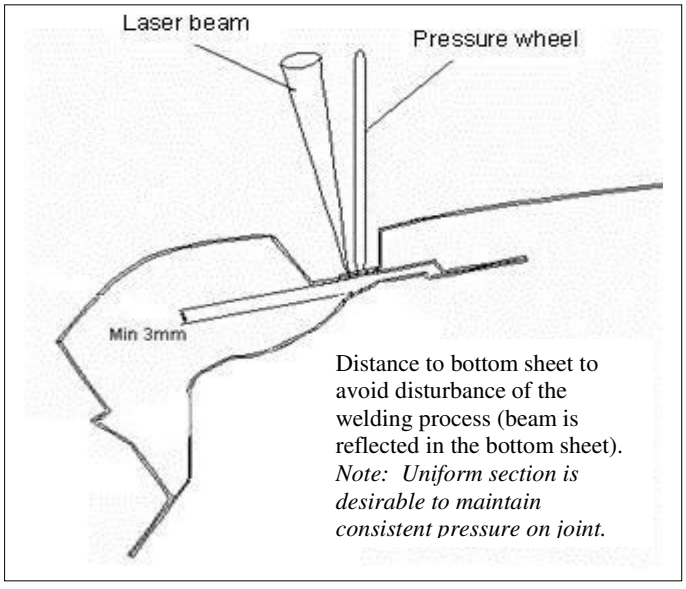

Figure 7: Design for Process Stability

Design for Welding Towards Visible Surfaces

Laser welding on visible surfaces, without using post-treatment, can only be realized on hem flanges (see Figure 8).

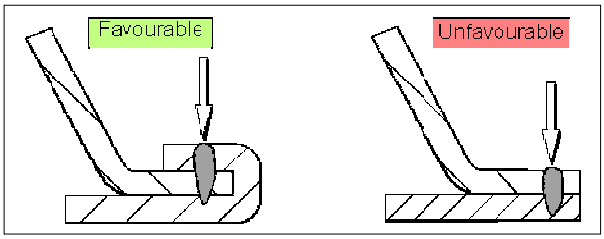

Figure 8: Welding towards Visible Surfaces

Design for joining of three sheets

Welding through three sheets in an overlap configuration should be avoided. Fixation of such a geometry is associated with big difficulties, resulting in bad weld quality in terms of undercut and lack of fusion. Therefore, two sheet joints are recommended for high volume production.

Additional design guidelines for laser-welding can be retrieved from the following weblink:
http://gbwlt025.gothenburg.vcc.ford.com/standard/static/vcc/design_instructions/joining/welding/met/laser_welding.html

I.3.4 s-value , Weld Length-Definitions, Joint Strength,

The width "s" of the laser-weld shall comply with the minimum requirements as shown in Figure 9 for 2-gauge combinations and in Figure 10 for 3-gauge combinations and their respective weld interfaces for individual gauges up to and including 1.5 mm. The s-value for gauges exceeding 1.5 mm need to be agreed on a case-by-case basis jointly between the relevant Body and Manufacturing Engineering departments.

Overlap Joint, Seam Weld	Overlap Joint, Seam Weld at Edge
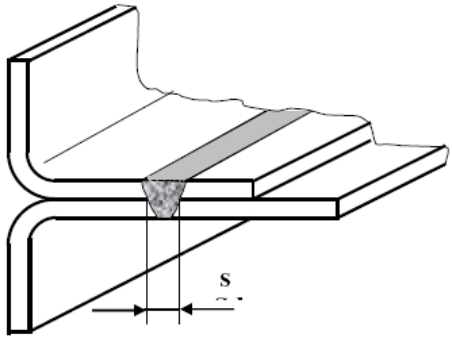	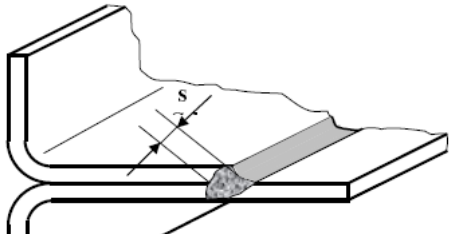
$s \geq 0.9 * t_{min}$ t_{min} = thickness of thinnest sheet	**$s \geq 0.7 * t_{top}$** t_{top} = thickness of top sheet

Figure 9: Minimum s-Dimension for 2-Gauge Combination

Overlap Joint, Seam Weld	Overlap Joint, Seam Weld at Edge
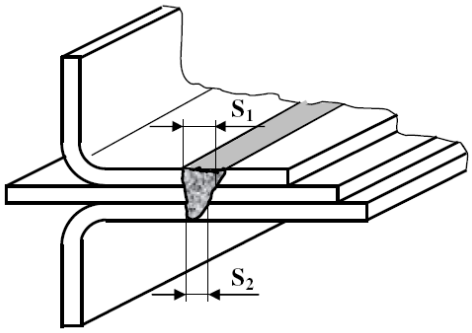	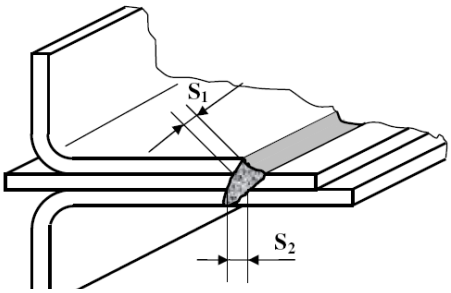
$s_1, s_2 \geq 0.9 * t_{min}$ t_{min} = thickness of thinnest sheet in each interface	$s_1 \geq 0.7 * t_{top}$ $s_2 \geq 0.9 * t_{min}$ t_{top} = thickness of top sheet t_{min} = thickness of thinnest sheet in lower interface

Figure 10: Minimum s-Dimension For 3-Gauge Combination

Values lower than the minimum s-value specified need the approval of the relevant Body and Manufacturing Engineering Departments.

A detailed description on how to measure the s-value during the section cut analysis of different bead geometries is contained in Section III.4.2.

Weld Length Definitions

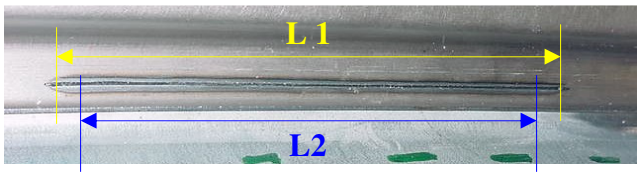

Figure 11: Weld Length Definitions

Minimum Design Weld Length
The minimum design length for individual welds is 25 mm.

Design Length vs. Effective Weld Length

- The weld length L_1 shown in the CAD-system is the design length and represents the minimum overall length inclusive of start and stop.
- The effective weld length L_2 is used for CAE-calculations only and should be the design length L_1 reduced by 5 mm (2.5 mm on each end for start and stop).

Continuous versus Stitch Weld Length
Individual welds having a design length of at least 50 mm are classified as continuous welds and are covered by a separate Engineering Specification – ESAU5A-1B312-A*.

Joint Strength

The following values are a guideline for strength estimates. If needed for CAE-analysis, actual strength values for the relevant combinations need to be determined in shear strength testing upfront.

Guideline: In case of an overlap joint and loading conditions perpendicular to the weld, a continuous weld can have a strength equivalent to a spot weld spacing of 20 mm in shear loading and 10 mm in peel loading for mild steels.

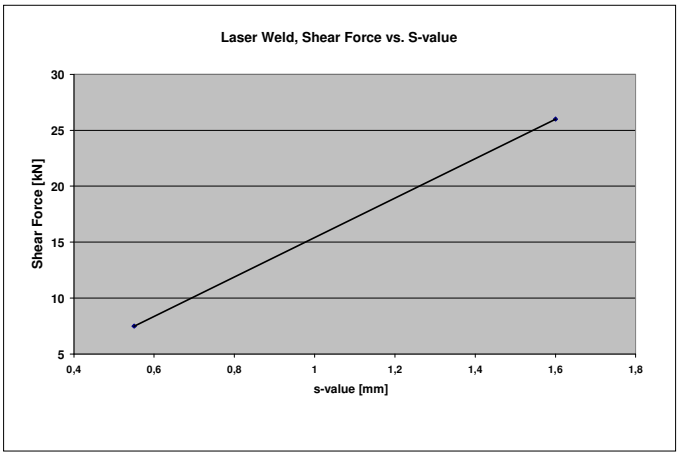

Figure 12: Shear Force vs. s-Value

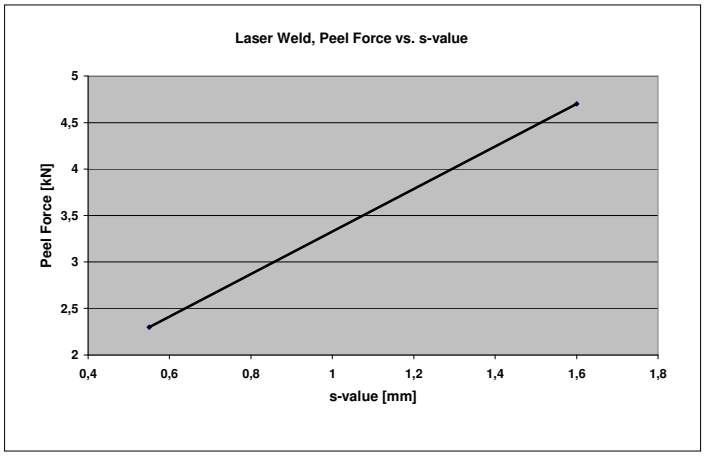

Figure 13: Peel Force vs. s-Value

Figure 12 illustrates the relationship between the s-value and shear strength for specimen with a 25 mm bead. Figure 13 illustrates the same for peel strength, all for overlap joint geometries.

I.3.5 Laser-Beam Welding In Combination With Sealants and Adhesives

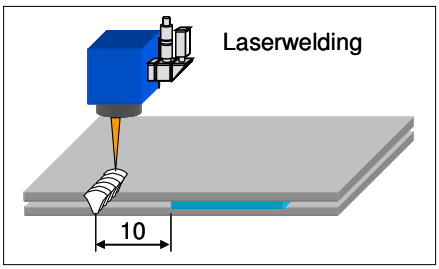

A distance of minimum 10 mm shall be maintained between the laser-weld and a potential sealer or adhesive bead in compressed condition as shown in Figure 14.

Figure 14: Distance to Sealer/Adhesive Bead

I.3.6 Parent Metal Gauge Ratio

There is no generic limitation to the gauge ratio of the parent metals. Applications which have no existing data or are described as not recommended in Figure 15 and 16 shall be analysed individually during the Design phase within the scope of tests outlined in Section III.

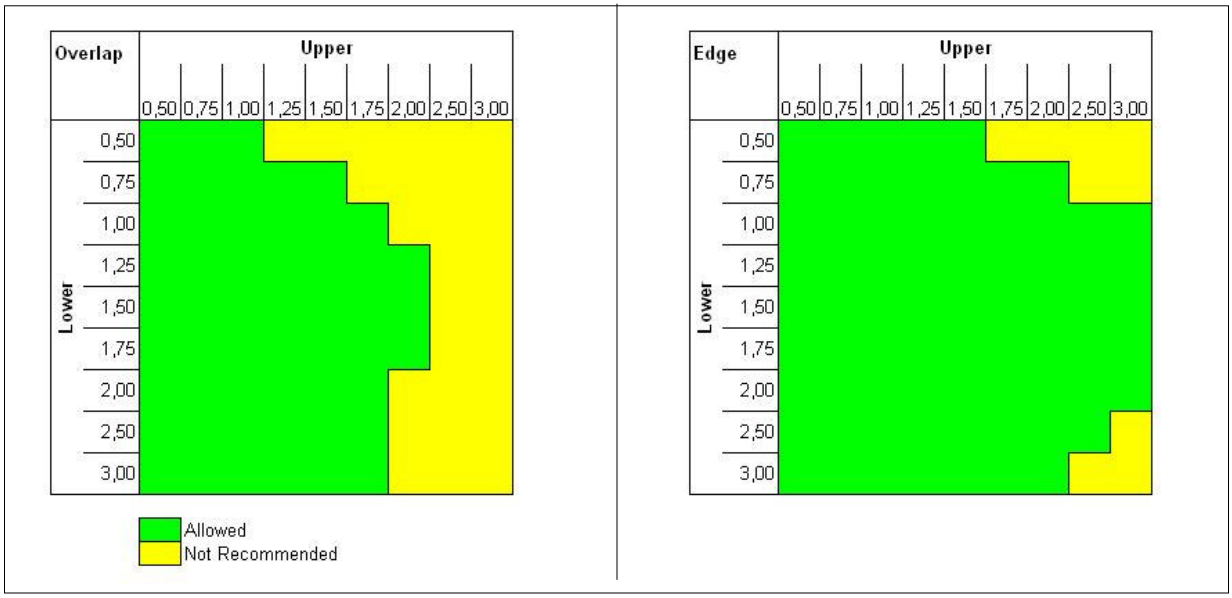

Figure 15: Gauge Ratio Limitations for Overlap Joint, Seam Weld

Figure 16: Gauge Ratio Limitations for Overlap Joint, Seam Weld at Edge

I.4 Applicable Materials

This Engineering Specification covers the use of the following steels categories in uncoated and coated condition:

		FORD MATERIAL SPECIFICATION NUMBER		
Category	**Types of Steel**	**Europe**	**North America**	**Global [3)]**
MS	Mild, Hot and Cold Rolled, Low Carbon	WSS-M1A344-A1/A2 WSS-M1A345-A1/A4	WSD-M1A333-A1/A4	WSS-M1A365-A11/A14 WSS-M1A365-A20/A23
DR	Dent Resistant incl. Bake Hardening, High Strength IF, Isotropic, and Rephosphorised	WSS-M1A341-A1/A10	WSS-M1A341-A1/A10	WSS-M1A367-A21/A23
HSLA	High Strength Low Alloy Steels	WSS-M1A346-A1/A3 WSS-M1A347-A1/A3	WSB-M1A215-E1/F1	WSS-M1A367-A35/A36 WSS-M1A367-A45/A46
DP [1)]	Dual Phase Steels	WSS-M1A348-A1/A9	WSS-M1A348-A1/A9	WSS-M1A368-A13/A14
TRIP [1)]	TRIP Steels	WSS-M1A351-A1/A3	WSS-M1A351-A1/A3	NA
MSW [1)]	Martensitic Steels	TBD	WSS-M1A183-D	WSS-M1A368-A81/A84 WSS-M1A368-A91/A92
BORON [1)]	Boron Steels	WSS-M1A322-A3	WSB-M1A322-A1 (Uncoated) WSS-M1A357-A1 (Coated) [2)] WSS-M1A358-A1 (Coated) [2)]	WSS-M1A357-A1 (Coated) [2)] WSS-M1A358-A1 (Coated) [2)]

1) DP, Trip, MSW, and Boron Steels are included in this Engineering Specification within a limited applicability. Use of these materials needs to be checked with the relevant Body and Manufacturing Engineering departments on a case-by-case basis.
2) WSS-M99P39-A1/A2/A3/A4 performance specification must be called out with these Boron steels.
3) Contact Materials Engineering for the applicability of Global specification numbers.

Table I.4-1: Applicable Categories of Base Sheet Steels Covered by this Specification

The text of the referenced Ford material specifications is available from the following web link http://www.mats.ford.com/mats/scripts/spec_by_mtlCat.html, Metals 1A-99A.

New steel types are under constant development. In the case of steel types not covered by Table I.4-1 the relevant Body and Manufacturing Engineering departments shall be contacted.

Standard Parent Metal Coatings

Laser-beam welding of coated sheet metal is possible as long as the total nominal thickness of zinc coating between overlapping sheets surfaces does not exceed 20 µm. Zinc coating between overlapping sheets in excess of 20 µm can have a critical influence on process stability resulting in porosity and overall joint strength.

Note: Coating combinations in excess of 20 µm require the approval of the relevant Body and Manufacturing Engineering departments. They can be granted on the basis of successful welding trials.

Specification Type	Specification No.	Coating Type
60G60G EL, 50G50G EL	WSS-M1P94-A	Electro-galvanized
55A55A HD	WSS-M1P94-A	Galvannealed
60G60G HD, 50G50G HD	WSS-M1P94-A	Hot Dip Galvanized
AlSi coating	WSD-M1A295-A2	Hot Dip Aluminized

Table I.4-2: Standard Base Metal Coatings Covered by this Specification

Shielding Gases
Shielding gases used for the laser-beam welding process shall preferably be either a standard inert or an active gas according to EN 439. Any other gas needs to be approved by Manufacturing and Materials Engineering.

Filler Metal Wire
Filler wires used for the laser-beam welding process shall be in compliance with WSS-M4A182-A. Any other filler wire needs to be approved by Manufacturing and Materials Engineering.

I.5 Laser-Beam Welded Joint Identification Symbols

The weld identification symbols shall be in accordance with the individual requirements of the Ford Motor Company Brands as outlined below:

- **Ford**

The laser-beam welded joint symbols shall be in accordance with Ford Engineering CAD and Drafting Standard D-3 (Welding Symbols and Specifications). The basic practices to identify laser-welded seams shall follow those standards outlined for the Fusion Welding Process. The process reference number according to ISO 4063 for Laser Welding is 52. Figures 17 and 18 show the method of identification for a 2-gauge overlap joints, both having five 25 mm long stitches, 30 mm apart, with the top sheet as the thinnest sheet at 1.0 mm gauge.

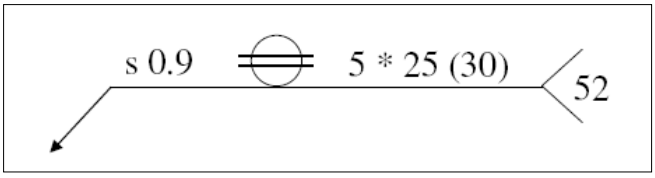

Figure 17: Identification of 2-Gauge Overlap Joint, Seam Weld

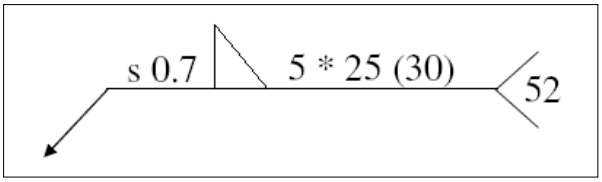

Figure 18: Identification of 2-Gauge Overlap Joint, Seam Weld at Edge

Figures 19 and 20 show examples for the identification of 3-gauge welding conditions, both having five 25 mm long stitches, 30 mm apart, with the top sheet as the thinnest sheet at 1.0 mm gauge. Please note that in the case of Figure 19, the second interface is then considered an overlap weld for the ISO symbol selection.

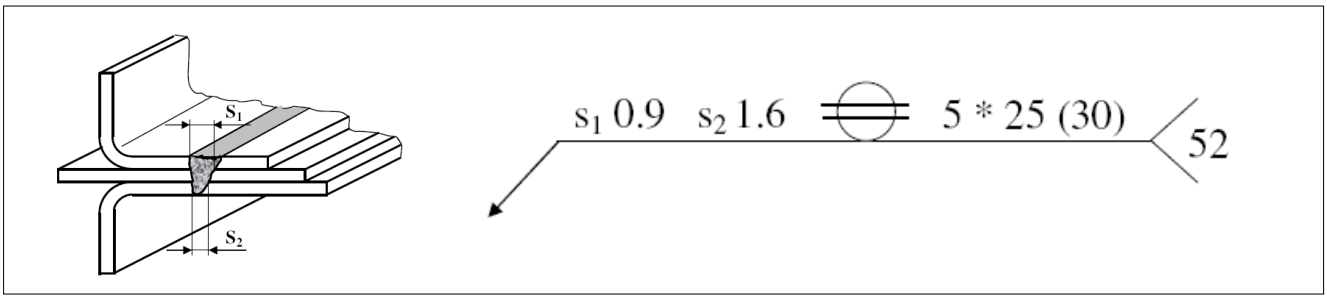

Figure 19: Identification of 3-Gauge Overlap Joint, Seam Weld

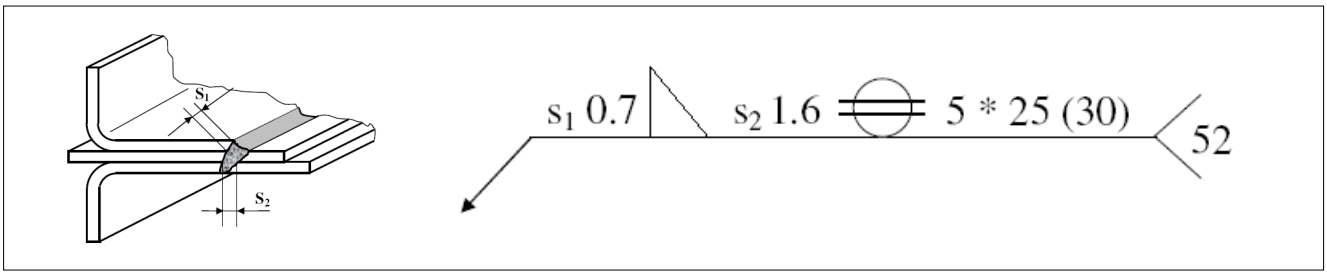

Figure 20: Identification of 3-Gauge Overlap Joint, Seam Weld at Edge

- **Volvo Car Corporation**

The structure of the weld symbols shall be in accordance with Volvo Car Corporation Standard VCS 5027,4, Section 2. Symbolic Representation of Welds, available at http://www.tech.volvo.se/standard/eng/stdnum.html.

I.6 Weld Groups

A weld group is defined as a set of welds (e.g. circular, staple or stitch welds) that join the same combination of sheets ("stackup"). In general, all welds in a stackup will be in one group. A metal condition change (e.g. when a tailor-welded part is in the stackup) requires designation of a new group. Because individual control welds may be identified as described in Section I.6, a group may contain both common and control welds. This situation is described further in Section I.8.

- A group size of one is not permitted, unless it is grouped with an adjacent continuous weld of the same stack up. If a single weld is essential, the joint should be redesigned to incorporate a redundant weld or a mechanical fastener.

- A group size of two is not recommended. If both welds are essential, the joint should be redesigned to incorporate a redundant weld or a mechanical fastener. If a second weld was added as noted above to avoid a one-weld group, a note can be added to the engineering drawing to allow one discrepant weld in the group. This requires approval of the relevant Body and Manufacturing Engineering departments.

I.7 Weld Classification

"Control welds" for laser beam welding are defined as welds that are important for structural integrity, safety, or Federal compliance (North America). They shall be identified jointly between Body Engineering (Core and Vehicle Program) and the Attribute Teams (Crash, Durability and, if applicable, NVH) on the basis of the relevant Design-FMEAs, CAE-analysis and physical verification testing.

"Control welds" are identified by 'Control / ∇'. This designation is attached to specific welds in the relevant CAD files. Welds not designated as "control welds" are considered "common welds".

I.8 Weld Quality Levels, Acceptance Criteria and Reaction Requirements

I.8.1 Weld Quality Levels

For this Engineering Specification, Table I.8.1 defines two distinct levels of quality for laser welds:

Satisfactory	Discrepant
A laser weld that meets the minimum s-value requirements at each interface and all the relevant requirements of Section III.	A laser weld that does not meet the minimum s-value requirements at each interface or all the relevant requirements of Section III. *Note: A missing laser weld is classified as discrepant.*

Table I.8.1: Levels of Laser Weld Quality

I.8.2 Acceptance Criteria

Table I.8.2 defines the requirements for determining weld group effectiveness based on the quantity of welds designated, the quantity of satisfactory welds, and the quantity of satisfactory.

Number of Welds in Group	Minimum Satisfactory Welds
2	2
3	2
4	3
5	4
6	5
7	6
8	6
9	7
N > 9	80% based on common rounding rules

Table I.8.2: Number of Minimum Satisfactory Welds in a Group

I.8.3 Reaction Requirements

Reaction plans for containment and repair according to local weld control plans shall be executed in any one of the following cases:

- the criteria in Table I.8.2 are not met,
- a single control weld is discrepant,
- adjacent welds are discrepant, even if they are from different groups.

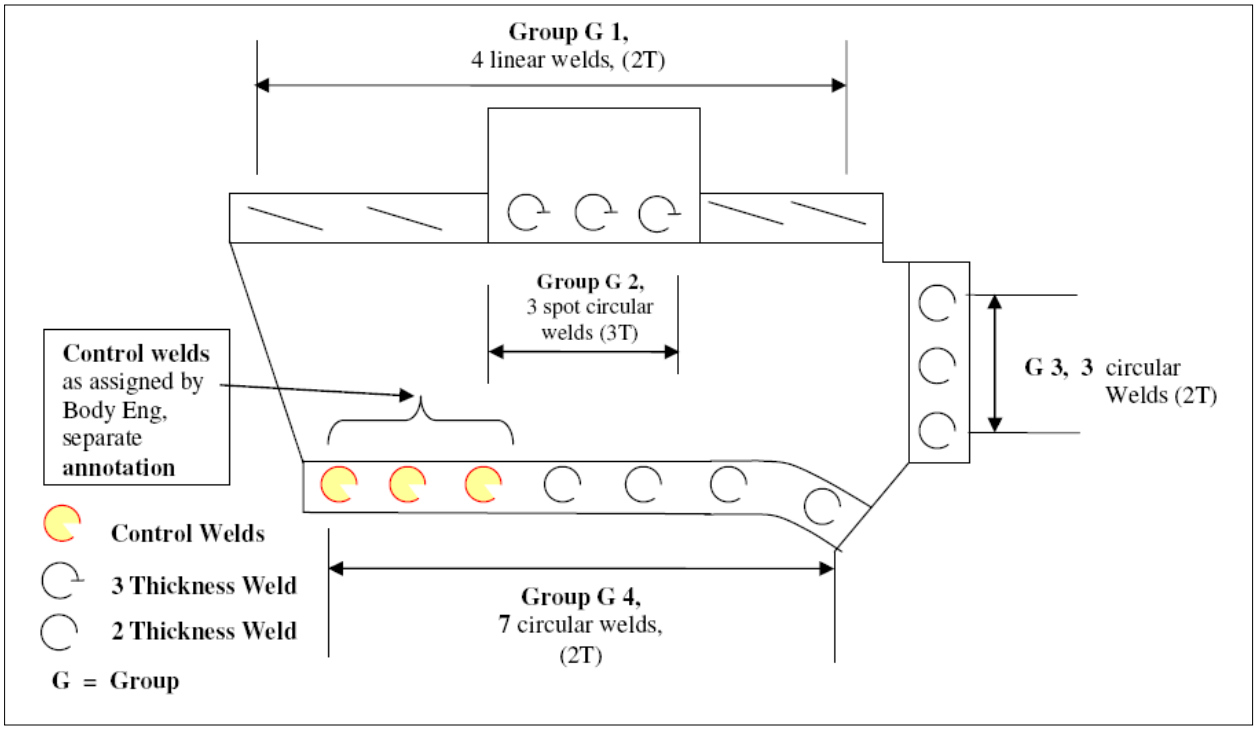

Figure 21: Weld Grouping Illustration

Examples of how to consider group testing in general and how to handle control welds in group testing:

- **Group 1**, 4 linear welds, 2 thickness combination, in general follow discrepancy rules in Table I.8-2
- **Group 2**, 3 circular welds, 3 thickness combination, in general follow discrepancy rules in Table I.8-2
- **Group 3**, 3 circular welds, 2 thickness combination, in general follow discrepancy rules in Table I.8-2
- **Group 4**, 7 circular welds, in general follow discrepancy rules in Table I.8-2, **but** none of the control welds shown above is allowed to be discrepant

NOTE: Start or end welds of groups relevant to attribute performance may be identified as control welds, as shown in this example.

II. SUMMARY OF PRODUCTION VALIDATION AND IN-PROCESS TESTS

Production Validation (PV) tests are used to obtain an initial estimate of the process potential to produce parts that conform to engineering requirements, and to identify causal or predictive relationships between significant design and process characteristics (to be used for process control). The tests must be completed successfully using initial parts from production tooling and production process before Part Submission Warrant (PSW) approval and authorization of production parts can be issued. Sampling plans for PV testing must be included in the control plan.

In addition, tests can be done on prototype level parts or vehicles to the same extent as outlined for PV-testing. This does not replace the necessity to run PV-phase testing as described above.

In-Process (IP) tests are used to further understand the relationship between significant design and process characteristics and to establish a basis for continuing improvement. Tests must be completed with production parts on an ongoing basis. Sampling plans for both IP testing and evaluation of the significant process characteristics must be included in the Control Plan. When the process is found to be out of control or the test acceptance criteria are not met, the reaction plan approved in the Control Plan shall be invoked.

Laser-welded joints that do not meet the requirements outlined in Chapters II (Summary of Production Validation and In-Process Tests) and III (Test Procedures and Requirements) of this Engineering Specification need to be repaired following the repair procedure according to Section III.5.

The table that follows summarizes the various PV and IP tests and the acceptance parameters for each. They form the basis upon which to develop a complete Control Plan for these and their related significant process characteristics. The Control Plan will include frequencies, sample sizes and reaction plans; see Quality Management Systems, ISO/TS 16949:2009.

II. SUMMARY OF PRODUCTION VALIDATION AND IN-PROCESS TESTS

Welding Parameter Monitoring (Characteristics monitored or established by Manufacturing through equipment settings)

Please see Section III.2 for a detailed description of the requirements.

Test Number	Test Characteristics	Lower Tolerance Limit	Target Value	Upper Tolerance Limit	Minimum Sample Size	Minimum Sample Frequency
III.2.2	**Laser Power [kW]**	As determined during PV testing	As determined during PV testing	As determined during PV testing	see [1)]	see [1)]
III.2.3	**Spot Size and Shape [mm]**	As determined during PV testing	As determined during PV testing	As determined during PV testing	see [1)]	see [1)]
III.2.4	**Flow of Shielding Gas V_G [l/min]**	Not Applicable	Gas Flow Sensor Signals Gas Flow	Not Applicable	see [1)]	see [1)]
III.2.5	**Welding Speed [m/min]**	As determined during PV testing	As determined during PV testing	As determined during PV testing	see [1)]	see [1)]
III.2.6	**Force of Clamping Device or Wheel [N]**	As determined during PV testing	As determined during PV testing	As determined during PV testing	see [1)]	see [1)]
III.2.7	**Filler Wire Speed [m/min]**	As determined during PV testing	As determined during PV testing	As determined during PV testing	see [1)]	see [1)]

[1)] **Ford**

Minimum Sample Size and Frequency to be determined by the manufacturing plant personnel responsible for the control plan, in conjunction with the design-responsible Body Engineering activity and the relevant quality departments, as well as other appropriate functions. Reference:

Ford of Europe: Document VOPQUE-612, available at http://wiki.ford.com:8888/confluence/display/QOS/VOPQUE-612+Uniform+Test+and+Evaluation+Program+for+Welding+and+other+joining+Operations

Ford North America: Document VOPSSN-008, available at http://www.vo.ford.com/ss/procedures

Volvo Car Corporation: Minimum Sample Size and Frequency to be defined by the relevant manufacturing unit.

II. SUMMARY OF PRODUCTION VALIDATION AND IN-PROCESS TESTS (cont.)

Inspection of the Visible Part of the Weld

Test Number	Test Characteristics	Overlap (O) Edge (E)	Lower Tolerance Limit	Target Value	Upper Tolerance Limit	Minimum Sample Size	Minimum Sample Frequency
ALL of III.3	**ALL**	ALL	**Cumulative effect of dimensional and visual test characteristics below must not exceed 30% of the design weld length.**				
III.3.2	**Bead Position**	O, E	Not applicable	As specified on assembly drawing or in CAD-system	O: center of seam +/- 3 mm E: seam must cover top sheet edge	see [1)]	see [1)]
III.3.3	**Weld Length**	O, E	Length as specified on assembly drawing or in CAD-system is the minimum design length	Meet at least the design length	Design length + 3 mm for all welds	see [1)]	see [1)]
III.3.4	**Top Surface Pores and Holes**	O, E	Not applicable	Not present	Maximum 20 % cumulative of the design length specified on assembly drawing or in CAD-system	see [1)]	see [1)]
III.3.5	**Top Surface Cracks**	O, E	Not applicable	Cracks visible without magnification are not permitted	Not applicable	see [1)]	see [1)]

[1)] **Ford**
Minimum Sample Size and Frequency to be determined by the manufacturing plant personnel responsible for the control plan, in conjunction with the design-responsible Body Engineering activity and the relevant quality departments, as well as other appropriate functions. Reference:
Ford of Europe: Document VOPQUE-612, available at http://wiki.ford.com:8888/confluence/display/QOS/VOPQUE-612+Uniform+Test+and+Evaluation+Program+for+Welding+and+other+joining+Operations
Ford North America: Document VOPSSN-008, available at http://www.vo.ford.com/ss/procedures

Volvo Car Corporation: Minimum Sample Size and Frequency to be defined by the relevant manufacturing unit.

Inspection of the Visible Part of the Weld, continued

Test Number	Test Characteristics	Overlap (O) Edge (E)	Lower Tolerance Limit	Target Value	Upper Tolerance Limit	Minimum Sample Size	Minimum Sample Frequency
III.3.6	**Top Surface Cut Through**	O, E	Not applicable	Not present	Maximum 20 % cumulative of the design length specified on assembly drawing or in CAD-system	see [1)]	see [1)]
III.3.7	**Spatter**	O, E	Not applicable	Not present	See III.3.7	see [1)]	see [1)]
III.3.8	**Weld Discontinuity**	O, E	Not applicable	Not present	Maximum 20 % cumulative of the design length specified on assembly drawing or in CAD-system	see [1)]	see [1)]
III.3.9	**Undercut**	O, E	Not applicable	Not present	Maximum 20 % cumulative of the design length specified on assembly drawing or in CAD-system	see [1)]	see [1)]

[1)] **Ford**

Minimum Sample Size and Frequency to be determined by the manufacturing plant personnel responsible for the control plan, in conjunction with the design-responsible Body Engineering activity and the relevant quality departments, as well as other appropriate functions. Reference:

Ford of Europe: Document VOPQUE-612, available at http://wiki.ford.com:8888/confluence/display/QOS/VOPQUE-612+Uniform+Test+and+Evaluation+Program+for+Welding+and+other+joining+Operations

Ford North America: Document VOPSSN-008, available at http://www.vo.ford.com/ss/procedures

Volvo Car Corporation: Minimum Sample Size and Frequency to be defined by the relevant manufacturing unit.

II. SUMMARY OF PRODUCTION VALIDATION AND IN-PROCESS TESTS (GENERIC REQUIREMENTS) (cont.)

Inspection of Section Cut

Test Number	Test Characteristics	Overlap (O) Edge (E)	Lower Tolerance Limit	Target Value	Upper Tolerance Limit	Minimum Sample Size	Minimum Sample Frequency
III.4.2	**s-Value**	O, E	See I.3.4	Exceed the s-value outlined in Section I.3.4	Not applicable	see [1)]	see [1)]
III.4.3	**Weld Penetration**	O, E	30% of bottom sheet thickness in double and triple panel welding	100% of bottom sheet thickness	Not applicable	see [1)]	see [1)]
III.4.4	**Root Convexity**	O, E	Not applicable	Not present	0.2 mm + 30% of bottom sheet thickness	see [1)]	see [1)]
III.4.5	**Weld Top Bead Concavity**	O, E	Not applicable	Not present	50% of top sheet thickness	see [1)]	see [1)]
III.4.6	**Encapsulated Pores, Inner Lack of Fusion, Pits, Enclosures**	O, E	Not applicable	Not present	Single discrepancy $\leq 30\%$ t_{min}, maximum two per section cut	see [1)]	see [1)]

[1)] **Ford**
Minimum Sample Size and Frequency to be determined by the manufacturing plant personnel responsible for the control plan, in conjunction with the design-responsible Body Engineering activity and the relevant quality departments, as well as other appropriate functions. Reference:
Ford of Europe: Document VOPQUE-612, available at http://wiki.ford.com:8888/confluence/display/QOS/VOPQUE-612+Uniform+Test+and+Evaluation+Program+for+Welding+and+other+joining+Operations
Ford North America: Document VOPSSN-008, available at http://www.vo.ford.com/ss/procedures

Volvo Car Corporation: Minimum Sample Size and Frequency to be defined by the relevant manufacturing unit.

Inspection of Section Cut, continued

Test Number	Test Characteristics	Overlap (O) Edge (E)	Lower Tolerance Limit	Target Value	Upper Tolerance Limit	Minimum Sample Size	Minimum Sample Frequency
III.4.7	**Cracks**	O, E	Not applicable	Not present	Not applicable	see [1)]	see [1)]
III.4.8	**Burn Through of Parent Metal**	O, E	Not applicable	Not present	Not applicable	see [1)]	see [1)]
III.4.9	**Hardness Increase**	O, E	See Section III.4.9 for details	See Section III.4.9 for details	See Section III.4.9 for details	see [1)]	see [1)]

[1)] **Ford**
Minimum Sample Size and Frequency to be determined by the manufacturing plant personnel responsible for the control plan, in conjunction with the design-responsible Body Engineering activity and the relevant quality departments, as well as other appropriate functions. Reference:
Ford of Europe: Document VOPQUE-612, available at http://wiki.ford.com:8888/confluence/display/QOS/VOPQUE-612+Uniform+Test+and+Evaluation+Program+for+Welding+and+other+joining+Operations
Ford North America: Document VOPSSN-008, available at http://www.vo.ford.com/ss/procedures

Volvo Car Corporation: Minimum Sample Size and Frequency to be defined by the relevant manufacturing unit.

II. SUMMARY OF PRODUCTION VALIDATION AND IN-PROCESS TESTS (GENERIC REQUIREMENTS) (cont.)

Destructive, Non-Destructive and Functional Testing

Test Number	Test Characteristics	Overlap (O) Edge (E)	Lower Tolerance Limit	Target Value	Upper Tolerance Limit	Minimum Sample Size	Minimum Sample Frequency
III.5.2	**Static Tensile Test**	O, E	Not applicable	Sample to separate in base sheet metal or in HAZ but not in weld bead	Not applicable	see [1)]	see [1)]
III.5.3	**Peel Test**	O, E	Not applicable	Sample to separate in base sheet metal or in HAZ but not in weld bead	Not applicable	see [1)]	see [1)]
III.5.4	**Impact Test**	O, E	Not applicable	Welded joint integrity in either component and/or subassembly testing; test set up and test conditions to be agreed with responsible Safety Attribute Team	Not applicable	see [1)]	see [1)]
III.5.5	**Chisel Test (Destructive)**	O, E	Tear out in 80 % of the design length specified on assembly drawing or in CAD-system	Base metal tears out with weld or weld fractures through throat with root fusion evident and visible over 100% of weld	Not applicable	see [1)]	see [1)]

[1)] **Ford**
Minimum Sample Size and Frequency to be determined by the manufacturing plant personnel responsible for the control plan, in conjunction with the design-responsible Body Engineering activity and the relevant quality departments, as well as other appropriate functions. Reference:
Ford of Europe: Document VOPQUE-612, available at http://wiki.ford.com:8888/confluence/display/QOS/VOPQUE-612+Uniform+Test+and+Evaluation+Program+for+Welding+and+other+joining+Operations
Ford North America: Document VOPSSN-008, available at http://www.vo.ford.com/ss/procedures

Volvo Car Corporation: Minimum Sample Size and Frequency to be defined by the relevant manufacturing unit.

Destructive, Non-Destructive and Functional Testing (cont.'d)

Test Number	Test Characteristics	Overlap (O) Edge (E)	Lower Tolerance Limit	Target Value	Upper Tolerance Limit	Minimum Sample Size	Minimum Sample Frequency
III.5.6	**Destructive Test using a Machine**	O, E	Tear out in 80 % of the design length specified on assembly drawing or in CAD-system	Base metal tears out with weld or weld fractures through throat with root fusion evident and visible over 100% of design length of weld	Not applicable	see [1)]	see [1)]
III.5.7	**Chisel Test (Non-Destructive)**	O, E	No separation in 80 % of the design length specified on assembly drawing or in CAD-system	No partial or complete separation of welded joint over 100% of design length of weld	Not applicable	see [1)]	see [1)]
III.5.8	**Durability / Fatigue Test**	O, E	Not applicable	No fatigue cracks in weld and no lack of compliance following completion of full vehicle PASCAR Phase 1 and 50% of PASCAR Phase 2 testing according to CETP 00.00-R310	Not applicable	see [1)]	see [1)]

[1)] **Ford**

Minimum Sample Size and Frequency to be determined by the manufacturing plant personnel responsible for the control plan, in conjunction with the design-responsible Body Engineering activity and the relevant quality departments, as well as other appropriate functions. Reference:

Ford of Europe: Document VOPQUE-612, available at http://wiki.ford.com:8888/confluence/display/QOS/VOPQUE-612+Uniform+Test+and+Evaluation+Program+for+Welding+and+other+joining+Operations

Ford North America: Document VOPSSN-008, available at http://www.vo.ford.com/ss/procedures

Volvo Car Corporation: Minimum Sample Size and Frequency to be defined by the relevant manufacturing unit.

III. TEST PROCEDURES AND REQUIREMENTS

III.1 Applicability of Test Procedures for PV- and IP-Test Phases

Table III.1 defines the applicability of the test procedures listed above for PV- and IP-testing

Test No.	Test Characteristics	PV-Test Phase	IP-Test Phase
III.2	**Weld Parameter Monitoring**	**Mandatory** To establish target values and tolerance limits ***Force of Clamping Device or Wheel [N] is optional in case of remote laser welding only***	**Mandatory** ***Force of Clamping Device or Wheel [N] is optional in case of remote laser welding only***
III.3	**Inspection of the Visible Part of the Weld**	**Mandatory** **Optional** Dye Penetration Test recommended to further analyze the occurrence of top surface pores, holes and cracks	**Mandatory** **Optional** Dye Penetration Test recommended to further analyze the occurrence of top surface pores, holes and cracks
III.4	**Inspection of Section Cuts**	**Mandatory**	**Mandatory** – for control welds **Optional** – for common welds **Recommended** for • root cause analysis in case of discrepancies and • weld quality evaluation as part of the revalidation (Section IV)
III.5	**Destructive, Non-Destructive and Functional Testing**	**Mandatory** Destructive Chisel Test (III.5.5) or Destructive Test Using a Machine (III.5.6) Body and Manufacturing Engineering expert departments to decide whether the following tests are required: Static Tensile Test (III.5.2), Peel Test (III.5.3), Impact Test (III.5.4), Durability /Fatigue Test (III.5.8), typically for unknown Laser-Beam Welding applications only.	**Mandatory** Destructive Chisel Test (III.5.5) or Destructive Test using a Machine (III.5.6) for those edge and overlap welds whose material combinations are considered non-pryable (for example having a gauge ≥ 2.0 mm and/or having a minimum yield strength ≥ 410 MPa). Non-Destructive Chisel Test (III.5.7) for pryable welds

Table III.1: Applicability of Test Procedures and Requirements

III.2 Welding Parameter Monitoring

III.2.1 Introduction

Each welding application requires an individual set of fixed equipment settings as well as controllable process parameters as outlined below - the so-called **Operating Window**. It consists of target values as well as the upper and lower tolerance limits and shall be determined in Production Validation tests individually for each Laser-Welded joint.

EQUIPMENT SETTINGS (Fixed)	PROCESS PARAMETERS (Controllable)
Laser Power [kW]	Laser Welding Speed [m/min]
Spot Size and Shape [mm]	Force of Clamping Device or Wheel [N]
	Flow of Shielding Gas V_G [l/min]
	Filler Wire Speed [m/min]

Table III.2.1: List of Process Parameters

The aim is to define a process window that protects for tolerances and process variations but still ensures a stable laser welding process in high volume production. The operating window shall be included in the process control plan. The parameter monitoring shall be applied on the basis of a 100 % sampling rate in IP-conformance testing.

III.2.2 Laser Power [kW]

The power of the laser beam is crucial for the appropriate energy input into the welded joint.

During IP-phase, the beam power shall be equal to the power setting determined during PV-testing. Compliance shall be checked using a power tester that correlates the laser energy intensity on the parent metal surface to the laser beam power.

III.2.3 Spot Size and Shape [mm]

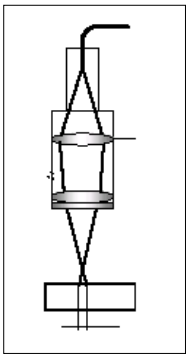

The size and shape of the spot created by the laser on the parent metal surface depends on the geometry of the laser optics.

During IP-phase, the size and shape of the spot shall match what has been determined during PV-testing individually for the relevant laser-welded joint application. The exchange of the laser head or of its subcomponents due to maintenance and repair shall trigger a revalidation of the laser optic geometry including the size and shape of the spot.

Figure 22: Laser Optics

III.2.4 Flow of Shielding Gas – if applicable [l/min]

In case shielding gas is used, a gas sensor shall continuously monitor during IP-phase whether or not a proper flow of gas is delivered to the vent.

III.2.5 Welding Speed [m/min]

During IP-monitoring, the laser welding speed patterns shall stay within the process window as defined in PV-testing individually for each laser welded joint application.

III.2.6 Force of Clamping Device or Wheel [N]

The force applied by the clamping device or wheel determines the gap condition between the parent sheet metal and thus the degassing condition for the zinc-gases. It typically varies during the welding operation. During IP-monitoring, the force shall stay within the process window as defined in PV-testing individually for each laser welded joint application.

III.2.7 Filler Wire Speed [m/min]

The filler metal wire speed determines the amount of filler material that is available for the actual welding operation in conjunction with the speed of the welding head (welding speed). Typically, the wire speed is set during PV-Phase jointly with the welding speed.
During IP-monitoring, the wire speed shall stay within the process window as defined in PV-testing individually for each laser welded joint application.

III.3 Inspection of the Visible Part of the Weld

III.3.1 Introduction

The visible part of the weld shall be inspected for discrepancies using the following two inspection methods. The applicability of the relevant test methods is defined in Section III.1.

- **Naked Eye Inspection**
  Visual inspections shall be performed (naked eye inspection) to detect those obvious discrepancies outlined in this Section. Scales or calliper gauges are required to verify dimensional compliance.
- **Dye Penetrant Testing**
  A dye penetrant test may be performed to further analyze the following discrepancies:
  - Top Surface Pores and Holes, see Section III.3.4 and
  - Top Surface Cracks, see Section III.3.5.

Cumulative effect of dimensional and visual test characteristics below must not exceed 30% of the design weld length.

III.3.2 Bead Position

The position of the laser weld shall be as specified on the assembly drawing or in the CAD-system. The upper tolerance limit for deviations of the position of the center of overlap seams is +/- 3 mm in both, lateral and longitudinal direction. In the case of edge welds, the weld must cover the top sheet edge.

III.3.3 Weld Length

The length of the weld must comply with the specified design length as outlined on the assembly drawing as it is considered the minimum length. An upper tolerance limit of 3 mm on top of the minimum design length is acceptable.

III.3.4 Top Surface Pores and Holes

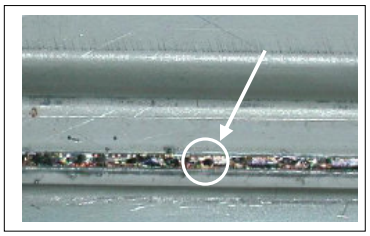

Figure 23: Top Surface Pores

The target is that top surface pores and holes as shown in Figure 23 shall not be present.

The upper tolerance for surface pores and holes is a cumulative discrepant length ≤ 20 % of the design length specified on the assembly drawing or in the CAD-system.

III.3.5 Top Surface Cracks

Cracks are fracture type discontinuities characterized by a sharp tip and high ratio of length to width. They typically result from an inhomogeneous heat distribution in the joint. Surface cracks visible without magnification must not be present and are unacceptable.

III.3.6 Top Surface Cut Through

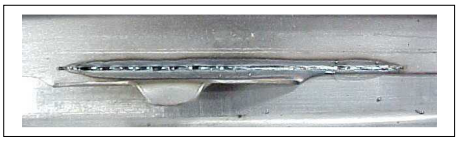

Figure 24: Top Surface Cut Through

The target is that top surface cut through as shown in Figure 24 shall not be present.

The upper tolerance for surface cut through is a cumulative discrepant length ≤ 20 % of the design length specified on the assembly drawing or in the CAD-system.

III.3.7 Spatter

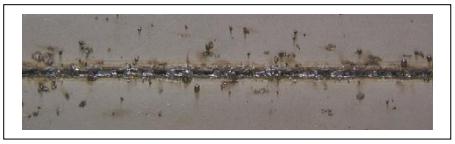

Figure 25: Spatter

Spatter is defined as metal particles that are expelled during the welding operation (illustrated in Figure 25).

The acceptance criteria for spatter depend on the class of surface finish defined in ESF75-B11007-AA as follows:

- **Ford Class 1 Finish, VCC Classes 1 and 2 Finish:**
  Spatter shall not be detectable.
- **Ford Class 2 Finish, VCC Classes 3 and 4 Finish:**
  Spatter shall not be detectable. Individual exemptions can be agreed between Body Engineering, Manufacturing Engineering and Craftsmanship.
- **Ford Class 3 Finish, VCC Class 5 Finish:**
  The minimum occurrence of spatter – as determined during the definition of the operating window in PV-testing - is acceptable if their height is less than 1.0 mm unless the drawing indicates that spatter is prohibited.

III.3.8 Weld Discontinuity

The target is that welds will not have their continuity broken.

The upper tolerance for weld discontinuity is a cumulative discrepant length ≤ 20 % of the design length specified on the assembly drawing or in the CAD-system.

III.3.9 Undercut

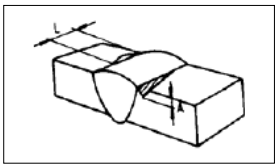

Figure 26: Undercut

The target is that undercut as shown in Figure 26 shall not be present.

The upper tolerance for undercut is a cumulative discrepant length ≤ 20 % of the design length specified on the assembly drawing or in the CAD-system.

III.4 Inspection of Section Cut

III.4.1 Introduction

The visual / dimensional inspection of a section cut gives the best insight into the weld properties and is therefore used during the series of PV-testing performed to define the operating window for each individual welding application. Its execution is mandatory for all welds during the PV test phase and for control welds during IP test phase. In addition, section cut analysis is recommended for root cause analysis in case of discrepancies during IP-phase and bead quality evaluations as part of the revalidation (Section IV).

Section cuts shall be performed perpendicular to the seam in the middle of a weld. In the case of a group of welds, Body and Manufacturing Engineering shall agree on the selection of welds and the scope of section cut testing individually for each application during PV-testing.

III.4.2 s-Value

The target for the s-value is to exceed the minimum value described in Section I.3.4. The s-value for gauges exceeding 1.5 mm need to be agreed on a case-by-case basis jointly between the relevant Body and Manufacturing Engineering departments

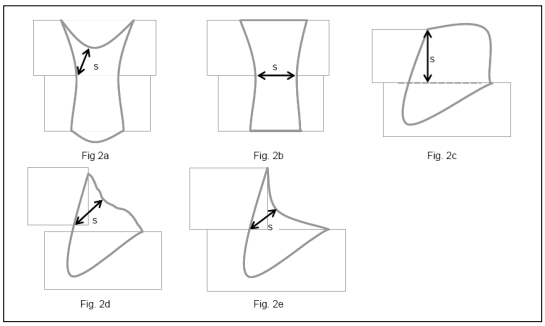

Figure 27 shall help to properly identify the s-value considering various joint types, weld and gap conditions.

Figure 27: Measurement of s-value

III.4.3 Weld Penetration

The target value for weld penetration is 100 % of bottom sheet thickness in double and triple panel welding. The lower tolerance limit for penetration depth is 30% of the bottom sheet thickness t2 and t3 respectively as shown in Figure 28 for double and triple panel welding.

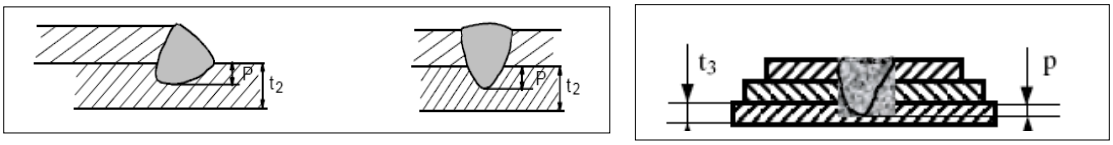

Figure 28: Minimum Weld Penetration into Bottom Sheet

III.4.4 Root Convexity

The target is that root convexity h_2 as shown in Figure 29 shall not be present.

The upper tolerance for h_2 is 0.2 mm + 30% of bottom sheet thickness.

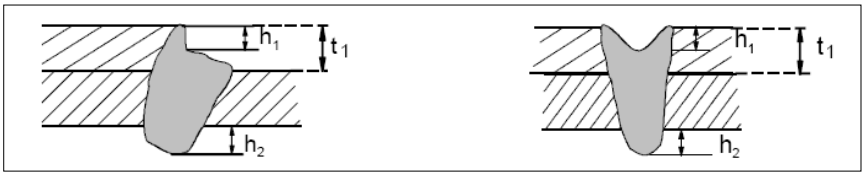

Figure 29: Weld Root Convexity and Top Bead Concavity

III.4.5 Weld Top Bead Concavity

The target is that weld top bead concavity h_1 as shown in Figure 28 shall not be present.

The upper tolerance limit for h_1 is 50% of top sheet thickness.

III.4.6 Encapsulated Pores, Inner Lack of Fusion, Pits, Enclosures

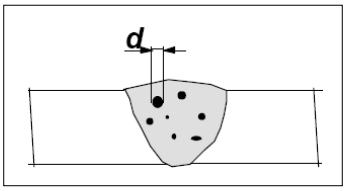

The target is that encapsulated pores, inner lack of fusion, pits or enclosures as shown in Figure 30 shall not be present.

The upper tolerance is ≤ 30 % of t_{min} for a single discrepancy with maximum two such discrepancies per section cut.

Figure 30: Encapsulated Pores

III.4.7 Cracks

Cracks in the bead are not acceptable.

III.4.8 Burn Through Of Parent Metal

Burn through of parent sheet metal is not acceptable.

III.4.9 Hardness Increase

Hardness testing shall be performed according to ISO 14271 on laser weld section cuts to determine the Vickers hardness (low load range, HV 1) of the weld, the heat affected zone and the parent sheet metal.

Initial Parent Sheet Metal Hardness [HV 1]	Hardness In Weld [HV 1]
< 120	< 350
> 120… < 200	< 450
> 200 … < 300	< 550
> 300	< 600

Table III.4.9: Hardness Increase Limits

Table III.4.9 lists the permissible increase in hardness based on the initial parent sheet metal hardness.

The material used and the welding techniques employed shall be such that the hardness of the weld and the heat-affected zone do not exceed the limits listed in Table III.4.9.

Note:
The relevant expert department shall be consulted in case that these limits cannot be met.

III.5 Destructive, Non-Destructive, and Functional Testing

III.5.1 Introduction

Welded bead strength tests are performed to ensure that the joint meets the individual performance requirements in terms of static and dynamic loads. The applicability of the relevant test methods is defined in Section III.1.

III.5.2 Static Tensile Test

The static tensile test shall be performed in accordance with:

- DIN EN 895, Destructive Testing Of Welds In Metallic Materials or
- Volvo Cars Standard 5601,039, Static Testing of Line Joints
- Auto/Steel Partnership Test Procedures for North America.

Alternative test specimen geometries suitable for static tensile testing are shown in Figure 31.

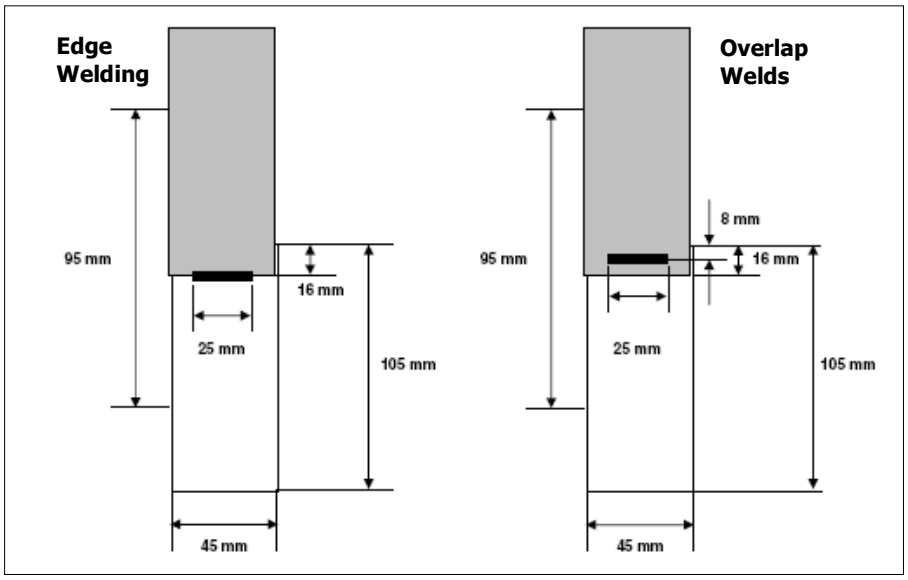

Figure 31: Typical Tensile Test Specimen for Edge and Overlap Welds

The test specimen shall be manufactured using base sheet metal as well as – if applicable - filler metal wire identical to production conditions in terms of material specification, gauge and base sheet metal coating. The test specimen shall be loaded gradually and continuously until separation occurs. Separation is acceptable in the base sheet metal or in the HAZ, but not in the weld bead.

III.5.3 Peel Test

The static peel test shall be performed in accordance with:

- Volvo Cars Standard 5601,039, Static Testing of Line Joints.
- Auto/Steel Partnership Test Procedures for North America.

Alternative test specimen geometries suitable for static tensile testing are shown in Figure 32.

The test specimen shall be manufactured using base sheet metal as well as – if applicable - filler metal wire identical to production conditions in terms of material specification, gauge and base sheet metal coating. The test specimen shall be loaded gradually and continuously until separation occurs. Separation is acceptable in the base sheet metal or in the HAZ, but not in the weld bead.

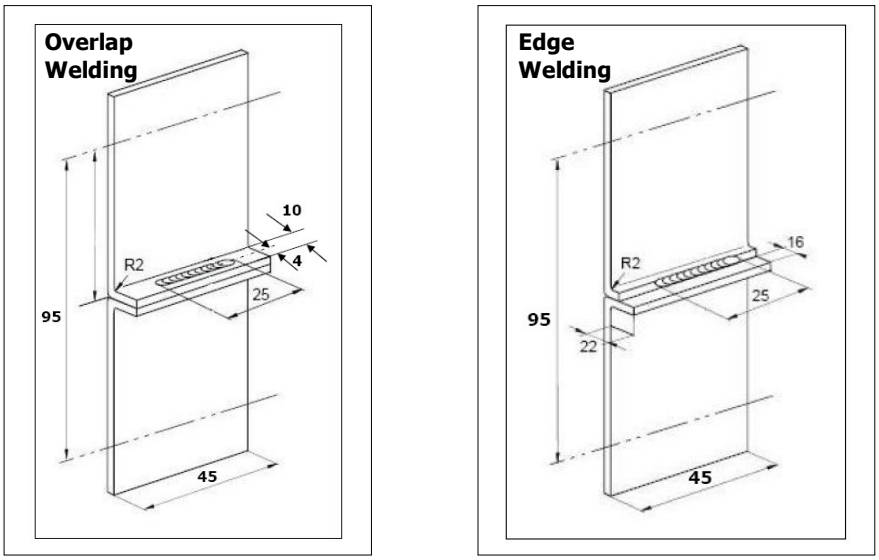

Figure 32: Typical Peel Test Specimen for Edge and Overlap Welds

III.5.4 Impact Test

Impact tests shall be performed with those welded joints that are subjected to loads at high speeds to verify integrity of the welded joint. The test set up and test conditions shall be agreed upon with the relevant Safety Attribute Team taking into consideration the location and loading condition of the relevant joint on the vehicle. Testing can be performed on either components or subassemblies (e.g. sled testing, drop testing) that contain the welded joint.

III.5.5 Chisel Test (Destructive)

In the destructive chisel test, the base sheet metal shall tear out with weld or weld fractures through the throat with root fusion evident and visible over 100% of the design length of the weld.

The lower tolerance limit for the destructive chisel test is that the base metal tears out with weld over 80% of the design length *specified on the assembly drawing or in the CAD-system.*

The chisel test can be applied on subassembly or complete bodies. It is applicable for those edge and overlap welds whose material combinations are considered non-pryable (typically having a gauge ≥ 2.0 mm and/or having a minimum yield strength ≥ 410 MPa).

Destructive chisel testing requires separating the base sheet metal adjacent to the weld in the direction parallel to the weld using a chisel. The chisel according to ISO 10447 is shown as an example in Figure 33 for Europe. Figure 34 shows the chisel used in North America.

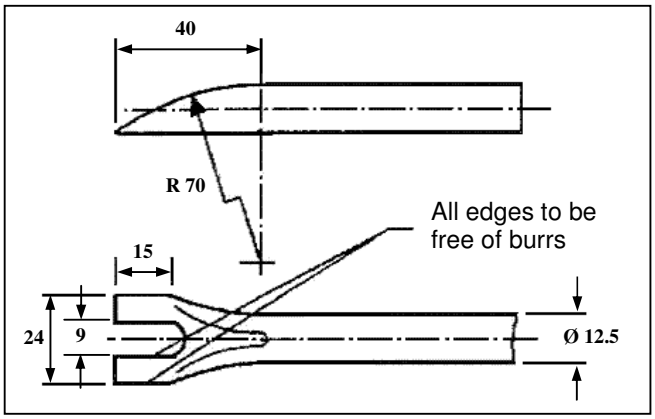

Figure 33: Chisel According to ISO 10447

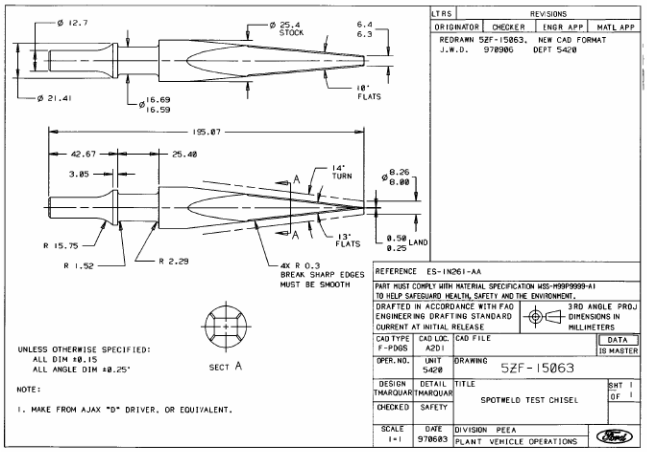

Figure 34: Test Chisel Used in North America (ref. tool # 5ZF-15063)

III.5.6 Destructive Test Using a Machine

A peel testing bench (weld teardown machine), tensile machine, and/or hydraulic tool ("jaws of life") may be utilized in lieu of a chisel for destructive inspection. Examples are documented in the Volvo Cars Standard VCS 8631.39. Welds are evaluated using the same criteria.

III.5.7 Chisel Test (Non-Destructive)

The non-destructive chisel test is applied to pryable welds without directing the chisel onto the weld itself.

In the non-destructive chisel test, there shall be no partial or complete separation of the joint over 100% of the design length of the weld *specified on the assembly drawing or in the CAD-system.* The operator - in contrast to the destructive chisel test – should apply the load gradually and exercise care to avoid permanent damage to the panels.

The lower tolerance limit for the destructive chisel test is that there shall be no partial or complete separation over 80% of the design length *specified on the assembly drawing or in the CAD-system.*

The non-destructive chisel test can also be used to verify the integrity of joints that were welded with parameters outside the operating window while showing no imperfections in a visual inspection (Section III.3).

Non-destructive chisel testing shall include test points at a maximum distance of 10 mm from weld start and stop respectively.

III.5.8 Durability/Fatigue Test

Full vehicle durability testing according to CETP 00.00-R310 (PASCAR Phase 1 and half of PASCAR Phase 2) shall be performed on a test vehicle equipped with the relevant welded joints. These joints shall be welded to meet all requirements of this specification. No fatigue cracks in the welded seam shall be observed following test completion.

III.6 Permissible Repair Methods

Repair can be performed as laser welding. Alternative joining processes that may be suitable are resistance spot welding, gas metal-arc welding [GMA-W], or – in certain cases - gas metal-arc brazing [GMA-B]. The selection of repair method shall be done on an individual basis for each joint, in order to minimize disturbance in running production.

Each repair method used must be approved by both Body and Manufacturing Engineering shall be documented in the Control Plan. Repair using the alternative joining processes shall follow the relevant process Engineering Specification.

IV. REVALIDATION REQUIREMENTS

Any of the following conditions that affect the welding operation require a re-run of Production Validation (PV) tests as agreed upon by the relevant Body and Manufacturing Engineering Departments.

- **Process Change -** Any change in the process which could alter its capability to meet the design requirements or durability of the product. This includes:
  - New, different, relocated, or refurbished production machinery or equipment
  - Any change in subcontracted products or services including the use of engineering-approved alternate materials
  - Changes to rework methods
  - Changes in the sequence of operations
  - Changes in chemical compounds such as lubricants, which are part of the product
  - Changes to filler metal or gas shielding type
- **Engineering Change -** Any change in the part(s) initiated by Ford Motor Company.
- **Material and Coating Change -** Any change in the material properties, or a change in sheet metal coating when the new/revised coating is not listed in Section I.4. A change in steel supplier for steels having a yield strength equal to or exceeding 310 MPa (representing DP600) in the "as received condition" is also considered a material change.
- **Sub-Supplier Change -** Any change in the source of subcontracted components.
- **Adopting Optional Design -** Any change where the supplier incorporates optional designs specified on the released engineering drawing or relevant CAD model.

Certain process parameters will have a significant influence on the Welded joint quality. The control plan, as defined in ISO/TS 16949:2009, Quality Management Systems, is an essential part of a quality product. Some recommended process variables to include in the control plan are:

- Operating Window defined by:
  a. Laser-Power [kW]
  b. Spot Size and Shape [mm]
  c. Flow of Shielding Gas [l/min]
  d. Welding Speed [m/min]
  e. Force of Clamping Device or Wheel [N]
  f. Filler Wire Speed [m/min]

V. INSTRUCTION AND NOTES

Control Plans address all significant design and process characteristics, which include all ES tests and Control Item characteristics. They describe the process potential studies that will be performed for product validation (including PV tests) and the ongoing product and process evaluation for continuing improvement (including IP tests). They include acceptance criteria, sample size, frequencies, data analysis methods and reaction plans.

The control plan is developed, and updated as necessary by the manufacturing source in conjunction with the design responsible Product Engineering activity and other appropriate functions such as Supplier Technical Assistance (STA). The control plan defines the management of the upstream production process and part variables (significant process characteristics) that affect the outcome of the ES tests or other significant design characteristics. The control plan also identifies the specific ES tests, with their sample sizes and frequencies which will be performed in order to:

- Confirm whether the process is being managed effectively.
- Further identify significant process characteristics.
- Evaluate performance of marginal processes.
- Better anticipate the customer effect of proposed process improvements.

For any part on which ES tests have been specified, the manufacturing source must present the control plan and any revisions to the design-responsible Product Design activity for review. This Product Engineering activity has flexibility to honour business relationships with suppliers having proprietary processes.

Examples of formats for control plans are shown in the AIAG Advanced Product Quality Planning and Control Plan (APQP) Guidelines. Internal reference documents can also be found in procedure VOPQUG-051 (*Control Plans – Vehicle Operations Procedure – Global*).

VI. COMPILATION OF REFERENCE DOCUMENTS

A. AIAG Production Part Approval Process (PPAP) Manual
https://www.lom.ford.com/launchomatic/download?objectId=09000c5180a4c4b5&contentType=pdf&rendition=pdf&contentSize=2410054
B. ISO/TS 16949:2009, Quality Management Systems
C. FAP02-001, Quality Planning & Process Control
http://www.lom.ford.com/launchomatic/launch/view.jsp?chronicleId=09000c51802afe89&docbase=edrdoc1
D. DIN EN 895, Destructive Testing Of Welds In Metallic Materials (05/1999)
E. ISO 14271, Vickers hardness testing of resistance, spot, projection and seam welds (low load and microhardness)
F. Volvo Cars Standard 5601,039, Static Testing of Line Joints
G. Volvo Cars Standard 8631,39, Quality Assurance, Spot Welding
H. Standard for Testing Line Welds, Auto/Steel Partnership
I. Ford Corporate Engineering Test Procedure 00.00-R-310, North Atlantic Durability Test for Passenger Cars
J. FNA Weld Quality Program Procedure VOPSSN-008 available at
http://www.vo.ford.com/ss/procedures/procd-files/ssn008c.pdf
K. ESF75B-11007-AA, Specification – Sheet Metal Surfaces and Edges available from
http://forddoc.secure24.ford.com/PNSearch.aspx
L. FoE Vehicle Operations Operating procedure VOP QUE-612, Uniform Test and Evaluation Program For Welding and other joining Operations; available at
http://wiki.ford.com:8888/confluence/display/QOS/VOPQUE-612+Uniform+Test+and+Evaluation+Program+for+Welding+and+other+joining+Operations